frontiers | Research Topics

Genomic and epigenomic applications in animal and veterinary sciences

Edited by
Nélida Rodríguez-Osorio, Abdul Rasheed Baloch and Jean Feugang

Published in
Frontiers in Veterinary Science
Frontiers in Genetics

FRONTIERS EBOOK COPYRIGHT STATEMENT

The copyright in the text of individual articles in this ebook is the property of their respective authors or their respective institutions or funders. The copyright in graphics and images within each article may be subject to copyright of other parties. In both cases this is subject to a license granted to Frontiers.

The compilation of articles constituting this ebook is the property of Frontiers.

Each article within this ebook, and the ebook itself, are published under the most recent version of the Creative Commons CC-BY licence. The version current at the date of publication of this ebook is CC-BY 4.0. If the CC-BY licence is updated, the licence granted by Frontiers is automatically updated to the new version.

When exercising any right under the CC-BY licence, Frontiers must be attributed as the original publisher of the article or ebook, as applicable.

Authors have the responsibility of ensuring that any graphics or other materials which are the property of others may be included in the CC-BY licence, but this should be checked before relying on the CC-BY licence to reproduce those materials. Any copyright notices relating to those materials must be complied with.

Copyright and source acknowledgement notices may not be removed and must be displayed in any copy, derivative work or partial copy which includes the elements in question.

All copyright, and all rights therein, are protected by national and international copyright laws. The above represents a summary only. For further information please read Frontiers' Conditions for Website Use and Copyright Statement, and the applicable CC-BY licence.

ISSN 1664-8714
ISBN 978-2-83252-084-0
DOI 10.3389/978-2-83252-084-0

About Frontiers

Frontiers is more than just an open access publisher of scholarly articles: it is a pioneering approach to the world of academia, radically improving the way scholarly research is managed. The grand vision of Frontiers is a world where all people have an equal opportunity to seek, share and generate knowledge. Frontiers provides immediate and permanent online open access to all its publications, but this alone is not enough to realize our grand goals.

Frontiers journal series

The Frontiers journal series is a multi-tier and interdisciplinary set of open-access, online journals, promising a paradigm shift from the current review, selection and dissemination processes in academic publishing. All Frontiers journals are driven by researchers for researchers; therefore, they constitute a service to the scholarly community. At the same time, the *Frontiers journal series* operates on a revolutionary invention, the tiered publishing system, initially addressing specific communities of scholars, and gradually climbing up to broader public understanding, thus serving the interests of the lay society, too.

Dedication to quality

Each Frontiers article is a landmark of the highest quality, thanks to genuinely collaborative interactions between authors and review editors, who include some of the world's best academicians. Research must be certified by peers before entering a stream of knowledge that may eventually reach the public - and shape society; therefore, Frontiers only applies the most rigorous and unbiased reviews. Frontiers revolutionizes research publishing by freely delivering the most outstanding research, evaluated with no bias from both the academic and social point of view. By applying the most advanced information technologies, Frontiers is catapulting scholarly publishing into a new generation.

What are Frontiers Research Topics?

Frontiers Research Topics are very popular trademarks of the *Frontiers journals series*: they are collections of at least ten articles, all centered on a particular subject. With their unique mix of varied contributions from Original Research to Review Articles, Frontiers Research Topics unify the most influential researchers, the latest key findings and historical advances in a hot research area.

Find out more on how to host your own Frontiers Research Topic or contribute to one as an author by contacting the Frontiers editorial office: frontiersin.org/about/contact

Genomic and epigenomic applications in animal and veterinary sciences

Topic editors

Nélida Rodríguez-Osorio — Universidad de la República, Uruguay

Abdul Rasheed Baloch — University of Karachi, Pakistan

Jean Feugang — Mississippi State University, United States

Citation

Rodríguez-Osorio, N., Baloch, A. R., Feugang, J., eds. (2023). *Genomic and epigenomic applications in animal and veterinary sciences*.

Lausanne: Frontiers Media SA. doi: 10.3389/978-2-83252-084-0

Table of contents

frontiers | Frontiers in Veterinary Science

TYPE Editorial
PUBLISHED 20 March 2023
DOI 10.3389/fvets.2023.1167079

Check for updates

OPEN ACCESS

EDITED AND REVIEWED BY
Martino Cassandro,
University of Padua, Italy

*CORRESPONDENCE
Nélida Rodríguez-Osorio
✉ nelida.rodriguez@unorte.edu.uy

SPECIALTY SECTION
This article was submitted to Livestock Genomics, a section of the journal Frontiers in Veterinary Science

RECEIVED 15 February 2023
ACCEPTED 01 March 2023
PUBLISHED 20 March 2023

CITATION
Baloch AR, Feugang JM and Rodríguez-Osorio N (2023) Editorial: Genomic and epigenomic applications in animal and veterinary sciences. *Front. Vet. Sci.* 10:1167079. doi: 10.3389/fvets.2023.1167079

COPYRIGHT
© 2023 Baloch, Feugang and Rodríguez-Osorio. This is an open-access article distributed under the terms of the Creative Commons Attribution License (CC BY). The use, distribution or reproduction in other forums is permitted, provided the original author(s) and the copyright owner(s) are credited and that the original publication in this journal is cited, in accordance with accepted academic practice. No use, distribution or reproduction is permitted which does not comply with these terms.

Editorial: Genomic and epigenomic applications in animal and veterinary sciences

Abdul Rasheed Baloch[1], Jean Magloire Feugang[2] and Nélida Rodríguez-Osorio[3]*

[1]Panjwani Center for Molecular Medicine and Drug Research, International Center for Chemical and Biological Sciences, University of Karachi, Karachi, Pakistan, [2]Department of Animal and Dairy Sciences, Mississippi State University, Starkville, MS, United States, [3]Unidad de Genómica y Bioinformática, Departamento de Ciencias Biológicas, Universidad de la República, Salto, Uruguay

KEYWORDS

animal genomics, animal epigenomics, domestic animals and wildlife, veterinary research, animal sciences

Editorial on the Research Topic
Genomic and epigenomic applications in animal and veterinary sciences

In the last two decades, all biological and health disciplines, from virology to ecology, have been revolutionized by genomics with the advances in sequencing technologies and bioinformatics software development. Animal and veterinary sciences have not been an exception; the impact of genomics, transcriptomics, proteomics, and other "omic" branches on animal selection, breeding, nutrition, and health is evident.

Among the plethora of genomic and epigenomic papers published each year, the proportion of publications involving non-model, domestic, or wild animals is still low. However, the availability of annotated genomes for most domestic and economically relevant species (Table 1 collects genome assembly information for some domestic animals) has made it possible for animal science and veterinary researchers to turn to cutting-edge genomic strategies to better identify genetic markers associated with productive traits, characterize pathologic agents, associate transcriptomic information with physiological responses, and evaluate the effect of epigenetic modifications on gene expression. Even multi-omic data integration approaches are being applied to animal research (11).

This Research Topic, on the application of genomic and epigenomic tools in animal and veterinary sciences, aimed at showcasing research that included genomic and epigenomic tools to solve questions relating to animal and veterinary science. The result is a set of nine original research papers and two review articles that explore a diverse array of applications of genomics to animal health, reproduction, production, and response to stress and pathogens in cattle, yak, Chinese forest musk deer, pig, rat, chicken, and carp.

Two papers focused on measuring microRNA expression in domestic animals: Wang H. et al. evaluated the role of miR-22 in Suhuai pig skeletal muscle and identified a SNP upstream of the miR-22 precursor sequence that correlates with pork color. The target of this microRNA is ELOVL6, an elongase that catalyzes *de novo* synthesis of fatty acids, previously linked with the regulation of muscle fiber type conversion, and that appears to be over-expressed in white muscle. Their findings provide a basis for future research on the molecular markers of pork color. The paper by Veshkini et al. studied circulating miRNAs in dairy cows to assess their roles in the metabolic adaptations the cow goes through before and after

TABLE 1 Assembly information for important domestic species genomes, organized chronologically according to the first assembly release.

Species	First assembly		Current reference assembly		
	Year	Submitter	Identifier	Accession	Last update
Dog, *Canis lupus familiaris*	2003	Kirkness et al. (1)	Dog10K_Boxer_Tasha	GCA_000002285.4	2020
Chicken, *Gallus gallus*	2004	International Chicken Genome Sequencing Consortium (2)	GRCg6a	GCA_000002315.5	2018
Cat, *Felis catus*	2007	Pontius et al. (3)	F.catus_Fca126_mat1.0	GCA_018350175.1	2021
Horse, *Equus caballus*	2007	Wade et al. (4)	EquCab3.0	GCA_002863925.1	2018
Cattle, *Bos taurus*	2009	Bovine Genome Sequencing and Analysis Consortium (5)	ARS-UCD1.3	GCA_002263795.3	2018
Rabbit, *Oryctolagus cuniculus*	2009	Unpublished	UM_NZW_1.0	GCA_009806435.2	2021
Pig, *Sus scrofa*	2009	Archibald et al. (6)	Sscrofa11.1	GCA_000003025.6	2017
Sheep, *Ovis aries*	2010	Archibald et al. (7)	ARS-UI_Ramb_v2.0	GCA_016772045.1	2021
Turkey, *Meleagris gallopavo*	2010	Dalloul et al. (8)	Turkey_5.1	GCA_000146605.4	2019
Tilapia, *Oreochromis niloticus*	2012	Brawand et al. (9)	O_niloticus_UMD_NMBU	GCA_001858045.3	2018
Buffalo, *Bubalus bubalis*	2013	Unpublished	NDDB_SH_1	GCA_019923935.1	2021
Goat, *Capra hircus*	2013	Bickhart et al., Unpublished	ARS1.2	GCA_001704415.2	2016
Duck, *Anas platyrhynchos*	2013	Huang et al. (10)	ZJU1.0	GCA_015476345.1	2020

calving. According to their results, calving significantly affects miRNA expression, disturbing signaling pathways related to energy, metabolism, and immunity.

Three additional papers used genomic tools for association and gene expression studies. Khan et al. genotyped *TRAPPC9* and *CD4* polymorphisms in Chinese Holstein cows and studied their association with milk production and mastitis resistance. They associated the identified SNPs with milk production, protein content, somatic cell count, somatic cell score, and the expression of interleukin 6 (IL-6) and interferon-gamma (IFN-γ), suggesting that polymorphisms in these genes could be useful markers for milk production and mastitis resistance in dairy cattle. The pioneering work by Chen et al. employed Nanopore long-read RNA-Seq to evaluate the genome-wide allelic differential expression in the lung and liver of domesticated cattle-yak hybrids (known as "yattle"). The authors found that genes related to hypoxia adaptation and immune response were predominantly expressed from the yak alleles. In contrast, lipid metabolism and endocrine secretion genes were expressed from the cattle alleles. This analysis of the differential contribution of parental alleles in hybrid animals could enhance our understanding of the genetic basis of hybrid vigor during crossbreeding. Thirdly, a weighted gene co-expression network analysis (WGCNA) was applied by Wang X. et al. to identify key genes involved in the regulation of subcutaneous adipose tissue. They identified 15 gene co-expression modules and selected 3, according to the correlation between modules and phenotype, from which eight hub lipid metabolism genes were identified. Their expression levels were measured in the heart, liver, spleen, lung, kidney, muscle, and adipose tissue. The results provide a theoretical basis for studying beef quality by identifying hub genes that regulate lipid metabolism.

A couple of papers in this Research Topic studied gene expression in brain tissue. Baker et al. explore the pattern of DNA methylation and gene expression in amygdala tissue from Brahman cows exposed to prenatal stress. Although they only found differential methylation in a few individual CpG sites and differentially expressed in two genes, this is one of the first studies on the impact of prenatal stress on cattle brain DNA methylation and transcriptomic profiles. The second paper by Gao et al. measured the protective effects of taurine in rats against the negative effect of formaldehyde, benzene, toluene, and xylene, which are common indoor volatile organic compounds (VOC) and associated them with intellectual and cognitive impairment in children. Taurine protected rats against VOC-induced cognitive-behavioral damage and restored their learning and memory. Therefore, suggesting that it could be a potential treatment for a cognitive behavioral disorder.

Given the association between bacterial infection and pneumonia and the threat, it poses to the endangered Chinese forest musk deer (*Moschus berezovskii*), Tang et al. relied on ITRAQ-based quantitative proteomics to understand pneumonia pathogenesis in this species. Since the forest musk deer genome is poorly annotated, the researchers used the bovine genome to identify the proteins and found a clear dysregulation of proteins involved in bacterial infection and immunity, in deer suffering from pneumonia. These results shed light on the molecular mechanisms, and pathways underlying pneumonia pathogenesis.

The paper by Xie et al. is one of the first attempts at optimizing common carp (*Cyprinus carpio*) germ cell culture, which could open new opportunities for the application of surrogate production, a biotechnological strategy that could be valuable in common carp breeding, the restoration and development of lines, and the conservation of genetic resources.

Finally, this Research Topic included two review papers: first, Gul et al. reviewed the recent genetic basis of poultry resistance against microbial pathogens and genomic modifications that increase resistance against pathogens in chickens. Understanding disease resistance genetics would enable the identification of resistance markers and the development of disease resistance breeds, which could reduce the dependency on vaccination and prophylactic antibiotics in the poultry industry. The last paper by Guo et al.'s team reviews the methods and advances in cell immortalization in livestock and poultry. Immortalized cell lines provide a reliable tool for biological research and stable infinite cell lines should guarantee proliferation, while maintaining normal cell function.

Author contributions

NR-O initiated the Research Topic and drafted the manuscript. AB, JF, and NR-O co-edited the Research Topic and participated in the editorial process. All authors revised and approved the manuscript.

Funding

JF acknowledges the support of USDA-ARS Biophotonics (grant # 6066-31000-015-00D).

Conflict of interest

The authors declare that the research was conducted in the absence of any commercial or financial relationships that could be construed as a potential conflict of interest.

Publisher's note

All claims expressed in this article are solely those of the authors and do not necessarily represent those of their affiliated organizations, or those of the publisher, the editors and the reviewers. Any product that may be evaluated in this article, or claim that may be made by its manufacturer, is not guaranteed or endorsed by the publisher.

References

1. Kirkness EF, Bafna V, Halpern AL, Levy S, Remington K, Rusch DB, et al. The dog genome: Survey sequencing and comparative analysis. *Science.* (2003) 301:1898–903. doi: 10.1126/science.1086432

2. International Chicken Genome Sequencing Consortium. Sequence and comparative analysis of the chicken genome provide unique perspectives on vertebrate evolution. *Nature.* (2004) 432:695–716. doi: 10.1038/nature 03154

3. Pontius JU, Mullikin JC, Smith DR, Team AS, Lindblad-Toh K, Gnerre S, et al. Initial sequence and comparative analysis of the cat genome. *Genome Res.* (2007) 17:1675–89. doi: 10.1101/gr.6380007

4. Wade CM, Giulotto E, Sigurdsson S, Zoli M, Gnerre S, Imsland F, et al. Genome sequence, comparative analysis, and population genetics of the domestic horse. *Science.* (2009) 326:865–7. doi: 10.1126/science.117 8158

5. Bovine Genome Sequencing and Analysis Consortium, Elsik CG, Tellam RL, Worley KC, Gibbs RA, Muzny DM, Weinstock GM, et al. The genome sequence of taurine cattle: A window to ruminant biology and evolution. *Science.* (2009) 324:522–8. doi: 10.1126/science.1169588

6. Archibald AL, Bolund L, Churcher C, Fredholm M, Groenen MA, Harlizius B, et al. Pig genome sequence—Analysis and publication strategy. *BMC Genomics.* (2010) 11:438. doi: 10.1186/1471-2164-11-438

7. Consortium ISG, Archibald AL, Cockett NE, Dalrymple BP, Faraut T, Kijas JW, et al. The sheep genome reference sequence: A work in progress. *Anim Genet.* (2010) 41:449–53. doi: 10.1111/j.1365-2052.2010.02100.x

8. Dalloul RA, Long JA, Zimin AV, Aslam L, Beal K, Blomber LA, et al. Multi-platform next-generation sequencing of the domestic turkey (*Meleagris gallopavo*): Genome assembly and analysis. *PLoS Biol.* (2010) 8:e1000475. doi: 10.1371/journal.pbio.1000475

9. Brawand D, Wagner CE, Li YI, Malinsky M, Keller I, Fan S, et al. The genomic substrate for adaptive radiation in African cichlid fish. *Nature.* (2014) 513:375–81. doi: 10.1038/nature13726

10. Huang Y, Li Y, Burt DW, Chen H, Zhang Y, Qian W, et al. The duck genome and transcriptome provide insight into an avian influenza virus reservoir species. *Nat Genet.* (2013) 45:776–83. doi: 10.1038/ng.2657

11. Kim DY, Kim JM. Multi-omics integration strategies for animal epigenetic studies—A review. *Anim Biosci.* (2021) 34:1271–82. doi: 10.5713/ab.21.0042

frontiers | Frontiers in Veterinary Science

ORIGINAL RESEARCH
published: 30 June 2022
doi: 10.3389/fvets.2022.892663

Favoring Expression of Yak Alleles in Interspecies F1 Hybrids of Cattle and Yak Under High-Altitude Environments

Shi-Yi Chen[1]*, *Cao Li*[1], *Zhihao Luo*[1,2], *Xiaowei Li*[2], *Xianbo Jia*[1] and *Song-Jia Lai*[1]

[1] *Farm Animal Genetic Resources Exploration and Innovation Key Laboratory of Sichuan Province, Sichuan Agricultural University, Chengdu, China,* [2] *Longri Breeding Farm of Sichuan Province, Hongyuan, China*

Both *cis*- and *trans*-regulation could cause differential expression between the parental alleles in diploid species that might have broad biological implications. Due to the relatively distant genetic divergence between cattle and yak, as well as their differential adaptation to high-altitude environments, we investigated genome-wide allelic differential expression (ADE) in their F1 hybrids using Nanopore long-read RNA-seq technology. From adult F1 hybrids raised in high-altitude, ten lung and liver tissues were individually sequenced for producing 31.6 M full-length transcript sequences. Mapping against autosomal homologous regions between cattle and yak, we detected 17,744 and 14,542 protein-encoding genes expressed in lung and liver tissues, respectively. According to the parental assignments of transcript sequences, a total of 3,381 genes were detected to show ADE in at least one sample. There were 186 genes showing ubiquitous ADE in all the studied animals, and among them 135 and 37 genes had consistent higher expression of yak and cattle alleles, respectively. Functional analyses revealed that the genes with favoring expression of yak alleles have been involved in the biological progresses related with hypoxia adaptation and immune response. In contrast, the genes with favoring expression of cattle alleles have been enriched into different biological progresses, such as secretion of endocrine hormones and lipid metabolism. Our results would support unequal contribution of parental genes to environmental adaptation in the F1 hybrids of cattle and yak.

Keywords: allele expression, Nanopore long-read RNA-seq, transcriptome, cattle, yak

OPEN ACCESS

Edited by:
Jean Feugang,
Mississippi State University,
United States

Reviewed by:
Xiaoyun Wu,
Lanzhou Institute of Husbandry and Pharmaceutical Sciences (CAAS), China
Xianrong Xiong,
Southwest Minzu University, China

***Correspondence:**
Shi-Yi Chen
sychensau@gmail.com

Specialty section:
This article was submitted to Livestock Genomics, a section of the journal Frontiers in Veterinary Science

Received: *09 March 2022*
Accepted: *01 June 2022*
Published: *30 June 2022*

Citation:
Chen S-Y, Li C, Luo Z, Li X, Jia X and Lai S-J (2022) Favoring Expression of Yak Alleles in Interspecies F1 Hybrids of Cattle and Yak Under High-Altitude Environments. Front. Vet. Sci. 9:892663. doi: 10.3389/fvets.2022.892663

INTRODUCTION

Within the *Bos* genus, the two species of cattle (*Bos taurus*) and yak (*B. grunniens*) evolutionally diverged ∼4.9 million years ago (1). However, there is no reproductive barrier to hybridization between cattle and yak regarding both reciprocal crosses, although the male F1 hybrids are sterile that may be possibly resulting from spermatogenesis failure (2). Most modern cattle breeds have evolved into high production performance in terms of economically important traits, whereas yak is well adapted to high-altitude environments due to long-term adaptive evolution (3). Meanwhile, both physiological fitness and production performance of cattle will considerably decrease when residing above 2,500 m altitude (4). In phenotype, therefore, the interspecies F1 hybrids of cattle and

yak have the significantly improved milk yield and growth, as well as great physiological adaptation to high-altitude environment. Yet, the underlying genomic basis remains poorly characterized.

For autosomal non-imprinted genes in diploid species, the two allelic copies that are inherited from parents could be differentially expressed, which is termed allelic differential expression (ADE) and has broad biological implications as an important regulatory variation (5, 6). Obviously, the most extreme case of ADE is monoallelic expression that was observed to be widespread (7, 8). The genome-wide landscape of ADE in humans and diverse species (such as cattle, chicken, and rice) have been investigated comprehensively using the large numbers of single nucleotide polymorphisms (SNPs) obtained by oligonucleotide array and high-throughput sequencing technologies (8–12). The degree of genetic differentiation between two parents would influence detection ability of allelic expression levels in offspring. The genomic heterozygosity of F1 hybrids of cattle and yak was recently estimated to be ∼1.2%, which is higher than cross-breed hybrids of taurine and indicine cattle (13). Therefore, the highly heterogeneous diploid genome of F1 hybrids of cattle and yak provides us a great opportunity to investigate ADE, especially in such case that two parents have differential production performance and adaptation to the local environments. Using the short reads of transcriptome sequencing, Wang et al. (14) first reported hundreds of genes (∼5% of all analyzed genes) showing ADE in the liver and ear tissues of F1 hybrids of cattle and yak.

Second-generation RNA sequencing technologies (i.e., short-read RNA-seq) have been becoming the most widely used approach for studying gene expression (15). However, two analytical methodological issues should be taken into consideration when studying ADE based on short sequencing reads. The first issue is mapping bias of short reads against reference genome, which would lead to an over-estimation of reference allele in relative to alternate allele (16, 17). Second, allelic expression is indirectly quantified by counting the distinguishable short reads instead of full transcript sequences, mainly as it is difficult to accurately assemble allele-specific transcripts (18). Recently, the long-read RNA sequencing technologies (i.e., long-read RNA-seq) have been increasingly used for quantifying allelic expression (19, 20). In this study, we employed single-molecule long-read sequencing technology from Oxford Nanopore Technologies (ONT) to investigate global gene expression in F1 hybrids of cattle and yak. After quantifying allelic expression based on the full transcript sequences, the genes with ADE and the possibly involved biological implications were analyzed. These results are expected to improve our understanding of parental contribution to F1 hybrids of cattle and yak regarding the environmental adaptation and production performance.

MATERIALS AND METHODS

Animals and Sample Preparation

Five adult (∼5 years of age, two males and three females) and healthy F1 hybrids of cattle and yak were randomly included in this study (**Figure 1A**), which had been raised in the Longri Breeding Farm of Sichuan Province at an altitude of ∼3,000 m. The five animals were individually sequenced as biological replicates. After being slaughtered with head-only electrical stunning, the tissue samples of lung and liver were immediately collected and frozen in liquid nitrogen. In parallel, the peripheral blood was collected and used for genome sequencing. Total RNA was extracted using RNASimple Total RNA Kit (Tiangen Biotech, Beijing, China) following manufacturer's instructions. RNA concentration and RNA integrity number (RIN) were analyzed using Nanodrop 2000C (Thermo Fisher Scientific, Waltham, USA) and Agilent 2100 Bioanalyzer (Agilent Technologies, Santa Clara, USA), respectively (**Supplementary Table S1**). Genomic DNA was isolated using TIANamp Genomic DNA Kit (Tiangen Biotech, Beijing, China) according to manufacturer's instructions.

RNA and DNA Sequencing

For transcriptome sequencing, 1 μg of total RNA was used for preparing libraries with cDNA-PCR Sequencing Kit (SQK-PCS109, Oxford Nanopore Technologies). In brief, the full-length cDNAs were enriched using template switching activity of reverse transcriptase. The PCR adapters were directly added to both ends of the first-strand cDNAs. PCR amplification was performed with 14 circles using LongAmp Tag (NEB), and then PCR products were subjected to ONT adaptor ligation using T4 DNA ligase (NEB). The Agencourt XP beads was used for DNA purification according to official protocol. The final cDNA libraries were added to FLO-MIN109 flowcells and run on PromethION platform at Biomarker Technology Company (Beijing, China).

For genome sequencing, the paired-end libraries with 350 bp of insert sizes were constructed according to Illumina's protocol (Illumina, San Diego, CA, USA). In brief, 0.5 μg of genomic DNA was fragmented, end-paired and ligated to adaptors, respectively. After the P2 adapter was added, DNA fragments were fractionated and purified by PCR amplification. Finally, the sequencing libraries were sequenced using Illumina HiSeq2000 at Biomarker Technology Company (Beijing, China).

Quality Controls of Sequencing Reads

Among raw long reads of transcriptome sequencing, full-length and non-chimeric (FLNC) transcript sequences were determined and extracted using Pychopper software with default parameters (https://github.com/nanoporetech/pychopper). The raw short reads of genome sequencing were subjected to quality filtering using fastp software (21); and low-quality reads were removed according to the three criteria: (i) containing adaptor sequences, (ii) more than five N base, or (iii) unqualified bases (Q-value <15) higher than 40% of total read length. After these quality controls, the clean reads were generated.

Construction of Transcriptome

To avoid potential mapping bias when using either cattle or yak genome sequence as reference, one pseudo genome sequence was constructed for mapping the FLNC transcript sequences (**Figures 1B,C**). First, interspecies autosomal homologous regions were detected according to pairwise alignment of

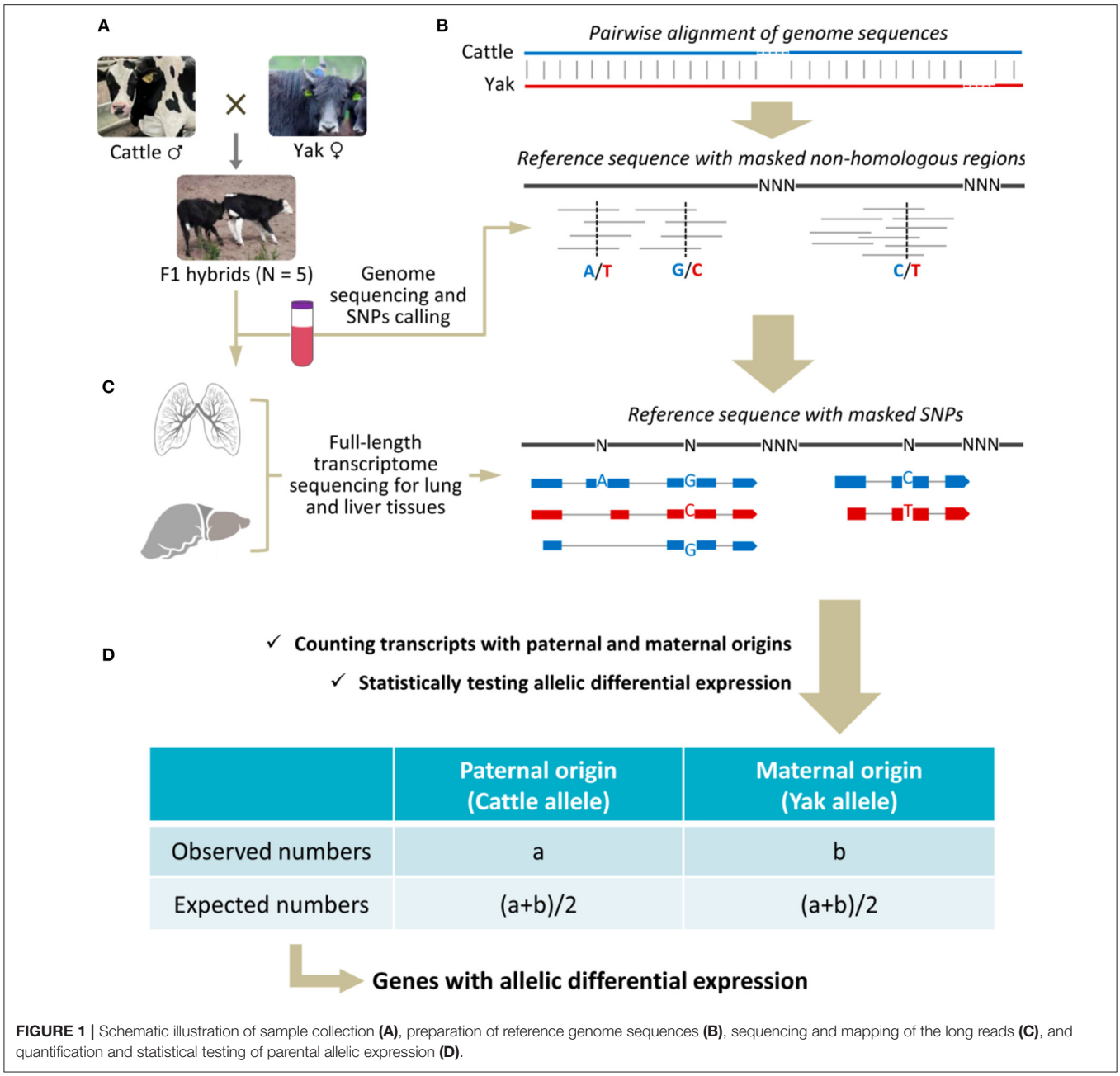

FIGURE 1 | Schematic illustration of sample collection **(A)**, preparation of reference genome sequences **(B)**, sequencing and mapping of the long reads **(C)**, and quantification and statistical testing of parental allelic expression **(D)**.

reference genome sequences between cattle (ARS-UCD1.2) and yak (BosGru3.0), which was performed using -asm5 module in minimap2 software (22). Herein, non-homologous genomic regions (i.e., species-specific sequences) were excluded from reference sequence to avoid falsely positive findings of ADE. Second, short sequencing reads of genome were aligned to reference sequence using BWA-MEM algorithm and default parameters in BWA software (23). The interspecies SNPs were called using bcftools (24) and masked to alleviate potential mapping bias of long reads. Third, FLNC transcript sequences were aligned to this custom reference genome sequence using minimap2 software with parameters of "-ax splice -p 0.9 -N 1" (22). To detect novel genes, the obtained mapping results of FLNC transcript sequences were compared with the known annotation information of cattle genome.

Quantification and Allelic Differential Expression

The expression levels of paternal and maternal alleles were quantified on each genic locus and statistically tested regarding their differential expressions (**Figure 1D**). First, the transcript

sequence was assigned to paternal or maternal origins according to distinguishable interspecies SNPs determined in previous steps. When multiple SNPs with inconsistent assignments were found in one transcript sequence, the mode rule was applied. Furthermore, the indistinguishable transcript sequences that did not contain any interspecies SNP were proportionally assigned according to other known assignments. Second, the expression levels of paternal and maternal alleles were quantified by directly counting their respective transcript sequences, and expression level was expressed as counts per million mapped reads (CPM). Finally, the differential expressions of alleles were statistically deduced using Fisher's exact test implemented in R software (25), and the directions of favoring expression were determined regarding paternal and maternal origins. Here, a gene with ADE was statistically determined as both the fold change > 2 and $P < 0.05$.

Functional Analyses of Candidate Genes

For candidate genes of interest, functional enrichment analyses were conducted using the g:GOSt function on g:Profiler web server (26), including the target cattle datasets of Gene Ontology (GO) terms (27) and Kyoto Encyclopedia of Genes and Genomes (KEGG) pathway (28). The default parameters and methods for adjusting for multiple hypotheses testing were used with an adjusted 5% level of significance.

RESULTS

Reference Genome Sequence and Interspecies SNPs

Genomic comparisons revealed that 93.92% of the autosomal region of cattle had homologous genomic sequences in yak (**Supplementary Figure S1**). According to the annotation information of reference genomes, there were 19,163 common protein-encoding genes located within these homologous regions, whereas cattle and yak had 1,558 and 1,669 species-specific genes, respectively. Genome sequencing of the five hybrid animals generated the clean paired-end short reads with an average depth of 15-fold coverage, from which average 19,426,851 interspecies heterozygous SNPs (± 268,073 of standard deviation) were found (**Supplementary Table S2**). These SNPs were evenly distributed among the 29 autosomes (**Supplementary Figure S2**), and about 6.5% of them were located within the annotated exons.

Sequencing and Construction of Transcriptome

For the ten sequenced samples of both lung and liver tissues, a total of 36,017,234 Nanopore long reads were initially generated, ranging from 3,237,972 to 4,091,924 per sample (**Supplementary Table S3**). More than 42% of raw reads were higher than 1 Kb in length, and their average N50 length was 1,372 bp. After quality controls, average 3,157,628 FLNC transcript sequences were obtained per sample (ranging from 2,803,438 to 3,680,467). Finally, average 98% of FLNC transcript sequences were successfully aligned to our custom reference genome.

There were 17,744 and 14,542 protein-encoding genes expressed in the lung and liver tissues, respectively. The rarefaction curve analysis revealed that the sequencing depth was enough for discovering the expressed genes (including the noncoding and pseudogenes, **Figure 2A**). After discarding the lowly expressed genes (i.e., with >2 mapped transcript sequences), the numbers of genes and quantified expression levels were shown in **Supplementary Table S4**; and the overall distribution of gene expression levels were comparable among the 10 sequenced samples (**Figure 2B**). The five biological replications within each tissue were demonstrated according to the pairwise Pearson correlation coefficients (**Figure 2C**).

Allelic Differential Expression and Functional Analyses

After quantifying the allelic expression levels, ADE were statistically tested for all the expressed genes in different tissues of each animal. A total of 3,381 genes were found to show ADE in at least one tissue of one animal (**Figure 3**). Furthermore, 186 genes showed ubiquitous ADE in lung and/or liver tissues among the five biological replications (**Figure 4A** and **Supplementary Table S5**). Among them, 135 and 37 genes had the consistent favoring expression of yak alleles and cattle alleles, respectively; whereas 14 genes showed variable direction of favoring expression between parental alleles. Meanwhile, 81 and 57 genes with ADE were specifically found in the lung and liver tissues, respectively; and 48 genes with ADE simultaneously observed in the two tissues.

The 135 genes that show consistent favoring expression of yak allele among all studied animals were significantly enriched into 28 GO terms and five KEGG pathways (**Figure 4B**). Among them, ten and nine genes were involved in the GO terms of "Oxidation-reduction process" and "Mitochondrion organization," respectively. Other biologically important functions included the immune responses, change in state or activity of a cell as a result of an oxygen-containing compound stimulus, structural constituent of ribosome, and carbon metabolism. By contrast, the 37 genes showing consistent favoring expression levels of cattle allele were significantly enriched onto 18 GO terms and one KEGG pathway (**Figure 4C**). Nine and seven genes were involved in the GO terms of "Cell surface receptor signaling pathway" and "Lipid metabolic process," respectively. Also, the GO terms of "Endocrine process," "Regulation of blood pressure" and "Blood circulation" were suggested.

DISCUSSION

Despite the widely acknowledged contribution of gene expression regulation to phenotypic variation, it remains difficult to quantify allelic expression levels mainly because of analytical methodological limitations. However, it is well-known in humans that both *cis*- and *trans*-regulation would differentially affect the two parental alleles and might have significant implications in

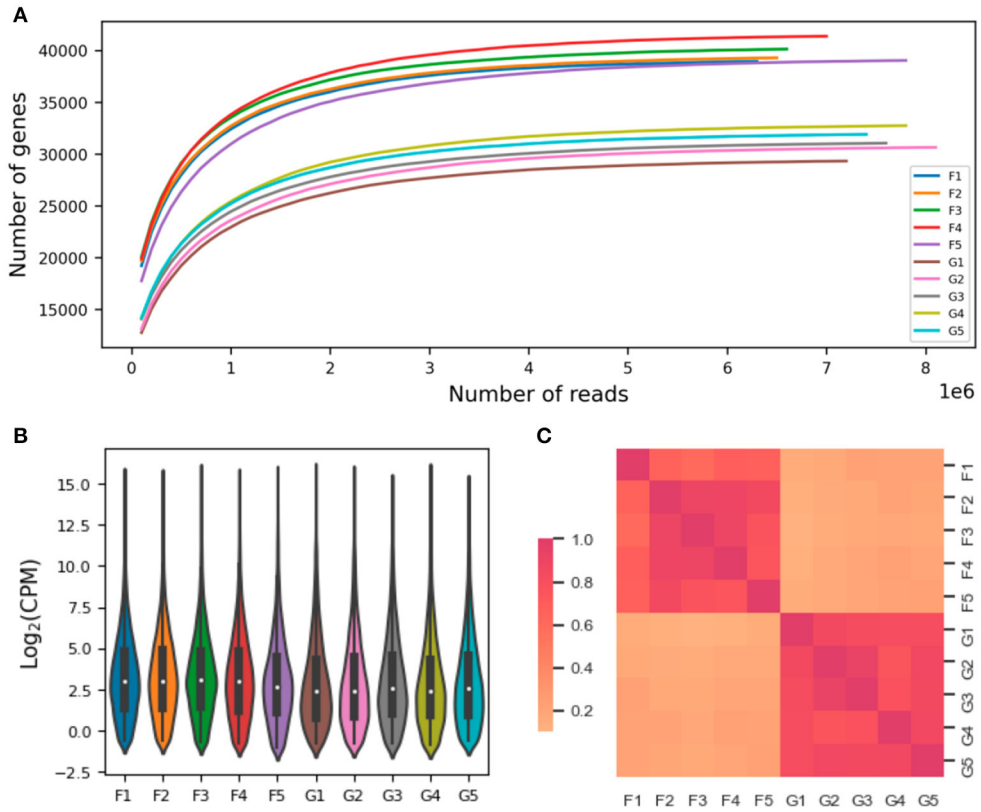

FIGURE 2 | Quantification of gene expression. The individual rarefaction curves indicate relationship between the sequencing depth and number of genes observed **(A)**. The overall distribution of gene expression levels and pairwise Pearson correlations of sequenced samples are shown in **(B, C)**, respectively. The sample names were denoted by prefix of "F" and "G" for lung and liver issues, respectively; such as, the "F1" denotes the sequenced lung issue for the first animal. CPM, counts per million mapped reads.

diverse biological functions (29). Recently, the widespread and dynamic allele-specific expression of immune-related genes were observed among different physiological states of human T cells (30). In farm species, the differential expression of parental alleles have been explored for discovering genetic basis of economically important traits, such as meat quality in cattle (31), disease susceptibility in pigs (32), and heterosis in rice (11). Based on the short RNA-seq reads of 18 tissues from a single cow, Chamberlain et al. (33) reported that about 90% of genes showed ADE in at least one tissue. In this study, we also revealed widespread occurrence of significantly differential expression between parental alleles in the F1 hybrids of cattle and yak.

Using the short-read RNA-seq datasets, Wang et al. (14) reported 883 genes in liver tissues and 592 genes in ear tissues showing significant differential expression between parental alleles in F1 hybrids of cattle and yak; and the long noncoding RNA, pseudo, and lowly expressed genes are more likely to show ADE. According to the direct counting of full-length transcripts from long-read RNA-seq, we found about 20% of the expressed protein-encoding genes showing ADE in at least one sequenced sample, which is higher than the former report of Wang et al. (14); however, such difference would be likely resulted from the different types of sequencing data and analysis methods. There are 186 genes found to show consistent ADE among all the studied animals, which would indicate their important biological implications in F1 hybrids of cattle and yak. As regulatory consequences, the tissue-specific occurrences of ADE have been extensively reported (10, 14, 33, 34). The similar pattern was revealed in the present study as only a small proportion of genes were observed to be simultaneous ADE in both studied tissues. Furthermore, we found that more genes showed ADE in lung tissue than that in liver tissue.

Among the 186 genes showing ubiquitous ADE in all studied animals, we found more genes consistently favoring the expression of yak allele in comparison with cattle allele ($N = 135$ vs. 37). This result is particularly interesting as it would indicate unequal contribution between parental genes to the F1 hybrids of cattle and yak; and the favoring expression of yak alleles might facilitate environmental adaptation as these animals had been raised in high-altitude environments. Our functional analyses further revealed that these genes have been significantly involved in the biological progresses, such as oxidation-reduction process and mitochondrion organization, that have been previously reported to be associated with hypoxia adaptation and immune response in high-altitude species (35, 36). Among the candidate genes found in this study, for example,

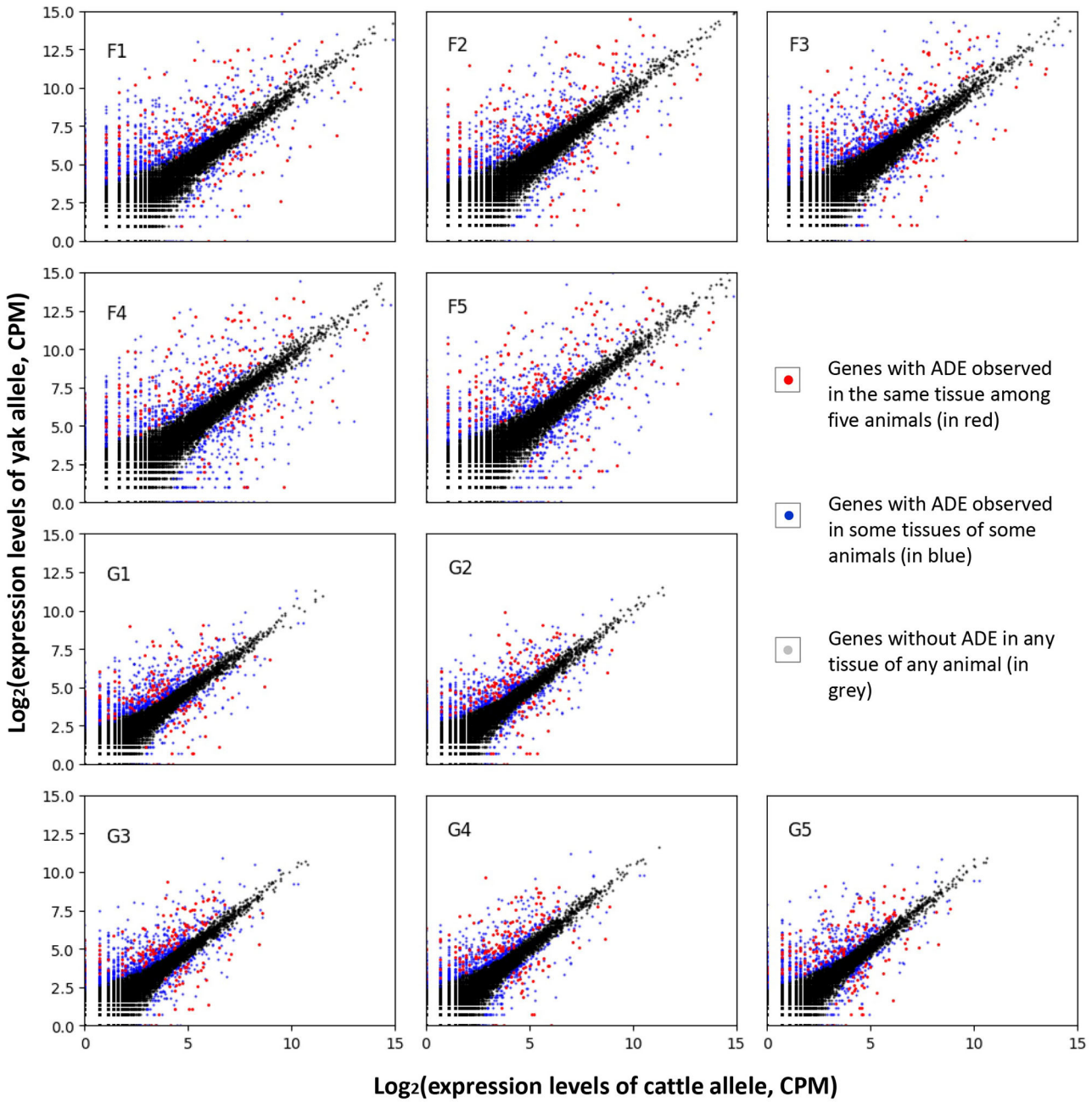

FIGURE 3 | Allelic differential expression among the sequenced samples. The sample names were denoted by prefix of "F" and "G" for lung and liver issues, respectively; such as, the "F1" denotes the sequenced lung issue for the first animal. CPM, counts per million mapped reads.

the cytochrome b5 type A (*CYB5A*) encodes membrane-bound cytochrome and was found to be one hypoxia-sensitive protein in rat erythrocytes (37); the UDP-glucose 6-dehydrogenase (*UGDH*) gene was involved in the metabolic adaptation to hypoxic stress in human glioblastoma cells (38). In contrast, the genes alternatively favoring expression of cattle alleles have been enriched into different biological progresses, such as the secretion of endocrine hormones and lipid metabolism. For instance, genetic associations with production traits have been reported for the genes of fatty acid binding protein 1 (*FABP1*), dystrophia myotonica protein kinase (*DMPK*), and proopiomelanocortin (*POMC*) in Nanyang, Hanwoo, and Nellore cattle (39–42). On the other hand, the genes with ADE, such as heat shock protein family B member 8 (*HSPB8*), transglutaminase 2 (*TGM2*), and phospholipase A2 group VII (*PLA2G7*), have been also found to play critical regulatory functions in development and

A

Number of genes with ADE consistently observed among all studied animals		Higher expressed allele			
		Yak	Cattle	Mixed	Sum
Tissues observed	Lung	56	17	8	**81**
	Liver	36	17	4	**57**
	Lung & Liver	43	3	2	**48**
	Sum	**135**	**37**	**14**	**186**

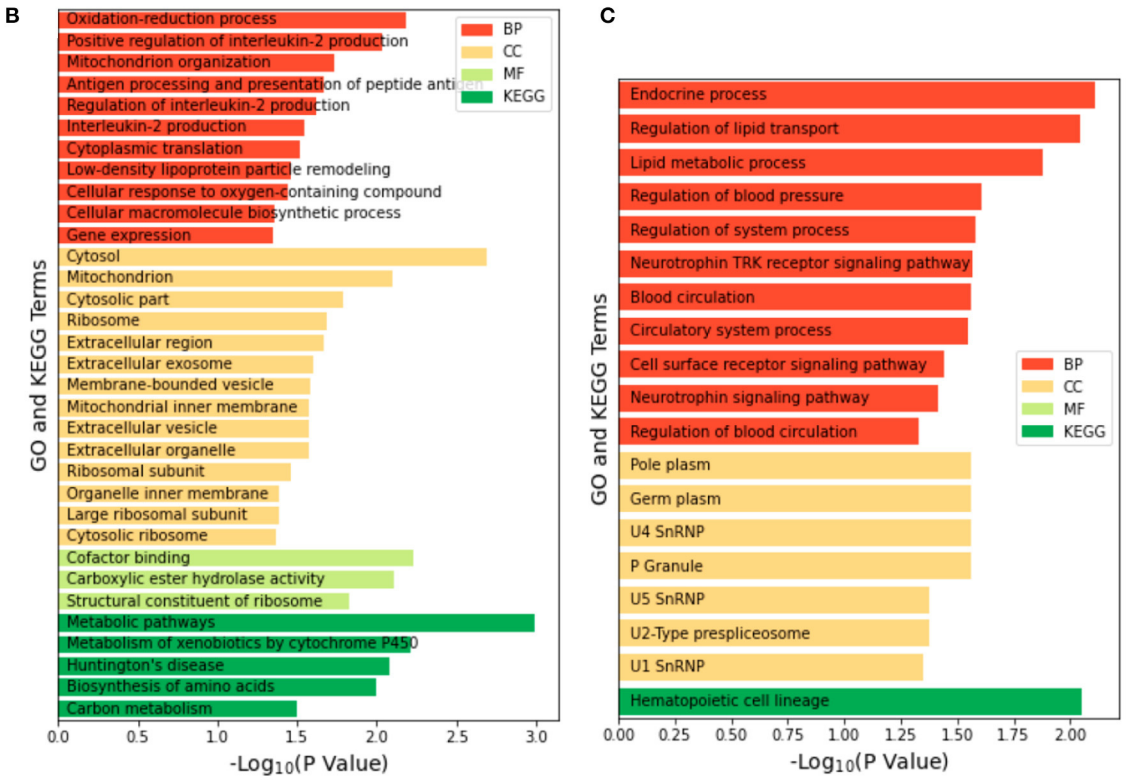

FIGURE 4 | The favoring direction and tissue distribution of allelic differential expression **(A)**. Functional analyses for 135 genes with the consistent higher expression of yak alleles **(B)** and for 35 genes with the consistent higher expression of cattle alleles **(C)**. BP, biological process; MF, molecular function; CC, cellular component; KEGG, Kyoto Encyclopedia of Genes and Genomes.

maintenance of muscle tissue in Nelore cattle (31). Therefore, we speculate that there would have the biological function-dependent selection pressures regarding the favoring direction of ADE in the F1 hybrids of cattle and yak. However, both *cis*- and *trans*-regulatory variations between parental genomes should be further investigated. Also, it is much interesting to investigate ADE pattern when F1 hybrids of cattle and yak are alternatively raised in low altitude.

To reduce mapping bias of sequencing reads in the F1 hybrids, only homologous regions between the parental genomes were used as reference sequences that account for about 94% of bovine autosome genome. Both inter- and intra-species SNPs were detected and further masked from reference sequence, which is a common strategy for studying the allelic expression (16, 36, 43). Instead of short-read RNA-seq datasets, we employed long sequencing reads in this study that have been proposed to be more robust in terms of assembly of full-length transcripts and quantification of gene expression (20, 44). In high-altitude species, lung and liver are the most important organs in maintaining respiratory and metabolism homeostasis of the entire body, which have been commonly included for studying physiological adaptation to environments

[e.g., (3, 14)]. Despite this, one of possible limitations of this study is that only two tissues were analyzed, and muscle tissue should be specifically taken into consideration in future studies (31). Regarding candidate genes found in this study, molecular biology experiments are also required to explore their biological mechanisms influencing the physiological adaptation to environments and the improved production performance for F1 hybrids of cattle and yak.

CONCLUSIONS

In this study, we employed Nanopore long-read RNA-seq technology to quantify genome-wide allelic expression in interspecies F1 hybrids of cattle and yak. Our results revealed many more genes with the favoring expression of yak allele, which would contribute to the physiological adaptation to high-altitude environments. Such unequal contribution of parental alleles will also help us understand the genetic basis of economically important traits in the hybrid animals.

DATA AVAILABILITY STATEMENT

The raw sequence data reported in this paper have been deposited in the Genome Sequence Archive of Chinese Academy of Sciences (GSA: CRA006347).

ETHICS STATEMENT

Ethical review and approval was not required for the animal study because Biological samples involved in this study were specially collected from commercial slaughterhouse in the Hongyuan County of Sichuan Province.

AUTHOR CONTRIBUTIONS

S-YC and CL: conceptualization, formal analysis, and writing—original draft preparation. ZL, XL, and XJ: resources. S-YC, XJ, and S-JL: writing—review and editing. All authors contributed to the article and approved the submitted version.

FUNDING

This work was supported by Innovative Research Team of Beef Cattle in Sichuan Province (SCCXTD-2022-13) and Science & Technology Department of Sichuan Province (2021YFYZ0007).

SUPPLEMENTARY MATERIAL

The Supplementary Material for this article can be found online at: https://www.frontiersin.org/articles/10.3389/fvets.2022.892663/full#supplementary-material

REFERENCES

1. Qiu Q, Zhang G, Ma T, Qian W, Wang J, Ye Z, et al. The yak genome and adaptation to life at high altitude. *Nat Genet.* (2012) 44:946–9. doi: 10.1038/ng.2343
2. Zhang GW, Wu Y, Luo Z, Guan J, Wang L, Luo X, et al. Comparison of Y-chromosome-linked *TSPY*, *TSPY2*, and *PRAMEY* genes in Taurus cattle, yaks, and interspecific hybrid bulls. *J Dairy Sci.* (2019) 102:6263–75. doi: 10.3168/jds.2018-15680
3. Qi X, Zhang Q, He Y, Yang L, Zhang X, Shi P, et al. The transcriptomic landscape of yaks reveals molecular pathways for high altitude adaptation. *Genome Biol Evol.* (2019) 11:72–85. doi: 10.1093/gbe/evy264
4. Newman JH, Holt TN, Cogan JD, Womack B, Phillips JA, Li C, et al. Increased prevalence of EPAS1 variant in cattle with high-altitude pulmonary hypertension. *Nat Commun.* (2015) 6:6863. doi: 10.1038/ncomms7863
5. Knight JC. Allele-specific gene expression uncovered. *Trends Genet.* (2004) 20:113–6. doi: 10.1016/j.tig.2004.01.001
6. Yan H, Zhou W. Allelic variations in gene expression. *Curr Opin Oncol.* (2004) 16:39–43. doi: 10.1097/00001622-200401000-00008
7. Chess A. Mechanisms and consequences of widespread random monoallelic expression. *Nat Rev Genet.* (2012) 13:421–842. doi: 10.1038/nrg3239
8. Guillocheau GM, El Hou A, Meersseman C, Esquerre D, Rebours E, Letaief R, et al. Survey of allele specific expression in bovine muscle. *Sci Rep.* (2019) 9:4297. doi: 10.1038/s41598-019-40781-6
9. Moyerbrailean GA, Richards AL, Kurtz D, Kalita CA, Davis GO, Harvey CT, et al. High-throughput allele-specific expression across 250 environmental conditions. *Genome Res.* (2016) 26:1627–38. doi: 10.1101/gr.209759.116
10. Zhuo Z, Lamont SJ, Abasht B. RNA-Seq analyses identify frequent allele specific expression and no evidence of genomic imprinting in specific embryonic tissues of chicken. *Sci Rep.* (2017) 7:11944. doi: 10.1038/s41598-017-12179-9
11. Shao L, Xing F, Xu C, Zhang Q, Che J, Wang X, et al. Patterns of genome-wide allele-specific expression in hybrid rice and the implications on the genetic basis of heterosis. *Proc Natl Acad Sci U S A.* (2019) 116:5653–8. doi: 10.1073/pnas.1820513116
12. Langmyhr M, Henriksen SP, Cappelletti C, Van De Berg WDJ, Pihlstrøm L, Toft M. Allele-specific expression of Parkinson's disease susceptibility genes in human brain. *Sci Rep.* (2021) 11:504. doi: 10.1038/s41598-020-79990-9
13. Rice ES, Koren S, Rhie A, Heaton MP, Kalbfleisch TS, Hardy T, et al. Continuous chromosome-scale haplotypes assembled from a single interspecies F1 hybrid of yak and cattle. *Gigascience.* (2020) 9:giaa029. doi: 10.1093/gigascience/giaa029
14. Wang Y, Gao S, Zhao Y, Chen WH, Shao JJ, Wang NN, et al. Allele-specific expression and alternative splicing in horse×donkey and cattle×yak hybrids. *Zool Res.* (2019) 40:293–304. doi: 10.24272/j.issn.2095-8137.2019.042
15. Stark R, Grzelak M, Hadfield J. RNA sequencing: the teenage years. *Nat Rev Genet.* (2019) 20:631–56. doi: 10.1038/s41576-019-0150-2
16. Degner JF, Marioni JC, Pai AA, Pickrell JK, Nkadori E, Gilad Y, et al. Effect of read-mapping biases on detecting allele-specific expression from RNA-sequencing data. *Bioinformatics.* (2009) 25:3207–12. doi: 10.1093/bioinformatics/btp579
17. Stevenson KR, Coolon JD, Wittkopp PJ. Sources of bias in measures of allele-specific expression derived from RNA-seq data aligned to a single reference genome. *BMC Genomics.* (2013) 14:536. doi: 10.1186/1471-2164-14-536
18. Dudley DM, Karl JA, Creager HM, Bohn PS, Wiseman RW, O'connor DH. Full-length novel MHC class I allele discovery by next-generation sequencing: two platforms are better than one. *Immunogenetics.* (2014) 66:15–24. doi: 10.1007/s00251-013-0744-3
19. Hughes AE, Montgomery MC, Liu C, Weimer ET. Quantification of allele-specific HLA expression with Nanopore long-read sequencing. *Blood.* (2020) 136:42–3. doi: 10.1182/blood-2020-140902
20. Hu Y, Fang L, Chen X, Zhong JF, Li M, Wang K. LIQA: long-read isoform quantification and analysis. *Genome Biol.* (2021) 22:182. doi: 10.1186/s13059-021-02399-8
21. Chen S, Zhou Y, Chen Y, Gu J. fastp: an ultra-fast all-in-one FASTQ preprocessor. *Bioinformatics.*

(2018) 34:i884–90. doi: 10.1093/bioinformatics/bty560
22. Li H. Minimap2: pairwise alignment for nucleotide sequences. *Bioinformatics.* (2018) 34:3094–100. doi: 10.1093/bioinformatics/bty191
23. Li H, Durbin R. Fast and accurate short read alignment with Burrows-Wheeler transform. *Bioinformatics.* (2009) 25:1754–60. doi: 10.1093/bioinformatics/btp324
24. Li H, Handsaker B, Wysoker A, Fennell T, Ruan J, Homer N, et al. The sequence alignment/map format and SAMtools. *Bioinformatics.* (2009) 25:2078–9. doi: 10.1093/bioinformatics/btp352
25. R Core Team. *R: A language and Environment for Statistical Computing*. R Foundation for Statistical Computing, Vienna, Austria (2019). Available online at: http://www.R-project.org/
26. Raudvere U, Kolberg L, Kuzmin I, Arak T, Adler P, Peterson H, et al. g:Profiler: a web server for functional enrichment analysis and conversions of gene lists (2019 update). *Nucl Acids Res.* (2019) 47:W191–8. doi: 10.1093/nar/gkz369
27. The Gene Ontology Consortium. The gene ontology resource: 20 years and still GOing strong. *Nucl Acids Res.* (2019) 47:D330–D338. doi: 10.1093/nar/gky1055
28. Kanehisa M, Sato Y, Furumichi M, Morishima K, Tanabe M. New approach for understanding genome variations in KEGG. *Nucl Acids Res.* (2019) 47:D590–5. doi: 10.1093/nar/gky962
29. Pastinen T. Genome-wide allele-specific analysis: insights into regulatory variation. *Nat Rev Genet.* (2010) 11:533–8. doi: 10.1038/nrg2815
30. Gutierrez-Arcelus M, Baglaenko Y, Arora J, Hannes S, Luo Y, Amariuta T, et al. Allele-specific expression changes dynamically during T cell activation in HLA and other autoimmune loci. *Nat Genet.* (2020) 52:247–53. doi: 10.1038/s41588-020-0579-4
31. De Souza MM, Zerlotini A, Rocha MIP, Bruscadin JJ, Diniz WJDS, Cardoso TF, et al. Allele-specific expression is widespread in *Bos indicus* muscle and affects meat quality candidate genes. *Sci Rep.* (2020) 10:10204. doi: 10.1038/s41598-020-67089-0
32. Wu H, Gaur U, Mekchay S, Peng X, Li L, Sun H, et al. Genome-wide identification of allele-specific expression in response to Streptococcus suis 2 infection in two differentially susceptible pig breeds. *J Appl Genet.* (2015) 56:481–91. doi: 10.1007/s13353-015-0275-8
33. Chamberlain AJ, Vander Jagt CJ, Hayes BJ, Khansefid M, Marett LC, Millen CA, et al. Extensive variation between tissues in allele specific expression in an outbred mammal. *BMC Genomics.* (2015) 16:993. doi: 10.1186/s12864-015-2174-0
34. Crowley JJ, Zhabotynsky V, Sun W, Huang S, Pakatci IK, Kim Y, et al. Analyses of allele-specific gene expression in highly divergent mouse crosses identifies pervasive allelic imbalance. *Nat Genet.* (2015) 47:353–60. doi: 10.1038/ng.3222
35. Zhang QL, Zhang L, Yang XZ, Wang XT, Li XP, Wang J, et al. Comparative transcriptomic analysis of Tibetan Gynaephora to explore the genetic basis of insect adaptation to divergent altitude environments. *Sci Rep.* (2017) 7:16972. doi: 10.1038/s41598-017-17051-4
36. Zhang QL, Li HW, Dong ZX, Yang XJ, Lin LB, Chen JY, et al. Comparative transcriptomic analysis of fireflies (Coleoptera: Lampyridae) to explore the molecular adaptations to fresh water. *Mol Ecol.* (2020) 29:2676–91. doi: 10.1111/mec.15504
37. Sidorenko SV, Ziganshin RH, Luneva OG, Deev LI, Alekseeva NV, Maksimov GV, et al. Proteomics-based identification of hypoxia-sensitive membrane-bound proteins in rat erythrocytes. *J Proteomics.* (2018) 184:25–33. doi: 10.1016/j.jprot.2018.06.008
38. Kucharzewska P, Christianson HC, Belting M. Global profiling of metabolic adaptation to hypoxic stress in human glioblastoma cells. *PLoS ONE.* (2015) 10:e0116740. doi: 10.1371/journal.pone.0116740
39. Zhang CL, Wang YH, Chen H, Lei CZ, Fang XT, Wang JQ, et al. The polymorphism of bovine *POMC* gene and its association with the growth traits of Nanyang cattle. *Yi Chuan.* (2009) 31:1221–5. doi: 10.3724/SP.J.1005.2009.01221
40. Park H, Seo S, Cho YM, Oh SJ, Seong HH, Lee SH, et al. Identification of candidate genes associated with beef marbling using QTL and pathway analysis in Hanwoo (Korean cattle). *Asian-Australas J Anim Sci.* (2012) 25:613–20. doi: 10.5713/ajas.2011.11347
41. Seong J, Kong HS. Association between polymorphisms of the *CRH* and *POMC* genes with economic traits in Korean cattle (Hanwoo). *Genet Mol Res.* (2015) 14:10415–21. doi: 10.4238/2015.September.8.2
42. Silva RP, Berton MP, Grigoletto L, Carvalho FE, Silva RMO, Peripolli E, et al. Genomic regions and enrichment analyses associated with carcass composition indicator traits in Nellore cattle. *J Anim Breed Genet.* (2019) 136:118–33. doi: 10.1111/jbg.12373
43. Tomlinson Iv MJ, Polson SW, Qiu J, Lake JA, Lee W, Abasht B. Investigation of allele specific expression in various tissues of broiler chickens using the detection tool VADT. *Sci Rep.* (2021) 11:3968. doi: 10.1038/s41598-021-83459-8
44. Amarasinghe SL, Su S, Dong X, Zappia L, Ritchie ME, Gouil Q. Opportunities and challenges in long-read sequencing data analysis. *Genome Biol.* (2020) 21:30. doi: 10.1186/s13059-020-1935-5

Conflict of Interest: The authors declare that the research was conducted in the absence of any commercial or financial relationships that could be construed as a potential conflict of interest.

Publisher's Note: All claims expressed in this article are solely those of the authors and do not necessarily represent those of their affiliated organizations, or those of the publisher, the editors and the reviewers. Any product that may be evaluated in this article, or claim that may be made by its manufacturer, is not guaranteed or endorsed by the publisher.

Copyright © 2022 Chen, Li, Luo, Li, Jia and Lai. This is an open-access article distributed under the terms of the Creative Commons Attribution License (CC BY). The use, distribution or reproduction in other forums is permitted, provided the original author(s) and the copyright owner(s) are credited and that the original publication in this journal is cited, in accordance with accepted academic practice. No use, distribution or reproduction is permitted which does not comply with these terms.

frontiers | Frontiers in Veterinary Science

TYPE Original Research
PUBLISHED 28 July 2022
DOI 10.3389/fvets.2022.939440

Check for updates

OPEN ACCESS

EDITED BY
Nelida Rodriguez-Osorio,
Universidad de la República, Uruguay

REVIEWED BY
María Muñoz,
INIA-CSIC, Spain
Xin Zhang,
China Agricultural University, China

*CORRESPONDENCE
Liming Hou
liminghou@njau.edu.cn

SPECIALTY SECTION
This article was submitted to Livestock Genomics, a section of the journal Frontiers in Veterinary Science

RECEIVED 09 May 2022
ACCEPTED 28 June 2022
PUBLISHED 28 July 2022

CITATION
Wang H, Shen Z, Huang R, Zhao A, Jiang J, Li P, Zhou X, Yang S and Hou L (2022) A polymorphism in porcine miR-22 is associated with pork color. *Front. Vet. Sci.* 9:939440. doi: 10.3389/fvets.2022.939440

COPYRIGHT
© 2022 Wang, Shen, Huang, Zhao, Jiang, Li, Zhou, Yang and Hou. This is an open-access article distributed under the terms of the Creative Commons Attribution License (CC BY). The use, distribution or reproduction in other forums is permitted, provided the original author(s) and the copyright owner(s) are credited and that the original publication in this journal is cited, in accordance with accepted academic practice. No use, distribution or reproduction is permitted which does not comply with these terms.

A polymorphism in porcine miR-22 is associated with pork color

Han Wang[1], Zhonghao Shen[1], Ruihua Huang[2], Ayong Zhao[1], Jiani Jiang[3], Pinghua Li[2], Xiaolong Zhou[1], Songbai Yang[1] and Liming Hou[2]*

[1]Key Laboratory of Applied Technology on Green-Eco-Healthy Animal Husbandry of Zhejiang Province, Department of Animal Breeding, College of Animal Science and Technology, College of Veterinary Medicine, Zhejiang A&F University, Hangzhou, China, [2]Institute of Swine Science, Department of Animal Breeding, College of Animal Science and Technology, Nanjing Agricultural University, Nanjing, China, [3]Department of Statistical Sciences, University of Toronto, Toronto, ON, Canada

MicroRNAs (miRNAs) are posttranscriptional regulators that play key roles in meat color regulation. Changes in miRNA expression affect their target mRNAs, leading to multifunctional effects on biological processes and phenotypes. In this study, a G > A mutation site located upstream of the precursor miR-22 sequence in Suhuai pigs was significantly correlated with the meat color parameter a*(redness) of the porcine longissimus dorsi (LD) muscle. AA genotype individuals had the highest average meat color a* value and the lowest miR-22 level. When G > A mutation was performed in the miR-22 overexpression vector, miR-22 expression significantly decreased. Considering that Ca^{2+} homeostasis is closely related to pig meat color, our results further demonstrated that *ELOVL6* is a direct target of miR-22 in pigs. The effects of miR-22 on skeletal muscle intracellular Ca^{2+} were partially caused by the suppression of *ELOVL6* expression.

KEYWORDS

pig, meat color, miR-22, *ELOVL6*, intracellular calcium concentration, mutation

Introduction

MicroRNAs (miRNAs) are posttranscriptional regulators that play key roles in meat color regulation (1). Among these, meat color has a major impact on consumer preference and market price (2). Pig meat color is a complex quantitative trait with low heritability, ranging from 0.14 to 0.25 (3). The International Commission on Illumination (CIE) defined a colorimetric system that is widely used in meat color detection (4). According to CIE, any kind of object color characteristics can be represented by tri-stimulus values (i.e., X, Y, and Z). Through mathematical relationship conversion, the colorimeter converts the original CIE tri-stimulus values into understandable values, such as L* (lightness), a*(redness), and b*(yellowness). Because meat color can only be obtained after slaughter, early breeding for meat color is difficult. Recent advances in porcine genomics studies have applied whole-genome sequencing (WGS) and genome-wide association study (GWAS) to improve our understanding of the genetic regulation of pork meat quality by identifying quantitative

trait loci (QTLs), candidate genes, and related genetic variants associated with pork meat quality traits (5). Thus, new tools are being developed to improve pig meat color traits using marker-associated selection (MAS) and genome selection (GS) approaches.

MicroRNAs are posttranscriptional regulators that play key roles in meat color regulation. Genetic variation in miRNA genes can alter precursor miRNA (pre-miRNA) transcription, affecting the processing or stability of pre-miRNA and the expression of mature miRNAs. These changes in turn affect target mRNAs, leading to multifunctional effects on individual phenotypes (6, 7). Genetic mutations in miR-208b and miR-1 precursor genes are significantly associated with pig muscle fiber characteristics and meat color traits (8, 9). The expression of miR-499 is significantly correlated with the expression of *myoglobin*, which typically reflects meat color (10). However, few studies have explored the mechanism of miRNA involvement in the regulation of pig meat color traits.

MiR-22 is a miRNA that plays key roles in multiple biological processes, including tumor suppression, cancer therapy, and the prevention of cardiac hypertrophy (11). Previous studies have shown that miR-22 inhibits the proliferation of porcine muscle satellite cells (PMSCs) and promotes their differentiation (12). MiR-22 is also involved in the regulation of muscle fiber type conversion *via* the inhibition of the *AMPK-SIRT1-PGC-1α* pathway in mouse muscle cells (13). Muscle fiber type is associated with meat color (14), and previous studies have demonstrated that Ca^{2+} homeostasis affects pig meat color (15, 16).

Through bioinformatics prediction, we discovered that elongase of very-long-chain fatty acids 6 (*ELOVL6*), an elongase that catalyzes *de novo* synthesis of fatty acids (17), is a direct potential target gene of miR-22. In our previous study, we showed that *ELOVL6* is more highly expressed in white longissimus dorsi (LD) muscle than in red soleus (SOL) muscle (18). In *ELOVL6*-knockout *Drosophila*, the proportion of stearic acid in mitochondria was repressed. However, when stearic acid was added to food consumed by *Drosophila*, stearoylation was promoted, which inhibited the *JNK* signaling pathway and reduced the ubiquitination of mitochondrial fusion proteins, thereby promoting mitochondrial metabolism and fusion and maintaining its normal function (19). Dysfunction due to the inhibition of mitochondrial fusion decreased the sensitivity of myofibroblasts to Ca^{2+} action (20). The *ELOVL6* gene may affect the concentration of Ca^{2+} in muscle cells, influencing pig meat color. However, few studies have investigated the involvement of *ELOVL6* in muscle cell Ca^{2+} concentration.

Therefore, we hypothesized the existence of a functional mutation site related to meat color in the precursor sequence gene of porcine miR-22, which regulates Ca^{2+} concentration in porcine muscle cells by affecting the expression of miR-22. In this study, we explored the role of miR-22 in regulating skeletal muscle intracellular Ca^{2+} by investigating a mutation site related to pork color in the miR-22 gene. Our findings will provide a useful theoretical basis for future research on genetic markers of pig meat color traits.

Materials and methods

Animals and phenotype measurements

All animal procedures were performed in accordance with the Guidelines for Care and Use of Laboratory Animals of Nanjing Agriculture University and approved by the Animal Ethics Committee of Nanjing Agriculture University. A total of 300 healthy Suhuai pigs (i.e., 194 castrated barrows and 106 sows) with the same market weight (80–90 kg) and approximately 7–8 months old were reared at the Huaiyin Breeding Farm (Huaian, China) under the same feeding conditions and slaughtered at Sushi Meat Products Co., Ltd. (Huaian, China).

Ear tissues from the end of the right ear were collected and stored in 75% alcohol for DNA extraction. Samples of the LD, SOL, psoas major (PM), masseter (MA), and biceps femoris (BF) muscles were collected for RNA extraction from four randomly selected healthy Suhuai pigs with similar body weight and age. LD muscle samples from the last rib of the carcass were collected and used to determine meat color. In China, traditional hot fresh meat is usually marketed immediately after slaughter, whereas chilled fresh meat is often cooled quickly to a stable 0–4°C within 24 h postmortem and maintained at this temperature until sold to the consumer (21). Therefore, meat color (L*a*and b*) was measured on the last rib at 2 (room temperature) and 24 h (4°C) postmortem using a chromameter (Minolta Camera Co., Osaka, Japan).

Cell culture

Porcine muscle satellite cells were isolated as described previously (22). LD muscles of 3-day-old healthy male piglets were disinfected with alcohol and aseptically dissected *in vitro*. Muscle samples were washed three times with phosphate-buffered saline (PBS) (HyClone, Logan, USA) containing 1% penicillin–streptomycin (Solarbio, Beijing, China), and the skin, fat, and connective tissue were removed. The muscle was crushed into meat paste and digested with 2 ml PBS containing 0.1% collagenase II at 37°C for 10 min. The samples were centrifuged three times at 500 rpm for 5 min each. The cell suspension was sequentially passed through 100 and 40 μm nylon cell filters and a 20 μm mesh filter. The filtrate was collected into a 15 ml centrifuge tube and centrifuged at 1,500 rpm for 10 min, and the supernatant was discarded to obtain the cell pellets. The pellets were washed three times with PBS, added to a Percoll gradient solution, and centrifuged

at 2,000 rpm for 1 h. Totally, 26% of the Percoll gradient solution was recovered, which then was cultured in growth medium (GM) and Dulbecco's modified Eagle medium (DMEM; HyClone, Logan, USA) supplemented with 10% fetal bovine serum (FBS) and 1% penicillin–streptomycin (Solarbio, Beijing, China). HEK293T cells and PK15 cells were cultured in 12-well plates in DMEM with 10% FBS and penicillin–streptomycin (50 mg/mL). All cells were incubated at 37°C under 5% CO_2.

Isolation of genomic DNA and single-nucleotide polymorphism genotyping

Genomic DNA was isolated from ear tissue using the standard phenol–chloroform protocol method (23). DNA concentration and integrity were measured using a Nanodrop 2000 spectrophotometer (Thermo Fisher Scientific Inc., Waltham, MA, USA). A 688 bp DNA fragment encompassing porcine pre-miR-22 and its flanking sequences was amplified by polymerase chain reaction (PCR) using pooled genomic DNA isolated from eight randomly selected pigs. The primer sequences (miR-22-SNP) are provided in Table 1. Polymorphisms were sequenced by TsingKe Inc. and analyzed using the Chromas software. The NC_010454.4:g.47913559 G > A SNP was selected for genotyping and named according to sequence variation nomenclature guidelines provided by the Human Genome Variation Society. Sequences for the 300 pigs were individually amplified and genotyped by PCR using the miR-22-SNP primers (Table 1).

Quantitative reverse transcription PCR

TRIzol reagent was used to extract total RNA (24). Briefly, TRIzol (Invitrogen, Waltham, MA, USA) was added to the culture dish to lyse the cells or tissue in the tubes. Then, 0.2 ml chloroform per 1 ml TRIzol reagent was added, and the samples were incubated at 15–30°C for 2–3 min. Then, the samples were centrifuged for 15 min at 12,000× g at 4°C. Following centrifugation, approximately 0.5 ml of the aqueous phase was transferred to a fresh tube, and 0.5 ml of isopropyl alcohol was added. Samples were incubated at 15–30°C for 10 min and centrifuged at 12,000× g for 10 min at 2–8°C. The supernatant was removed, and the RNA pellet was washed once with 75% ethanol and air-dried for 5–10 min. qRT-PCR analyses were performed as described previously (25). Reverse transcription of miRNA was performed using the RR014a reverse transcription kit (Takara, Kusatsu, Japan). Differential expression was analyzed using the $2^{-\Delta\Delta Ct}$ method (26). *U6* and *GAPDH* were selected as housekeeping genes for miR-22 and protein coding genes, respectively. The primer sequences used in these analyses are provided in Table 1.

Plasmid construction

To construct the pcDNA3.1-miR-22 expression vector, a fragment of the first intron containing the NC_010454.4:g.47913559 G > A SNP and the entire second exon of the miR-22 host gene (TLC-domain containing 2, *TLCD2*) was amplified and cloned into the pcDNA 3.1 plasmid, which was digested with the *EcoRI* and *XhoI* restriction enzymes (Invitrogen). The primer sequences were 5'-GAATTCGGGACCAAGTCAGTTCGG-3′ and 5′-CTCGAGCCAGACTTAGGCAATACAGG-3′. The pcDNA3.1-miR-22 expression point mutant vector was generated using the Mut Express II Fast Mutagenesis kit (Vazyme Biotech Co., Ltd., Nanjing, China). The pcDNA3.1-*ELOVL6* expression vector, *ELOVL6* Psicheck-2 dual-luciferase reporter, and *ELOVL6* point mutant vectors were generated by Tsingke (Hangzhou, China).

RNA oligonucleotides and transfection

MiR-22 mimics, miR-22 mimics NC, miR-22 inhibitor, miR-22 inhibitor NC, small interfering RNA (siRNA) against pig *ELOVL6*, and the negative control scramble siRNA (NC) were designed and synthesized by RiboBio (Guangzhou, China). The primer sequences are provided in Table 2. The Lipofectamine 3000 system (Invitrogen) was used for transfection according to the manufacturer's instructions.

Dual-luciferase reporter assay

In 12-well plates, miR-22 or NC mimics (50 nM) were transfected into HEK293T cells with 1 μg Psicheck-2 *ELOVL6* luciferase vector (wild-type or mutated) using Lipofectamine 3000. The assays were performed 24 h after transfection according to the manufacturer's instructions (Promega, Madison, WI, USA).

Immunofluorescence staining

Porcine muscle satellite cells were cultured in 12-well cell culture plates with cell slides. When cells reached 70–80% confluence, they were washed three times with precooled PBS for 5 min and fixed with 4% paraformaldehyde for 15 min. Furthermore, the cells were permeabilized with 0.25% Triton X-100 for 10 min, blocked at 4°C overnight, and incubated with anti-*Pax7* primary antibody (Abcam, Shanghai, China) or anti-*Desmin* primary antibody (Abcam, Shanghai, China) for 1 h at room temperature. Then, a fluorescent secondary antibody (Thermo Fisher, Shanghai, China) was incubated with the cells for 1 h at room temperature. We added

TABLE 1 The primers used for PCR in this study.

Name	Sequence (5′-3′)	Accession number
miR-22	F: CAGGAAGCTGCCAGTTGAA	NR_038580.1
	R: TCAACTGGTGTCGTGGAGTC	
RT-loop-miR-22	CTCAACTGGTGTCGTGGAGTCGGCAATTCAGTTGAGACAGTTC	NR_038580.1
U6	F: GCTTCGGCAGCACATATACT	XM_003357006.5
	R: TTCACGAATTTGCGTGTCA	
miR-22-SNP	F: GGTCCACATGCTCACCTA	N/A
	R: CGCACGAGGACCAACTAA	
GAPDH	F: GATGGTGAAGGTCGGAGTG	NM_001206359.1
	R: CCAAGTTGTCATGGATGACC	
Myhc I	F: CGACACACCTGTTGAGAAG	NM_213855.2
	R: AGATGCGGATGCCCTCCA	
MyhcIIb	F: GTTCTGAAGAGGGTGGTAC	NM_001123141.1
	R: AGATGCGGATGCCCTCCA	
Myoglobin	F: GGATGAGATGAAGGCCTCTG	NM_214236.1
	R: AACCTGGATGATGGCTTCTG	
ELOVL6	F: AGCAGTTCAACGAGAACGAAGCC	XM_021100707.1
	R: TGCCGACCGCCAAAGATAAAG	

TABLE 2 Sequence of RNA oligonucleotides.

Name	Forward (5′-3′)	Reverse (5′-3′)
Negative control	UUCUCCGAACGUGUCACGUdTdT	ACGUGACACGUUCGGAGAAdTdT
miR-22-mimics	AAGCUGCCAGUUGAAGAACUGU	AGUUCUUCAACUGGCAGCUUUU
miR-22-inhibitor	CAGUUCUUCAACUGGCAGCUU	
Inhibitor NC	UCUACUCUUUCUAGGAGGUUGUGA	
siRNA-*ELOVL6*	UGAACAAGCGCGCGAAGUU	AACUUCGCGCGCUUGUUCA
siRNA-Negative control	UUCUCCGAACGUGUCACGU	ACGUGACACGUUCGGAGAA

4′,6-diamidino-2-phenylindole (DAPI) (Invitrogen) to stain the nuclei, and the cells were incubated for 10 min at room temperature. A fluorescence microscope (Olympus, Tokyo, Japan) was used to observe the samples.

Detection of intracellular calcium concentration

The cells were washed twice with PBS and once with D-Hank's solution. Fura-2/AM (5 μM) was added, and the cells were incubated at 37°C for 30 min. The samples were washed three times and incubated with D-Hank's solution at 37°C for 20–30 min. A fluorescence spectrophotometer with excitation wavelengths of 340 and 380 nm, and an emission wavelength of 510 nm was used to measure R, F_{max}, and F_{min}, respectively. The following formula was used to calculate intracellular calcium concentration ($[Ca^{2+}]i$): $[\boldsymbol{Ca^{2+}}]\boldsymbol{i}=\boldsymbol{Kd}[\boldsymbol{R}-\boldsymbol{Rmin})/(\boldsymbol{Rmax}-\boldsymbol{R})](\boldsymbol{Fmin}/\boldsymbol{Fmax})$, where Kd = 224 nmol/L, R is the ratio of fluorescence intensity measured at excitation wavelengths of 340/380 nm, R_{max} is the same ratio after adding Triton X-100, and R_{min} is the same ratio after adding ethylene glycol tetraacetic acid (EGTA). F_{max} and F_{min} are the maximum and minimum fluorescence intensities measured at 340 nm after adding Triton X-100 and EGTA, respectively.

Statistical analysis

Association analysis of the SNP for meat color was performed using the PROC GLM procedure in the SAS v9.2 software (SAS Institute Inc., Cary, NC, USA), with both sex and SNP as fixed effects and slaughter age as a covariate (27, 28). Kinship was not taken into account in this statistical model. The associated genotype mean eigenvalues were compared using the Tukey–Kramer program in SAS to detect significant differences. All data were expressed as mean ± standard error of the mean (SEM). Unpaired Student's *t*-tests were used to calculate *P*-values using the SPSS v20.0 software (SPSS Inc., Chicago, IL, USA). Significant differences were evaluated at a level of $P < 0.05$ and highly significant differences at $P < 0.01$.

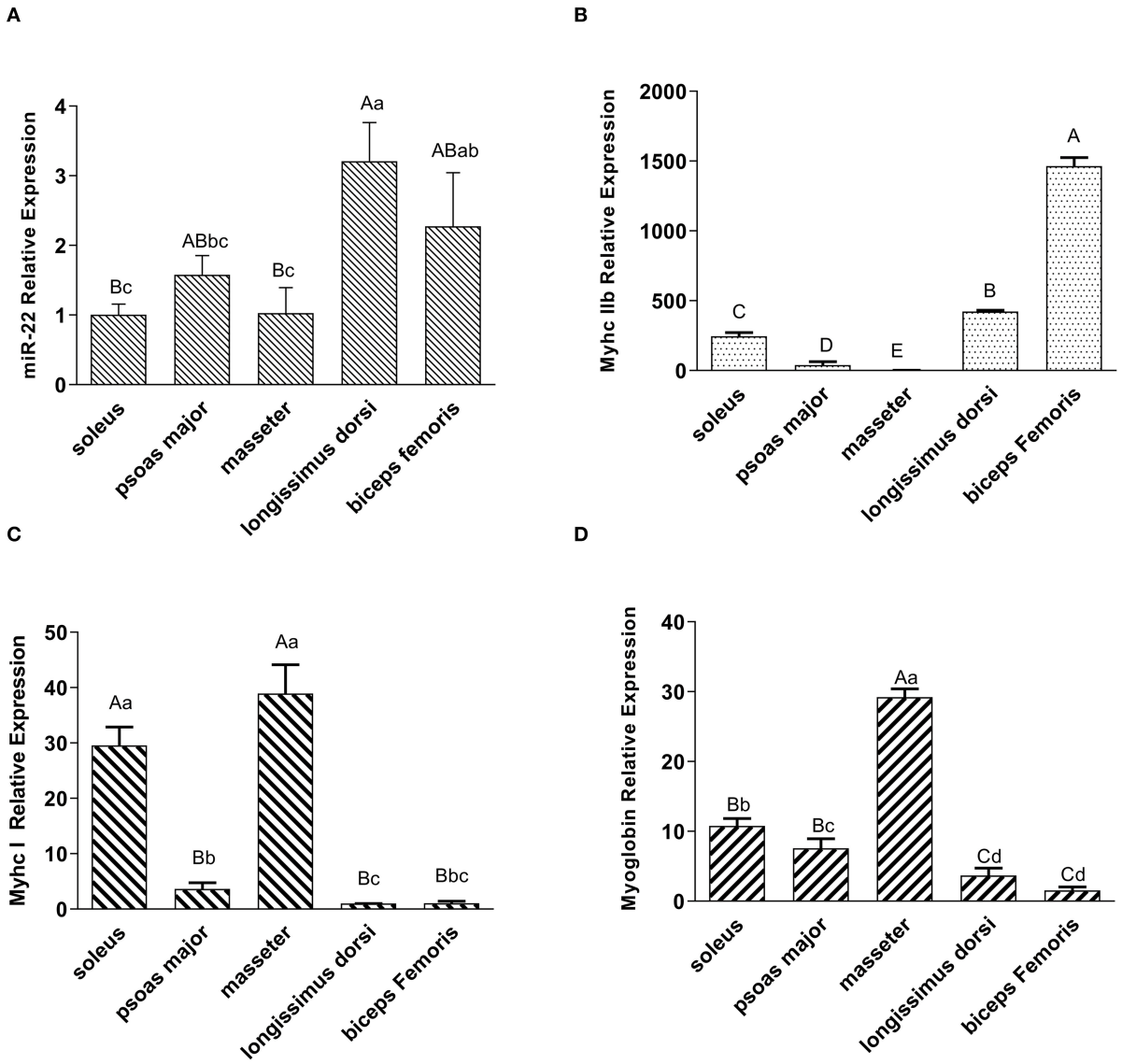

FIGURE 1
Expression profiling of miR-22, muscle fiber type marker genes, and myoglobin in different types of porcine muscle. **(A)** Expression of miR-22 in different type of skeletal muscles (i.e., SOL, psoas major, masseter, longissimus dorsi, and biceps femoris) in Suhuai pigs. **(B)** Expression of the glycolytic type IIb fiber marker gene *MyhcIIb* in different muscle types. The masseter group was treated as the control group. **(C)** Expression of oxidized type I fiber marker gene *Myhc I* in different muscle types. The longissimus dorsi group was treated as the control group. **(D)** Expression of myoglobin in different types of skeletal muscles. The biceps femoris group was treated as the control group. Capital letters indicate highly significant differences ($P < 0.01$); lowercase letters indicate significant differences ($P < 0.05$) ($n = 4$).

Results

Expression profiling of miR-22 in different porcine muscle types

To investigate the expression profile of miR-22 in various muscle types, we performed a qRT-PCR assay. MiR-22 expression was significantly lower in the SOL, PM, and MA muscle than in the LD and BF muscle ($P < 0.05$) (Figure 1A). *Myhc IIb*, a marker gene for fast glycolytic muscle fibers (29), was more highly expressed in the LD and BF muscles than in the SOL, PM, and MA muscles (Figure 1B). However, *Myhc I*, a marker gene for slow oxidative muscle fibers (29), was highly expressed in the SOL and MA muscles (Figure 1C). We also found that *myoglobin* expression patterns were similar to those of *Myhc I* in different muscle types (Figure 1D).

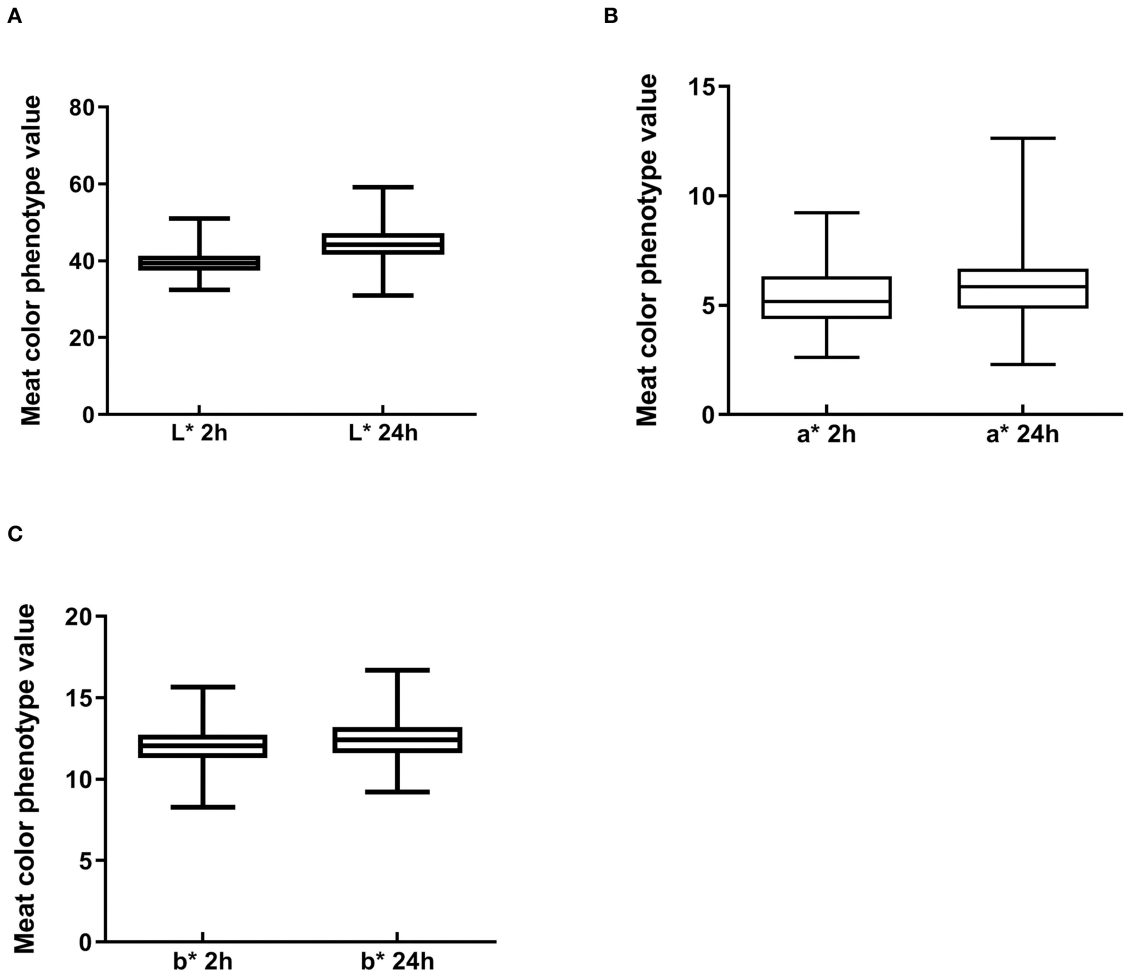

FIGURE 2
Boxplot of meat color index values in Suhuai pigs at 2 and 24 h after slaughter, including **(A)** lightness (L*), **(B)** redness (a*), and **(C)** yellowness (b*).

Descriptive statistics for meat color phenotypes

To understand the characteristics of the Suhuai pig population, we performed descriptive statistical analysis of meat color trait values. Mean values of meat color traits in this group were within the normal range, although there was a large difference between the maximum and minimum values (Figures 2A–C). The coefficient of variation for meat color a* reached 28.35% at 24 h postmortem (Table 3) and 25.82% at 2 h postmortem (Table 3). The coefficients of variation for all other meat color parameters were <10% (Table 3). These results indicate that the breeding of Suhuai pig meat color should be studied further.

Detection of SNP in the miR-22 gene and association analysis of meat color traits

After sequencing the miR-22 genes of eight Suhuai pigs, we found a G/A mutation at NC_010454.4:g.47913559 (Figure 3A) within the 1st intron of the miR22 host gene (*TLCD2*), located 147 bp upstream of pre-miR-22 (Figure 3B). After sequencing the 688 bp DNA amplicons of 300 Suhuai pigs, we found 152, 111, and 37 GG, GA, and AA genotype individuals, respectively (Table 4). The frequency of allele G was 0.735 and that of allele C was 0.265 (Table 4). The NC_010454.4:g.47913559 G > A SNP was significantly associated with meat color a* at 2 h postmortem but not with other meat color parameters (Table 5). At 2 h postmortem, the AA genotype had the highest meat color

TABLE 3 Descriptive statistics analysis of meat color traits in 300 Suhuai pigs.

Meat color	*N*	Range	Mean ± SE	CV (%)	median
L* value after slaughter 2 h	300	32.52–51.05	39.54 ± 0.18	7.64%	39.34
a* value after slaughter 2 h	300	2.61–9.22	5.38 ± 0.08	25.82%	5.18
b* value after slaughter 2 h	300	8.28–15.67	12.01 ± 0.06	8.98%	12.04
L* value after slaughter 24 h	300	31.04–59.19	44.43 ± 0.23	8.8%	44.2
a* value after slaughter 24 h	300	2.28–19.18	5.94 ± 0.1	28.35%	5.85
b* value after slaughter 24 h	300	9.22–16.71	12.51 ± 0.07	9.43%	12.41

a* value among all genotypes, and a* was higher for the GA genotype than for the GG genotype (Table 5).

Association between miR-22 expression levels and the g.47913559 G > A mutation

To determine the effect of NC_010454.4: g.47913559 G > A on the expression of miR-22 in pig skeletal muscle, we randomly selected six individuals from each genotype to detect the relative expression of miR-22. MiR-22 expression was lowest for the AA genotype, whereas no significant differences were detected between the GG and GA genotypes (Figure 4A). When G > A mutation was performed in the miR-22 overexpression vector, miR-22 expression decreased in the AA genotype compared with the GG genotype (Figure 4B). Together, these results suggest that the NC_010454.4:g.47913559 G > A SNP affects miR-22 expression.

MiR-22 promotes intracellular Ca^{2+} concentration by targeting *ELOVL6* in porcine skeletal muscle satellite cells

Isolated PMSCs adhered completely to the cell dish after 12 h of isolation, and the cells were spindle-shaped (Figure 5A). After 24 h, the cells increased in number and grew in a regular manner in one direction. These results indicated that the PMSCs showed vigorous cell viability and normal skeletal muscle satellite cell morphology. To further validate the isolated cells, we performed immunofluorescence staining with the skeletal muscle satellite cell-specific marker proteins *Pax7* and *Desmin* (30). *Pax7* and *Desmin* were positive in the nucleus and cytoplasm, respectively (Figure 5B), further demonstrating that the isolated cells were PMSCs.

Compared with the NC, overexpression of miR-22 effectively increased the intracellular Ca^{2+} concentration, whereas knockdown of miR-22 reduced the intracellular Ca^{2+} concentration of PMSCs (Figures 5C,D). Using the TargetScan online prediction program, we discovered that *ELOVL6* was a potential target of miR-22, with an miR-22 binding site in its 3′UTR region, which is highly conserved in multiple species (Figure 5E). Furthermore, we conducted a dual-luciferase reporter assay to test whether *ELOVL6* is a real target gene of miR-22. The predicted sequence of the *ELOVL6* 3′UTR was inserted into the Renilla luciferase report vector Psicheck-2 (Figure 5E). The mutated Psicheck-2 *ELOVL6* luciferase vector, which has three mutant sites in the binding site of miR-22, was also generated. Overexpression of miR-22 significantly inhibited luciferase activity when co-transfected with Psicheck-2 *ELOVL6* luciferase vector in HEK293T cells (Figure 5F). However, no significant changes in luciferase activity were observed when miR-22 was co-transfected with mutated Psicheck-2 *ELOVL6* luciferase vector.

The expression of *ELOVL6* was significantly downregulated after miR-22 overexpression (Figure 5G) in PMSCs. In contrast, loss of miR-22 upregulated the mRNA expression of *ELOVL6*. SiRNA-mediated knockdown of *ELOVL6* increased the intracellular Ca^{2+} concentration in PMSCs, and overexpressing *ELOVL6* decreased the intracellular Ca^{2+} concentration (Figures 5H,I). These results suggest that miR-22 increases the concentration of intracellular Ca^{2+} by targeting *ELOVL6* in PMSCs.

Discussion

Genetic and nutritional factors such as breed, muscle fiber type, and feed nutrition, as well as physiological and biochemical factors such as mitochondrial function and lipid oxidation, regulate pig meat color by affecting the content or redox state of myoglobin (31). In this study, we found that miR-22 expression was significantly lower in red muscles with high proportions of oxidative fibers such as porcine SOL, PM, and MA muscles than in white muscles containing high proportions of glycolytic fibers such as the LD and BF. Previous studies have also found that porcine SOL, PM, and MA muscles are mainly composed of oxidized type I and type IIa muscle fibers, whereas muscles such as the LD and BF are mainly glycolytic type IIb muscle fibers (32). Among the reported target genes of miR-22, we discovered genes such as *Sirt1* and *HDAC4*, which promote the formation of red muscles (33, 34). A previous study found that miR-22 eliminated the effects of resveratrol on slow *MyHC* and fast

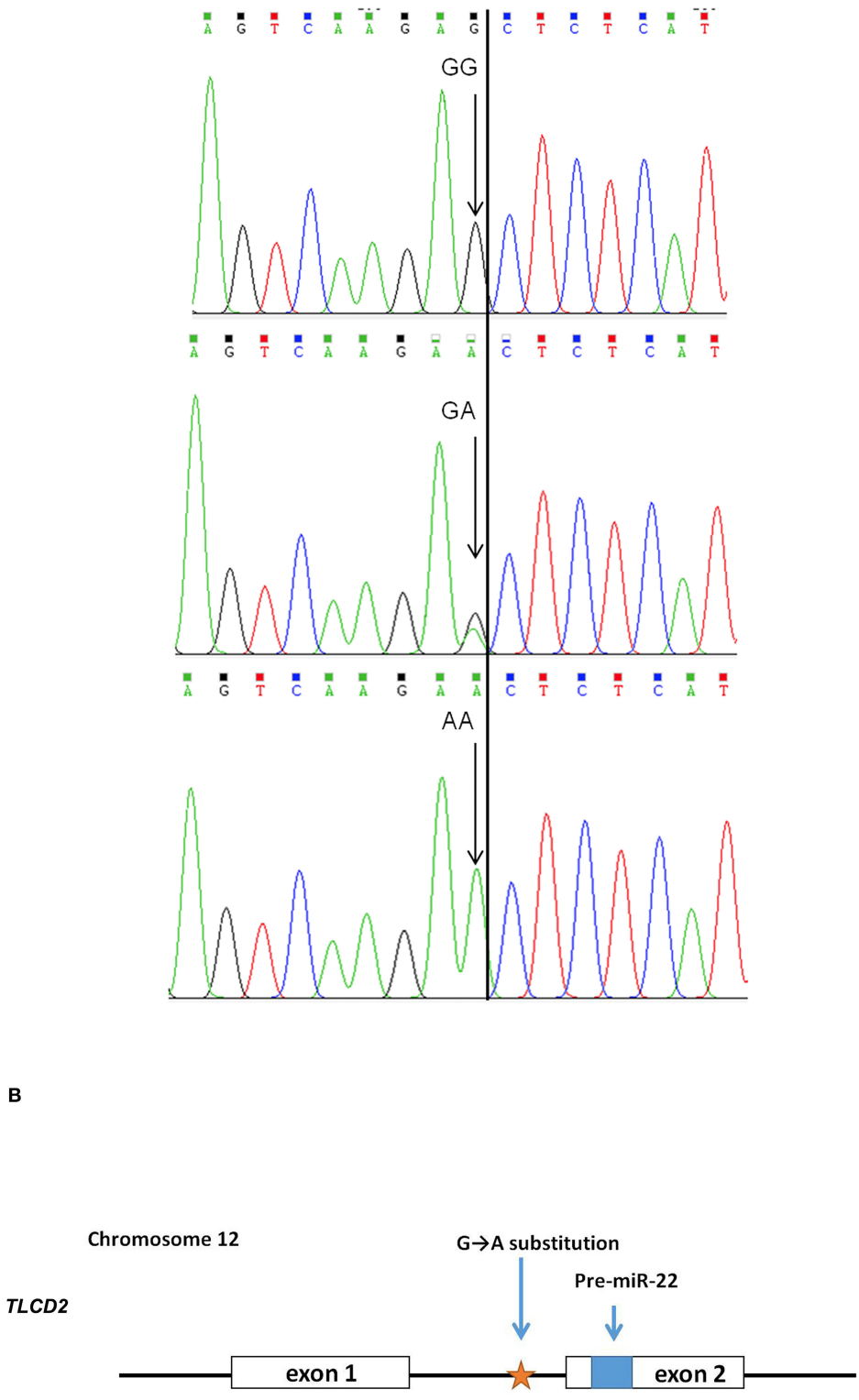

FIGURE 3
Scheme of the NC_010454.4: g.47913559 G > A mutation in the miR-22 gene. **(A)** Sequencing peak map of the GG, GA, and AA genotypes. Eight individuals were randomly divided into two groups, and each group of four was mixed for sequencing. Arrow indicates the target site. **(B)** Positional relationship between the NC_010454.4: g.47913559 site, ssc-miR-22 precursor, and its host gene *TLCD 2*.

TABLE 4 Allele frequencies of the G > A substitution of miR-22 primary transcript in the Suhuai pig population.

Population	No. of pigs	Genotypes			Allele frequency	
Suhuai pig	300	GG	GA	AA	G	A
		152	111	37	0.735	0.265

TABLE 5 Association results for the G > A polymorphism in miR-22 transcript with meat color traits.

Genotype	No.	Meat color L^* at 2 h postmortem	Meat color a^* at 2 h postmortem	Meat color b^* at 2 h postmortem	Meat color L^* at 24 h postmortem	Meat color a^* at 24 h postmortem	Meat color b^* at 24 h postmortem
GG	152	39.65 ± 0.26	5.08 ± 0.12Bb	11.99 ± 0.09	53.25 ± 7.24	5.83 ± 0.15	12.60 ± 0.10
GA	111	39.46 ± 0.29	5.57 ± 0.13ABa	12.00 ± 0.10	43.66 ± 8.21	6.01 ± 0.17	12.41 ± 0.12
AA	37	38.73 ± 0.50	5.91 ± 0.26Aa	11.91 ± 0.18	43.85 ± 14.02	6.12 ± 0.28	12.37 ± 0.20
P-Value		0.2672	0.0008**	0.8933	0.6297	0.5648	0.3659

Capital letters indicate highly significant differences (P < 0.01), and lowercase letters indicate significant differences (P < 0.05).

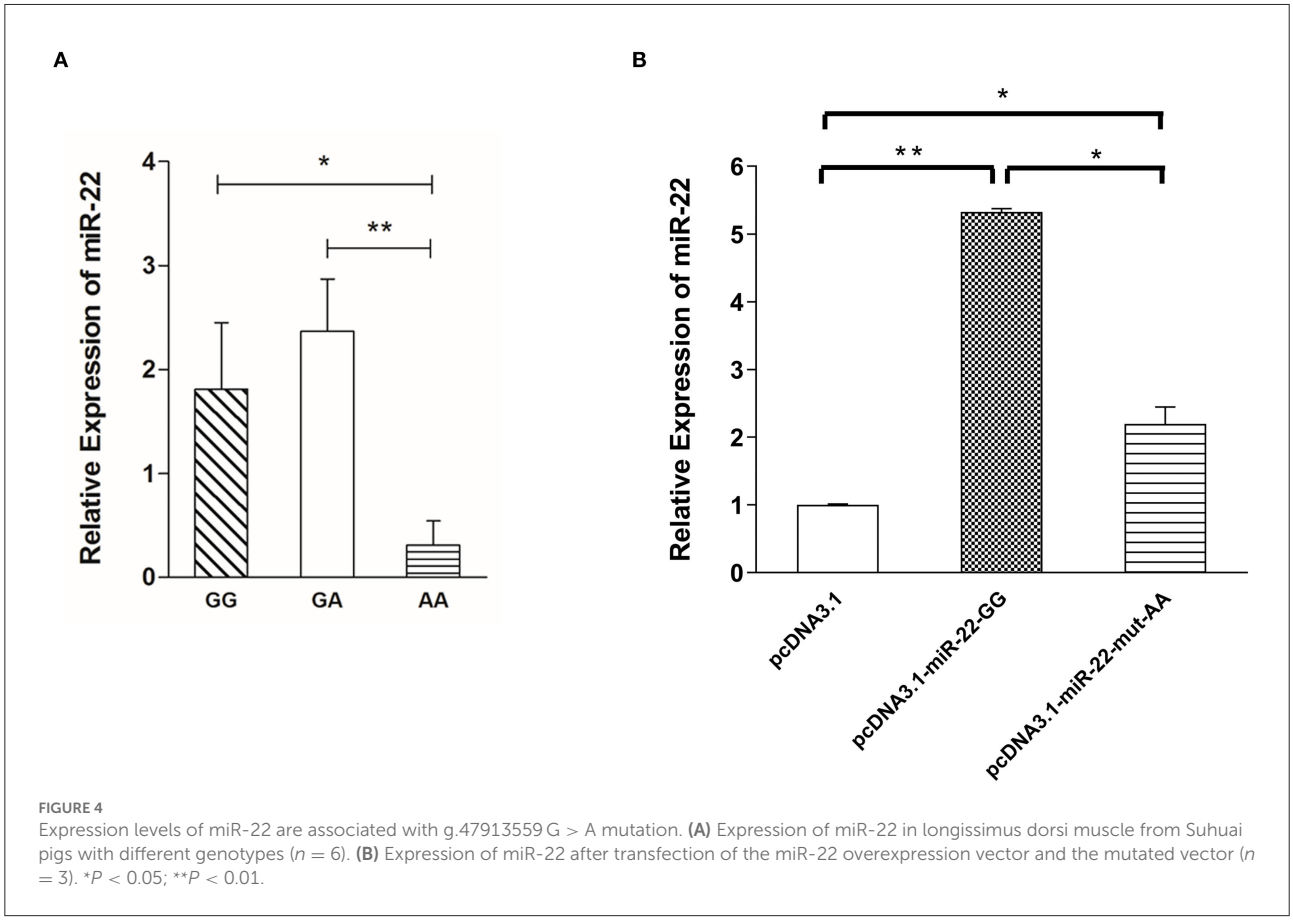

FIGURE 4
Expression levels of miR-22 are associated with g.47913559 G > A mutation. **(A)** Expression of miR-22 in longissimus dorsi muscle from Suhuai pigs with different genotypes ($n = 6$). **(B)** Expression of miR-22 after transfection of the miR-22 overexpression vector and the mutated vector ($n = 3$). $^*P < 0.05$; $^{**}P < 0.01$.

MyHC expression in porcine myotubes (35). Our results also showed that *myoglobin* expression was higher in red muscles than in white muscles and that the pattern was opposite to that of miR-22 in different pig muscle types. This finding further suggests that miR-22 expression may be lower in muscles with higher redness values. Therefore, further studies are needed to explore the genes or signaling pathways related to pig meat color regulated by miR-22.

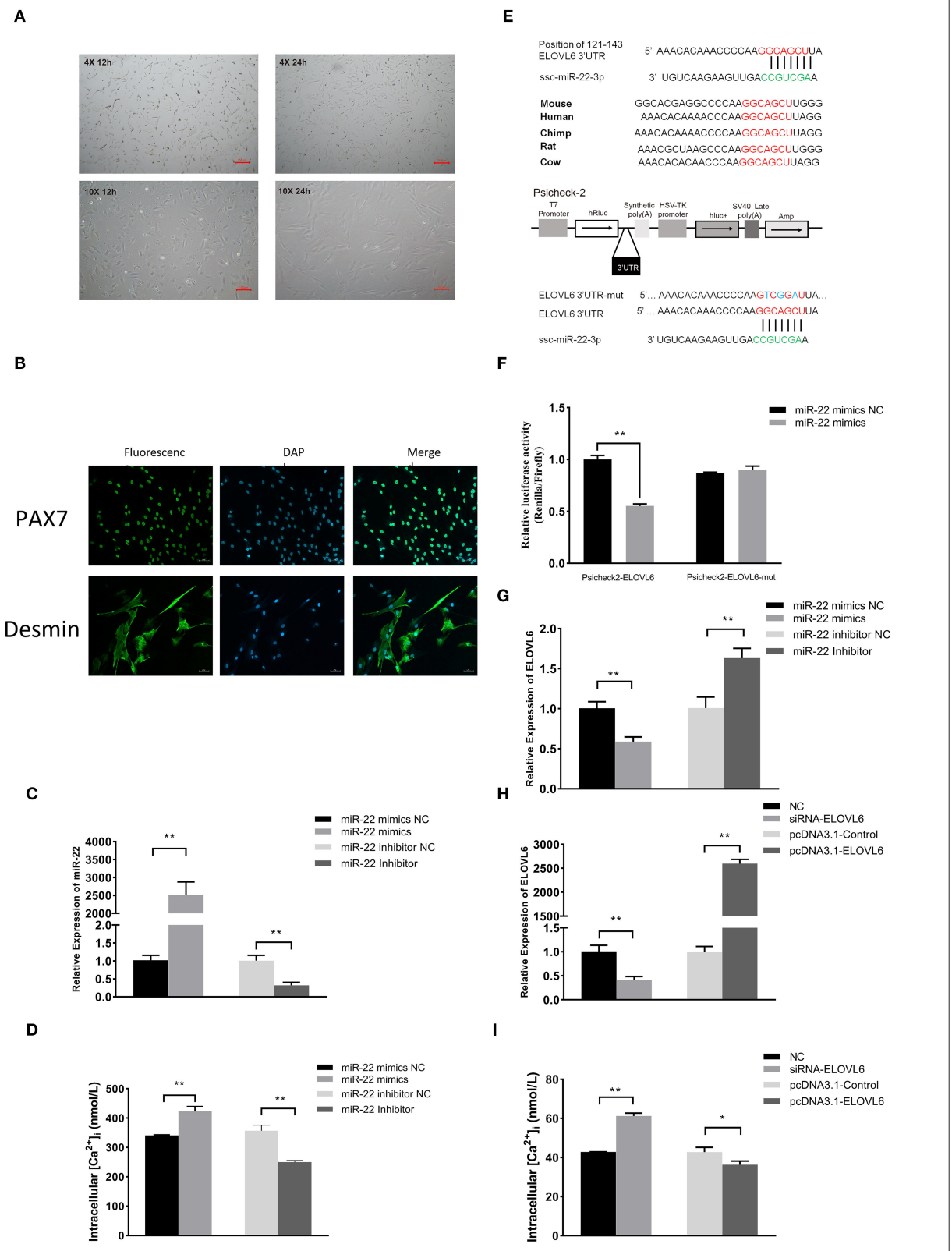

FIGURE 5
The miR-22 gene promotes intracellular calcium concentration by targeting the elongase of very long chain fatty acids 6 (*ELOVL6*) gene in porcine skeletal muscle satellite cells (PMSCs). Microscopic morphological observation of PMSC growth for 12 and 24 h at **(A)** 4× (upper panel)
(Continued)

FIGURE 5
and 10× (bottom panel) magnification. **(B)** Immunofluorescence staining of satellite cell marker proteins (Pax7 and Desmin) in PMSCs. **(C)** Expression of miR-22 in PMSCs after transfection of miR-22 mimics and its NC and miR-22 inhibitor and its NC. **(D)** Intracellular calcium concentration was measured after PMSCs were transfected with miR-22 mimics, miR-22 mimics NC, miR-22 inhibitor, or miR-22 inhibitor NC for 24 h. **(E)** Sequence of miR-22 and its predicted conserved binding region in *ELOVL6* 3′UTR (red). Structural diagram of the dual-luciferase reporter vector Psicheck-2. The predicted miR-22 target site of the *ELOVL6* 3′UTR and mutated target site were inserted into the 3′-end of the Renilla luciferase gene (hRluc). Firefly luciferase gene (hluc+) expression was used as the standard control. **(F)** HEK293T cells transfected with miR-22 mimics or NC were co-transfected with the Psicheck-2 *ELOVL6* vector or its mutated vector. Relative luciferase activity was determined after 24 h. **(G)** Expression of *ELOVL6* mRNA in PMSCs following transfection of miR-22 mimics, miR-22 mimics NC, miR-22 inhibitor, or miR-22 inhibitor NC. **(H)** Expression of *ELOVL6* mRNA in PMSCs following transfection of siRNA-*ELOVL6*, NC, pcDNA3.1-*ELOVL6*, or pcDNA3.1-Control. **(I)** Intracellular calcium concentration was measured after PMSCs were transfected with siRNA-*ELOVL6*, NC, pcDNA3.1-*ELOVL6*, or pcDNA3.1-Control for 24 h ($n = 3$). $^{*}P < 0.05$; $^{**}P < 0.01$.

Many studies have analyzed the association between miRNA and economic traits in farm animals through the detection of SNPs in miRNA genes. A T/C mutation in the miR-27a gene, which is associated with litter size in large white pigs, may be a potential molecular marker for litter size trait breeding (36). An SNP on the miR-206 gene is associated with the proportions of type IIa and IIb fibers in muscle and also with meat quality traits including drip loss and backfat and lean meat percentages (37). An SNP on miR-133b is significantly associated with the total number of muscle fibers, loin eye muscle area, and pH (37). In this study, we showed that the coefficient of variation for meat color a* at 2 h postmortem reached 25.82%, such that the meat redness trait has great breeding potential in Suhuai pigs.

Through sequencing, we found a G > A mutation site in the ssc-miR-22 gene that was highly significantly correlated with meat color a* at 2 h postmortem in Suhuai pigs. AA genotype individuals had the highest a*value and the lowest miR-22 expression. However, GG genotype individuals had lower a*values at 2 h postmortem than GA genotype individuals, but there were no significant differences in miR-22 expression between these genotypes. The G > A mutation in the miR-22 overexpression vector decreased miR-22 expression levels. Thus, this mutation may promote the binding of transcription factors that inhibit miR-22 expression; however, this phenomenon may be fully effective only for AA homozygous genotype. Future studies should further explore the mechanism underlying the effects of this mutation on miR-22 expression.

In a previous study, we found that the *ELOVL6* gene was differentially expressed in different types of muscles in pigs (18), which was in contrast to the expression trend observed in miR-22 in this study. In this study, we also discovered that porcine miR-22 targets *ELOVL6* to regulate the Ca^{2+} concentrations in PMSCs. The calcium/calmodulin kinase II (*CaMK II*) gene is a significantly enriched phosphorylation motif of *ELOVL6*$^{-/-}$ zebrafish compared with wild-type zebrafish (38). In skeletal muscle, *CaMK II* phosphorylation can stimulate intracellular Ca^{2+} levels. Therefore, we speculated that *CaMK II* may be downstream of miR-22 or its target gene *ELOVL6*, where it regulates intracellular Ca^{2+} in PMSCs (39).

In summary, a G/A mutation in the miR-22 gene was discovered to be associated with pig meat color a* at 2 h postmortem, and this mutation influences miR-22 expression. The NC_010454.4: g.47913559 G > A mutation site may act as a molecular marker for meat color in pig breeding. In addition, *ELOVL6* is a direct target of miR-22 in pigs. The effects of miR-22 on skeletal muscle intracellular Ca^{2+} concentrations may be partly due to the inhibition of *ELOVL6* expression.

Data availability statement

The raw data supporting the conclusions of this article will be made available by the authors, without undue reservation.

Ethics statement

The animal study was reviewed and approved by the Animal Ethics Committee of Nanjing Agriculture University.

Author contributions

LH and RH conceived and designed the experiments. HW and ZS performed the experiments. HW, XZ, SY, and JJ analyzed the data. AZ and PL helped to write the manuscript. JJ helped to revise the language. All authors read and approved the final manuscript.

Funding

This study was supported by the National Natural Science Foundation of China (Nos. 31802030, 32002149, and 32172710).

Conflict of interest

The authors declare that the research was conducted in the absence of any commercial or financial relationships that could be construed as a potential conflict of interest.

Publisher's note

All claims expressed in this article are solely those of the authors and do not necessarily represent those of their affiliated organizations, or those of the publisher, the editors and the reviewers. Any product that may be evaluated in this article, or claim that may be made by its manufacturer, is not guaranteed or endorsed by the publisher.

References

1. Nonneman D, Shackelford S, King D, Wheeler T, Wiedmann R, Snelling W, et al. Genome-wide association of meat quality traits and tenderness in swine. *J Anim Sci.* (2013) 91:4043–50. doi: 10.2527/jas.2013-6255

2. Brewer M, Jensen J, Sosnicki A, Fields B, Wilson E, McKeith F. The effect of pig genetics on palatability, color and physical characteristics of fresh pork loin chops. *Meat Sci.* (2002) 61:249–56. doi: 10.1016/S0309-1740(01)00190-5

3. Van Wijk H, Arts D, Matthews J, Webster M, Ducro B, Knol E. Genetic parameters for carcass composition and pork quality estimated in a commercial production chain. *J Anim Sci.* (2005) 83:324–33. doi: 10.2527/2005.832324x

4. Wu D, Sun D-W. Colour measurements by computer vision for food quality control–a review. *Trends Food Sci Tech.* (2013) 29:5–20. doi: 10.1016/j.tifs.2012.08.004

5. Davoli R, Braglia S. Molecular approaches in pig breeding to improve meat quality. *Brief Funct Genomics.* (2007) 6:313–21. doi: 10.1093/bfgp/elm036

6. Georges M, Coppieters W, Charlier C. Polymorphic miRNA-mediated gene regulation: contribution to phenotypic variation and disease. *Curr Opin Genet Dev.* (2007) 17:166–76. doi: 10.1016/j.gde.2007.04.005

7. Slaby O, Bienertova-Vasku J, Svoboda M, Vyzula R. Genetic polymorphisms and microRNAs: new direction in molecular epidemiology of solid cancer. *J Cell Mol Med.* (2012) 16:8–21. doi: 10.1111/j.1582-4934.2011.01359.x

8. Hong J-S, Noh S-H, Lee J-S, Kim J-M, Hong K-C, Lee YS. Effects of polymorphisms in the porcine microRNA miR-1 locus on muscle fiber type composition and miR-1 expression. *Gene.* (2012) 506:211–6. doi: 10.1016/j.gene.2012.06.050

9. Kim J, Lim K, Hong J, Kang J, Lee Y, Hong KC, et al. polymorphism in the porcine miR Y, Hong KCoRNA miR-1 locus on muscle fiber type composition and miR-1 expression coufects on muscle fibre characteristics and meat quality. *Anim Genet.* (2015) 46:73–7. doi: 10.1111/age.12255

10. Jiang A, Yin D, Zhang L, Li B, Li R, Zhang X, et al. Parsing the microRNA genetics basis regulating skeletal muscle fiber types and meat quality traits in pigs. *Anim Genet.* (2021) 52:292–303. doi: 10.1111/age.13064

11. Xiong J. Key roles of microRNA-22 family in complex organisms inferred from its evolution. *Microrna.* (2014) 3:64–74. doi: 10.2174/2211536603666140609232335

12. Dang HQ, Xu G-l, Hou L-J, Jian X, Hong G-l, Chingyuan H, et al. MicroRNA-22 inhibits proliferation and promotes differentiation of satellite cells in porcine skeletal muscle. *J Integr Agric.* (2020) 19:225–33. doi: 10.1016/S2095-3119(19)62701-2

13. Wen W, Chen X, Huang Z, Chen D, Zheng P, He J, et al. miR-22-3p regulates muscle fiber-type conversion through inhibiting AMPK/SIRT1/PGC-1α pathway. *Anim Biotechnol.* (2021) 32:254–61. doi: 10.1080/10495398.2020.1763375

14. Offer G. Modelling of the formation of pale, soft and exudative meat: Effects of chilling regime and rate and extent of glycolysis. *Meat Sci.* (1991) 30:157–84. doi: 10.1016/0309-1740(91)90005-B

15. Cheah K, Cheah A, Crosland A, Casey J, Webb A. Relationship between Ca^{2+} release, sarcoplasmic Ca2+, glycolysis and meat quality in halothane-sensitive and halothane-insensitive pigs. *Meat Sci.* (1984) 10:117–30. doi: 10.1016/0309-1740(84)90064-0

16. Chai J, Xiong Q, Zhang P, Shang Y, Zheng R, Peng J, et al. Evidence for a new allele at the SERCA1 locus affecting pork meat quality in part through the imbalance of Ca^{2+} homeostasis. *Mol Biol Rep.* (2010) 37:613–9. doi: 10.1007/s11033-009-9872-0

17. Matsuzaka T, Shimano H, Yahagi N, Kato T, Atsumi A, Yamamoto T, et al. Crucial role of a long-chain fatty acid elongase, Elovl6, in obesity-induced insulin resistance. *Nat Med.* (2007) 13:1193–202. doi: 10.1038/nm1662

18. Li B, Dong C, Li P, Ren Z, Wang H, Yu F, et al. Identification of candidate genes associated with porcine meat color traits by genome-wide transcriptome analysis. *Sci Rep.* (2016) 6:1–12. doi: 10.1038/srep35224

19. Senyilmaz D, Virtue S, Xu X, Tan CY, Griffin JL, Miller AK, et al. Regulation of mitochondrial morphology and function by stearoylation of TFR1. *Nature.* (2015) 525:124–8. doi: 10.1038/nature14601

20. Gandra PG, Shiah AA, Nogueira L, Hogan MC, A. mitochondrialh Argeted antioxidant improves myofilament Ca2+ sensitivity during prolonged low frequency force depression at low. *J Physiol.* (2018) 596:1079–89. doi: 10.1113/JP275470

21. Liu R, Xing L, Zhou G, Zhang W. What is meat in China? *Animal Frontiers.* (2017) 7:53–6. doi: 10.2527/af.2017.0445

22. Yue T, Fang Q, Yin J, Li D, Li W. S-adenosylmethionine stimulates fatty acid metabolism-linked gene expression in porcine muscle satellite cells. *Mol Biol Rep.* (2010) 37:3143–9. doi: 10.1007/s11033-009-9893-8

23. Russell DW, Sambrook J. *Molecular Cloning: A Laboratory Manual.* New York: Cold Spring Harbor Laboratory Cold Spring Harbor (2001).

24. Rio DC, Ares M, Hannon GJ, Nilsen TW. Purification of RNA using TRIzol (TRI reagent). *Cold Spring Harb Protoc.* (2010) 2010:pdb. prot5439. doi: 10.1101/pdb.prot5439

25. Wang H, Shi L, Liang T, Wang B, Wu W, Su G, et al. MiR-696 regulates C2C12 cell proliferation and differentiation by targeting CNTFRα. *Int J Biol Sci.* (2017) 13:413. doi: 10.7150/ijbs.17508

26. Livak KJ, Schmittgen TD. Analysis of relative gene expression data using real-time quantitative PCR and the 2– ΔΔCT method. *methods.* (2001) 25:402–8. doi: 10.1006/meth.2001.1262

27. Iqbal A, Kim Y-S, Kang J-M, Lee Y-M, Rai R, Jung J-H, et al. Genome-wide association study to identify quantitative trait loci for meat and carcass quality traits in Berkshire. *Asian-Australas J Anim Sci.* (2015) 28:1537. doi: 10.5713/ajas.15.0752

28. Reardon W, Mullen A, Sweeney T, Hamill R. Association of polymorphisms in candidate genes with colour, water-holding capacity, and composition traits in bovine M. *longissimus* and *M semimembranosus. Meat Sci.* (2010) 86:270–5. doi: 10.1016/j.meatsci.2010.04.013

29. Lefaucheur L, Milan D, Ecolan P, Le Callennec C. Myosin heavy chain composition of different skeletal muscles in Large White and Meishan pigs. *J Anim Sci.* (2004) 82:1931–41. doi: 10.2527/2004.8271931x

30. Li B-j, Li P-h, Huang R-h, Sun W-x, Wang H, Li Q-f, et al. Isolation, culture and identification of porcine skeletal muscle satellite cells. *Asian-Australas J Anim Sci.* (2015) 28:1171. doi: 10.5713/ajas.14.0848

31. Purslow PP. *New Aspects of Meat Quality: From Genes to Ethics*. Woodhead Publishing (2017).

32. Karlsson A, Klont R, Fernandez X. Skeletal muscle fibres as factors for pork quality. *Livest Prod Sci.* (1999) 60:255–69. doi: 10.1016/S0301-6226(99)00098-6

33. Ljubicic V, Burt M, Lunde JA, Jasmin BJ. Resveratrol induces expression of the slow, oxidative phenotype in mdx mouse muscle together with enhanced activity of the SIRT1-PGC-1α axis. *Am J Physiol Cell Physiol.* (2014) 307:C66–82. doi: 10.1152/ajpcell.00357.2013

34. Cohen TJ, Choi M-C, Kapur M, Lira VA, Yan Z, Yao T-P. HDAC4 regulates muscle fiber type-specific gene expression programs. *Mol Cells.* (2015) 38:343. doi: 10.14348/molcells.2015.2278

35. Wen W, Chen X, Huang Z, Chen D, Yu B, He J, et al. Resveratrol regulates muscle fiber type gene expression through AMPK signaling pathway and miR-22-3p in porcine myotubes. *Anim Biotechnol.* (2022) 2022:1–7. doi: 10.1080/10495398.2022.2046599

36. Lei B, Gao S, Luo L, Xia X, Jiang S, Deng C, et al. A SNP in the miR-27a gene is associated with litter size in pigs. *Mol Biol Rep.* (2011) 38:3725–9. doi: 10.1007/s11033-010-0487-2

37. Lee JS, Kim JM, Lim KS, Hong JS, Hong KC, Lee YS. Effects of polymorphisms in the porcine micro RNA MIR206/MIR133B cluster on muscle fiber and meat quality traits. *Anim Genet.* (2013) 44:101–6. doi: 10.1111/j.1365-2052.2012.02362.x

38. Wang X, Sun S, Cao X, Gao J. Quantitative phosphoproteomic analysis reveals the regulatory networks of Elovl6 on lipid and glucose metabolism in zebrafish. *Int J Mol Sci.* (2020) 21:2860. doi: 10.3390/ijms21082860

39. Chin ER. Role of Ca^{2+}/calmodulin-dependent kinases in skeletal muscle plasticity. *J Appl Physiol.* (2005) 99:414–23. doi: 10.1152/japplphysiol.00015.2005

frontiers | Frontiers in Genetics

TYPE Original Research
PUBLISHED 05 August 2022
DOI 10.3389/fgene.2022.949309

Check for updates

OPEN ACCESS

EDITED BY
Nelida Rodriguez-Osorio,
Universidad de la República, Uruguay

REVIEWED BY
Rodrigo Urrego,
CES University, Colombia
Gokhan Akkoyunlu,
Akdeniz University, Turkey

*CORRESPONDENCE
David G. Riley,
david.riley@ag.tamu.edu

SPECIALTY SECTION
This article was submitted to Livestock Genomics,
a section of the journal
Frontiers in Genetics

RECEIVED 20 May 2022
ACCEPTED 30 June 2022
PUBLISHED 05 August 2022

CITATION
Baker EC, Earnhardt AL, Cilkiz KZ, Collins HC, Littlejohn BP, Cardoso RC, Ghaffari N, Long CR, Riggs PK, Randel RD, Welsh TH and Riley DG (2022), DNA methylation patterns and gene expression from amygdala tissue of mature Brahman cows exposed to prenatal stress.
Front. Genet. 13:949309.
doi: 10.3389/fgene.2022.949309

COPYRIGHT
© 2022 Baker, Earnhardt, Cilkiz, Collins, Littlejohn, Cardoso, Ghaffari, Long, Riggs, Randel, Welsh and Riley. This is an open-access article distributed under the terms of the Creative Commons Attribution License (CC BY). The use, distribution or reproduction in other forums is permitted, provided the original author(s) and the copyright owner(s) are credited and that the original publication in this journal is cited, in accordance with accepted academic practice. No use, distribution or reproduction is permitted which does not comply with these terms.

DNA methylation patterns and gene expression from amygdala tissue of mature Brahman cows exposed to prenatal stress

Emilie C. Baker[1], Audrey L. Earnhardt[1,2,3], Kubra Z. Cilkiz[1], Haley C. Collins[1], Brittni P. Littlejohn[1,3], Rodolfo C. Cardoso[1], Noushin Ghaffari[4], Charles R. Long[1,3], Penny K. Riggs[1], Ronald D. Randel[1,3], Thomas H. Welsh Jr[1,2] and David G. Riley[1]*

[1]Department of Animal Science, Texas A&M University, College Station, TX, United States, [2]Texas A&M AgriLife Research, College Station, TX, United States, [3]Texas A&M AgriLife Research, Overton, TX, United States, [4]Department of Computer Science, Prairie View A&M University, Prairie View, TX, United States

Prenatal stress can alter postnatal performance and temperament of cattle. These phenotypic effects may result from changes in gene expression caused by stress-induced epigenetic alterations. Specifically, shifts in gene expression caused by DNA methylation within the brain's amygdala can result in altered behavior because it regulates fear, stress response and aggression in mammals Thus, the objective of this experiment was to identify DNA methylation and gene expression differences in the amygdala tissue of 5-year-old prenatally stressed (PNS) Brahman cows compared to control cows. Pregnant Brahman cows (n = 48) were transported for 2-h periods at 60 ± 5, 80 ± 5, 100 ± 5, 120 ± 5, and 140 ± 5 days of gestation. A non-transported group (n = 48) were controls (Control). Amygdala tissue was harvested from 6 PNS and 8 Control cows at 5 years of age. Overall methylation of gene body regions, promoter regions, and cytosine-phosphate-guanine (CpG) islands were compared between the two groups. In total, 202 genes, 134 promoter regions, and 133 CpG islands exhibited differential methylation (FDR ≤ 0.15). Following comparison of gene expression in the amygdala between the PNS and Control cows, 2 differentially expressed genes were identified (FDR ≤ 0.15). The minimal differences observed could be the result of natural changes of DNA methylation and gene expression as an animal ages, or because this degree of transportation stress was not severe enough to cause lasting effects on the offspring. A younger age may be a more appropriate time to assess methylation and gene expression differences produced by prenatal stress.

KEYWORDS

amygdala, Brahman, DNA methylation, gene expression, prenatal stress

1 Introduction

The amygdala is a cell mass composed of nuclei that are classified into three cell groups located in the temporal cortex of the brain: 1) the basolateral amygdala; 2) cortical like cells; and 3) centromedial cells (Yang and Wang, 2017). The cell groups have neural connections that receive stimuli from areas of the brain including the sensory cortex, the prefrontal cortex, and the hippocampus. It is through those connections the amygdala processes and influences emotions including fear, anxiety, and stress response (Rasia-Filho et al., 2000; Davis and Whalen, 2001). Loss of amygdala function causes emotional based memory loss and aberrant social behavior (Fine and Blair, 2000). In contrast, increased amygdala activity has been linked to various disorders including schizophrenia and bipolar disorder (Lawrie et al., 2003; Kalmar et al., 2009). Increased activation of amygdala neurons can increase vigilance, anxiety, and stress.

The amygdala is a part of the body's system for detecting stressful and frightening stimuli and then initiating the body's coping response (LeDoux, 1994). Chronic stress can cause increased anxiety and behavior changes potentially due to hyperexcitability of the amygdala (Rosenkranz et al., 2010). Prenatal stress influences how the amygdala functions by shaping the development and connectivity within it and the tissues it communicates with (Kraszpulski et al., 2006; Scheinost et al., 2016). Shifts in gene expression in the amygdala of prenatally stressed offspring have been observed in mice and sheep (Ward et al., 2000; Petit et al., 2015). The shifts of gene expression in the amygdala may be responsible for the behavioral differences observed in prenatally stressed offspring. Prenatally stressed rhesus monkeys showed altered social behavior including a decrease in play and an increase in clinging to others. When alone the prenatally stressed monkeys showed more inactivity relative to those who did not experience prenatal stress (Clarke et al., 1996). Calves subjected to prenatal transportation stress showed an increase in exit velocity from a restraining chute as well as an increase in temperament score (Littlejohn et al., 2016).

Gene expression shifts in the amygdala of prenatally stressed animals could result from stress-induced DNA methylation alterations. Prenatal stress in Brahman cattle resulted in changes of DNA methylation patterns of leukocytes from 28-day old bull and heifer calves, with differences persisting through 5 years of age (Littlejohn et al., 2018; Baker et al., 2020; Cilkiz et al., 2021). Shifts in DNA methylation patterns have been linked to prenatal stress and changes in temperament of the offspring (Littlejohn et al., 2016; Gartstein and Skinner, 2018; Littlejohn et al., 2018). Methylation of DNA is the addition of a methyl group to the nitrogenous bases in the DNA sequence. In mammals, the addition of the methyl group often occurs to the 5′ carbon of the nitrogenous base cytosine (Razin and Riggs, 1980). Methylation is primarily found within Cytosine-Phosphate-Guanine (CpG) dinucleotides. Methylated cytosines can lead to inhibition of gene expression, while demethylation can promote gene expression. (Tate and Bird, 1993). The methylome changes drastically throughout fetal development and therefore can be influenced by maternal environment. Methylation patterns continue to change postnatally (Salpea et al., 2012). These stress-induced epigenetic modifications can be transgenerational and have the potential to affect many generations in the production system (Feeney et al., 2014; Thompson et al., 2020).

In cattle, the amygdala tissue had the highest percent genome wide DNA methylation relative to other tissues in the limbic system (Cantrell et al., 2019). Considering the amygdala's important role in behavioral and stress response, modifications to the DNA methylation patterns and gene expression within the amygdala could cause phenotypic differences in the offspring. The long-term phenotypic changes observed in prenatally stressed livestock, including temperament changes, can impact production, animal welfare, and profitable traits (Lay et al., 1997; Cooke, 2014; Serviento et al., 2020). Suckling calves that were exposed to prenatal stress were more temperamental and have a greater serum cortisol concentration than control calves. The early life difference in serum cortisol concentration appears to have been sustained cows selected for harvest at 5 years of age (Control: 29.5 ± 9.8 ng/ml; Prenatally Stressed: 40.34 ± 5.2 ng/ml).

Early life alterations in DNA methylation patterns in humans has measurable effects on behavior and is associated with depression and anxiety (Vonderwalde, 2019). The effects of prenatal stress on methylation and gene expression patterns in the amygdala have been well studied in mice, but less so in livestock species (Kundakovic and Jaric, 2017). Thus, the objective of this study was to investigate whether prenatal stress alters DNA methylation and gene expression in the amygdala of 5-year-old prenatally stressed Brahman cows relative to control cows.

2 Methods and materials

All procedures were done in compliance with the Guide for the Care and Use of Agricultural Animals in Research and Teaching (Federation of Animal Science Societies, 2020), and its earlier versions, and approved by the Texas A&M AgriLife Research Animal Care and Use Committee.

2.1 Animal procedures

Details of the experimental design and animal handling were described in Littlejohn et al. (2016), Littlejohn et al. (2018), and Cilkiz et al. (2021). Briefly, 96 cows were determined pregnant by rectal palpation 45 days after the breeding date. Cows were then

assigned randomly to groups with respect to age, parity, and temperament assessment. The treatment group (n = 48) was transported for a duration of 2 h on 60 ± 5, 80 ± 5, 100 ± 5, 120 ± 5, and 140 ± 5 days of gestation (Price et al., 2015). The physiological and metabolic variables measured in the PNS cows were: vaginal temperature (recorded by use of an indwelling vaginal temperature monitoring device), the percentage of weight lost (shrink), and serum concentrations of cortisol and glucose. The dams of the cows used in the present study experienced significantly increased vaginal temperature, shrink, and serum concentrations of cortisol and glucose in response to the transportation events. The findings of Price et al. (2015) reaffirmed our prior reports that transportation constitutes a stressor for pregnant cattle and thereby could influence post-natal development and physiology (Lay et al., 1997; Chen et al., 2015). A group of non-transported cows (n = 48) was maintained as a control. Both groups were managed together under the same nutrient and environmental conditions at the Texas A&M AgriLife Research and Extension Center at Overton.

Twenty bull calves and 21 heifer calves were born from the transported cows (PNS), and 26 bull and 18 heifer calves were born to cows that had not been transported (Control). The 39 heifer calves entered a development regimen typical of cows in the herd, which included exposure to bulls for mating at 1 year of age and annually thereafter. Of those females remaining when the group was 5 years old, 8 Control and 6 PNS nonpregnant cows were slaughtered and the whole amygdala from each was harvested and stored at −80°C.

2.2 RNA and DNA extraction

Frozen amygdala tissue samples were submitted to the Texas A&M Institute for Genome Sciences and Society (TIGSS) Experimental Genomics Core Laboratory for RNA sequence analysis. The TRIzol Plus RNA Purification Kit (Thermo Scientific, Waltham, MA) was utilized to extract purified RNA from each amygdala sample (approximately 20 mg per sample). Quantification of purified RNA was performed with the Qubit RNA Fluorometric Assay Kit (Thermo Scientific) and the quality was assessed using the RNA ScreenTape Assay (Agilent Technologies, Santa Clara, CA, United States). The RNA was prepared and sequenced with the HS protocol of the Illumina TruSeq Stranded mRNA library preparation kit and mRNA isolated with globin and ribosomal RNA depletion. Paired-end sequencing by the NovaSeq 6000 Sequencing System Illumina Inc.) produced raw RNA FASTQ files as the final output.

Approximately 20 mg of each amygdala tissue sample were digested to extract DNA for methylation analysis. First, 150 µl of sodium chloride-Tris-EDTA buffer, 25 µl of Proteinase K (20 mg/ml) and 25 µl 20% sodium dodecyl sulfate were added to the microcentrifuge tube containing the tissue and gently mixed. Samples were then incubated in a 56°C water bath for 2 h, then 20 µl of RNAse A (10 mg/ml) were added to the sample tubes and the mixture was incubated at 37°C for 30 min. Purified DNA was isolated from the digested amygdala tissue using the protocol for the GeneJET Genomic DNA Purification Kit (Thermo Scientific). Once purified, DNA was quantified with a NanoDrop Spectrophotometer (NanoDrop Technologies, Rockland, DE) and stored at −80°C until further analysis.

2.3 DNA methylation library preparation and sequence alignments

Isolated DNA was submitted to Zymo Research (Irvine, CA) for reduced representation bisulfite sequencing methylation analysis. Input DNA was digested with 60 units of TaqαI followed by 30 units of MspI, and then purified with DNA Clean & ConcentratorTM-5. Purified DNA was then ligated to adapters containing 5′-methyl-cytosine. Adapter-ligated fragments of 150–250 bp and 250 to 350 bp were recovered using the ZymocleanTM Gel DNA Recovery Kit. Fragments were then bisulfite-treated using the EZ DNA Methylation-LightningTM Kit followed by preparative-scale PCR and purification.

Standard Illumina base calling was used to identify sequence reads from bisulfite-treated libraries and the raw FASTQ files were trimmed with the TrimGalore 0.6.4 software based upon adapter content and quality. The trimmed sequences were then aligned to the *Bos taurus* genome (ARS-UCD1.2) (Rosen et al., 2020) using Bismark 0.19.0 (Babrahman Bioinformatics, Cambridge, United Kingdom). Methylated and unmethylated read totals at each CpG site were quantified from the aligned binary alignment map (BAM) files using MethylDackel 0.5.0 (Zymo Research).

2.4 DNA methylation analysis

2.4.1 Feature specific

Overall methylation of defined features was compared between the PNS and Control groups. The features analyzed included gene bodies, promoter regions (defined as 1,000 bp upstream to 500 bp downstream of the transcription start site), and CpG islands. These features are CpG rich areas of the genome that are vital to epigenetic regulation (Papin et al., 2021). Binary alignment map files that were produced by Zymo Research were read into the SeqMonk program (Babrahman Bioinformatics, Cambridge, United Kingdom). Each feature type was defined, and a bisulfite feature methylation pipeline (SeqMonk) was applied with the requirement of the sites within the feature to have at least 5x coverage, a threshold utilized in other livestock methylation studies (Livernois et al., 2021). Reduced representation bisulfite sequencing can provide

accurate analysis at lower coverage, allowing for more biological replicates (Ziller at al., 2015; Crary-Dooley et al., 2017). The pipeline calculates a percentage methylation for each cytosine within the feature and averages these to give an overall value. After the quantification pipeline was applied, a logistic regression was fit, and chi square tests for each feature was performed with the contrast of Control minus PNS. Because this experiment was a very early investigation of methylation in this tissue and species, the false discovery rate (Benjamini and Hochberg, 1995) was controlled at 0.15.

2.4.2 Genome wide methylation

Individual CpG sites across the genome, that is, without regard to predefined features, were also tested. Using the information provided by the methylation call tables the total coverage count, percent methylation, methylated counts, and unmethylated counts were calculated. Sites were filtered in edgeR (Robinson et al., 2010) by requiring 5x coverage at the site in all 14 samples as well as removing sites that were always methylated or unmethylated. A negative binomial generalized linear model was fit to the methylation counts for each site, and a likelihood ratio test was performed at each site using the contrast of Control minus PNS. The false discovery rate (Benjamini and Hochberg, 1995) was controlled at 0.15. Locations in the genome of the significant sites were identified using Ensembl BioMart tool, Ensembl Release 104 (Howe et al., 2020). Multi-Dimensional Scaling (MDS) analysis and plotting were conducted utilizing the M values. The M values are the base 2 logit transformation of the proportion of methylated to unmethylated signal at each locus.

2.5 RNA sequence analysis and differential gene expression

Raw RNA FASTQ files were subjected to a 3-step pipeline to generate gene counts. The Trim Galore program (Babrahman Bioinformatics) was used to remove any remaining adapter content. The Spliced Transcripts Alignment to a Reference (STAR) (Dobin et al., 2012) program was used to first create an index file using the ARS-UCD1.2 genome assembly. The trimmed reads were then aligned to the index using the default STAR parameters which had been optimized for alignment of mammalian genomes (Dobin et al., 2012). The BAM files produced by STAR were subjected to procedures of the HTSeq program (Anders et al., 2014) to generate gene counts for each sample.

Differential gene expression analysis was performed in edgeR using a matrix consisting of gene counts from each sample. Genes with no counts were filtered and the remaining counts were normalized using the trimmed mean of M-values method. Tagwise dispersion was calculated, and a negative binomial generalized log-linear model was fit to the read counts for each gene. Finally, a likelihood ratio test corresponding to each gene was calculated with a contrast of Control minus PNS. The false discovery rate was controlled at 0.15 (Benjamini and Hochberg, 1995). Multi-dimensional scaling analysis and plotting were calculated utilizing the normalized read counts.

2.6 Cell processes and pathway identification

Further analysis of the significant features and differentially expressed genes was conducted with the PANTHER Classification System 16.0 (Thomas et al., 2003) to identify cellular processes and biological pathways corresponding to identified genes.

3 Results and Discussion

3.1 DNA methylation

3.1.1 Feature specific-bodies

Gene bodies of 26,900 genes were assessed for methylation status. Of those, 202 were differentially methylated between the PNS and Control (FDR ≤ 0.15), with 104 having increased methylation in the PNS group and 98 having decreased methylation (Supplementary Table S1). The top 10 differentially methylated genes in amygdala tissue of prenatally stressed mature Brahman cows relative to Control cows are presented in Table 1. A heatmap of the mean methylation levels of the 202 differentially methylated genes in each sample is presented in Figure 1. Gene body methylation can lead to a decrease in gene expression which can then impact cellular processes (Klose and Bird, 2006). Through use of the PANTHER Classification System, numerous cell processes and biological pathways, including response to stimulus, growth, and metabolic processes, were associated with the differentially methylated genes (Supplementary Table S2). *Dual specificity phosphatase 26* (DUSP26) is active in the oxidative stress response biological pathway, which, in the amygdala contributes to pain response and pain related behavior (Sagalajev et al., 2018). Another highlighted pathway is the ubiquitin proteasome pathway, which is involved in the formation of fear memory within the amygdala (Jarome et al., 2011). Deviations in methylation patterns of genes involved in these pathways could result in altered response to fear and pain in animals.

3.1.2 Feature specific--promoter regions

A total of 134 gene promoters were identified as differentially methylated (FDR ≤ 0.15) in the amygdala tissue of PNS cows when compared to the Control group. Seventy promoter regions had increased methylation in the PNS group, and 64 had

TABLE 1 Top 10 differentially methylated genes in amygdala tissue of prenatally stressed mature to Control cows.

Gene name	Chr	FDR	Difference[a]
Eukaryotic translation initiation factor 5A2	1	0.044	15.86
Homeobox D1	2	0.061	11.45
Centrosomal protein 41	4	0.044	25.61
Salvador family WW domain containing protein 1	10	0.003	−17.05
Brain expressed associated with NEDD4 1	18	0.003	15.87
Translocase of outer mitochondrial membrane 40	18	0.045	17.81
5S ribosomal RNA	21	5.68E-18	−3.34
Ornithine aminotransferase	26	0.047	12.57
5.8S ribosomal RNA	27	0.003	−1.00
Mitochondrial ribosomal protein L21	29	0.044	29.03

[a]A positive (negative) difference indicates the prenatally stressed cows had decreased (increased) methylation of the gene relative to the Control cows.

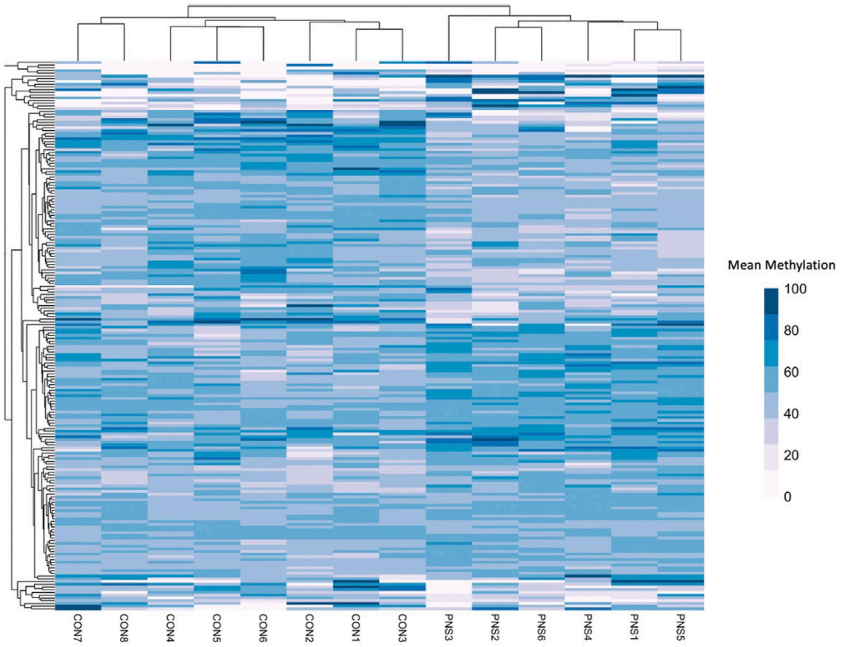

FIGURE 1
Heatmap showing the mean methylation of the differentially methylated (n = 202) genes in the prenatally Stressed (PNS) cows and the Control (CON).

decreased methylation (Supplementary Table S3). The top 10 (lowest FDR value) differentially methylated promoter regions are presented in Table 2. Methylation shifts in promoter regions of genes impact gene expression mainly by influencing the accessibility of the promoter region to transcription factors (Klose and Bird, 2006). One stress-related gene that had increased methylation in its promoter region was *Brain derived neutrophic factor* (*BDNF*). This gene is critical for neural development and function of the amygdala. Alterations of methylation patterns of *BDNF* have been associated with increased anxiety behavior in rats and psychiatric disorders in humans (Redlich et al., 2020). Increased methylation of *BDNF* was observed in individuals that experienced early life stress (Doherty et al., 2016; Blaze et al., 2017). Because of the relationship between *BDNF*, aberrant behavior, and changes in DNA methylation, the methylation of *BDNF* is considered a

TABLE 2 Top 10 differentially methylated promoter[a] regions of genes in amygdala of prenatally stressed mature Brahman cows relative to Control cows.

Gene name	Chr	FDR	Difference[b]
Oxysterol binding protein like 8	5	0.005	9.88
RNA terminal phosphate cyclase like 1	8	0.001	−13.90
Maspardin	10	0.0002	23.28
WD repeat domain 34	11	0.005	10.08
Crumbs cell polarity complex component 1	16	0.005	−6.87
5S ribosomal RNA	21	0.003	-2.24
Dual Specificity Phosphatase 26	27	0.006	13.11
N-deacetylase and N-sulfotransferase 2	28	0.002	−14.98
Annexin A8 like 1	28	0.003	23.37
Hepatic and glial cell adhesion molecule	29	0.002	14.75

[a]Promoter regions were defined as 1,000 base pairs upstream and 500 base pairs downstream from the transcription start site of the gene.
[b]A positive (negative) difference indicates the prenatally stressed cows had decreased (increased) methylation of the promoter region relative to control cows.

TABLE 3 Top 10 differentially methylated CpG Islands[a] in amygdala tissue of prenatally stressed mature Brahman cows relative to Control cows.

Chr	Start	End	FDR	Difference[b]
4	94192085	94192593	0.040	26.19
7	106955324	106955725	0.058	−35.11
10	43554822	43555817	0.018	−18.35
16	47324909	47326146	0.058	−16.63
18	34194169	34195605	0.003	15.87
19	49916310	49917178	0.058	20.85
20	71009252	71009654	0.058	30.51
21	33001944	33003266	6.99e-18	−3.34
21	33023989	33026059	0.002	2.36
29	42549665	42551050	0.002	14.03

[a]Cytosine-Phosphate-Guanine rich locations within the genome.
[b]A positive (negative) difference indicates the prenatally stressed cows had decreased (increased) methylation of the promoter region relative to control cows.

potential biomarker for early life stress in mammals (Kundakovic et al., 2015). Changes in methylation of this gene could be responsible for the temperament differences that have been observed in prenatally stressed livestock. The stressed group also had decreased methylation of the promoter region of *synapse 1* (*SYN1*). This gene has a role in synaptic function in the amygdala. Male mice who were exposed to early life stress showed an increase in synapse formation and altered synaptic responses (Guadagno et al., 2020). Shifts in gene expression of *SYN1* because of methylation changes could result in altered brain plasticity in the prenatally stress cows. Rats subjected to early maternal separation exhibited increased methylation of *SYN1* (Park et al., 2014) which is contrary to our results of decreased methylation was reported.

3.1.3 Feature specific--CpG islands

Islands of CpG are often located in promoters of genes, are typically resistant to DNA methylation, and are rarely found in tissue specific genes (Bird, 1986). Because of this it is hypothesized that these regions are in genes that are regularly used in cell function and do not need to be repressed (Bird, 1986). In total 22,188 CpG islands were tested and 133 (FDR ≤ 0.15) were differentially methylated; 77 had increased methylation in the PNS cows and 56 had decreased methylation (Supplementary Table S4). Table 3 has the locations of the top 10 (lowest FDR values) differentially methylated CpG islands identified. A CpG island located within *BDNF* also had increased methylation in the PNS while a CpG island located within the defined promoter region of *SYN1* had decreased methylation. The decrease in methylation of the CpG island within *SYN1* is consistent with what has been reported in aging mice, where decreased methylation of CpG islands within the promoter region coincides with an increase in expression of this gene (Haberman et al., 2012). A CpG island with decreased methylation was located within *Nuclear receptor corepressor 2* (*NCOR2*), which is involved in amygdala development and anxiety behavior (Jessen et al., 2010). The influence of DNA methylation on gene expression of *NCOR2* is relatively unknown, but the location of a CpG island in the regulatory region of the gene suggests the possibility of epigenetic control.

3.1.4 Genome wide methylation

Minimal methylation differences of gene bodies, promoter regions and CpG islands were observed in amygdala tissue between PNS and Control cows at 5 years of age when methylation across the genome was considered in its entirety. Of the genome wide CpG sites, 63,255 sites passed filtering. Only 29 of those sites (Supplementary Table S5) were differentially methylated between the Control and PNS (FDR ≤ 0.15). The significant sites were only 0.046% of the sites tested, indicating that substantial differences in global CpG methylation were not observed between the PNS and Control groups. Visualization of the lack of distinction between treatments is shown in the MDS plot (Figure 2). No distinct grouping of PNS and Control samples occurred and many of the samples from the two treatments were closely positioned. The proximity of the samples to each other in the MDS plot reflects the minimal differences in methylation between groups when evaluated globally. These results differ from analysis of DNA methylation of leukocytes in prenatally stressed Brahman bulls and heifers at 28 days of age which revealed vast differences relative to the Control, some of which were identified in the heifer calves (the cows in this study) and were found in leukocytes 5 years later (Littlejohn et al., 2018; Baker et al., 2020; Cilkiz et al., 2021).

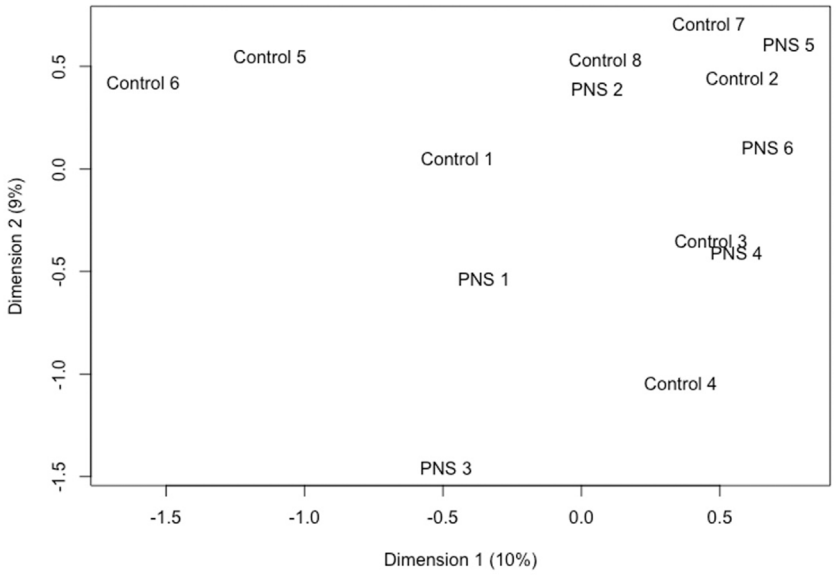

FIGURE 2
Multidimensional scaling plot utilizing the base 2 logit transformation of the proportion of methylated signal at each locus to plot distances between methylation profiles (M-Values) of amygdala tissue of 5-year-old prenatally stressed (PNS) Brahman cows relative to control cows.

Changes in the epigenetic landscape continue postnatally, with evident differences observed in saliva samples from infants from 6 to 52 weeks of age (Wikenius et al., 2019). In humans, a general trend of demethylation is observed with aging, but some sites that have low methylation at a young age do increase in methylation over time (Wilson et al., 1987; Jones et al., 2015). Differences in methylation caused by the prenatal stress could be present at an early age in cattle but diminish over time. However, severe prenatal stress (i.e., famine and extreme weather) led to lasting DNA methylation changes that were transgenerational (Heijmans et al., 2008; Cao-Lei et al., 2014). The severity of prenatal stress can result in very different outcomes of changes in methylation patterns in the brain (Mychasiuk et al., 2011). Transportation stress during mid to late gestation might not be a severe enough stress to cause enduring epigenetic changes in amygdala tissue in cattle that persist throughout life.

3.2 Gene expression

From expression analyses, 22,867 genes remained after filtering. Even in the context of a permissive FDR (<0.15), only two genes were differentially expressed in the amygdala of the PNS cows compared to the Controls. The *Solute carrier family 28 member 3* (*SLC28A3*) had decreased expression in the PNS cows relative to the Control, while the *Fc fragment of IgG receptor IIa* (*FCGR2A*) had increased expression. Fc fragment of IgG receptor IIa has an essential role in protecting the body from foreign antigens (Hibbs et al., 1988). Deletion of *FCGR2A* inhibited the invasion of glimoa cells into the brain suggesting the gene product is important for transportation across the blood brain barrier. Members of the solute carrier family are active in the brain, aiding in the transport of hormones, sugars, and amino acids; however, the role of *SLC28A3* in the brain and stress response has not been documented (Hu et al., 2020). The lack of differences is illustrated by the MDS plot (Figure 3) which shows no distinct clustering and some overlap of individual samples from the two groups. There were no methylation differences within the promoter region or gene body of these two differentially expressed genes.

Prenatally stressed Brahman cows had only slight differences in gene expression relative to Controls at 5 years of age. In contrast, in rats, prenatal stress has caused gene expression disturbances in the brain that persisted into adulthood (Fumagalli et al., 2005; Baier et al., 2015). Similar to the DNA methylation results, the timing and severity of a prenatal stressor can dictate the effect on gene expression. Maternal nutrient restriction in cattle has resulted in varying gene expression changes in the offspring depending on timing of restriction during gestation and the tissue analyzed (Mohrhauser et al., 2015; Sanglard et al., 2018). The stress caused by transportation during mid to late gestation may be insufficient to influence gene expression in the offspring. Expression of genes at the proper level is complex, regulated by many different factors, and varies with aging (Berchtold et al., 2008). Corrections may have occurred over time to compensate for aberrant gene expression caused by prenatal stress.

This is this first study to incorporate the effect of prenatal stress on DNA methylation and gene expression in the amygdala

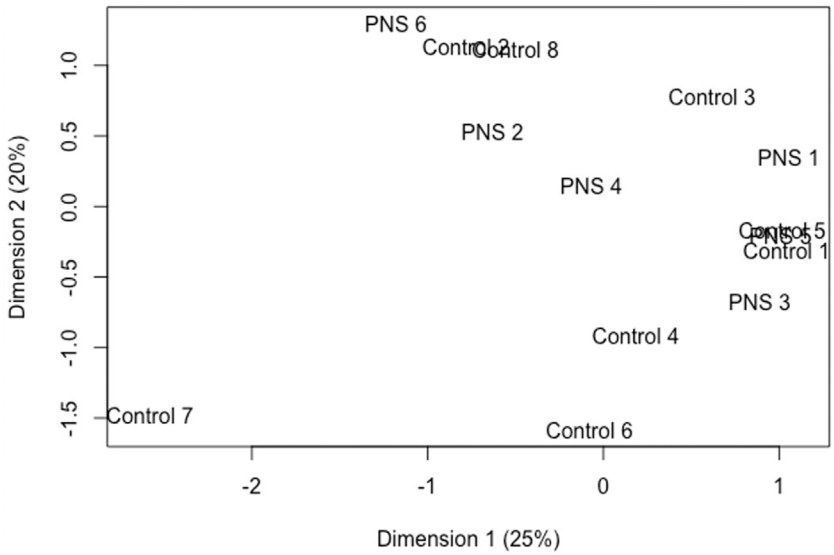

FIGURE 3
Multidimensional scaling plot utilizing normalized read counts to plot distances between expression profiles of amygdala tissue of 5-year-old prenatally stressed (PNS) Brahman cows relative to Control cows.

of cattle. Overall methylation of important genes and promoter regions were significantly different between the PNS and Control groups. While gene expression analysis resulted in only two significant genes, the two genes are involved in essential biological functions. These novel results provide a foundation for future research on how prenatal stress effects the amygdala in cattle.

4 Conclusion

Gene expression and DNA methylation comparison of amygdala tissue from mature Brahman cows that were prenatally stressed relative to non-stressed mature Control cows revealed minimal differences between the groups. A small number of individual CpG sites and a low proportion of genes, promoters and CpG islands were differentially methylated. Two genes were differentially expressed in amygdala tissue when PNS and Control groups were compared. Methylation controls gene expression of many genes; however, no overlap between differentially methylated genes and differentially expressed genes was observed. Since both DNA methylation and gene expression are complex mechanisms that shift and adapt over time, it is feasible that any differences that were caused by the prenatal stress are no longer present at 5 years of age. The timing and severity of the stressor may also be a major influence on the extent of the alterations. Therefore, prenatal transportation stress during mid to late gestation may not be significant enough to cause lasting effects. Increasing the severity of the transportation stress, such as transport for an extended period and over poorer quality of roadways could potentially result in lasting effects. Also, further investigation is needed to determine if there are differences present at younger ages, which could cause expression changes during important postnatal developmental periods. However, much of the current knowledge of the effects of prenatal stress on methylation is from model organisms; thus, the novel information and candidate regions and genes reported are valuable for understanding the effects stress induced epigenetic modifications have on livestock.

Data availability statement

The datasets presented in this study can be found in online repositories. The names of the repository/repositories and accession numbers can be found below: https://www.ncbi.nlm.nih.gov/; SAMN29182872 - SAMN29182885. Data has been uploaded to the NCBI SRA under BioProject PRJNA850510.

Ethics statement

The animal study was reviewed and approved by the Texas A&M AgriLife Animal Care and Use Committee.

Author contributions

RR, TW, and CL designed the study. EB, AE, KC, HC, RC, PR, TW, RR, and DR collected samples. EB, AE, KC, and HCC

conducted data analyses under supervision of DR and NG. EB wrote the manuscript with input from all authors.

Funding

This work was supported by the USDA-NIFA [2018-67015-28131], Western Regional Project TEX03212, Hatch Projects H-9022 and H-TEX09377, Texas A&M University One Health Initiative and Texas A&M AgriLife Research, Overton.

Acknowledgments

The authors thank Don Neuendorff, Andy Lewis, and Catherine Wellman (Texas A&M AgriLife Research Center, Overton, TX), Dr. Keith Booher (Zymo Research Corporation), Dr. Andrew Hillhouse, Sarah Sharpton (Texas A&M Institute for Genome Sciences and Society) for contributing their expertise. The authors thank Lacey Quail, Mari Mund Calloway, Dr. Rui d'Orey Branco, Charlotte Whitaker and Ray Riley for assistance with collection of tissue samples at the TAMU Rosenthal Meat Science & Technology Center.

Conflict of interest

The authors declare that the research was conducted in the absence of any commercial or financial relationships that could be construed as a potential conflict of interest.

Publisher's note

All claims expressed in this article are solely those of the authors and do not necessarily represent those of their affiliated organizations, or those of the publisher, the editors and the reviewers. Any product that may be evaluated in this article, or claim that may be made by its manufacturer, is not guaranteed or endorsed by the publisher.

Supplementary material

The Supplementary Material for this article can be found online at: https://www.frontiersin.org/articles/10.3389/fgene.2022.949309/full#supplementary-material

References

Anders, S., Pyl, P. T., and Huber, W. (2014). HTSeq—a Python framework to work with high-throughput sequencing data. *Bioinformatics* 31 (2), 166–169. doi:10.1093/bioinformatics/btu638

Baier, C. J., Pallarés, M. E., Adrover, E., Monteleone, M. C., Brocco, M. A., Barrantes, F. J., et al. (2015). Prenatal restraint stress decreases the expression of alpha-7 nicotinic receptor in the brain of adult rat offspring. *Stress* 18 (4), 435–445. doi:10.3109/10253890.2015.1022148

Baker, E. C., Cilkiz, K. Z., Riggs, P. K., Littlejohn, B. P., Long, C. R., Welsh, T. H., et al. (2020). Effect of prenatal transportation stress on DNA methylation in Brahman heifers. *Livest. Sci.* 240, 104116. doi:10.1016/j.livsci.2020.104116

Benjamini, Y., and Hochberg, Y. (1995). Controlling the false discovery rate: A practical and powerful approach to multiple testing. *J. R. Stat. Soc. Ser. B* 57 (1), 289–300. doi:10.1111/j.2517-6161.1995.tb02031.x

Berchtold, N. C., Cribbs, D. H., Coleman, P. D., Rogers, J., Head, E., Kim, R., et al. (2008). Gene expression changes in the course of normal brain aging are sexually dimorphic. *Proc. Natl. Acad. Sci. U. S. A.* 105(40), 15605–15610. doi:10.1073/pnas.0806883105

Bird, A. P. (1986). CpG-rich islands and the function of DNA methylation. *Nature* 321 (6067), 209–213. doi:10.1038/321209a0

Blaze, J., Asok, A., Borrelli, K., Tulbert, C., Bollinger, J., Ronca, A. E., et al. (2017). Intrauterine exposure to maternal stress alters Bdnf IV DNA methylation and telomere length in the brain of adult rat offspring. *Int. J. Dev. Neurosci.* 62 (1), 56–62. doi:10.1016/j.ijdevneu.2017.03.007

Cantrell, B., Lachance, H., Murdoch, B., Sjoquist, J., Funston, R., Weaber, R., et al. (2019). Global DNA Methylation in the limbic system of cattle. *Epigenomes* 3 (2), 8. doi:10.3390/epigenomes3020008

Cao-Lei, L., Massart, R., Suderman, M. J., Machnes, Z., Elgbeili, G., Laplante, D. P., et al. (2014). DNA methylation signatures triggered by prenatal maternal stress exposure to a natural disaster: Project Ice Storm. *PLOS ONE* 9 (9), e107653. doi:10.1371/journal.pone.0107653

Chen, Y., Arsenault, R., Napper, S., and Griebel, P. (2015). Models and methods to investigate acute stress responses in cattle. *Animals* 5 (4), 1268–1295. doi:10.3390/ani5040411

Cilkiz, K. Z., Baker, E. C., Riggs, P. K., Littlejohn, B. P., Long, C. R., Welsh, T. H., et al. (2021). Genome-wide DNA methylation alteration in prenatally stressed Brahman heifer calves with the advancement of age. *Epigenetics* 16 (5), 519–536. doi:10.1080/15592294.2020.1805694

Clarke, A. S., Soto, A., Bergholz, T., and Schneider, M. L. (1996). Maternal gestational stress alters adaptive and social behavior in adolescent rhesus monkey offspring. *Infant Behav. Dev.* 19 (4), 451–461. doi:10.1016/S0163-6383(96)90006-5

Cooke, R. F. (2014). Bill E. Kunkle Interdisciplinary Beef Symposium: Temperament and acclimation to human handling influence growth, health, and reproductive responses in *Bos taurus* and *Bos indicus* cattle. *J. Anim. Sci.* 92 (12), 5325–5333. doi:10.2527/jas.2014-8017

Crary-Dooley, F. K., Tam, M. E., Dunaway, K. W., Hertz-Picciotto, I., Schmidt, R. J., LaSalle, J. M., et al. (2017). A comparison of existing global DNA methylation assays to low-coverage whole-genome bisulfite sequencing for epidemiological studies. *Epigenetics* 12 (3), 206–214. doi:10.1080/15592294.2016.1276680

Davis, M., and Whalen, P. J. (2001). The amygdala: vigilance and emotion. *Mol. Psychiatry* 6 (1), 13–34. doi:10.1038/sj.mp.4000812

Dobin, A., Davis, C. A., Schlesinger, F., Drenkow, J., Zaleski, C., Jha, S., et al. (2012). Star: ultrafast universal RNA-seq aligner. *Bioinformatics* 29 (1), 15–21. doi:10.1093/bioinformatics/bts635

Doherty, T. S., Forster, A., and Roth, T. L. (2016). Global and gene-specific DNA methylation alterations in the adolescent amygdala and hippocampus in an animal model of caregiver maltreatment. *Behav. Brain Res.* 298 (Pt A), 55–61. doi:10.1016/j.bbr.2015.05.028

Federation of Animal Science Societies (FASS) (2020). *Guide for the care and use of agricultural animals in research and teaching*. 4th ed. Champaign, IL: FASS.

Feeney, A., Nilsson, E., and Skinner, M. K. (2014). Epigenetics and transgenerational inheritance in domesticated farm animals. *J. Anim. Sci. Biotechnol.* 5 (1), 48. doi:10.1186/2049-1891-5-48

Fine, C., and Blair, R. J. R. (2000). The cognitive and emotional effects of amygdala damage. *Neurocase* 6 (6), 435–450. doi:10.1080/13554790008402715

Fumagalli, F., Bedogni, F., Slotkin, T. A., Racagni, G., and Riva, M. A. (2005). Prenatal stress elicits regionally selective changes in basal FGF-2 gene expression in adulthood and alters the adult response to acute or chronic stress. *Neurobiol. Dis.* 20 (3), 731–737. doi:10.1016/j.nbd.2005.05.005

Gartstein, M. A., and Skinner, M. K. (2018). Prenatal influences on temperament development: The role of environmental epigenetics. *Dev. Psychopathol.* 30 (4), 1269–1303. doi:10.1017/s0954579417001730

Guadagno, A., Verlezza, S., Long, H., Wong, T. P., and Walker, C.-D. (2020). It is all in the right amygdala: Increased synaptic plasticity and perineuronal nets in

male, but not female, juvenile rat pups after exposure to early-life stress. *J. Neurosci.* 40 (43), 8276–8291. doi:10.1523/JNEUROSCI.1029-20.2020

Haberman, R. P., Quigley, C. K., and Gallagher, M. (2012). Characterization of CpG island DNA methylation of impairment-related genes in a rat model of cognitive aging. *Epigenetics* 7 (9), 1008–1019. doi:10.4161/epi.21291

Heijmans, B. T., Tobi, E. W., Stein, A. D., Putter, H., Blauw, G. J., Susser, E. S., et al. (2008). Persistent epigenetic differences associated with prenatal exposure to famine in humans. *Proc. Natl. Acad. Sci. U. S. A.* 105 (44), 17046–17049. doi:10.1073/pnas.0806560105

Hibbs, M. L., Bonadonna, L., Scott, B. M., McKenzie, I. F., and Hogarth, P. M. (1988). Molecular cloning of a human immunoglobulin G Fc receptor. *PNAS* 85 (7), 2240–2244. doi:10.1073/pnas.85.7.2240

Howe, K. L., Achuthan, P., Allen, J., Allen, J., Alvarez-Jarreta, J., Amode, M. R., et al. (2020). Ensembl 2021. *Nucleic Acids Res.* 49 (D1), D884–D891. doi:10.1093/nar/gkaa942

Hu, C., Tao, L., Cao, X., and Chen, L. (2020). The solute carrier transporters and the brain: Physiological and pharmacological implications. *Asian J. Pharm. Sci.* 15 (2), 131–144. doi:10.1016/j.ajps.2019.09.002

Jarome, T. J., Werner, C. T., Kwapis, J. L., and Helmstetter, F. J. (2011). Activity dependent protein degradation is critical for the formation and stability of fear memory in the amygdala. *PLoS One* 6 (9), e24349. doi:10.1371/journal.pone.0024349

Jessen, H. M., Kolodkin, M. H., Bychowski, M. E., Auger, C. J., and Auger, A. P. (2010). The nuclear receptor corepressor has organizational effects within the developing amygdala on juvenile social play and anxiety-like behavior. *Endocrinology* 151 (3), 1212–1220. doi:10.1210/en.2009-0594

Jones, M. J., Goodman, S. J., and Kobor, M. S. (2015). DNA methylation and healthy human aging. *Aging Cell* 14 (6), 924–932. doi:10.1111/acel.12349

Kalmar, J. H., Wang, F., Chepenik, L. G., Womer, F. Y., Jones, M. M., Pittman, B., et al. (2009). Relation between amygdala structure and function in adolescents with bipolar disorder. *J. Am. Acad. Child. Adolesc. Psychiatry* 48 (6), 636–642. doi:10.1097/CHI.0b013e31819f6fbc

Klose, R. J., and Bird, A. P. (2006). Genomic DNA methylation: the mark and its mediators. *Trends Biochem. Sci.* 31 (2), 89–97. doi:10.1016/j.tibs.2005.12.008

Kraszpulski, M., Dickerson, P. A., and Salm, A. K. (2006). Prenatal stress affects the developmental trajectory of the rat amygdala. *Stress* 9 (2), 85–95. doi:10.1080/10253890600798109

Kundakovic, M., Gudsnuk, K., Herbstman, J. B., Tang, D., Perera, F. P., Champagne, F. A., et al. (2015). DNA methylation of BDNF as a biomarker of early-life adversity. *Proc. Natl. Acad. Sci. U. S. A.* 112 (22), 6807–6813. doi:10.1073/pnas.1408355111

Kundakovic, M., and Jaric, I. (2017). The Epigenetic link between prenatal adverse environments and neurodevelopmental disorders. *Genes* 8 (3), 104. doi:10.3390/genes8030104

Lawrie, S. M., Whalley, H. C., Job, D. E., and Johnstone, E. C. (2003). Structural and functional abnormalities of the amygdala in Schizophrenia. *Ann. N. Y. Acad. Sci.* 985 (1), 445–460. doi:10.1111/j.1749-6632.2003.tb07099.x

Lay, D. C., Jr., Randel, R. D., Friend, T. H., Jenkins, O. C., Neuendorff, D. A., Bushong, D. M., et al. (1997). Effects of prenatal stress on suckling calves. *J. Anim. Sci.* 75 (12), 3143–3151. doi:10.2527/1997.75123143x

LeDoux, J. E. (1994). The amygdala: contributions to fear and stress. *Seminars Neurosci.* 6 (4), 231–237. doi:10.1006/smns.1994.1030

Littlejohn, B. P., Price, D. M., Banta, J. P., Lewis, A. W., Neuendorff, D. A., Carroll, J. A., et al. (2016). Prenatal transportation stress alters temperament and serum cortisol concentrations in suckling Brahman calves. *J. Anim. Sci.* 94 (2), 602–609. doi:10.2527/jas.2015-9635

Littlejohn, B. P., Price, D. M., Neuendorff, D. A., Carroll, J. A., Vann, R. C., Riggs, P. K., et al. (2018). Prenatal transportation stress alters genome-wide DNA methylation in suckling Brahman bull calves. *J. Anim. Sci.* 96 (12), 5075–5099. doi:10.1093/jas/sky350

Livernois, A. M., Mallard, B. A., Cartwright, S. L., and Cánovas, A. (2021). Heat stress and immune response phenotype affect DNA methylation in blood mononuclear cells from Holstein dairy cows. *Sci. Rep.* 11 (1), 11371. doi:10.1038/s41598-021-89951-5

Mohrhauser, D. A., Taylor, A. R., Gonda, M. G., Underwood, K. R., Pritchard, R. H., Wertz-Lutz, A. E., et al. (2015). The influence of maternal energy status during mid-gestation on beef offspring tenderness, muscle characteristics, and gene expression. *Meat Sci.* 110, 201–211. doi:10.1016/j.meatsci.2015.07.017

Mychasiuk, R., Ilnytskyy, S., Kovalchuk, O., Kolb, B., and Gibb, R. (2011). Intensity matters: brain, behaviour and the epigenome of prenatally stressed rats. *Neuroscience* 180, 105–110. doi:10.1016/j.neuroscience.2011.02.026

Papin, C., Le Gras, S., Ibrahim, A., Salem, H., Karimi, M. M., Stoll, I., et al. (2021). CpG Islands shape the epigenome landscape. *J. Mol. Biol.* 433 (6), 166659. doi:10.1016/j.jmb.2020.09.018

Park, H.-J., Kim, S.-K., Kang, W.-S., Chung, J.-H., and Kim, J.-W. (2014). Increased activation of synapsin 1 and mitogen-activated protein kinases/extracellular signal-regulated kinase in the amygdala of maternal separation rats. *CNS Neurosci. Ther.* 20 (2), 172–181. doi:10.1111/cns.12202

Petit, B., Boissy, A., Zanella, A., Chaillou, E., Andanson, S., Bes, Lévy F., et al. (2015). Stress during pregnancy alters dendritic spine density and gene expression in the brain of new-born lambs. *Behav. Brain Res.* 291, 155–163. doi:10.1016/j.bbr.2015.05.025

Price, D. M., Lewis, A. W., Neuendorff, D. A., Carroll, J. A., Burdick Sanchez, N. C., Vann, R. C., et al. (2015). Physiological and metabolic responses of gestating Brahman cows to repeated transportation. *J. Anim. Sci.* 93 (2), 737–745. doi:10.2527/jas.2013-7508

Rasia-Filho, A. A., Londero, R. G., and Achaval, M. (2000). Functional activities of the amygdala: an overview. *J. Psychiatry Neurosci.* 25 (1), 14–23.

Razin, A., and Riggs, A. D. (1980). DNA methylation and gene function. *Science* 210 (4470), 604–610. doi:10.1126/science.6254144

Redlich, R., Schneider, I., Kerkenberg, N., Opel, N., Bauhaus, J., Enneking, V., et al. (2020). The role of BDNF methylation and Val(66) Met in amygdala reactivity during emotion processing. *Hum. Brain Mapp.* 41 (3), 594–604. doi:10.1002/hbm.24825

Robinson, M. D., McCarthy, D. J., and Smyth, G. K. (2010). edgeR: a Bioconductor package for differential expression analysis of digital gene expression data. *Bioinformatics* 26 (1), 139–140. doi:10.1093/bioinformatics/btp616

Rosen, B. D., Bickhart, D. M., Schnabel, R. D., Koren, S., Elsik, C. G., Tseng, E., et al. (2020). De novo assembly of the cattle reference genome with single-molecule sequencing. *Gigascience* 9 (3), giaa021. doi:10.1093/gigascience/giaa021

Rosenkranz, J. A., Venheim, E. R., and Padival, M. (2010). Chronic stress causes amygdala hyperexcitability in rodents. *Biol. Psychiatry* 67 (12), 1128–1136. doi:10.1016/j.biopsych.2010.02.008

Sagalajev, B., Wei, H., Chen, Z., Albayrak, I., Koivisto, A., and Pertovaara, A. (2018). Oxidative stress in the amygdala contributes to neuropathic pain. *Neuroscience* 387, 92–103. doi:10.1016/j.neuroscience.2017.12.009

Salpea, P., Russanova, V. R., Hirai, T. H., Sourlingas, T. G., Sekeri-Pataryas, K. E., Romero, R., et al. (2012). Postnatal development- and age-related changes in DNA-methylation patterns in the human genome. *Nucleic Acids Res.* 40 (14), 6477–6494. doi:10.1093/nar/gks312

Sanglard, L. P., Nascimento, M., Moriel, P., Sommer, J., Ashwell, M., Poore, M. H., et al. (2018). Impact of energy restriction during late gestation on the muscle and blood transcriptome of beef calves after preconditioning. *BMC Genomics* 19 (1), 702. doi:10.1186/s12864-018-5089-8

Scheinost, D., Kwon, S. H., Lacadie, C., Sze, G., Sinha, R., Constable, R. T., et al. (2016). Prenatal stress alters amygdala functional connectivity in preterm neonates. *Neuroimage. Clin.* 12, 381–388. doi:10.1016/j.nicl.2016.08.010

Serviento, A. M., Lebret, B., and Renaudeau, D. (2020). Chronic prenatal heat stress alters growth, carcass composition, and physiological response of growing pigs subjected to postnatal heat stress. *J. Anim. Sci.* 98 (5), skaa161. doi:10.1093/jas/skaa161

Tate, P. H., and Bird, A. P. (1993). Effects of DNA methylation on DNA-binding proteins and gene expression. *Curr. Opin. Genet. Dev.* 3 (2), 226–231. doi:10.1016/0959-437x(93)90027-m

Thomas, P. D., Campbell, M. J., Kejariwal, A., Mi, H., Karlak, B., Daverman, R., et al. (2003). PANTHER: A library of protein families and subfamilies indexed by function. *Genome Res.* 13 (9), 2129–2141. doi:10.1101/gr.772403

Thompson, R. P., Nilsson, E., and Skinner, M. K. (2020). Environmental epigenetics and epigenetic inheritance in domestic farm animals. *Anim. Reprod. Sci.* 220, 106316. doi:10.1016/j.anireprosci.2020.106316

Vonderwalde, I. (2019). DNA Methylation within the amygdala early in life increases susceptibility for depression and anxiety disorders. *J. Neurosci.* 39 (45), 8828–8830. doi:10.1523/JNEUROSCI.0845-19.2019

Ward, H. E., Johnson, E. A., Salm, A. K., and Birkle, D. L. (2000). Effects of prenatal stress on defensive withdrawal behavior and corticotropin releasing factor systems in rat brain. *Physiol. Behav.* 70 (3-4), 359–366. doi:10.1016/s0031-9384(00)00270-5

Wikenius, E., Moe, V., Smith, L., Heiervang, E. R., and Berglund, A. (2019). DNA methylation changes in infants between 6 and 52 weeks. *Sci. Rep.* 9 (1), 17587. doi:10.1038/s41598-019-54355-z

Wilson, V. L., Smith, R. A., Ma, S., and Cutler, R. G. (1987). Genomic 5-methyldeoxycytidine decreases with age. *J. Biol. Chem.* 262 (21), 9948–9951. doi:10.1016/s0021-9258(18)61057-9

Yang, Y., and Wang, J. Z. (2017). From structure to behavior in basolateral amygdala-hippocampus circuits. *Front. Neural Circuits* 11, 86. doi:10.3389/fncir.2017.00086

Ziller, M. J., Hansen, K. D., Meissner, A., and Aryee, M. J. (2015). Coverage recommendations for methylation analysis by whole-genome bisulfite sequencing. *Nat. Methods* 12 (3), 230–232. doi:10.1038/nmeth.3152

frontiers | Frontiers in Genetics

TYPE Original Research
PUBLISHED 23 August 2022
DOI 10.3389/fgene.2022.946211

Check for updates

OPEN ACCESS

EDITED BY
Jean Feugang,
Mississippi State University,
United States

REVIEWED BY
Haji Akbar,
University of Illinois at Urbana-Champaign, United States
Axel Heiser,
AgResearch Ltd., New Zealand

*CORRESPONDENCE
Fabrizio Ceciliani,
fabrizio.ceciliani@unimi.it

SPECIALTY SECTION
This article was submitted to Livestock Genomics,
a section of the journal
Frontiers in Genetics

RECEIVED 17 May 2022
ACCEPTED 25 July 2022
PUBLISHED 23 August 2022

CITATION
Veshkini A, Hammon HM, Lazzari B, Vogel L, Gnott M, Tröscher A, Vendramin V, Sadri H, Sauerwein H and Ceciliani F (2022), Investigating circulating miRNA in transition dairy cows: What miRNAomics tells about metabolic adaptation.
Front. Genet. 13:946211.
doi: 10.3389/fgene.2022.946211

COPYRIGHT
© 2022 Veshkini, Hammon, Lazzari, Vogel, Gnott, Tröscher, Vendramin, Sadri, Sauerwein and Ceciliani. This is an open-access article distributed under the terms of the Creative Commons Attribution License (CC BY). The use, distribution or reproduction in other forums is permitted, provided the original author(s) and the copyright owner(s) are credited and that the original publication in this journal is cited, in accordance with accepted academic practice. No use, distribution or reproduction is permitted which does not comply with these terms.

Investigating circulating miRNA in transition dairy cows: What miRNAomics tells about metabolic adaptation

Arash Veshkini[1,2,3], Harald Michael Hammon[2], Barbara Lazzari[4], Laura Vogel[2], Martina Gnott[2], Arnulf Tröscher[5], Vera Vendramin[6], Hassan Sadri[7], Helga Sauerwein[1] and Fabrizio Ceciliani[3]*

[1]Institute of Animal Science, Physiology Unit, University of Bonn, Bonn, Germany, [2]Research Institute for Farm Animal Biology (FBN), Dummerstorf, Germany, [3]Department of Veterinary Medicine, Università degli Studi di Milano, Lodi, Italy, [4]Institute of Agricultural Biology and Biotechnology of the CNR, Milan, Italy, [5]BASF SE, Lampertheim, Germany, [6]IGA Technology Services, Udine, Italy, [7]Department of Clinical Science, Faculty of Veterinary Medicine, University of Tabriz, Tabriz, Iran

In the current study, we investigated dairy cows' circulating microRNA (miRNA) expression signature during several key time points around calving, to get insights into different aspects of metabolic adaptation. In a trial with 32 dairy cows, plasma samples were collected on days −21, 1, 28, and 63 relative to calving. Individually extracted total RNA was subjected to RNA sequencing using NovaSeq 6,000 (Illumina, CA) on the respective platform of IGA Technology Services, Udine, Italy. MiRDeep2 was used to identify known and novel miRNA according to the miRbase collection. Differentially expressed miRNA (DEM) were assessed at a threshold of fold-change > 1.5 and false discovery rate < 0.05 using the edgeR package. The MiRWalk database was used to predict DEM targets and their associated KEGG pathways. Among a total of 1,692 identified miRNA, 445 known miRNA were included for statistical analysis, of which 84, 59, and 61 DEM were found between days −21 to 1, 1 to 28, and 28 to 63, respectively. These miRNA were annotated to KEGG pathways targeting the insulin, MAPK, Ras, Wnt, Hippo, sphingolipid, T cell receptor, and mTOR signaling pathways. MiRNA-mRNA network analysis identified miRNA as master regulators of the biological process including miR-138, miR-149-5p, miR-2466-3p, miR-214, miR-504, and miR-6523a. This study provided new insights into the miRNA signatures of transition to the lactation period. Calving emerged as a critical time point when miRNA were most affected, while the following period appeared to be recovering from massive parturition changes. The primarily affected pathways were key signaling pathways related to establishing metabolic and immune adaptations.

KEYWORDS

miRNA, post-calving, systemic inflammation, negative energy balance, posttranscriptional regulation, immune-related pathways

Introduction

In dairy cows, the transition from pregnancy into lactation often coincides with metabolic stress associated with a negative energy balance (NEB), a result of an imbalance between feed intake and milk production (Drackley, 1999). Several factors such as excessive fat mobilization, impaired liver function, and systemic inflammation during this period may lead to metabolic disorders and also economic losses (Wankhade et al., 2017). Nevertheless, most dairy cows can adapt and maintain their internal organization to deal with transition period challenges, which require an orchestrated array of regulatory mechanisms at the hormonal, metabolic, and immunological levels (Horst et al., 2021).

MicroRNAs (miRNA) are evolutionary conserved small non-coding (approximately 17–24 nucleotides) RNA molecules involved in the post-transcriptional regulation of most protein-coding mRNA, including degradation and translational repression (O'Brien et al., 2018). Since miRNA are involved in almost all metabolic pathways, including energy metabolism, lipid metabolism, insulin sensitivity, and glucose homeostasis (Lin et al., 2020), it is not surprising that their function is crucial during the transition period. As tissue-specific miRNA can enter the circulation system (Barutta et al., 2018) embedded into stable structures such as exosomes and lipoproteins (Condrat et al., 2020), plasma and other body fluids may carry signatures related to the pathophysiological status. Various physiological conditions including heat stress (Lee et al., 2020), different levels of NEB (Hailay et al., 2019), and over-conditioning in dairy cows (Webb et al., 2020), induce changes to the circulating miRNA pattern. In particular, the stage of lactation and transition period affect the miRNA profile. In this regard, the microRNAome of dairy cows' dry secretions during the first 3 weeks of the dry period revealed differentially expressed miRNA related to reproduction and embryo development (i.e. bta-miR-130b and bta-miR-106a), lactation (i.e. bta-miR-29a, bta-miR-21-3p, bta-miR-130a), as well as inflammation and disease (bta-let-7 family) (Putz et al., 2019).

Markers of the metabolic adaptation during the transition period have been characterized in dairy cows by univariate analyses and, increasingly, via multivariate OMICs technologies (Ceciliani et al., 2018). On the other hand, the post-transcriptional regulation of gene expression has received relatively little attention in this context (Webb et al., 2020). Despite the progress in identifying the origin and the function of miRNA and developing databases, further knowledge of circulating miRNA in dairy cows is still lacking. We, therefore, aimed to characterize the longitudinal changes of the circulating miRNAome profile in dairy cows during the transition period using next-generation sequencing (NGS) and bioinformatics analysis.

Material and methods

Experimental design

The samples used herein were from an animal experiment described in detail by Vogel (Vogel et al., 2020), performed according to the animal welfare guidelines, and approved by the local authority, i.e. the State Mecklenburg-Western Pomerania, Germany (LALLF M-V/TSD/7221.3-1-038/15). In brief, 32 Holstein dairy cows in their second lactation and without clinical signs of disease were housed in free-stall barns with ad libitum access to a corn silage-based total mixed ration (TMR), formulated according to recommendations provided by the Society for Nutrition Physiology (GfE, 2001 (GfE, Gesellschaft für Ernährungsphysiologie (German Society of Nutrition Physiology), 2001), 2008 (GfE, Gesellschaft für Ernährungsphysiologie (German Society of Nutrition Physiology), 2008), 2009 (GfE, Gesellschaft für Ernährungsphysiologie (German Society of Nutrition Physiology), 2009)) and Deutsche Landwirtschaftliche Gesellschaft (DLG, 2013) (DLG (Deutsche Landwirtschafts-Gesellschaft and German Agricultural Society), 2013), from day 63 ante-partum (AP) to day 63 post-partum (PP). The dairy cows were randomly assigned to one of four treatment groups receiving different fat supplements as abomasal infusion: **CTRL** (n = 8; coconut oil, Bio-Kokosöl #665, Kräuterhaus Sanct Bernhard, KG, Bad Ditzenbach, Germany; 38 and 76 g/d in AP and PP), Essential fatty acids (**EFA**, n = 8, a combination of linseed oil (DERBY® Leinöl #4026921003087, DERBY Spezialfutter GmbH, Münster, Germany; 39 and 78 g/d in AP and PP), and safflower oil (GEFRO Distelöl, GEFRO Reformversand Frommlet KG, Memmingen, Germany; 2 and 4 g/d in AP and PP), conjugated linoleic acid (**CLA**, n = 8, Lutalin®; cis-9, trans-11, 10 g/d trans- 10, cis-12 CLA, BASF SE, Lampertheim, Germany; 19 and 38 g/d in AP and PP), and **EFA + CLA**, a combination of linseed oil, safflower oil and Lutalin® from day 63 AP to day 63 PP (Figure 1). The ingredients and the chemical composition of the basal diet were reported elsewhere (Vogel et al., 2020). The present investigation was focused on longitudinal changes only.

Blood sampling

Four blood samples were collected from each cow on days -21, 1, 28, and 63 relative to calving (Figure 1), immediately after the morning milking and before feeding, using the Vacuette system (Greiner Bio-One International GmbH, Kremsmünster, Austria) containing 1.8 g potassium-EDTA (K3EDTA)/L. Samples were immediately cooled on ice and transferred to the lab within 2 h of collection. The plasma fraction was

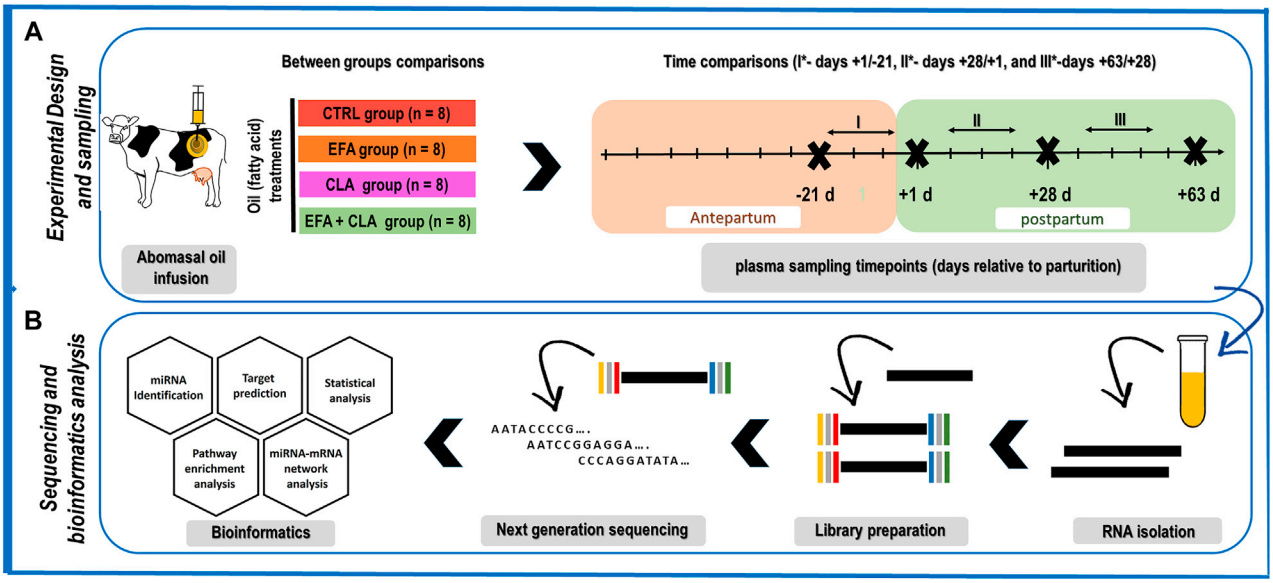

FIGURE 1
Schematic representation of **(A)** the animal experimental design and sampling time points, consisting of four groups CTRL: control (n = 8), EFA: essential fatty acids (n = 8), CLA: conjugated linoleic acid (n = 8), and EFA + CLA (n = 8), and four plasma sampling (days −21, +1, +28, and +63 relative to parturition). The focus of this study is primarily on time comparisons since the effect of treatments was negligible **(B)** Sequencing analysis and bioinformatics. CTRL: control, EFA: essential fatty acids, CLA: conjugated linoleic acid.

harvested after centrifugation at 1,500 × g (4°C) for 20 min and stored at −80°C until analysis.

Isolation of total RNA

Total RNA was extracted from 128 plasma samples using the QIAGEN miRNeasy serum/plasma kit (Qiagen GmbH, Hilden, Germany) according to the manufacturer protocol. The miRNeasy Serum/Plasma Spike-In Control (lyophilized *C. elegans* miR-39 miRNA) was used to verify extraction quality and normalize TaqMan qPCR results. The RNA yield and purity were assessed using an Agilent Small RNA kit on a 2100 Bioanalyzer (Agilent Technologies, Santa Clara, CA, United States). In samples with low miRNA concentration (<100 pg/μl), the isolation procedure was repeated using the double initial plasma volume (400 μl).

Library preparation and next-generation sequencing

The QIAseq miRNA library kit (QIAGEN, Hilden, Germany) was used for library preparation following the manufacturer's serum/plasma samples instructions. Final libraries were checked with Qubit 2.0 Fluorometer (Invitrogen, Carlsbad, CA) and Caliper (PerkinElmer, Waltham, MA). Afterward, libraries were sequenced on single-end 100 bp mode on the NovaSeq 6,000 (Illumina, San Diego, CA) on IGA Technology Services platform, Udine, Italy (https://igatechnology.com/).

Raw-sequencing data was checked for quality (format conversion to FASTQ, demultiplexing, adapter trimming, and UMI removal) using the Illumina Bcl2fastq2 Conversion Software (version 2.20). A summary of nucleotide sequence data, including FastQC merge reads produced for each sample, sequence quality histograms, per sequence quality scores, per base sequence content, per sequence GC content, per base N content, sequence length distribution, alignment-free estimation of sequences duplication levels, overrepresented sequences, adapter content (multiQC file, version 1.6) is available in the ArrayExpress database (http://www.ebi.ac.uk/arrayexpress) under the "ArrayExpress accession E-MTAB-11725".

Sequence analysis

Detected sequences were analyzed with the miRDeep2 (miRDeep2.pl) software package (version 2.0.0.5) (Friedländer, Mackowiak, Li, Chen, Rajewsky) to detect known miRNA and predict putative novel miRNA. MiRDeep2 was fed with the *Bos taurus* miRNA collection available at miRBase (www.mirbase.org (Kozomara et al., 2019)) for known cow miRNA detection. In

contrast, the miRBase human, ovine, and goat miRNA datasets were added to support the identification of novel miRNA. Read counts for each known and novel miRNA were compiled using HTSeq-count (Putri et al., 2022).

Statistical analysis and bioinformatics

The quantified counts were normalized using the TMM method via the edgeR (version 3.12.0) package in R software (Version 4.0). Only miRNA with at least one count per million over at least two samples were considered for the analysis. After normalization, differentially expressed miRNA (DEM) during time were identified by performing generalized linear model (GLM) likelihood ratio tests (glmLRT) using the GLM approach in edgeR to deal with the time series paired effects. Between each two consecutive time points, miRNA with an FDR <0.05 and log2 (FC) > 1.3 were considered as DEM, and visualised by Volcano plot according to their expression (EnhancedVolcano R package). DEM between treatment groups were identified at each time point using the same criterion (FDR <0.05 and log2 (FC) > 1.3). The miRWalk database (2022_01, Bos Taurus, http://mirwalk.umm.uni-heidelberg.de/) was used to compile consensus lists of predicted miRNA targets and to perform gene ontology and KEGG functional enrichment analysis. Network analysis was performed and visualized (yFiles Tree layout) using the combination of miRNet (version 2.0) web-based platform, StringApp, and Centiscape 2.2 in Cytoscape software (version 3.9) (Figure 1). The networks were filtered by two well-established criteria: degree centrality (number of connections with the other nodes) and betweenness centrality (the number of shortest paths connecting the node). The network has been constructed, visualized, and analyzed using the combination of miRanda, miRNet, and Cytoscape. The miRanda database was replaced with the miRWalk database to filter the number of target genes. As yet there is no possibility for target filtration in miRWalk based on Targetscan (http://www.targetscan.org/vert_80/), miRtarbase (https://mirtarbase.cuhk.edu.cn/~miRTarBase/miRTarBase_2022/php/index.php), and mirdb (http://mirdb.org/faq.html) for dairy cows.

Results

In total, 183,772,507 cleaned reads were processed and mapped to the bovine reference genome; in detail, 51,086,403, 46,288,086, 44,508,614, and 41,889,404 reads were processed at days -21, 1, 28, and 63, respectively. From these sequences, 846 miRNA were matched to previously known mature bovine miRNA (equal to 846/1025 = 82.5% of total identified miRNA in cattle until January 2021 (Do et al., 2021), and 846/6808 = 12.42% total theoretical number available in the RumimiR 2022 database, http://rumimir.sigenae.org/). In addition, 1,274 novel miRNA hairpins were identified, including 836 completely novel bovine miRNA (named according to their absolute genomic position), 374 miRNA similar to known *Homo sapiens* miRNA (has-miR), 58 similar to *Capra hircus* known miRNA (ch-miR), and six similar to *Ovis aries* known miRNA (oar-miR) (Supplementary Table S1). The statistical and functional enrichment analyses were limited to 445 cleaned known miRNA with ten counts or more in at least 50% of samples (Supplementary Table S2). Figure 2 represents the 25 miRNA with the highest mean reads (ranging from 2.1×10^5 to 7×10^6) across all samples and time points (sorted by time point). Oil treatments had negligible minor effects on miRNA profile and only one miRNA, bta-miR-1 (log2 (FC) = -5.65, FDR <0.001), was found to be differentially expressed between the CTRL and the CLA group at day -21 AP. There was no other difference in miRNA expression between CTRL, EFA, CLA, and EFA + CLA at days -21, 1, 28, and 63, respectively (Supplementary Table S3). Therefore, data from all four treatment groups were merged to study time-affected miRNA (regardless of the treatment effect).

Differentially expressed miRNA over time

Figure 3 shows the multidimensional scaling (MDS) plot of the individual miRNA profiles obtained on the different sampling days. Using a two-dimensional scatterplot, the distances between samples were approximated by their expression differences. The analysis differentiates the AP (day -21) and PP (days 1, 28, and 63) periods as two well-separated clusters, suggesting that most of the variance in the miRNAome data resulted from the transition to lactation. Even if PP time points partially overlap, clustering according to lactation periods is observable.

Differentially expressed miRNA during the transition from day −21 to +1 relative to parturition

Comparing day −21 to 1, 84 miRNA were differentially expressed (log2 (FC) > 1.3, q-value < 0.05), including 14 downregulated and 70 upregulated miRNA (Figure 4A). The most significantly downregulated miRNA was bta-miR-1 (log2 (FC) = −3.62, q-value < 0.001), and the most significantly upregulated was bta-miR-143 (log2 (FC) = 2.5, q-value < 0.001). Using the miRWalk cow database, 25,224 genes were targeted by the downregulated miRNA. These targeted genes were annotated to 29 KEGG pathways (adjusted *p*-value (FDR) < 0.05), mainly related to insulin pathways (insulin signaling pathway bta04910 and insulin resistance bta04931) and cell communication and signaling pathways (mitogen-activated

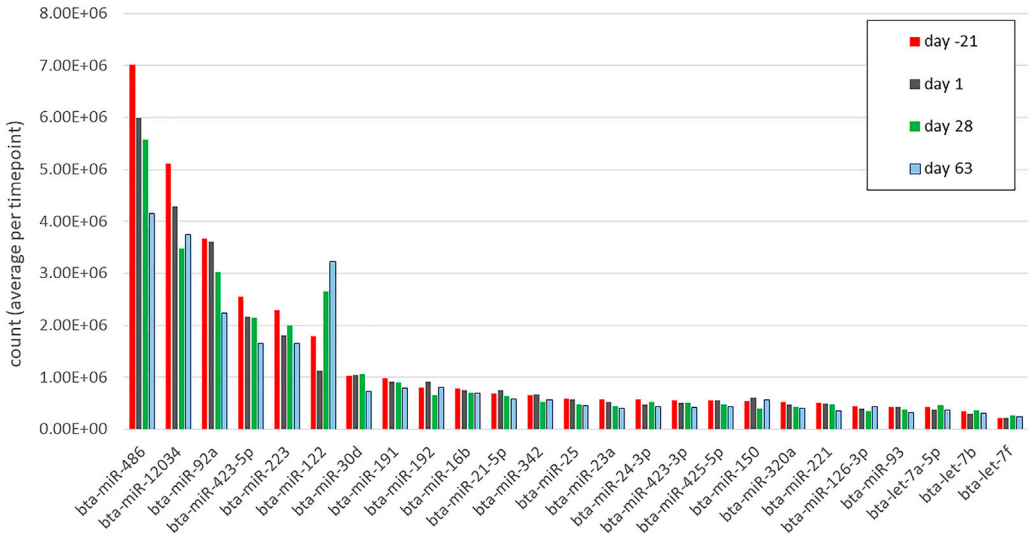

FIGURE 2
The top 25 miRNAs (by mean counts (million) per time point) in circulation during days −21, 1, 28, and 63 relative to parturition. Different colors correspond to different time points.

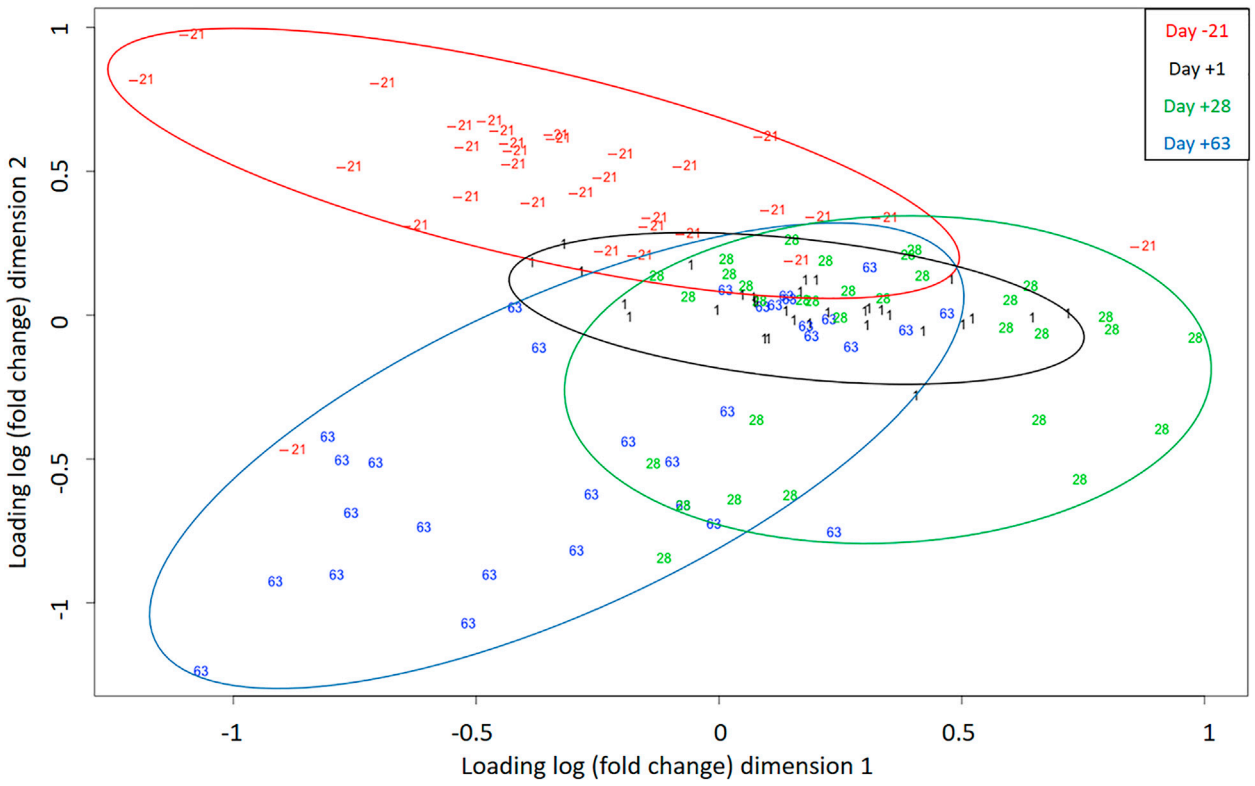

FIGURE 3
Multidimensional scaling (MDS) plot indicates samples (individual sequencing) separation during days -21, 1, 28, and 63 relative to parturition. Different colors correspond to different time points.

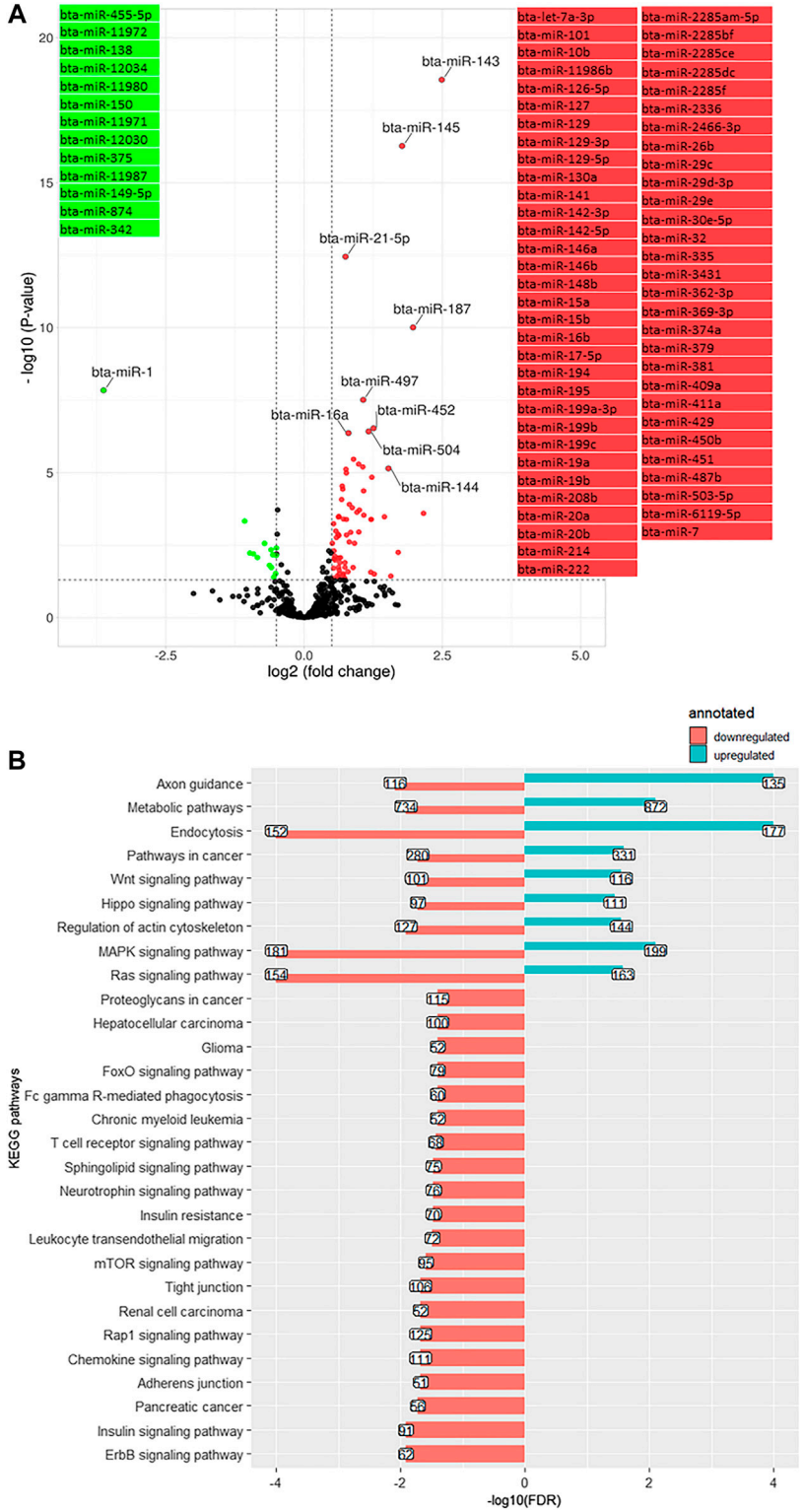

FIGURE 4
(A). Volcano plot representing differentially expressed miRNA (DEM) between day -21 and +1 relative to parturition (day +1/-21); increased (red dots) and decreased (green dots) miRNA in d+1/d-21 are highlighted ($p < 0.05$ and log2 fold change (FC) > 1.3). **(B)**. KEGG pathways annotated to DEM; Bars indicate proportional to the false discovery rate (FDR) adjusted p-value, and the box on each bar represents the gene counts (GC).

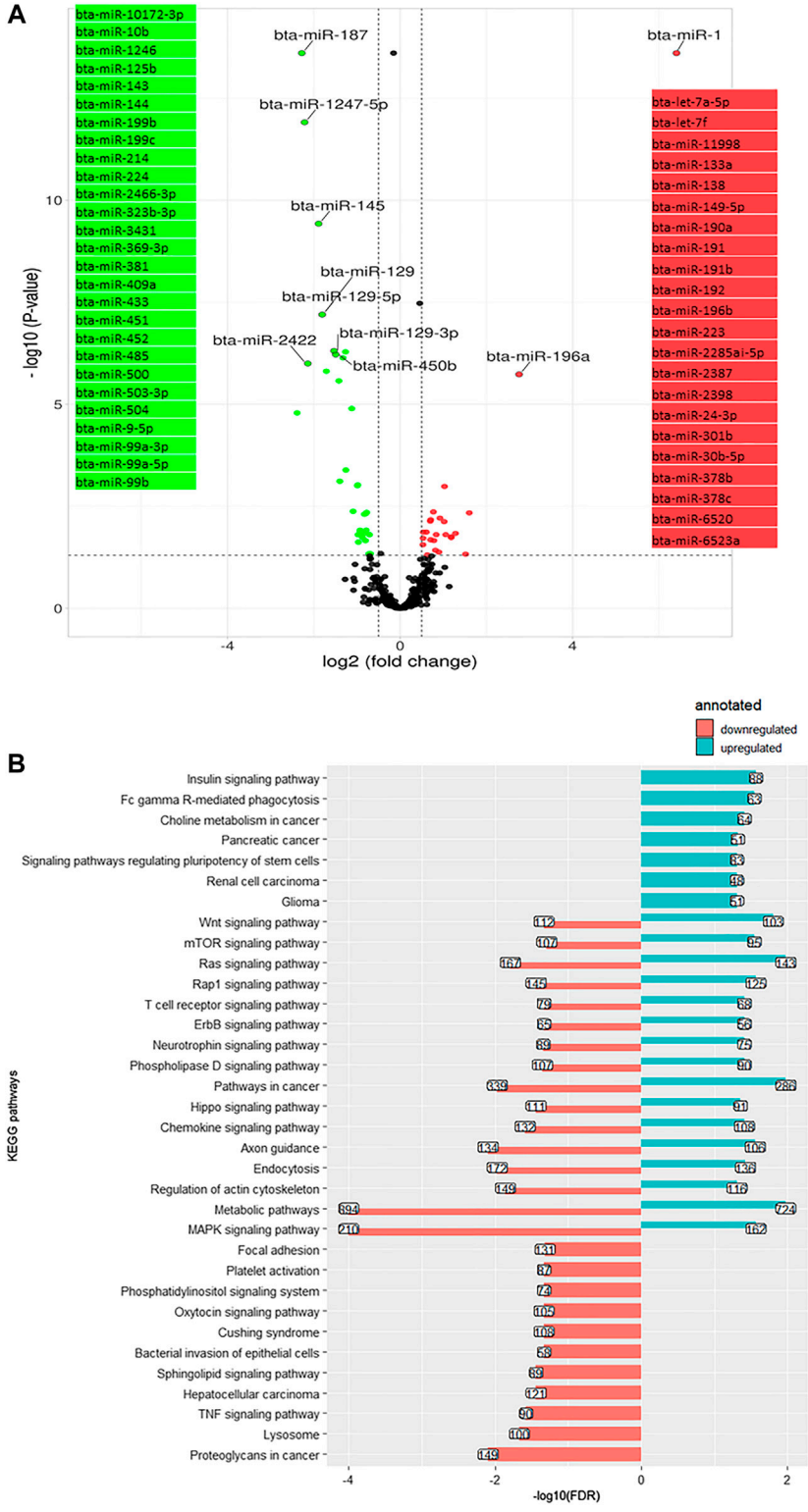

FIGURE 5
(A). Volcano plot representing differentially expressed miRNA (DEM) between day +1 and +28 relative to parturition; increased (red dots in top right) and decreased (green dots in top left) miRNA in d+28/d+1 are highlighted ($p < 0.05$ and log2 fold change (FC) > 1.3). **(B)**. KEGG pathways annotated to DEM; Bars indicate proportional to the false discovery rate (FDR) adjusted p-value, and the box on each bar represents the genes count (GC).

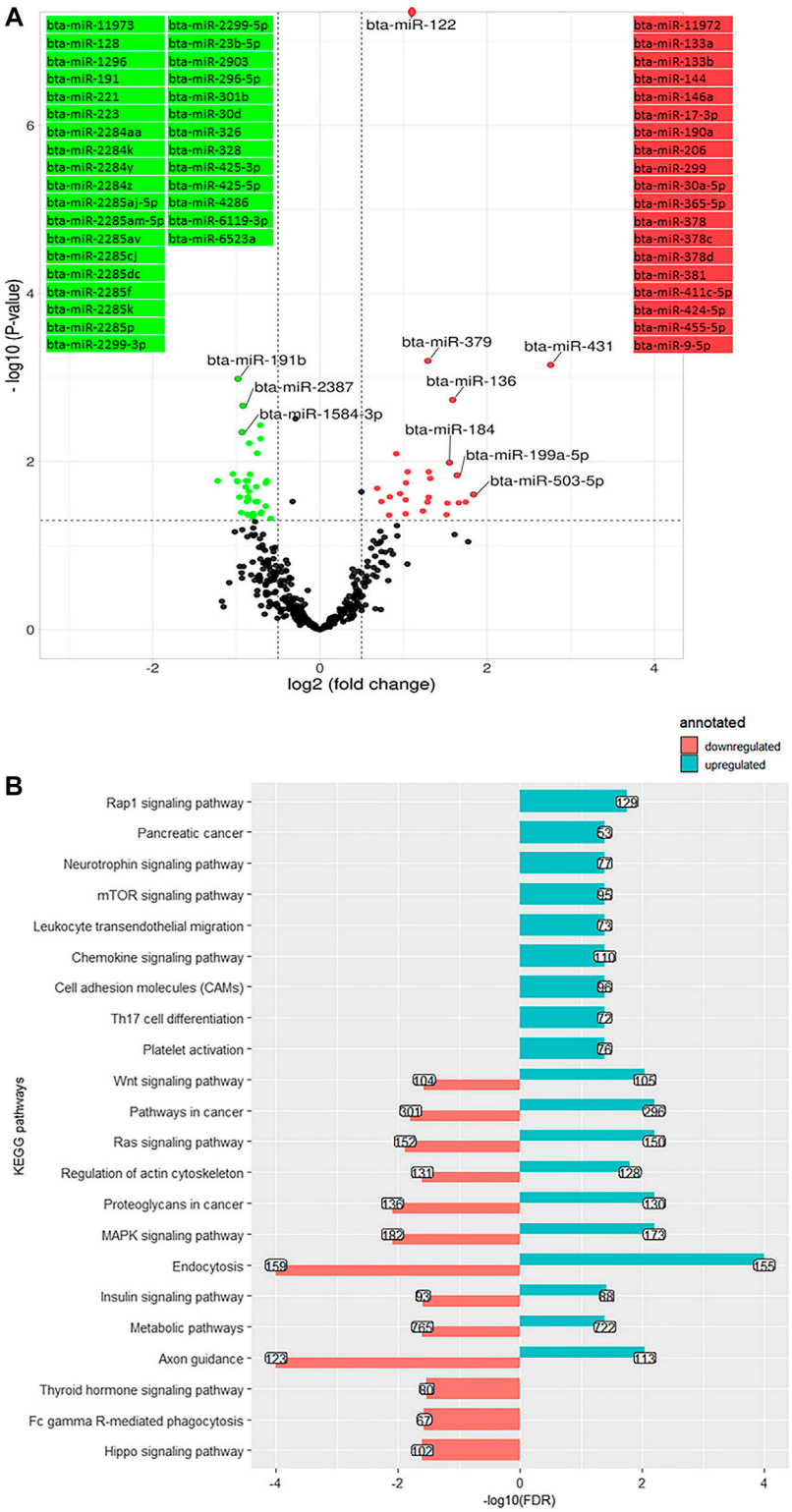

FIGURE 6
(A). Volcano plot representing differentially expressed miRNA (DEM) between day +28 and +63 relative to parturition; increased (red dots in top right) and decreased (green dots in top left) miRNA in d+63/d+28 are highlighted ($p < 0.05$ and log2 fold change (FC) > 1.3). **(B)**. KEGG pathways annotated to DEM; Bars indicate proportional to the false discovery rate (FDR) adjusted p-value, and the box on each bar represents the genes count (GC).

protein kinase (MAPK) signaling pathway bta04010, rat sarcoma (Ras) signaling pathway bta04014, mammalian telomere-binding protein (Rap1) signaling pathway bta04015, endocytosis bta04144, Wnt signaling pathway bta04310, Hippo signaling pathway bta04390, adherens junction bta04520, tight junction bta04530, the mammalian target of rapamycin or mTOR signaling pathway bta04150, sphingolipid signaling pathway bta04071, and T cell receptor (TCR) signaling pathway bta04660) (Figure 4B). The upregulated miRNA predicted targets (50,782 genes) were annotated to nine KEGG (Figure 4B), including the Ras/MAPK pathway, Hippo signaling pathway, and Wnt signaling pathway. Repetition of pathways indicates that a pathway is affected by up and downregulated target genes through possible feedback mechanisms.

Differentially expressed miRNA between days +1 and +28 of lactation

On day 28, compared with day 1, the relative expression was decreased for 35 miRNA and increased for 24 miRNA (Figure 5A). The most significantly downregulated miRNA was bta-miR-187 (log2 (FC) = −2.27, q-value < 0.001), and the most significantly upregulated was bta-miR-1 (log2 (FC) = 6.28, q-value < 0.001). A number of 47,968 genes were predicted as the target of downregulated miRNA annotated to 26 KEGG pathways. The KEGG pathways were mostly signaling pathways including MAPK signaling pathway, Ras signaling pathway, Wnt signaling pathway, Hippo signaling pathway, sphingolipid signaling pathway, TCR signaling pathway, lysosome bta04142, tumor necrosis factor (TNF) signaling pathway bta04668, and oxytocin signaling pathway bta04921, as well as bacterial invasion of epithelial cells bta05100 (Figure 5B). The overexpressed miRNA targeted (prediction) 26,570 genes were related to 23 KEGG pathways, including the Ras signaling pathway, Wnt signaling pathway, MAPK signaling pathway, insulin signaling pathway, mTOR signaling pathway, endocytosis, and TCR signaling pathway (Figure 5B).

Differentially expressed miRNA on day +28 versus +63 of lactation

A total of 61 DEM were identified on day 63 compared to day 28, including 35 downregulated and 26 upregulated ones, with bta-miR-122 (log2 (FC) = 0.89, q-value < 0.001) and bta-miR-191b (log2 (FC) = -0.97, q-value < 0.001) being the two extremes (Figure 6A). A number of 33,924 genes were predicted as the target of downregulated DEM which were annotated to 13 KEGG pathways, consisting of a cluster of signaling pathways: MAPK signaling pathway, Ras signaling pathway, Hippo signaling pathway, insulin signaling pathway, Wnt signaling pathway, and thyroid hormone signaling pathway bta04919 (Figure 6B). The overabundant miRNA (putatively targeting 31,531 genes) were annotated to 19 cell communication and signaling KEGG pathways, including MAPK signaling pathway, Ras signaling pathway, Hippo signaling pathway, Wnt signaling pathway, insulin signaling pathway, mTOR signaling pathway, and cell adhesion molecules (CAMs) bta04514 (Figure 6B).

Pattern identification of commonly affected miRNA during time

Venn diagram analysis of DEM across the time points revealed that the expression pattern of specific miRNA was time-dependent (Figure 7). Among time-dependent DEM, a cluster (Figure 8A) was affected at parturition and turned back to initial levels within 4 weeks, while another cluster (Figure 8B) was affected at day 28 PP and returned to parturition level at day 63 PP.

miRNA-target interaction networks

The biological relevance of miRNA is based on their interaction with their target genes (Lee et al., 2020), although correctly interpreting miRNA-mRNA regulatory pathways is challenging due to numerous potential target genes. Based on the "graph theory" (León and Calligaris, 2017), we analyzed the miRNA-mRNA interaction networks to identify critical nodes and hubs that could act as master regulators, to narrow down the focus of the discussion.

Accordingly, from day -21 to 1, bta-mir-874, bta-mir-149-5p, bta-mir-138, bta-mir-150, and bta-mir-342 from downregulated (Figure 9A) and bta-mir-2466-3p, bta-mir-214, bta-mir-504, bta-mir-497, bta-mir-3431, bta-mir-145, bta-mir-187, bta-mir-127, bta-mir-199b, bta-mir-146b, bta-mir-143, bta-mir-20a, and bta-mir-195 out of the upregulated miRNA (Figure 9B) were considered as master regulators.

From day 1–28 PP, bta-mir-2466-3p, bta-mir-2422, bta-mir-214, bta-mir-504, bta-mir-1247-5p, bta-mir-485, bta-mir-125b, bta-mir-3431, bta-mir-145, bta-mir-187, bta-mir-199b, bta-mir-224, bta-mir-433, and bta-mir-143 from the downregulated cluster (Figure 10A), and bta-mir-149-5p, bta-mir-2387, bta-mir-6523a, bta-mir-24-3p, bta-mir-138, bta-mir-133a, bta-mir-378c, and bta-mir-378b from the upregulated cluster (Figure 10B) were selected according to centrality and betweenness.

Furthermore, the highest betweenness was detected between bta-mir-328, bta-mir-326, bta-mir-1584-3p, bta-mir-2387, bta-mir-6523a, bta-mir-2299-3p, bta-mir-296-5p, bta-mir-4286, bta-mir-1296, bta-mir-23b-5p, bta-mir-128, and bta-mir-425-3p from the downregulated miRNA (Figure 11A), and bta-mir-378, bta-mir-365-5p, bta-mir-199a-5p, bta-mir-122, bta-mir-

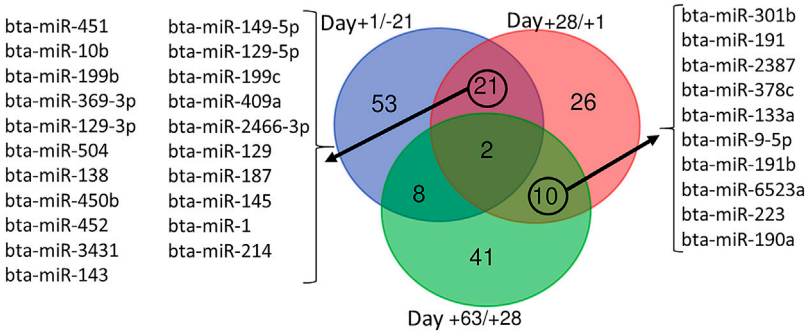

FIGURE 7
Venn diagram representing the overlap between differentially expressed miRNA during time series comparisons, including Day +1/-21 (blue), Day +28/+1 (red), and Day +63/+28 (green).

184, bta-mir-378c, bta-mir-133a, bta-mir-431, and bta-mir-378d from the upregulated miRNA (Figure 11B) when comparing day 28 and 63 PP.

Discussion

MiRNA play an essential role in the post-transcriptional regulation during the endocrine, metabolic, and immune reactions induced by an imbalance between energy requirements and supply during the transition to lactation. Previous studies have shown that severe states of NEB affect the expression of multiple hepatic miRNA and their target genes involved in lipid and glucose metabolism and homeostasis (McCarthy et al., 2010; McCabe et al., 2012; Fatima et al., 2014).

Nevertheless, less information is available regarding the circulating miRNA signature of late gestation and early lactation dairy cows. We used longitudinal miRNAome analysis to characterize DEM at critical time points around parturition and analyze the miRNA-gene network in plasma samples of transition dairy cows to identify candidate miRNA as master regulators of metabolic adaptation. The experimental dairy cows were abomasally supplemented with various fatty acids, and accordingly grouped to CTRL, EFA, CLA, and EFA + CLA. The effects of oil treatment on miRNA expression were negligible, except for the day -21 AP, when bta-miR-1 was differentially expressed between CTRL and CLA groups. No other significant differences were found between the treatment groups. Even though fatty acids treatment altered energy balance in cows of the present study (Vogel et al., 2020), it did not affect miRNA expression or post-transcriptional regulation of energy metabolism. Therefore, the discussion was limited to time-affected miRNA.

Highly abundant miRNA in plasma of ante and postpartum dairy cows

At day -21 AP and day 1 PP, the top five highly expressed miRNA were bta-miR-486, bta-miR-12034, bta-miR-92a, bta-miR-423-5p, and bta-miR-223, while during days 28 and 63 PP, bta-miR-122 got the position of bta-miR-223 in the top 5. Bta-miR-122 is a hepatic dominant conserved miRNA in dairy cows (Jin et al., 2009) and humans (Jopling, 2012), and is involved in regulating cholesterol and fatty acid metabolism (Wu et al., 2017), but also expressed, albeit at lesser values, in the mammary gland, digestive tract, and extracellular vesicular (serum extracted) exosomes (Sun et al., 2019). When profiling the liver miRNA in early lactation, bta-miR-122 was the highest expressed miRNA in dairy cows with mild and severe NEB (Fatima et al., 2014). Consistent with our results, the dominant expression of bta-miR-486 (highest), bta-miR-92a, and bta-miR-423-5p (among the top five) was previously reported in dairy cows' blood exosomes (Sun et al., 2019). In mice, there is evidence that miR-486 and miR-92a are involved in hepatic lipid and cholesterol regulatory pathways by targeting sterol-regulatory element-binding transcription factor-1 (SREBF1) and ATP-binding cassette G4 (ABCG4), respectively (Niculescu et al., 2018). Also in humans, these two miRNA are identified in the high-density circulating lipoproteins (HDL) associated with lipid metabolism (Niculescu et al., 2015). Moreover, bta-miR-30d, bta-miR-21-5p, bta-miR-320a, bta-let-7a-5p, bta-let-7b, and bta-let-7f were reported among the most highly expressed miRNA in dairy cows' dry secretions (Putz et al., 2019). These miRNA have been involved in many aspects of dairy cows' pregnancy, lactation, inflammation, and disease (Putz et al., 2019).

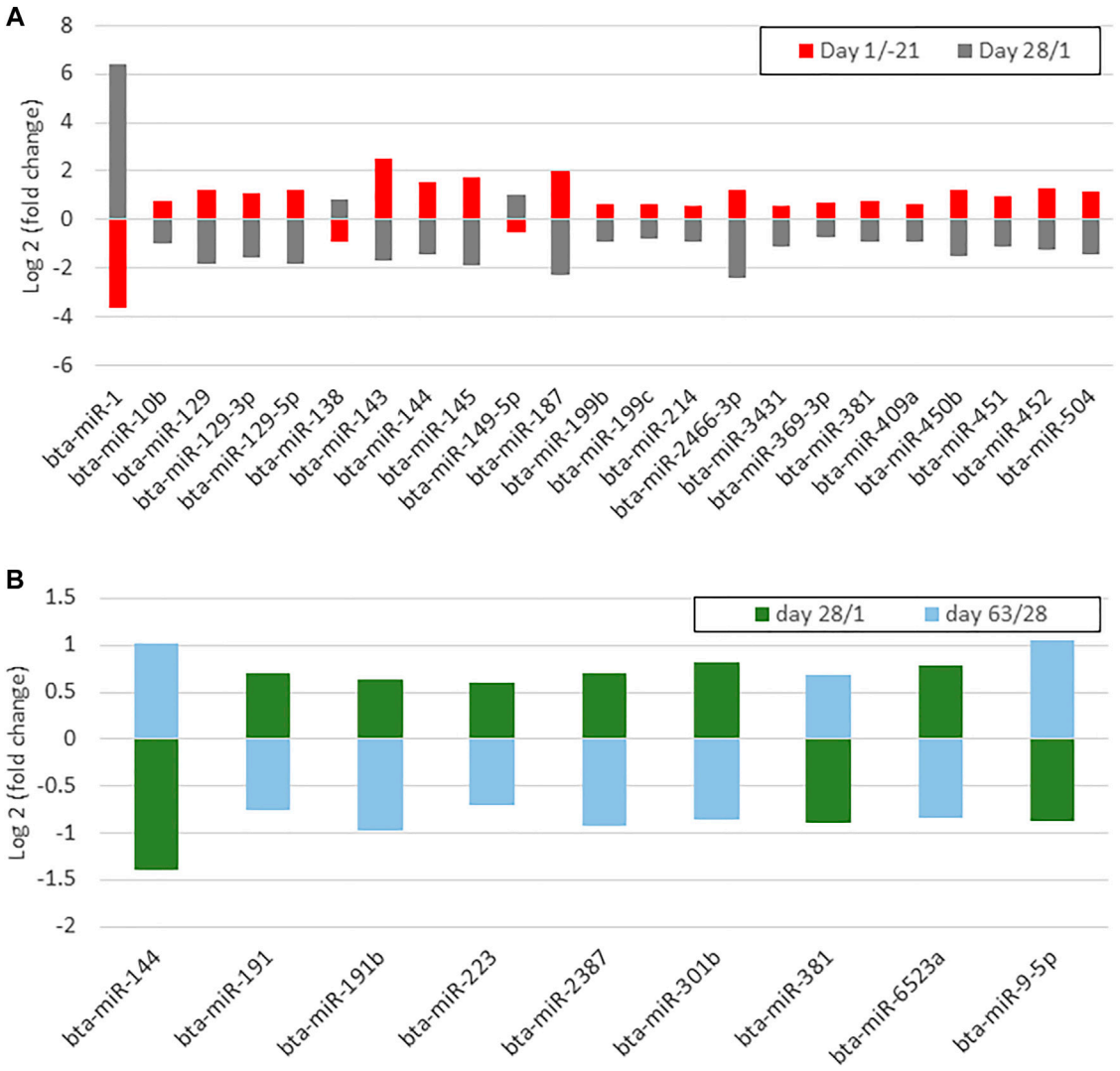

FIGURE 8
(A) A bar chart shows differentially expressed miRNAs whose up- or downregulation occurred on day 1 postpartum and returned antepartum levels on day 28 postpartum **(B)** A bar chart shows differentially expressed miRNAs whose up- or downregulation occurred on day 28 postpartum and returned to day 1 levels on day 63 postpartum.

Differentially expressed miRNA over time

To ensure comparability, the time points were chosen based on physiological reasons and previously collected data (zootechnical, performance, metabolite, hormone levels, as well as plasma proteomics data) (Vogel et al., 2020; Veshkini et al., 2022), under the identical experimental design. The MDS plot revealed a comprehensive perspective of miRNAome profile in individual samples over time, in which the AP period stands as a separate cluster, while there was a high degree of overlap between days 1 and 28 PP, and day 63 tended to be separated from them and form an independent cluster. Interestingly, the cluster separation was in line with dairy cows' energy balance (data are shown in (Vogel et al., 2020)), with positive energy balance (day -21) standing out as a distinct cluster, duration of the lowest energy balance (days 1 and 28 PP) as a second cluster, and the last cluster (day 63) appearing to correspond to a period when the energy balance was turning back to positive values. In this regard, miR-143 was differentially expressed in hepatic miRNA profiles of dairy cows at different levels of energy balance and was mainly related to lipid and energy metabolism (Fatima et al., 2014). Therefore, it might be concluded that energy balance is one of the significant determinants of critical pathways in which miRNA are subsequently necessary for initiating and regulating adaptation processes. As recently reviewed (Kinoshita et al., 2016), glucose

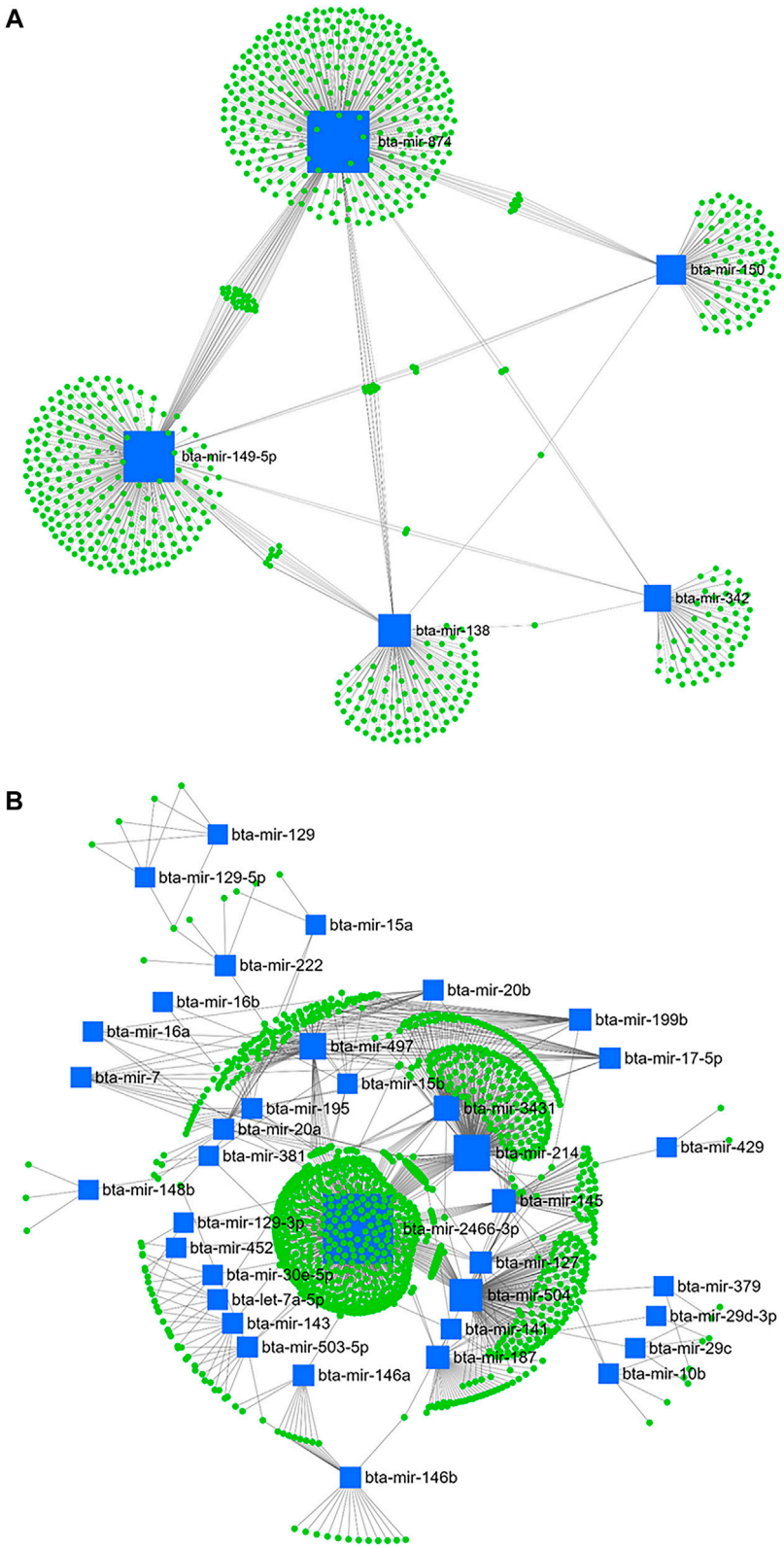

FIGURE 9
miRNA/mRNA network analysis. The regulation network of downregulated **(A)** and upregulated **(B)** miRNAs and predicted target mRNAs in d+1/-21 is illustrated by Cytoscape software. The nodes represent the mRNA (green), and the boxes represent the miRNA (blue). The box size corresponds to the centrality and betweenness of miRNA in constructing the network.

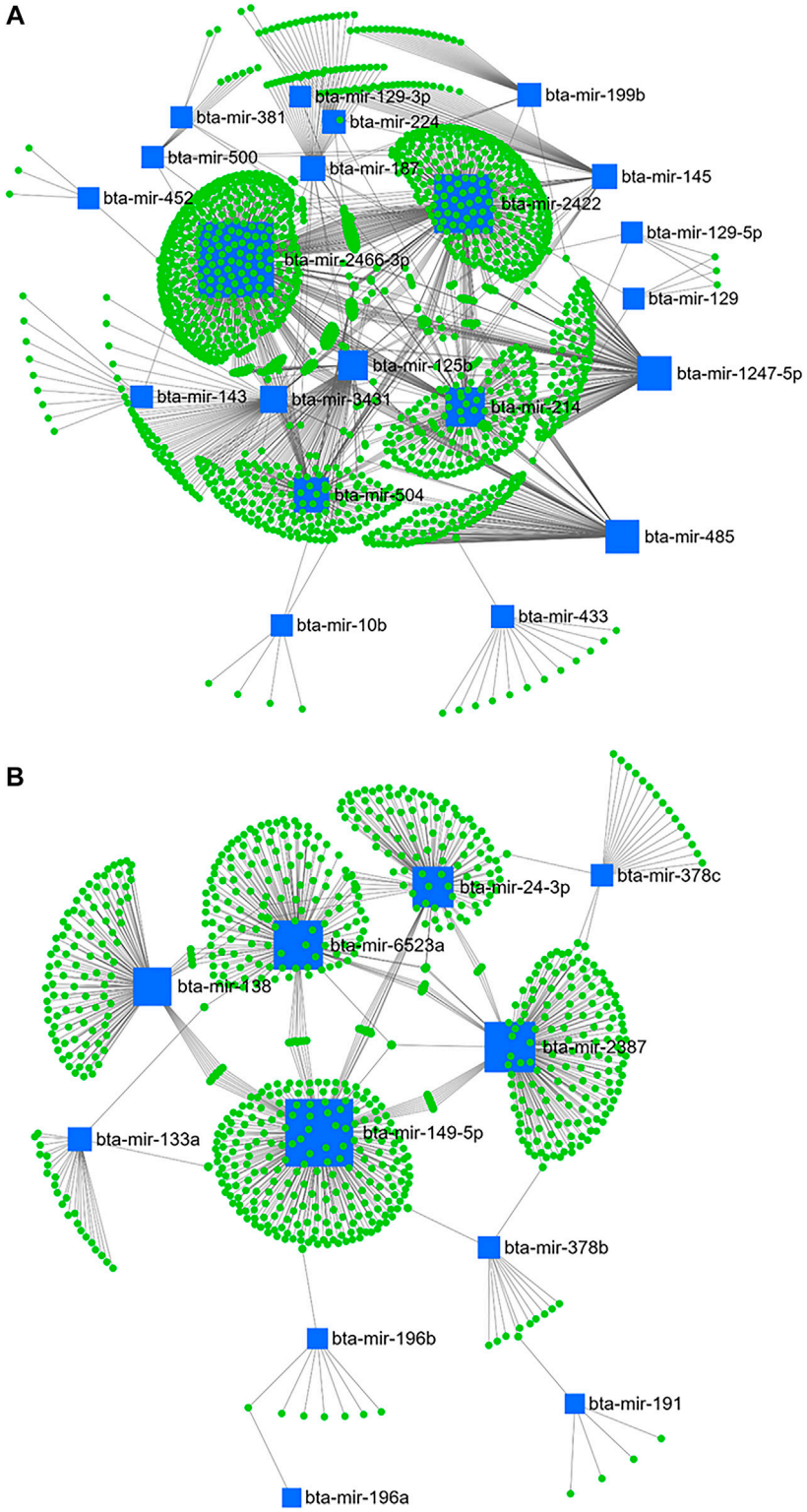

FIGURE 10
miRNA/mRNA network analysis. The regulation network of downregulated **(A)** and upregulated **(B)** miRNAs and predicted target mRNAs in d+28/+1 is illustrated by Cytoscape software. The nodes represent the mRNA (green), and the boxes represent the miRNA (blue). The box size corresponds to the centrality and betweenness of miRNA in constructing the network.

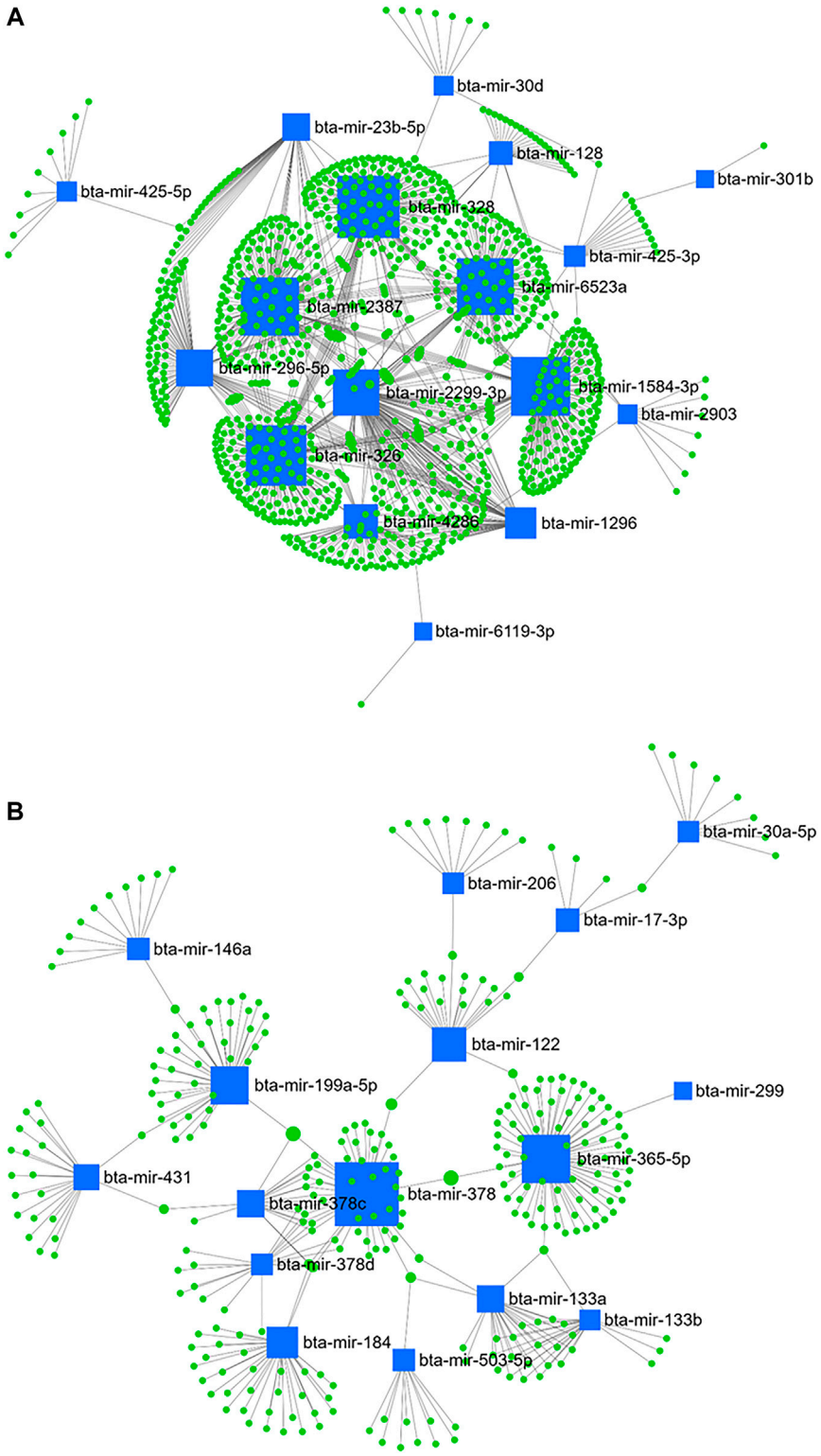

FIGURE 11
miRNA/mRNA network analysis. The regulation network of downregulated **(A)** and upregulated **(B)** miRNAs and predicted target mRNAs in d+63/+28 is illustrated by Cytoscape software. The nodes represent the mRNA (green), and the boxes represent the miRNA (blue). The box size corresponds to the centrality and betweenness of miRNA in constructing the network.

and lipid metabolism are systemically controlled by a complex orchestrated network containing a plethora of different molecules, such as hormones, lipoproteins, and miRNA. Although there are likely other players involved such as inflammation and immune activation, since in the current design fatty acid treatment significantly affected energy balance (Vogel et al., 2020), but not miRNA expression, which requires further investigation. Therefore, cluster separation was due to time-dependent miRNA expression, in which specific sets of miRNA were probably associated with the physiological state at that time. It should be noted that miRNA expression does not necessarily follow a linear order over time. Thus, there might be other up or downregulated miRNA during the AP and PP periods which were not detected according to our selected time points.

Differentially expressed miRNA and their associated pathways during the transition period

The transition from gestation to lactation considerably alters miRNA expression, with five times more upregulated miRNA than those downregulated. This might be biologically relevant since most miRNA induce mRNA degradation and translational repression (O'Brien et al., 2018), thereby as part of the adaptation process switching to several organs and tissues' catabolic status to prioritize milk production over other biological pathways (Veshkini et al., 2022). Although, in the following time points, some of the DEM showed reverse expression, which gradually inverted adaptations to restore normal metabolic and physiological conditions. In this regard, we have previously shown for various metabolites and the proteome that different aspects of the immune system (such as the complement system) (Veshkini et al., 2022) and lipid metabolism including lipoprotein content (Vogel et al., 2020) and apolipoprotein protein abundance (Veshkini et al., 2022) were temporarily downregulated at the time of parturition, and then gradually recovered within the next few weeks after parturition.

The DEM at day 1 PP were annotated to critical immune functions and energy metabolism pathways, including insulin, Ras, MAPK, Wnt, Hippo, sphingolipid, mTOR, and TCR signaling pathways. These signaling pathways are critical to establishing metabolic adaptation at the onset of lactation; therefore, they are strictly controlled. Their dysregulation results in immune and metabolic dysfunction and diseases (Sebastian-Leon et al., 2014). These results align with our recent findings, whereupon metabolic adaptations around calving are most prominent in two distinct but tightly interconnected physiological processes: lipid (energy) metabolism and immune function (Veshkini et al., 2022). The identified adaptation signaling pathways are tightly interconnected and exhibit functions that regulate a diverse array of physiological processes and cellular processes like proliferation, differentiation, transformation, inflammatory responses, apoptosis, and homeostasis in dairy cows (Sigdel et al., 2021). There is also evidence from a human study that circulating and tissue-derived miRNA play a crucial role in the cross-talk between different organs, acting as endocrine and paracrine messengers in intercellular communication (Kiran et al., 2021).

It is important to emphasize that targeted genes may overlap between up and downregulated miRNA; indeed, several pathways were annotated by both up and downregulated miRNA. Information regarding the source or target tissues of DEM is unavailable; therefore, discussing each pathway's direction according to the direction of miRNA expression seems inefficient. Instead, signaling pathways are discussed according to the literature and our previously published results at the proteome (OMICS based) and metabolite and hormones (classical kit measurements) level from the same experiment, in which the AP period was taken into consideration as the basis and calving as the critical time point for the initiation of the adaptation process.

A major component of immune adaptation was probably triggered by activating the TCR signaling pathway, which activates the NF-κb and downstream signaling cascades that regulate cytokine production, cell survival, proliferation, and differentiation (Hwang et al., 2020). In addition, the TCR signaling pathway initiates intracellular signals essential for T cell development and recruits macrophages for ingesting apoptotic and damaged cells (Moro-García et al., 2018; Shah et al., 2021), which is crucial during the rapid tissue remodeling at calving. Numerous miRNA have been reported to be associated with TCR signaling pathways (Rodríguez-Galán et al., 2018) of which miR-26b, miR-142, miR-146, miR-150, miR-342, and miR-451 were among our DEM.

Specific annotated pathways are downstream targets of the NF-κb pathway, and thus they might have ignited a state of inflammation already underway before parturition. In this regard, intracellular signaling pathways such as Wnt (Jeong et al., 2018), Hippo (Feng et al., 2017), TCR (Adachi and Davis, 2011), Rap1 (Pizon and Baldacci, 2000), and mTOR (Wang et al., 2013) are reportedly related to various physiological and pathological conditions depending on the specific cellular context. The Wnt pathway consists of a large family of highly conserved glycoproteins that cross-talk with MAPK in development, determining cell fate, tissue regeneration, and maintaining tissue homeostasis (Zhang et al., 2014). Previous studies have shown that Wnt and MAPK pathways are essential for normal mammary gland development (Roarty and Serra, 2007; Li et al., 2018) and are involved in immune system-related signaling pathways (Luoreng et al., 2021). These studies reported candidate miRNA including bta-miR-19a, bta-miR-19b, bta-miR-21-5p, bta-miR-29c, bta-miR-143, bta-miR-145, and bta-miR-146b are associated with

Wnt signals and MAPK pathway (Li et al., 2018; Luoreng et al., 2021). Mounting evidence from recent human studies also suggested that Wnt is involved in immune signaling, thus regulating immune cell maintenance and renewal, modulation of inflammatory cytokine production, such as NF-κB signaling, and bridging innate and adaptive immunity (Patel et al., 2019; Jridi et al., 2020). Furthermore, Rap1 is shown to function as a transcriptional cofactor that regulates the NF-κB pathway (Yeung et al., 2013).

The current results follow a challenging hypothesis proposed by Bradford et al. (Bradford et al., 2015) as the presence of a sub-acute inflammation during the peripartum period, which has been reviewed later and related to tissue damage and remodeling during this prenatal period in critical organs such as the mammary glands, liver, and adipose tissue (for review, see (Horst et al., 2021)). An earlier study reported that low-grade systemic inflammation, also known as "metabolic inflammation" and "sub-acute inflammation", plays an important role in developing insulin resistance and hepatic steatosis in mice activating NF-κB signaling pathways (Zeng et al., 2016). As low-grade systemic inflammation in early lactation is a non-infectious inflammatory response, it may activate a type of non-canonical NF-κB that exhibits slower but continuous function (for review, see (Sun, 2011)). Coordinating these signaling pathways develops an immune adaptation process during the transition period in which miRNA play a crucial role (for review, see (Lawless et al., 2014; Chandan et al., 2019)). However, the tissue and cellular level of individual miRNA require further investigation. Further, the current study design did not determine precisely when the systemic inflammation began, reached its peak, and diminished.

Metabolic adaptations are at least partly mediated by alterations in the insulin signaling pathway during early lactation, which is a highly conserved regulatory network coordinating animal metabolism (Zachut et al., 2013). Insulin resistance in the periparturient cow has been ascribed to multiple factors, including low-grade inflammation as one of the primary ones (Rehman and Akash, 2016). Dairy cows in the periparturient period have moderately reduced peripheral tissue insulin sensitivity, which promotes the mobilization of body fat and protein reserves and prioritizes nutrients to the fetus and mammary gland (Zachut et al., 2013). *In vivo* measurements revealed a considerable drop ($p < 0.001$) in plasma insulin levels in the PP period over the AP period (Supplementary Figure S1) and there is a distinct decrease in the insulin release in the PP transition cow (Weber et al., 2016). As a result, we hypothesized that insulin metabolism pathways were partially downregulated. Some of the DEM found herein were previously reported to be associated with the insulin signaling pathway in humans (Nigi et al., 2018). Among those, miR-15b and miR-195 directly regulate the insulin receptor and miR-1 regulates the IGF-1 and IGF1-receptor. Also, miR-122, miR-144, miR-145, miR-146a, miR-214, and miR-375 indirectly affect insulin signaling pathways (Nigi et al., 2018).

The insulin signaling pathways and the sphingolipid signaling pathways, are interrelated: sphingolipid accumulation at the onset of lactation may inhibit insulin signaling and cause insulin resistance in various tissues of dairy cows (McFadden and Rico, 2019), although they are not the sole mediator of insulin antagonism (Petersen and Jurczak, 2016). In that sense, modulating insulin signaling by the sphingolipid signaling pathway and in particular ceramides may considerably impact on regulating glucose utilization, maintaining PP health, and milk production in dairy cows (for review, see (McFadden and Rico, 2019)). Within the sphingolipid pathway, miR-1, miR-101, miR-125b, and miR-128 interact with sphingosine kinases, sphingosine-1 phosphate, and sphingosine-1 phosphate receptors (for review, see (Xu et al., 2021)). The knowledge of sphingolipids in inflammation and endocrine function of dairy cows will continue to grow with the increased accessibility of lipidomics technologies.

In association with the insulin signaling pathway, Ras/Raf/MAPK (rat sarcoma/rapidly accelerated fibrosarcoma/mitogen-activated protein kinases) as major signaling pathways are triggered to transduce signals from the extracellular milieu to the cell nucleus where specific genes are activated to promote gluconeogenesis, lipolysis, re-adjust insulin sensitivity, and regulate the cellular response to various stimuli (Saltiel and Kahn, 2001; Wang et al., 2013). The MAPK family members were also shown to be involved in hepatic and systemic inflammation and apoptosis in dairy cows (Li et al., 2020; Horst et al., 2021), and thus in the initiation of the innate immune system and cytokine receptor-mediated responses, as well as in the adaptive immune system through regulating T and B lymphocyte differentiation (Krzyzowska et al., 2010). Several human miRNA were suggested to be associated with the MAPK signaling pathway (in chronic myeloid leukemia (Chakraborty et al., 2016)), including miR-196a, miR-196b, miR-30a, miR-138, miR-126, miR-221, miR-128, miR-15a, miR-17, and miR-19a that were found as DEM during different time points in the present study.

Also, mTOR is one of the main signaling factors for metabolic adaptation and responds to growth factors, energy and amino acid levels, and cellular stress to regulate transcription, protein and lipid synthesis, sphingolipid biosynthesis, membrane homeostasis, cell cycle progression, endocytosis, and nutrient transport and autophagy (Madrid et al., 2016; Sadri et al., 2016). The mTOR and MAPK signaling pathways may cross-talk to maintain essential cellular functions (Madrid et al., 2016) and probably direct protein synthesis toward the mammary gland and, thus, milk production in early lactating dairy cows. In accordance, a recent study on dairy goats suggested the involvement of the AMPK-mTOR pathway in mammary milk protein synthesis (Cai et al., 2020). The DEM identified herein were predominantly involved

in signaling cross-talk regulatory mechanisms that determine energy homeostasis as a part of metabolic adaptations.

As discussed earlier, the expression level of several DEMs was reversed within a few weeks of lactation and then returned to AP expression, which resulted in normalized insulin, mTOR, and Ras signaling pathways. These results are consistent with our previous proteomics findings in which indicators of metabolic and immune adaptation such as acute phase proteins (haptoglobin, lipopolysaccharide-binding protein, alpha-2-Heremans-Schmid glycoprotein, and adiponectin) and various complement proteins at the onset of lactation were restored within four to 9 weeks of lactation (Veshkini et al., 2022).

Beside those affected pathways, the TNF signaling pathway was annotated by downregulated miRNA on day 28 PP. The NF-κB pathway is activated through TNF signalling pathways, producing various proinflammatory cytokines (including TNF-α). Moreover, lipoprotein lipase is inhibited thus decreasing fatty acid uptake and lipogenesis, and increasing lipolysis in adipose tissue (Kim et al., 2014). Conversely, TNF-α promotes the hepatic expression of SREBP1c, a major regulatory transcription factor in hepatic lipogenesis and the development of hepatic steatosis in humans (Kim et al., 2014). In addition, TNF-α, besides being a well-known major proinflammatory cytokine, induces in part insulin resistance through phosphorylation of Jun and insulin receptors (Kim et al., 2014). Accordingly, a possible explanation could be that early lactation inflammation induces TNF-α, affecting downstream pathways, including insulin signaling pathways. Then, TNF signaling was also reduced in conjunction with attenuated systemic inflammation at 28 days PP.

Determination of key miRNA and their target mRNA in regulatory pathways

As discussed earlier, a group of miRNA had a time-dependent expression including overexpression of bta-miR-10b, bta-miR-129 family, bta-miR-143, bta-miR-144, bta-miR-145, bta-miR-187, bta-miR-199b, bta-miR-214, bta-miR-369-3p, bta-miR-381, bta-miR-409a, bta-miR-450b, bta-miR-451, bta-miR-452, bta-miR-504, and bta-miR-2466-3p and downregulation of miR-1, bta-miR-138, and bta-miR-149-5p at parturition. These miRNA returned to AP expression after 28 days. During the transition from day 1–28 PP, another cluster, including bta-miR-133a, bta-miR-144, and bta-miR-378c, was downregulated, whereas bta-miR-9-5p, bta-miR-190a, bta-miR-191, bta-miR-191b, bta-miR-223, bta-miR-301b, bta-miR-381, bta-miR-2387, and bta-miR-6523a were upregulated. These miRNA regained their parturition levels on day 63 PP. Based on bioinformatics analysis, time-dependent DEM and their predicted target genes have been annotated to insulin secretion, sphingolipids, TNF, NF-κB, B cell receptor, and MAPK signaling pathways, the key indicators in determining metabolic and immune adaptation success.

We determined which miRNA are the central hub of those enriched pathways using miRNA-mRNA network analysis. Considering time-dependent expression and network analysis, bta-miR-138, miR-149-5p, bta-miR-214, bta-miR-504, bta-miR-2387, bta-miR-2466-3p, and bta-miR-6523a were selected as the central hub regulating annotated signaling pathways. Significant positive correlations were observed between bta-miR-504 and bta-miR-2466-3p ($r = 0.51$, p-value < 0.001), and bta-miR-504 and bta-miR-214 ($r = 0.6$, p-value < 0.001) (Supplementary Figure S2). According to bioinformatics analysis, these miRNA and their target genes are among the key regulators of the NF-κB signaling pathway, insulin secretion, sphingolipid, TNF, B cell receptor, and MAPK signaling pathways. Several target genes were common to these signaling pathways including, MAPK3, MAPK14, MAP3K14, MAP2K2, JUN, MYD88, NRAS (neuroblastoma RAS viral (V-ras) oncogene homolog), FOS, IKBKG (inhibitor of nuclear factor-kappa B kinase regulatory subunit gamma), IKBKB (inhibitor of nuclear factor-kappa B kinase subunit beta), and RELA (Supplementary Figure S3), which were the key genes in previously annotated metabolic and immune pathways. Also, protein-protein interaction network analysis revealed that all these genes are biologically connected (Supplementary Figure S4). Overall, bioinformatics provided a subset of miRNA considered the regulatory hub for metabolic and immune adaptation processes, which can be used as candidates to assess the metabolic health of dairy cows during the transition period. Nevertheless, future studies should focus on the specific role of these miRNA in metabolic disorders.

Conclusion

Investigating circulating miRNA revealed novel insights into miRNA signatures associated with metabolic and immune adaptation in late gestation and early lactation dairy cows. There were time-dependent differences in the expression of specific miRNA, in which the calving effect predominated, such that their expression was differential during the parturition time and returned to normal after a few weeks (days 28 and 63 PP). Calving prevailing was partially caused by DEM associated with a state of systemic inflammation. Bioinformatics analysis suggested that metabolic adaptation initiated by systemic inflammation, and DEM orchestrates critical signaling pathways, including TCR, NF-κB, MAPK, and insulin, which facilitate cross-talk between energy metabolism and immunity in target tissues across the whole body. In particular, the miRNA-mRNA network analysis revealed circulating DEM including bta-miR-138, miR-149-5p, bta-miR-2466-3p, bta-miR-214, bta-miR-504, and bta-miR-6523a and their targeted genes as central hubs that regulate key signal transduction pathways associated with energy homeostasis and immune response in transition dairy cows. However, a more in-depth analysis of the identified miRNA and their target genes is required to develop them as biomarkers of metabolic homeostasis.

Data availability statement

The data presented in the study are deposited in the ArrayExpress database (http://www.ebi.ac.uk/arrayexpress) repository, accession number E-MTAB-11725.

Ethics statement

The animal study was reviewed and approved by The State Mecklenburg-Western Pomerania, Germany (LALLF M-V/TSD/7221.3-1-038/15).

Author contributions

HMH and AT suggested the main idea of the basic animal study; AT supplied materials. HMH designed and performed the animal study and collected performance and blood and tissue data. HMH, FC, and HS elaborated the concept for the current analyses, contributed to the research's design and implementation, and supervised the related works. VV conducted the NGS analysis and the related works. BL designed and conducted the statistical analyses. LV and MG planned and performed the farm trial. AV and HaS performed sample preparation and laboratory analysis and provided methodologies, respectively. AV curated and visualized the NGS data, did the bioinformatics analysis, and wrote the paper. HaS, BL, HMH, FC, and HS revised the manuscript. All authors reviewed the results and approved the final version of the manuscript.

Funding

This project has received funding from the European Union's Horizon 2020 research and innovation programme H2020-MSCA-ITN-2017-EJD: Marie Skłodowska-Curie Innovative Training Networks (European Joint Doctorate)—Grant agreement n°: 765423. The animal study was supported by BASF SE (Ludwigshafen, Germany).

Acknowledgments

The authors express their appreciation to Inga Hofs and Hannah Schell (Institute of Animal Science, Physiology Unit, University of Bonn, Germany) and to the Fraunhofer Institute for Translational Medicine technicians Pharmacology ITMP (Frankfurt, Germany) for their technical assistance.

Conflict of interest

AT was employed by BASF and author VV was employed by IGA Technology Services.

The authors declare that the research was conducted in the absence of any commercial or financial relationships that could be construed as a potential conflict of interest.

Publisher's note

All claims expressed in this article are solely those of the authors and do not necessarily represent those of their affiliated organizations, or those of the publisher, the editors and the reviewers. Any product that may be evaluated in this article, or claim that may be made by its manufacturer, is not guaranteed or endorsed by the publisher.

Supplementary material

The Supplementary Material for this article can be found online at: https://www.frontiersin.org/articles/10.3389/fgene.2022.946211/full#supplementary-material

References

Adachi, K., and Davis, M. (2011). T-cell receptor ligation induces distinct signaling pathways in naïve vs. antigen-experienced T cells. *Proc. Natl. Acad. Sci. U.S.A.* 108, 1549–1554. doi:10.1073/pnas.1017340108

Barutta, F., Bellini, S., Mastrocola, R., Bruno, G., and Gruden, G. (2018). MicroRNA and microvascular complications of diabetes. *Int. J. Endocrinol.* 2018, 6890501. doi:10.1155/2018/6890501

Bradford, B. J., Yuan, K., Farney, J. K., Mamedova, L. K., and Carpenter, A. J. (2015). Invited review: Inflammation during the transition to lactation: New adventures with an old flame. *J. Dairy Sci.* 98, 6631–6650. doi:10.3168/jds.2015-9683

Cai, J., Wang, D., Zhao, F-Q., Liang, S., and Liu, J. (2020). AMPK-mTOR pathway is involved in glucose-modulated amino acid sensing and utilization in the mammary glands of lactating goats. *J. Anim. Sci. Biotechnol.* 11, 32. doi:10.1186/s40104-020-0434-6

Ceciliani, F., Lecchi, C., Urh, C., and Sauerwein, H. (2018). Proteomics and metabolomics characterizing the pathophysiology of adaptive reactions to the metabolic challenges during the transition from late pregnancy to early lactation in dairy cows. *J. Proteomics* 178, 92–106.

Chakraborty, C., Sharma, A. R., Patra, B. C., Bhattacharya, M., Sharma, G., and Lee, S-S. (2016). MicroRNAs mediated regulation of MAPK signaling pathways in chronic myeloid leukemia. *Oncotarget* 7, 42683–42697. doi:10.18632/oncotarget.7977

Chandan, K., Gupta, M., and Sarwat, M. (2019). Role of host and pathogen-derived MicroRNAs in immune regulation during infectious and inflammatory diseases. *Front. Immunol.* 10, 3081. doi:10.3389/fimmu.2019.03081

Condrat, C. E., Thompson, D. C., Barbu, M. G., Bugnar, O. L., Boboc, A., Cretoiu, D., et al. (2020). miRNAs as biomarkers in disease: Latest findings regarding their role in diagnosis and prognosis. *Cells* 9, 276. doi:10.3390/cells9020276

DLG (Deutsche Landwirtschafts-Gesellschaft, German Agricultural Society) (2013). *Stellungnahme des DLG-Arbeitskreises Futter und Fütterung*.Leitfaden zur Berechnung des Energiegehaltes bei Einzel-und Mischfuttermitteln für die Schweine-und Rinderfütterung (Guidelines for calculation of energy content of single and mixed feedstuff for pigs and cattle)

Do, D. N., Dudemaine, P-L., Mathur, M., Suravajhala, P., Zhao, X., and Ibeagha-Awemu, E. M. (2021). miRNA regulatory functions in farm animal diseases, and biomarker potentials for effective therapies. *Ijms* 22, 3080. doi:10.3390/ijms22063080

Drackley, J. K. (1999). Biology of dairy cows during the transition period: The final frontier? *J. Dairy Sci.* 82, 2259–2273. doi:10.3168/jds.s0022-0302(99)75474-3

Fatima, A., Lynn, D. J., O'Boyle, P., Seoighe, C., and Morris, D. (2014). The miRNAome of the postpartum dairy cow liver in negative energy balance. *BMC Genomics* 15, 279. doi:10.1186/1471-2164-15-279

Feng, R., Gong, J., Wu, L., Wang, L., Zhang, B., Liang, G., et al. (2017). MAPK and Hippo signaling pathways crosstalk via the RAF-1/MST-2 interaction in malignant melanoma. *Oncol. Rep.* 38, 1199–1205. doi:10.3892/or.2017.5774

Friedländer, M. R., Mackowiak, S. D., Li, N., Chen, W., and Rajewsky, N. (2012). miRDeep2 accurately identifies known and hundreds of novel microRNA genes in seven animal clades. *Nucleic Acids Res.* 40, 37–52. doi:10.1093/nar/gkr688

GfE Gesellschaft für Ernährungsphysiologie (German Society of Nutrition Physiology) (2001). *Empfehlungen zur Energie- und Nährstoffversorgung der Milchkühe und Aufzuchtrinder (Recommended energy and nutrient suply of dairy cows and growing cattle)*, Vol. 8. Germany: DLGVerlag, Frankfurt a. M.

GfE Gesellschaft für Ernährungsphysiologie (German Society of Nutrition Physiology) (2009). New equations for predicting metabolizable energy of compound feeds for cattle. Communications of the Committee for Requirement Standards of the Society of Nutrition Physiology. *Proc. Soc. Nutr. Physiol.* 18, 143–146.

GfE Gesellschaft für Ernährungsphysiologie (German Society of Nutrition Physiology) (2008). New equations for predicting metabolizable energy of grass and maize products for ruminants. Communications of the Committee for Requirement Standards of the Society of Nutrition Physiology. *Proc. Soc. Nutr. Physiol.* 17, 191–198.

Hailay, T., Hoelker, M., Poirier, M., Gebremedhn, S., Rings, F, Saeed-Zidane, M., et al. (2019). Extracellular vesicle-coupled miRNA profiles in follicular fluid of cows with divergent post-calving metabolic status. *Sci. Rep.* 9, 12851. doi:10.1038/s41598-019-49029-9

Horst, E. A., Kvidera, S. K., and Baumgard, L. H. (2021). Invited review: The influence of immune activation on transition cow health and performance-A critical evaluation of traditional dogmas. *J. Dairy Sci.* 104, 8380–8410. doi:10.3168/jds.2021-20330

Hwang, J-R., Byeon, Y., Kim, D., and Park, S-G. (2020). Recent insights of T cell receptor-mediated signaling pathways for T cell activation and development. *Exp. Mol. Med.* 52, 750–761. doi:10.1038/s12276-020-0435-8

Jeong, W-J., Ro, E. J., and Choi, K-Y. (2018). Interaction between Wnt/β-catenin and RAS-ERK pathways and an anti-cancer strategy via degradations of β-catenin and RAS by targeting the Wnt/β-catenin pathway. *npj Precis. Onc* 2, 5. doi:10.1038/s41698-018-0049-y

Jin, W., Grant, J. R., Stothard, P., Moore, S. S., and Guan, L. L. (2009). Characterization of bovine miRNAs by sequencing and bioinformatics analysis. *BMC Mol. Biol.* 10, 90. doi:10.1186/1471-2199-10-90

Jopling, C. (2012). Liver-specific microRNA-122: Biogenesis and function. *RNA Biol.* 9, 137–142. doi:10.4161/rna.18827

Jridi, I., Canté-Barrett, K., Pike-Overzet, K., and Staal, F. J. T. (2020). Inflammation and Wnt signaling: Target for immunomodulatory therapy? *Front. Cell. Dev. Biol.* 8, 615131. doi:10.3389/fcell.2020.615131

Kim, J., and Bajaj, M. (2014). "Normal adipose tissue biology: Adipocytokines and inflammation," in *Pathobiology of human disease*. Editors L. M. McManus and R. N. Mitchell (San Diego: Academic Press), 488–497. doi:10.1016/b978-0-12-386456-7.02006-2

Kinoshita, A., Kenéz, Á., Locher, L., Meyer, U., Dänicke, S., Rehage, J., et al. (2016). Insulin signaling in liver and adipose tissues in periparturient dairy cows supplemented with dietary nicotinic acid. *PLoS One* 11, e0147028. doi:10.1371/journal.pone.0147028

Kiran, S., Kumar, V., Kumar, S., Price, R. L., and Singh, U. P. (2021). Adipocyte, immune cells, and miRNA crosstalk: A novel regulator of metabolic dysfunction and obesity. *Cells* 10, 1004. doi:10.3390/cells10051004

Kozomara, A., Birgaoanu, M., and Griffiths-Jones, S. (2019). miRBase: from microRNA sequences to function. *Nucleic Acids Res.* 47, D155–D162. doi:10.1093/nar/gky1141

Krzyzowska, M., Swiatek, W., Fijalkowska, B., Niemialtowski, M., and Schollenberger, A. (2010). The role of map kinases in immune response. *Adv. Cell. Biol.* 1, 1–14. doi:10.2478/v10052-010-0007-5

Lawless, N., Vegh, P., O'Farrelly, C., and Lynn, D. J. (2014). The role of microRNAs in bovine infection and immunity. *Front. Immunol.* 5, 611. doi:10.3389/fimmu.2014.00611

Lee, J., Lee, S., Son, J., Lim, H., Kim, E., Kim, D., et al. (2020). Analysis of circulating-microRNA expression in lactating Holstein cows under summer heat stress. *PLoS One* 15, e0231125. doi:10.1371/journal.pone.0231125

León, L. E., and Calligaris, S. D. (2017). Visualization and analysis of MiRNA-targets interactions networks. *Methods Mol. Biol.* 1509, 209–220. doi:10.1007/978-1-4939-6524-3_19

Li, Q., Yang, C., Du, J., Zhang, B., He, Y., Hu, Q., et al. (2018). Characterization of miRNA profiles in the mammary tissue of dairy cattle in response to heat stress. *BMC Genomics* 19, 975. doi:10.1186/s12864-018-5298-1

Li, Y., Ding, H., Liu, L., Song, Y., Du, X., Feng, S., et al. (2020). Non-esterified fatty acid induce dairy cow hepatocytes apoptosis via the mitochondria-mediated ROS-JNK/ERK signaling pathway. *Front. Cell. Dev. Biol.* 8. doi:10.3389/fcell.2020.00245

Lin, H., Tas, E., Børsheim, E., and Mercer, K. E. (2020). Circulating miRNA signatures associated with insulin resistance in adolescents with obesity. *Dmso* Vol. 13, 4929–4939. doi:10.2147/dmso.s273908

Luoreng, Z-M., Yang, J., Wang, X-P., Wei, D-W., and Zan, L-S. (2021). Expression profiling of microRNA from peripheral blood of dairy cows in response to Staphylococcus aureus-infected mastitis. *Front. Vet. Sci.* 8, 691196. doi:10.3389/fvets.2021.691196

Madrid, M., Vázquez-Marín, B., Franco, A., Soto, T., Vicente-Soler, J., Gacto, M., et al. (2016). Multiple crosstalk between TOR and the cell integrity MAPK signaling pathway in fission yeast. *Sci. Rep.* 6, 37515. doi:10.1038/srep37515

McCabe, M., Waters, S., Morris, D., Kenny, D., Lynn, D., and Creevey, C. (2012). RNA-seq analysis of differential gene expression in liver from lactating dairy cows divergent in negative energy balance. *BMC Genomics* 13, 193. doi:10.1186/1471-2164-13-193

McCarthy, S. D., Waters, S. M., Kenny, D. A., Diskin, M. G., Fitzpatrick, R., Patton, J., et al. (2010). Negative energy balance and hepatic gene expression patterns in high-yielding dairy cows during the early postpartum period: A global approach. *Physiol. Genomics* 42A, 188–199. doi:10.1152/physiolgenomics.00118.2010

McFadden, J. W., and Rico, J. E. (2019). Invited review: Sphingolipid biology in the dairy cow: The emerging role of ceramide. *J. Dairy Sci.* 102, 7619–7639. doi:10.3168/jds.2018-16095

Moro-García, M. A., Mayo, J. C., Sainz, R. M., and Alonso-Arias, R. (2018). Influence of inflammation in the process of T lymphocyte differentiation: Proliferative, metabolic, and oxidative changes. *Front. Immunol.* 9, 339. doi:10.3389/fimmu.2018.00339

Niculescu, L., Simionescu, N., Fuior, E., Stancu, C., Carnuta, M., Dulceanu, M., et al. (2018). Inhibition of miR-486 and miR-92a decreases liver and plasma cholesterol levels by modulating lipid-related genes in hyperlipidemic hamsters. *Mol. Biol. Rep.* 45, 497–509. doi:10.1007/s11033-018-4186-8

Niculescu, L. S., Simionescu, N., Sanda, G. M., Carnuta, M. G., Stancu, C. S., Popescu, A. C., et al. (2015). MiR-486 and miR-92a identified in circulating HDL discriminate between stable and vulnerable coronary artery disease patients. *PLoS One* 10, e0140958. doi:10.1371/journal.pone.0140958

Nigi, L., Grieco, G. E., Ventriglia, G., Brusco, N., Mancarella, F., Formichi, C., et al. (2018). MicroRNAs as regulators of insulin signaling: Research updates and potential therapeutic perspectives in type 2 diabetes. *Ijms* 19, 3705. doi:10.3390/ijms19123705

O'Brien, J., Hayder, H., Zayed, Y., and Peng, C. (2018). Overview of MicroRNA biogenesis, mechanisms of actions, and circulation. *Front. Endocrinol. (Lausanne)* 9, 402. doi:10.3389/fendo.2018.00402

Patel, S., Alam, A., Pant, R., and Chattopadhyay, S. (2019). Wnt signaling and its significance within the tumor microenvironment: Novel therapeutic insights. *Front. Immunol.* 10, 2872. doi:10.3389/fimmu.2019.02872

Petersen, M. C., and Jurczak, M. J. (2016). CrossTalk opposing view: Intramyocellular ceramide accumulation does not modulate insulin resistance. *J. Physiol.* 594, 3171–3174. doi:10.1113/jp271677

Pizon, V., and Baldacci, G. (2000). Rap1A protein interferes with various MAP kinase activating pathways in skeletal myogenic cells. *Oncogene* 19, 6074–6081. doi:10.1038/sj.onc.1203984

Putri, G. H., Anders, S., Pyl, P. T., Pimanda, J. E., and Zanini, F. (2022). Analyzing high-throughput sequencing data in Python with HTSeq 2.0. *Bioinformatics*.

Putz, E. J., Putz, A. M., Jeon, H., Lippolis, J. D., Ma, H., Reinhardt, T. A., et al. (2019). MicroRNA profiles of dry secretions through the first three weeks of the dry period from Holstein cows. *Sci. Rep.* 9, 19658. doi:10.1038/s41598-019-56193-5

Rehman, K., and Akash, M. S. H. (2016). Mechanisms of inflammatory responses and development of insulin resistance: How are they interlinked? *J. Biomed. Sci.* 23, 87. doi:10.1186/s12929-016-0303-y

Roarty, K., and Serra, R. (2007). Wnt5a is required for proper mammary gland development and TGF-β-mediated inhibition of ductal growth. *Development* 134, 3929–3939. doi:10.1242/dev.008250

Rodríguez-Galán, A., Fernández-Messina, L., and Sánchez-Madrid, F. (2018). Control of immunoregulatory molecules by miRNAs in T cell activation. *Front. Immunol.* 9. doi:10.3389/fimmu.2018.02148

Sadri, H., Giallongo, F., Hristov, A. N., Werner, J., Lang, C. H., Parys, C., et al. (2016). Effects of slow-release urea and rumen-protected methionine and histidine on mammalian target of rapamycin (mTOR) signaling and ubiquitin proteasome-related gene expression in skeletal muscle of dairy cows. *J. Dairy Sci.* 99, 6702–6713. doi:10.3168/jds.2015-10673

Saltiel, A. R., and Kahn, C. R. (2001). Insulin signalling and the regulation of glucose and lipid metabolism. *Nature* 414, 799–806. doi:10.1038/414799a

Sebastian-Leon, P., Vidal, E., Minguez, P., Conesa, A., Tarazona, S., Amadoz, A., et al. (2014). Understanding disease mechanisms with models of signaling pathway activities. *BMC Syst. Biol.* 8, 121. doi:10.1186/s12918-014-0121-3

Shah, K., Al-Haidari, A., Sun, J., and Kazi, Kazi (2021). T cell receptor (TCR) signaling in health and disease. *Sig Transduct. Target Ther.* 6, 412. doi:10.1038/s41392-021-00823-w

Sigdel, A., Bisinotto, R. S., and Peñagaricano, F. (2021). Genes and pathways associated with pregnancy loss in dairy cattle. *Sci. Rep.* 11, 13329. doi:10.1038/s41598-021-92525-0

Sun, H-Z., Chen, Y., and Guan, L. L. (2019). MicroRNA expression profiles across blood and different tissues in cattle. *Sci. Data* 6, 190013. doi:10.1038/sdata.2019.13

Sun, S. C. (2011). Non-canonical NF-κB signaling pathway. *Cell. Res.* 21, 71–85. doi:10.1038/cr.2010.177

Veshkini, A., Hammon, H. M., Vogel, L., Viala, D., Delosière, M., Tröscher, A., et al. (2022). Plasma proteomics reveals crosstalk between lipid metabolism and immunity in dairy cows receiving essential fatty acids and conjugated linoleic acid. *Sci. Rep.* 12, 5648. doi:10.1038/s41598-022-09437-w

Vogel, L., Gnott, M., Kröger-Koch, C., Dannenberger, D., Tuchscherer, A., Tröscher, A., et al. (2020). Effects of abomasal infusion of essential fatty acids together with conjugated linoleic acid in late and early lactation on performance, milk and body composition, and plasma metabolites in dairy cows. *J. Dairy Sci.* 103, 7431–7450. doi:10.3168/jds.2019-18065

Wang, C., Cigliano, A., Delogu, S., Armbruster, J., Dombrowski, F., Evert, M., et al. (2013). Functional crosstalk between AKT/mTOR and ras/MAPK pathways in hepatocarcinogenesis: Implications for the treatment of human liver cancer. *Cell. Cycle* 12, 1999–2010. doi:10.4161/cc.25099

Wankhade, P. R., Manimaran, A., Kumaresan, A., Jeyakumar, S., Ramesha, K. P., Sejian, V., et al. (2017). Metabolic and immunological changes in transition dairy cows: A review. *Vet. World* 10, 1367–1377.

Webb, L. A., Ghaffari, M. H., Sadri, H., Schuh, K., Zamarian, V., Koch, C., et al. (2020). Profiling of circulating microRNA and pathway analysis in normal- versus over-conditioned dairy cows during the dry period and early lactation. *J. Dairy Sci.* 103, 9534–9547. doi:10.3168/jds.2020-18283

Weber, C., Schäff, C. T., Kautzsch, U., Börner, S., Erdmann, S., Görs, S., et al. (2016). Insulin-dependent glucose metabolism in dairy cows with variable fat mobilization around calving. *J. Dairy Sci.* 99, 6665–6679. doi:10.3168/jds.2016-11022

Wu, G., Rui, C., Chen, J., Sho, E., Zhan, S., Yuan, X., et al. (2017). MicroRNA-122 inhibits lipid droplet formation and hepatic triglyceride accumulation via yin yang 1. *Cell. Physiol. Biochem.* 44, 1651–1664. doi:10.1159/000485765

Xu, G., Yang, Z., Sun, Y., Dong, H., and Ma, J. (2021). Interaction of microRNAs with sphingosine kinases, sphingosine-1 phosphate, and sphingosine-1 phosphate receptors in cancer. *Discov. Onc* 12, 33. doi:10.1007/s12672-021-00430-9

Yeung, F., Ramírez, C. M., Mateos-Gomez, P. A., Pinzaru, A., Ceccarini, G., Kabir, S., et al. (2013). Nontelomeric role for Rap1 in regulating metabolism and protecting against obesity. *Cell. Rep.* 3, 1847–1856. doi:10.1016/j.celrep.2013.05.032

Zachut, M., Honig, H., Striem, S., Zick, Y., Boura-Halfon, S., and Moallem, U. (2013). Periparturient dairy cows do not exhibit hepatic insulin resistance, yet adipose-specific insulin resistance occurs in cows prone to high weight loss. *J. Dairy Sci.* 96, 5656–5669. doi:10.3168/jds.2012-6142

Zeng, T., Zhou, J., He, L., Zheng, J., Chen, L., Wu, C., et al. (2016). Blocking nuclear factor-kappa B protects against diet-induced hepatic steatosis and insulin resistance in mice. *PLoS One* 11, e0149677. doi:10.1371/journal.pone.0149677

Zhang, Y., Pizzute, T., and Pei, M. (2014). A review of crosstalk between MAPK and Wnt signals and its impact on cartilage regeneration. *Cell. Tissue Res.* 358, 633–649. doi:10.1007/s00441-014-2010-x

frontiers | Frontiers in Veterinary Science

TYPE Review
PUBLISHED 02 September 2022
DOI 10.3389/fvets.2022.956357

Check for updates

OPEN ACCESS

EDITED BY
Abdul Rasheed Baloch,
University of Karachi, Pakistan

REVIEWED BY
Shanti Choudhary,
Guru Angad Dev Veterinary and Animal Sciences University, India
Anjali Somal,
Chaudhary Sarwan Kumar Himachal Pradesh Krishi Vishvavidyalaya, India

*CORRESPONDENCE
Shudai Lin
linsd89sylvia@163.com

†These authors have contributed equally to this work

SPECIALTY SECTION
This article was submitted to Livestock Genomics, a section of the journal Frontiers in Veterinary Science

RECEIVED 30 May 2022
ACCEPTED 10 August 2022
PUBLISHED 02 September 2022

CITATION
Guo D, Zhang L, Wang X, Zheng J and Lin S (2022) Establishment methods and research progress of livestock and poultry immortalized cell lines: A review. *Front. Vet. Sci.* 9:956357. doi: 10.3389/fvets.2022.956357

COPYRIGHT
© 2022 Guo, Zhang, Wang, Zheng and Lin. This is an open-access article distributed under the terms of the Creative Commons Attribution License (CC BY). The use, distribution or reproduction in other forums is permitted, provided the original author(s) and the copyright owner(s) are credited and that the original publication in this journal is cited, in accordance with accepted academic practice. No use, distribution or reproduction is permitted which does not comply with these terms.

Establishment methods and research progress of livestock and poultry immortalized cell lines: A review

Dongxue Guo†, Li Zhang†, Xiaotong Wang, Jiahui Zheng and Shudai Lin*

College of Coastal Agricultural Sciences, Guangdong Ocean University, Zhanjiang, China

An infinite cell line is one of the most favored experimental tools and plays an irreplaceable role in cell-based biological research. Primary cells from normal animal tissues undergo a limited number of divisions and subcultures *in vitro* before they enter senescence and die. On the contrary, an infinite cell line is a population of non-senescent cells that could proliferate indefinitely *in vitro* under the stimulation of external factors such as physicochemical stimulation, virus infection, or transfer of immortality genes. Cell immortalization is the basis for establishing an infinite cell line, and previous studies have found that methods to obtain immortalized cells mainly included physical and chemical stimulations, heterologous expression of viral oncogenes, increased telomerase activity, and spontaneous formation. However, some immortalized cells do not necessarily proliferate permanently even though they can extend their lifespan compared with primary cells. An infinite cell line not only avoids the complicated process of collecting primary cell, it also provides a convenient and reliable tool for studying scientific problems in biology. At present, how to establish a stable infinite cell line to maximize the proliferation of cells while maintaining the normal function of cells is a hot issue in the biological community. This review briefly introduces the methods of cell immortalization, discusses the related progress of establishing immortalized cell lines in livestock and poultry, and compares the characteristics of several methods, hoping to provide some ideas for generating new immortalized cell lines.

KEYWORDS

livestock and poultry, immortalization, cell line, methods, telomerase activity

Introduction

As the basic structural and functional unit of life activities, cells are widely used as experimental tools in various studies, especially in the fields of molecular biology and biomedical research. Currently, there are two types of animal cells commonly used in laboratories: primary cells and infinite cell lines (1). Primary cells refer to cells that are directly collected from organism tissues and cultured in a simulated *in vivo* environment (2). Most of them are collected from tissues of experimental animals such as mice

and rabbits, and chicken embryos (3, 4). Take myoblast cells as an example to briefly describe the general process for collecting adherent cells. First, collect fresh muscle tissue samples from a slaughterhouse and transport them to a cell culture laboratory under sterile conditions (5). Small-sized experimental animals such as chicken embryos, whose muscle tissue can also be separated directly on the laboratory sterile bench (6). Then, wash the muscle tissue with 70% ethanol or 1 × phosphate buffered saline (PBS) containing 1% penicillin-streptomycin to remove surface dirt, and cut it into small pieces. Obtain the suspension containing myoblasts after mechanical dispersion and enzymatic digestion (commonly used are 0.1% collagenase and 0.25% trypsin solutions) (7, 8). Finally, remove tissue and cell debris in the suspension using a 40-μM cell strainer and perform low-speed centrifugation to collect primary myoblast cells (9–12). It is worth mentioning that the collected primary cells are suspended in a complete medium supplemented with an appropriate amount of fetal bovine serum (FBS) and cultured in monolayers at 37°C in a humidified atmosphere containing 5% carbon dioxide (simulating the environment in which cells survive and replicate *in vivo*) (13, 14).

The collected primary cells are almost identical to their source cells in morphology and characteristics. However, their ability to rapidly proliferate and differentiate *in vitro* is limited (15, 16). Even primary tumor-derived cells cannot continue to proliferate after a certain number of passages *in vitro* (17). In contrast, an infinite cell line is a population of non-senescent cells that escape cell cycle restriction and can proliferate indefinitely *in vitro* (18). In other words, achieving cell immortality is the basis for establishing infinite cell lines. Cell immortalization is one of the hotspots in biological research. It refers to the process of making cells cultured *in vitro* escape the senescence period of cell proliferation under the influence of external factors to obtain the ability of infinite division (1). Previous research has revealed that telomeres and telomerase activity were closely related to cell immortalization (19). Telomeres, special DNA-protein complexes presenting at the ends of eukaryotic chromosomes, are comprised of simple repetitive and highly conserved DNA sequences with guanine (G) base-rich and related proteins. They are involved in DNA replication and play important roles in maintaining a stable and complete replication of chromosomes (20). Along with proliferation and division of cells from normal animal tissues (nerve tissue, muscle tissue, etc.), telomeres get shortened, and cell proliferation will be inhibited to enter the senescence period. At this time, if the activity of telomerase is extremely low, the cell will reach the crisis stage and finally enter apoptosis under gene regulation. On the contrary, immortalized cells or tumor cells can maintain constant telomere length because of the activation of telomerase (21). In addition, the expression of tumor suppressor gene *p53* or *Rb* is also an important regulatory point in the process of cell immortalization (22, 23).

Cell lines bypass ethical issues associated with the use of animal and human tissues, providing an endless supply of a homogeneous cellular material that is cost-effective and very convenient to use. In addition, a cell line avoids collection of animal tissues from slaughterhouses, reducing the risk of endogenous contamination (24). Previous studies have suggested that many established immortalized cell lines could maintain the shape, characteristics, and functions of primary cells, and replace primary cells to provide convenient and reliable experimental materials for basic scientific research studies, clinical treatments, bioengineering pharmaceuticals, and vaccine research and development (25–27). However, some immortalized cells do not proliferate permanently despite their extended lifespan compared with primary cells (28). After multiple population doublings (PDs), cells will gradually senesce and loss important genetic characteristics (15, 18). Therefore, we summarized the established livestock and poultry cell lines and compared different methods to generate a stable infinite cell line hoping to find a better way to maximize the PDs of cells while maintaining their normal functions.

Abbreviations: PBS, Phosphate buffered solution; FBS, fetal bovine serum; PDs, population doublings; MNNG, N-methyl-N-nitro-N-nitrosoguanidine; SV40-LT, Simian virus 40 large T antigen; HPV E6/E7, human papilloma virus E6 or E7 protein; EBV, Epstein-Barr virus; *c-myc*, cellular-myelocytomatosis viral oncogene; hTERT, human telomerase reverse transcriptase; TR, telomerase RNA; PAI, plasminogen activator inhibitor; iPMSCs, immortalized porcine mesenchymal stem cells; EE, endocardial endothelium; SUVECs, swine umbilical vein endothelial cells; AEC, alveolar epithelial cell; BME, bovine microvascular endothelium; STCs, sheep trophoblast cells; bMECs, bovine mammary epithelial cells; Bag-1, Bcl-2-associated athanogene 1; TRPS-1, transcriptional repressor 1; CDKN2A, cyclin-dependent kinase inhibitor 2A; Dox, doxycyline; RKCs, rat Kupffer cells; EOE, enamel organ epithelial; MSCs, mesenchymal stem cells; CDK4, cyclin-dependent kinase 4; chTERT, chicken telomerase reverse transcriptase; ASV, avian sarcoma virus; ALSV, avian leukosis sarcoma virus; DEFs, duck embryo fibroblasts.

Methods for obtaining immortalized cells

Currently, the methods for obtaining the immortalization of human and animal cells are mainly divided into four categories (1, 29): (i) destroying the regulation of proto-oncogenes or tumor suppressor genes on the cell cycle through physical and chemical stimulation, which was a technique often utilized in early research (Figure 1), (ii) inducing the heterologous expression of viral oncogenes to help cells escape the cell cycle control (Figure 2), (iii) stimulating the activity of cellular telomerase to overcome the replicative senescence caused by telomere shortening and realize the infinite proliferation of cells *in vitro* (Figure 3), and (iv) spontaneous formation.

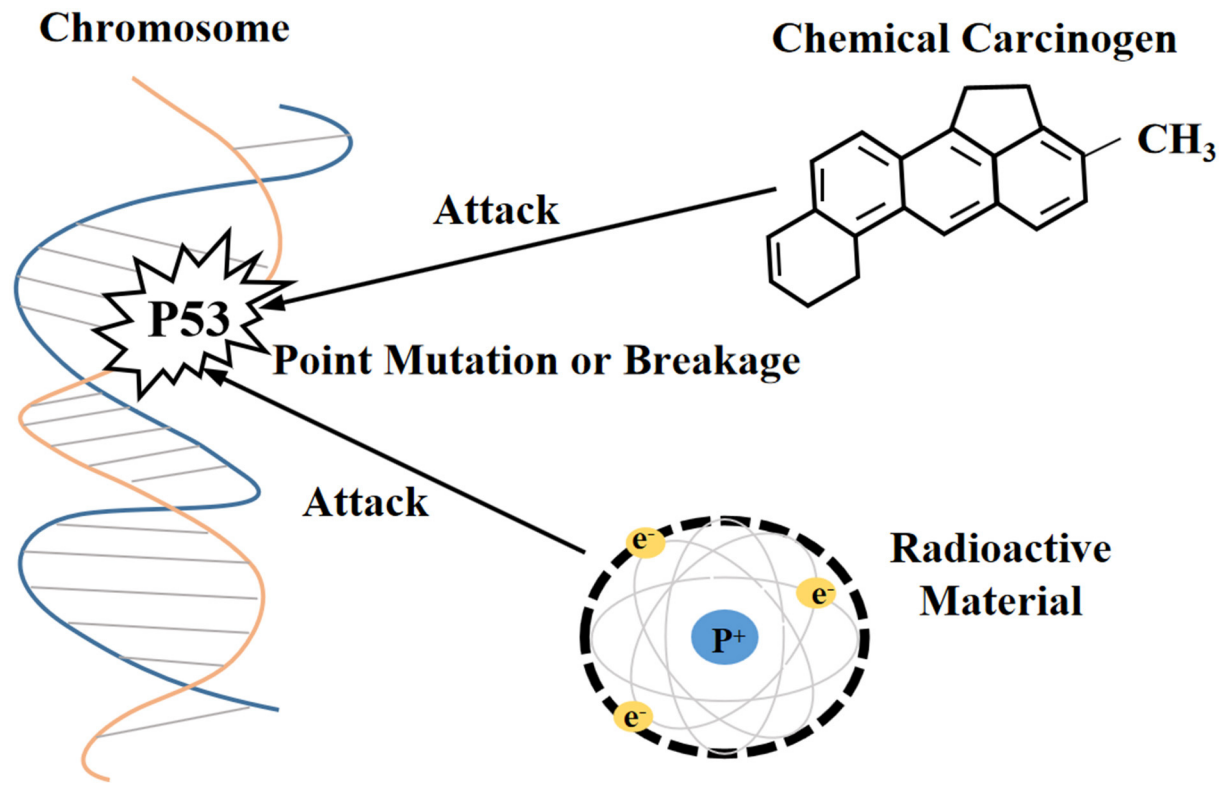

FIGURE 1
Physicochemical stimulation disrupts the molecular structure of proto-oncogenes and tumor suppressor genes.

Physical and chemical stimulation

Immortalization of cells induced by radioactive factors

In previous studies, researchers have attempted to induce cells with unlimited proliferation using X-rays or gamma rays. For example, results from an experiment indicated that human skin fibroblasts with a mutant *p53* allele could proliferate continually and exceeded 450 PDs *in vitro* after periodic X-ray irradiation, whereas the unirradiated control group cells could only be cultured to 37 PDs (30). Relevant phenotypes of immortalized cells obtained with such methods could be transferred by DNA transfection, which has been demonstrated in mouse cells (31). Previous study has shown that in place of it was suggested that treatment with Harvery murine sarcoma virus (Ha-MSV) alone did not promote the transformation of normal human fibroblasts into immortalized or tumorigenic cells, while immortalized fibroblasts KMST-6 formed by Co60γ-ray irradiation after treatment of Ha-MSV, and transplanted them into nude mice could acquire anchorage independent growth potential and eventually generated tumors (32). Therefore, radioactive factor-induced immortalized cells may increase the risk of tumorigenesis.

Immortalization of cells induced by chemical carcinogens

N-methyl-N-nitro-N-nitrosoguanidine (MNNG) (33) and 3-methylcholanthrene (34) are chemical carcinogens that induce cell immortalization. A previous study has observed that rabbit tracheal epithelial cells proliferated exponentially in the second week of culture and reached plateau in the third week. However, after experiencing the MNNG process, some rabbit tracheal epithelial cells showed a relative delay in the onset of proliferation and recovered clonal activity in a later stage of the plateau phase (35). Nevertheless, immortalized cells induced by chemical carcinogens do not necessarily retain normal morphology and are adhesion-dependent (33). Therefore, their carcinogenesis risk cannot be neglected.

Heterologous expression of viral oncogenes

It is well-known that the simian virus 40 large T antigen (*SV40-LT*), human papilloma virus E6 or E7 protein (*HPV E6/E7*), and Epstein-Barr Virus (*EBV*) are oncogenes. Among them, the *SV40-LT* gene fragment is one of the most commonly

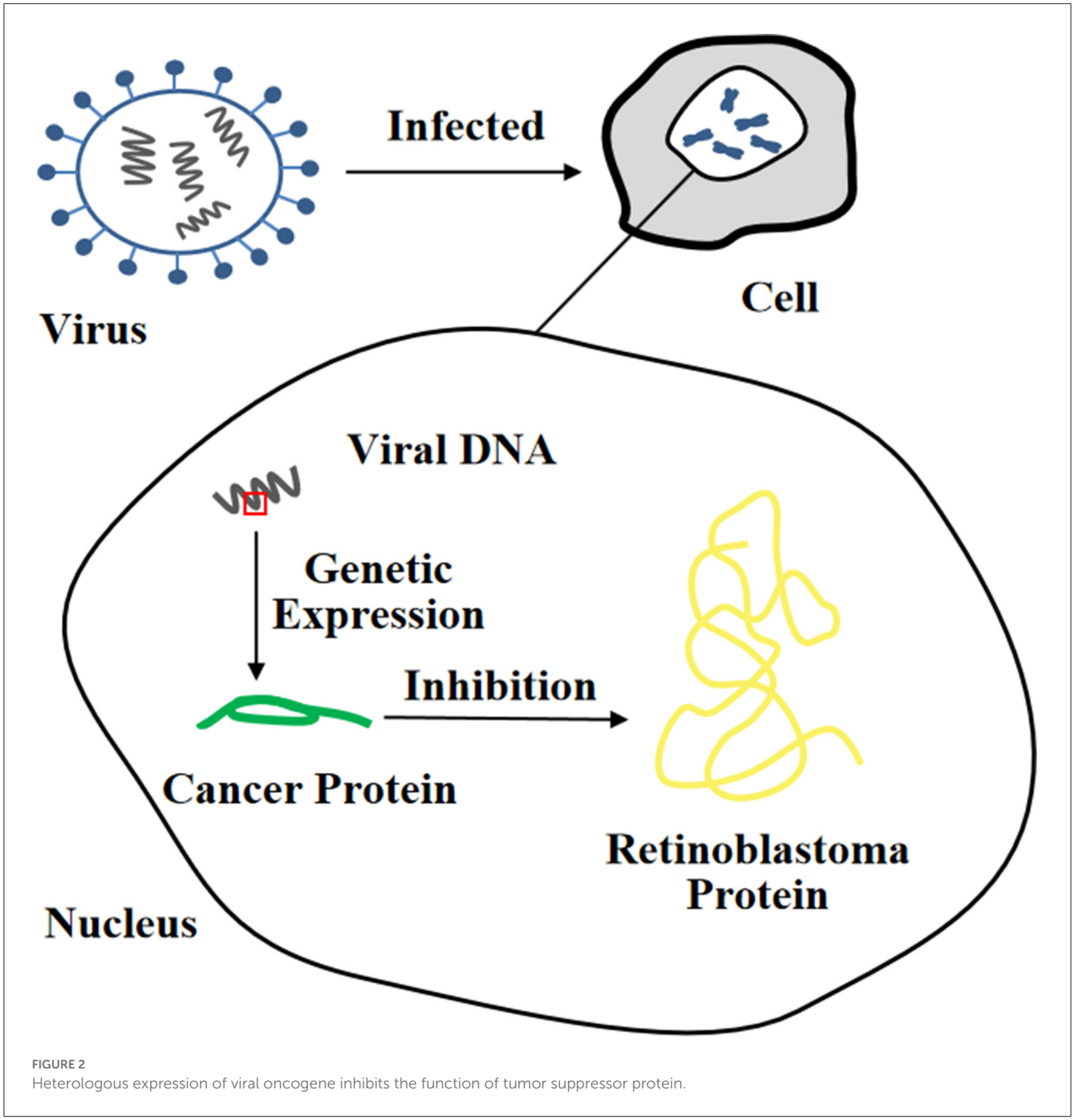

FIGURE 2
Heterologous expression of viral oncogene inhibits the function of tumor suppressor protein.

used target fragments for inducing cell immortalization. Integrating it into the target cell nucleus for expression can cause inactivation of the p53 and Rb proteins, thereby changing cell proliferation activity and prolonging cell lifespan (36). However, the length of telomeres will gradually shorten until cells stop growing, and only a few cells can completely leave the cell cycle and continue to proliferate, eventually forming immortalized cell lines (37). In recent years, *SV40-LT* has been successfully used in the establishment of immortalized cell lines of livestock and poultry such as pigs (38), cattle (25), sheep (24), and ducks (39).

In addition, infection with *HPV E6/E7* can also immortalize a large number of different types of cells (40, 41). The HPV E6 protein, as one of the most common transforming proteins, can cause degradation of the p53 protein and upregulate the expression level of cellular-myelocytomatosis viral oncogene (*c-myc*) (42). Furthermore, it can also induce the expression of human telomerase reverse transcriptase (*hTERT*) and enable cells to acquire the ability of indefinite proliferation (43). There are many binding sites for c-myctranscription factor on the promoter of *hTERT*, so c-myc can mediate *hTERT* transcriptional activation and rapidly induce *hTERT* mRNA to express (44). The HPV E7 protein can lead to degradation of the Rb protein (45). It was reported that retroviruses containing the *HPV E6/E7* gene was used to infect human pancreatic duct epithelial cells to establish the corresponding immortalized cell

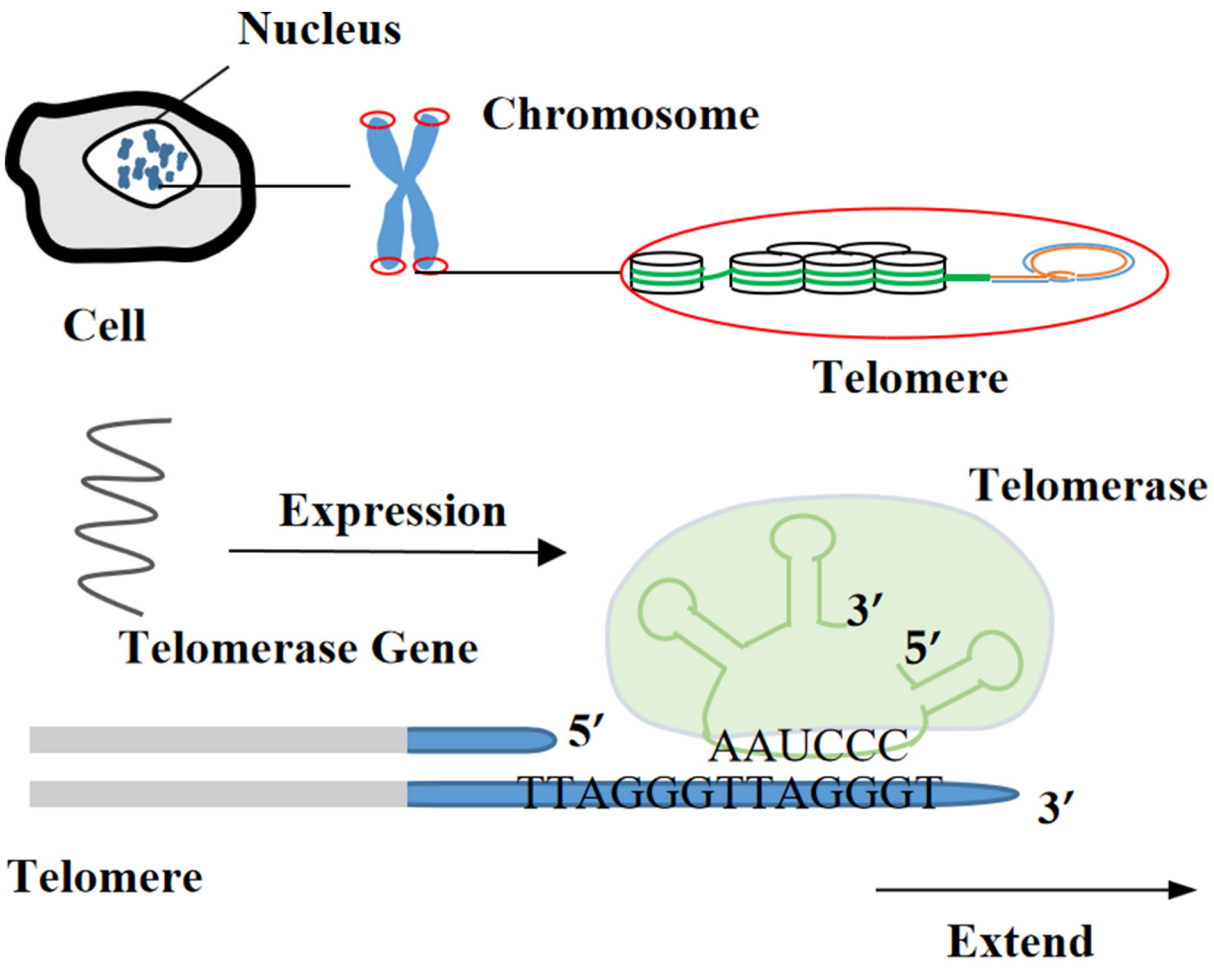

FIGURE 3
Mechanism of expressing telomerase reverse transcriptase gene.

line, which could be passaged more than 20 times, retaining the anchorage dependence of mammalian cells with non-carcinogenic effects (40). Currently, the EBV is mostly used to immortalize B lymphocytes. The EBV genome contains more than 100 genes, and only a few genes (so-called latent genes) can be expressed in EBV-infected B lymphocytes. For instance, it is capable of infecting B lymphoblastoid cells *in vitro*, activating the interaction of cytokines with their receptors by expressing latent proteins, and forming immortalized lymphoblastoid cell lines. It is worth noting that the most notable feature of immortalized B cells induced by *EBV* is increased telomerase activity (46).

Telomerase causing cell immortalization

Telomerase

Telomerase is a kind of a specific reverse transcriptase and includes three components: telomerase RNA (TR), telomerase-associated protein, and telomerase reverse transcriptase (TERT) or telomerase catalytic subunit. Using its own RNA as a template to extend telomeres from the 3′-OH end of telomeric DNA or synthesize new telomeric DNA, it can compensate for the shortening of chromosome ends during cell division, so as to maintain the length of telomeres and prevent cells from the apoptosis caused by telomere depletion (47). Telomerase almost has no activity in normal cells but with expression in stem cells and germ cells. The activity of telomerase is elevated in most immortalized cell lines and various human tumor tissues, suggesting that telomerase activity is closely related to occurrence and development of tumors (48).

Rebuild telomerase activity to immortalize cells

In 1998, it was first reported that after the exogenous *hTERT* gene was introduced into telomerase-negative normal human retinal pigment epithelial cells, the intracellular telomerase was activated and the endogenous β-galactosidase (senescent

TABLE 1 Immortalized livestock cell lines established by transfecting *hTERT* alone.

Species	Cell line name	Cell line source	Immortality	References
Swine	Fibroblast cell line	Primary fibroblasts prepared from pig ears, fetuses, and lung tissues	Cultured for 30–45 passages	(60)
	hTERT-POMECs	Primary porcine oral mucosal epithelial cells (POMECs) from the neonatal piglet.	Cultured for more than 150 passages *in vitro*	(61)
	iPMSCs	Fetal porcine pancreas mesenchymal stem cells	More than 80 passages	(62)
	EE cell line	Endocardial endothelium cells	Over 100 generations	(63)
	SUVECs	Umbilical vein endothelial cells	Passaged 50 times	(64)
Cattle	HTERT-AEC II	Type II alveolar epithelial cells	More than 50 passages	(4)
	hTERT-BME	Microvascular endothelial cells isolated from adrenal cortex	Over 80 passages	(65)
	BMET	Muscle epithelial cells	Cultured for 59 passages	(66)
Sheep	Fibroblast cell line	Lung fibroblasts	Cultured for about 120 days (50–80 PDS)	(67)
	hTERT-STCs	Primary trophoblast cells (STCs)	Cultured for 50 passages	(7)
	Microglia cell line	Brain macrophage	Passage up to 100 times	(26)
	Fibroblasts cell line	Fetal sheep fibroblasts	More than 180 PDs	(68)

marker) was significantly reduced (49). Besides, a previous study has claimed that after transfection with retrovirus-mediated exogenous *hTERT* gene, normal human breast epithelial cells gained stable telomere length, longer lifespan (40 PDs more than primary cells), less obvious β-galactosidase staining, and unchanged plasminogen activator inhibitor expression (PAI, another senescent marker) (50).

Furthermore, it has been determined that *hTERT* could improve telomerase activity, stabilize telomere length in cells, increase the number of cellular PDs, slow down cell senescence, and prolong the lifespan of culture *in vitro* (51–56). Certain cells can maintain their original morphology and function while obtaining the ability to proliferate indefinitely (57, 58). For example, immortalized human bone marrow mesenchymal stem cell line carrying *hTERT* has been subjected to 290 PDs without losing cell contact inhibitory function. By observing cell morphology at 95 and 275 PDs, it was found that transfected cells had the ability to transform into adipocytes, chondrocytes, and osteoblasts (59). Currently, *hTERT* transfection alone can immortalize many livestock and poultry cells (Table 1), or it can be combined with viral oncogenes to improve the success rate of obtaining immortalized cells (69).

Spontaneously generated immortalized cells

During cell culture *in vitro*, some spontaneously immortalized cells are occasionally generated and show high proliferative potential without gene transfer (70–73). These cells achieve serum-independent growth and have higher saturation densities (74).

Rodent cells have a higher incidence of spontaneous immortalization, up to 10^{-5} or 10^{-6} (44). Previous research has discussed that human cells could escape aging only if both the *p53* and *Rb* genes were inactivated simultaneously, and that dysregulation of the ARF-p53 pathway alone in rodent cells was sufficient for eternal proliferation (75). By comparing the expression of multiple genes in early passage bovine mammary epithelial cells (bMECs), senescent bMECs, spontaneously immortalized bMECs (BME65Cs), and human breast cancer MCF-7 cell line (76), it was found that BME65Cs had the general features of normal BMECs in terms of morphology and karyotype etc., accompanied by endogenous *TERT* activity and telomeres stability. Compared with MCF-7 cells, the oncogene *c-myc* was only slightly upregulated in BME65Cs, and the breast tumor-related genes Bcl-2-associated athanogene 1 (*Bag-1*) and transcriptional repressor 1 (*TRPS-1*) were not detected. Likewise, the expression of tumor suppressor gene *p53* and cycle-dependent kinase inhibitory factor *p16INK4a* (also known as cyclin-dependent kinase inhibitor 2A, *CDKN2A*) in BME65Cs was decreased but not completely inactivated compared to earlier passages, indicating that spontaneous immortalized cell lines were not caused by mutations in the *p53* or *p16INK4a* gene. In addition, the expression level of DNA methyltransferase was upregulated, suggesting that the co-suppression of cell aging and mitochondrial apoptosis pathways orchestrated the immortalization process of BME65Cs (76). That means the mechanism by which spontaneously immortalized cells escape replicative senescence is poorly understood.

TABLE 2 Establishment of different cell lines in mammals.

Species	Cell line	Establishment method	Immortality	References
Rat	RKC2	*SV40-LT* was expressed in passaged kupffer cells	–	(83)
Mouse	EOE-2M and EOE-3M	Induced the expression of *HPV16 E6/E7* oncogene in primary enamel organ epithelial (EOE) dental cells	Maintained more than 30 generations	(84)
	FP5-1-3 cell line	Spontaneous generation from mammary buds in *p53*-null female embryos	–	(85)
	LmcMF	Introducted of *SV40-LT* into primary intestinal myofibroblasts.	At least 20 generations	(86)
	SmcMF	Spontaneous immortalized intestinal myofibroblasts	At least 20 generations	(86)
	AD-MSC	Knockout of *p53* gene in adipose-derived mesenchymal stem cells (MSCs)	Passaged more than 50 times	(87)
	Osteoblast cell line	Transfection of primary floxed Bmp2/4 mouse osteoblasts with *SV40-LT*	Grown more than 50 PDs	(27)
	Epithelial cell line	Embryonic mouse neuroepithelial cells were infected with a retrovirus containing the *c-myc* oncogene	–	(88)
Rabbit	Fibroblast cell line	Co-expression of mutant *CDK4*, *cyclin D1* and *hTERT* in fibroblasts	More than 11 generations	(89)
	Articular cartilage cell line	Transfected with plasmid encoding SV40 early functional gene	Up to 130 generations	(90)
	ImRMC	Induced lentivirus-mediated *SV40-LT* expression in primary melanocytes	–	(91)
	Epithelial cell line	Infection of primary corneal epithelial cells with recombinant *SV40*-adenovirus vector	Grown over hundreds of generations	(92)
Swine	Granulosa cell line	Conditionally expressed *SV40-LT* gene in primary granulosa cells using tetracycline-induced Tet-On 3G system	Stable proliferation for at least 6 months	(93)
	siNEC and siTEC	Transfer of *SV40-LT* into nasal and tracheal epithelial cells	Over 30 passages, the doubling time is cut in half	(94)
	Ttag and Puro	Transfer of lentiviral vector expressing *SV40-LT* into primary porcine spermatogonial stem cells	More than 35 passages	(95)
	GalT-KO-hep and WT	GalT-KO and wild-type pig primary hepatocytes were transfected with *SV40-LT* lentiviral vector	More than 20 generations	(82)
	Fibroblast cell line	Sleeping beauty transposon-mediated ectopic expression system of porcine *TERT*	Over 40 generations	(96)
	Endothelial cell line	Primary endothelial cells were transfected with plasmid pRNS-1 carrying neomycin resistance gene and *SV40-LT*	The doubling time was about 17.6 h	(80)
Cattle	Epithelial cell line	Mammary epithelial cells were infected by retrovirus with the *SV40-LT* plasmid	Up to 80 PDs in 10 months	(18)
	Epithelial cell line	Transfer of lentiviral vectors encoding *cyclin D1*, mutant *CDK4*, and *hTERT* genes into colon-derived epithelial cells	Over 15 generations	(97)
	Germ cell line	Constructed pEGFP-*c-myc* and pEGFP-*hTERT* expression vectors and transfected 5-month-old calf sperm stem cells	About 100 PDs in 140 days	(69)
	BMES	Muscular epithelial cell spontaneously immortalized	Cultured for 62 generations	(66)
Sheep	Endothelial cell line	*HPV16 E6/E7* open reading frames were permanently transfected into fifth generation fetal pulmonary artery endothelial cells	At least 28 passages	(98)
	mMTSV-54/93 and TIGEF	Transfection of plasmid DNA encoding *SV40-LT* gene into goat fibroblasts	Faster doubling time	(99)

Indicates that immortality is not mentioned in the citation in place of previous sentence.

TABLE 3 Characteristics of immortalized pig cell lines established by transfecting *SV40-LT* and *hTERT*.

Establishment method	Cell line	Characteristics	Immortality	References
Transfection of *TERT* gene	Fibroblast cell line	It had anchorage dependency, and did not form any colonies on soft agar	Cultured for 30–45 passages	(60)
	hTERT-POMECs	No chromosome abnormality and tumorigenicity transformation	Cultured for more than 150 passages *in vitro*	(61)
	Fibroblast cell line	The cell line continued to grow after more than 40 passages, and *pTERT* maintained stable expression	Over 40 generations	(96)
	iPMSCs	With the ability to differentiate into neurons, cardiomyocytes, germ cells, and islet-like cells	More than 80 passages	(62)
	EE cell line	It had similar phenotypic and functional characteristics to the primary endocardial endothelium cells	Over 100 generations	(63)
	SUVECs	It had contact inhibition, serum demand and anchorage dependent growth	50 generations	(64)
Induced the expression of *SV40-LT*	Granulosa cell line	Able to reproduce stably for at least 6 months, with reduced cell proliferation following withdrawal from Dox	Stable proliferation for at least 6 months	(93)
	siNEC and siTEC	Retained the biological characteristics of primary epithelial cells and no abnormal chromosomes	Over 30 passages, the doubling time is cut in half	(94)
	Ttag and Puro	No morphological abnormalities	More than 35 passages within seven months	(95)
	GalT-KO-hep	Retained the characteristics of primary porcine hepatocytes. No tumorigenicity	More than 20 generations	(82)
	MSCs	Possessed higher proliferative capacity, shown no signs of senescence and displayed a common phenotype similar to primary MSCs	Serially passages more than 20–30 times	(38)
	Endothelial cell line	The original features of endothelial cells were preserved	The doubling time was about 17.6 h	(80)

Indicates that immortality is not mentioned in the citation in place of previous sentence.

Establishment and current status of livestock and poultry immortalized cell lines

The common methods for establishing non-carcinogenic immortalized cell lines

It is well known that cancer cells also have the ability to proliferate indefinitely, and that cells may become cancerous during the process of establishing cell lines. Soft agar assay and nude mouse tumorigenesis assay are widely recognized methods for testing whether immortalized cell lines are tumorigenic (77, 78). Studies have found that immortalized cell lines induced by radioactive substances and chemical carcinogens may increase the formation of cancer cells, which are rarely used today (32, 33). Immortalized cell lines established by inducing the combined expression of immortality genes, proto-oncogenes, and cell cycle regulators are also tumorigenic, such as porcine pancreatic ductal epithelial cells, which are often used to generate tumor models (79, 80).

However, some immortalized cell lines can still avoid the generation of cancer cells while maintaining the morphological and physiological characteristics of primary cells (63, 81). The current common immortalization methods that do not cause any cancer growth are mainly by *hTERT* or *SV40-LT* expression induction, such as porcine oral mucosal epithelial cell line (hTERT-POMEC) (61), canine bronchiolar epithelial cell line (hTERT-CBECs) (77), and pig liver cell line (GalT-KO-hep) (82). So far, anchorage-independent growth, chromosomal abnormalities, and tumorigenic transformation have not been observed during the culture of these cell lines.

Small mammalian and livestock cell lines

By comparing the establishment status of common small mammal (rats, mice, and rabbits) and livestock (such as pigs, cattle, and sheep) immortalized cell lines (Table 2), it is not difficult to find that most expression vectors carrying the *SV40-LT* or *hTERT* gene are transfected into cells to prolong their lifespan. Notably,

TABLE 4 Existing poultry cell lines and their characteristics.

Species	Cell Line	Characteristics	Immortality	References
Chick	CSC-1-5	Spontaneous emergence, the fibroblast cell line had a high proliferative state, high homogeneity and the same genetic background, normal cell cycle distribution without tumorigenesis, and transformation	Stable passage over 3 months	(100)
	ICP1 and ICP2	Acquired by transducting *chTERT* alone or in combination with *chTR*. They showed fibroblast-like morphology without signs of malignant transformation, revealed high telomerase activity and retained adipocyte differentiation capacity	Cultured *in vitro* over 100 passages	(13)
	CEL-im	Spontaneous generation without oncogenic treatment, 0.8–1.1 PDs per day, and negative for telomerase activity	Cultured over 120 passages	(101)
	DF-1	Spontaneous emergence, they demonstrated a fibroblast-like morphology during culture, did not contain endogenous sequences associated with ASV or ALSV, and supported replication of avian retroviruses	–	(102)
	LMH	It obtained from liver tumor tissue after injecting diethylnitrosamine, had triploid karyotype and 6 marker chromosomes. After the 40th passage, the growth rate gradually increased and the cell morphology changed	Cultured 120 passages in 5 years	(103)
Duck	DEE cell line	It had good adhesion ability and proliferative activity, no tumorigenicity, and the doubling time was about 17.6 h	50 generations	(104)
	DEF-TA	Expressing *SV40-LT* (obtained after more than 8 rounds of puromycin selection), PDs number increased every 30 to 48 h, and maintain fibroblast morphology	Passaged more than 30 times	(39)
Goose	Epithelial cell line	Spontaneous formation with a cubic morphology and constant chromosomal characteristics, they could efficiently transfect some plasmids carrying avian virus reporter genes and did not transform into tumorigenic cells	Grown over 65 passages	(105)
Quail	QM l-4 and QM 6-8	Seven avian myogenic cell lines derived from the fibrosarcoma cell line QT6	–	(106)
	Myocardial cell line	It obtained by injection of MC29 virus carrying the *v-myc*, without morphological changes, showing decreased growth and enhanced differentiation	More than 60 passages in 6 months	(107)
	QT	Injected with 7,12-dimethylbenzylanthracene, MNNG and 3-methylcholanthrene (carcinogens) and isolated from tumor tissue. The fibrosarcoma cell line had undergone ∼10 passages and was characteristic by tumorigenic transformation	Undergone ∼10 passages	(108)
	Cartilage cell line	Acquired by infection with MC29, it stimulates chondrocyte proliferation and progressively reduces doubling time	About 70 generations in 16 months	(109)

Indicates that immortality is not mentioned in the citation in place of previous sentence.

the cell immortalization induced by the tetracycline Tet-on 3G system is reversible, and cell proliferation can be controlled with doxycycline (Dox), which is more flexible (93).

As an example, the characteristics of immortalized pig cell lines separately obtained by transfecting *SV40-LT* and *hTERT* are compared (Table 3). It is observed that immortalization effects can be evaluated from the aspects of cell lifespan, telomerase activity, passage times, PDs, cell morphology, and tumorigenicity.

Establishment of poultry cell lines

We summarized poultry cell lines and their characteristics, including chickens, ducks, geese, and quails (Table 4). It

was found that few immortalized cell lines were successfully established in poultry compared with mammals, and that the existing poultry cell lines were mainly obtained from tumor tissues; some chemical carcinogens or oncogenic viruses were used to immortalize specific types of bird cells, and some continuous cell lines were spontaneously generated. There are two points worth noting: (i) the preadipocyte lines "ICP1" and "ICP2" successfully established by transfection with the chicken telomerase reverse transcriptase (*chTERT*) have a high proliferation potential without malignant transformation after long-term culture, which provides a new idea and theoretical reference for the acquisition of other immortalized poultry cell lines (7), and (ii) during the whole process of establishing immortalized cell lines, specific antibiotics can be used to screen out positive cells expressing the *SV40-LT* gene or other target genes and then select a single transforming focus for subculture, which is not only simple but also safer (27).

Conclusions

Establishing an ideal immortalized cell line with infinite proliferation ability and maintaining the characteristics of its source tissue cells cannot only avoid the complicated process of primary cell separation and purification, reduce the time and energy consumption of researchers, and save the cost of experiments, it is also conducive to the research on scientific issues such as gene function of livestock and poultry, and rapidly promotes the development of science. Since immortalized cells can be passaged multiple times *in vitro*, researchers can immortalize cells that are difficult to passage, slow to proliferate, and prone to senescence, and provide more cell resources for related experiments. Nevertheless, whether the functional cells from different species adopt the same immortalization method, and how to quickly and efficiently prepare immortalized cells and to ensure the immortalized cells maintaining the original characteristics have not yet been solved and require more in-depth research. In summary, the application of immortalized cells has broad prospects. The continuous improvement of immortalized cell line establishment technology is conducive to further research in molecular biology and other scientific fields.

Author contributions

DG participated in literature collection, drafted the manuscript, and revised it. LZ participated in the design of this review and revised it. XW participated in literature collection. JZ helped draft the manuscript. SL conceived the review, participated in literature collection, revised the manuscript, and finally agreed to publish it. All authors read and approved the final version of the manuscript.

Funding

This research was funded by the National Natural Science Foundation of China (Grant No. 31972550), Guangdong Province (Grant Nos. 2020A1515011576 and 2020B1515420008), and College of Coastal Agricultural Sciences—Ph.D. Start-up Fee and Postgraduate Training Fund (Grant No. 060302052104).

Acknowledgments

Thanks to SL for the English revision.

Conflict of interest

The authors declare that the research was conducted in the absence of any commercial or financial relationships that could be construed as a potential conflict of interest.

Publisher's note

All claims expressed in this article are solely those of the authors and do not necessarily represent those of their affiliated organizations, or those of the publisher, the editors and the reviewers. Any product that may be evaluated in this article, or claim that may be made by its manufacturer, is not guaranteed or endorsed by the publisher.

References

1. Stacey G, MacDonald C. Immortalization of primary cells. *Cell Biol Toxicol.* (2001) 17:231–46. doi: 10.1023/A:1012525014791

2. Matsuda A, Shimizu Y, Kanda T, Ohnishi A, Maeta N, Miyabe M, et al. Establishment of a canine lens epithelial cell line. *Can J Vet Res.* (2021) 85:236–40.

3. Wang JM, Chen AF, Zhang K. Isolation and primary culture of mouse aortic endothelial cells. *J Vis Exp.* (2016) 19:e52965. doi: 10.3791/52965

4. Su F, Liu X, Liu G, Yu Y, Wang Y, Jin Y, et al. Establishment and evaluation of a stable cattle type II alveolar epithelial cell line. *PLoS ONE.* (2013) 8:e76036. doi: 10.1371/journal.pone.0076036

5. Sadkowski T, Ciecierska A, Oprzadek J, Balcerek E. Breed–dependent microRNA expression in the primary culture of skeletal muscle cells subjected to myogenic differentiation. *BMC Genomics.* (2018) 19:109. doi: 10.1186/s12864-018-4492-5

6. Souza YRM, Manso PPA, Oliveira BCD, Terra MABL, Paschoal T, Caminha G, et al. Generation of yellow fever virus vaccine in skeletal muscle cells of chicken embryos. *Mem Inst Oswaldo Cruz.* (2019) 114:e190187. doi: 10.1590/0074-02760190187

7. Zhang Y, Shi J, Liu S. Establishment and characterization of a telomerase–immortalized sheep trophoblast cell line. *Biomed Res Int.* (2016) 2016:5808575. doi: 10.1155/2016/5808575

8. Luo W, Lin Z, Chen J, Chen G, Zhang S, Liu M, et al. TMEM182 interacts with integrin beta 1 and regulates myoblast differentiation and muscle regeneration. *J Cachexia Sarcopenia Muscle.* (2021) 12:1704–23. doi: 10.1002/jcsm.12767

9. Choi KH, Yoon JW, Kim M, Lee HJ, Jeong J, Ryu M, et al. Muscle stem cell isolation and *in vitro* culture for meat production: a methodological review. *Compr Rev Food Sci Food Saf.* (2021) 20:429–57. doi: 10.1111/1541-4337.12661

10. Liu P, Bian Y, Zhong J, Yang Y, Mu X, Liu Z. Establishment and characterization of a rat intestinal microvascular endothelial cell line. *Tissue Cell.* (2021) 72:101573. doi: 10.1016/j.tice.2021.101573

11. Lojk J, Mis K, Pirkmajer S, Pavlin M. siRNA delivery into cultured primary human myoblasts—-optimization of electroporation parameters and theoretical analysis. *Bioelectromagnetics.* (2015) 36:551–63. doi: 10.1002/bem.21936

12. Bautista–Amorocho H, Silva–Sayago JA, Goyeneche–Patino DA, Pérez–Cala TL, Macías–Gómez F, Arango–Viana JC, et al. A novel method for isolation and culture of primary swine gastric epithelial cells. *BMC Mol Cell Biol.* (2021) 2021:1. doi: 10.1186/s12860-020-00341-7

13. Wang W, Zhang T, Wu C, Wang S, Wang Y, Li H, et al. Immortalization of chicken preadipocytes by retroviral transduction of chicken TERT and TR. *PLoS ONE.* (2017) 12:e0177348. doi: 10.1371/journal.pone.0177348

14. Chenari N, Khademi B, Razmkhah M. EZB–ICR cell line: a new established and characterized oral squamous cell carcinoma cell line from tongue. *Asian Pac J Cancer Prev.* (2021) 22:99–103. doi: 10.31557/APJCP.2021.22.1.99

15. Bukowy–Bieryłło Z. Long–term differentiating primary human airway epithelial cell cultures: how far are we? *Cell Commun Signal.* (2021) 19:63. doi: 10.1186/s12964-021-00740-z

16. Martinovich KM, Iosifidis T, Buckley AG, Looi K, Ling KM, Sutanto EN, et al. Conditionally reprogrammed primary airway epithelial cells maintain morphology, lineage and disease specific functional characteristics. *Sci Rep.* (2017) 7:17971. doi: 10.1038/s41598-017-17952-4

17. Liu Y, Wang CH, Fan J, Peng JX, Pan J, Zhang X, et al. Establishing a papillary craniopharyngioma cell line by SV40LT–mediated immortalization. *Pituitary.* (2021) 24:159–69. doi: 10.1007/s11102-020-01093-5

18. Hu H, Zheng N, Gao H, Dai W, Zhang Y, Li S, et al. Immortalized bovine mammary epithelial cells express stem cell markers and differentiate *in vitro*. *Cell Biol Int.* (2016) 40:861–72. doi: 10.1002/cbin.10624

19. de Lange T. Protection of mammalian telomeres. *Oncogene.* (2002) 21:532–40. doi: 10.1038/sj.onc.1205080

20. Blackburn EH. Structure and function of telomeres. *Nature.* (1991) 350:569–73. doi: 10.1038/350569a0

21. Cerni C. Telomeres, telomerase, and myc. An update. *Mutat Res.* (2000) 462:31–47. doi: 10.1016/S1383-5742(99)00091-5

22. Sharpless N.E, Ramsey MR, Balasubramanian P, Castrillon DH, DePinho RA. The differential impact of p16 (INK4a) or p19 (ARF) deficiency on cell growth and tumorigenesis. *Oncogene.* (2004) 23:379–85. doi: 10.1038/sj.onc.1207074

23. D'Amico M, Wu K, Fu M, Rao M, Albanese C, Russell RG, et al. The inhibitor of cyclin–dependent kinase 4a/alternative reading frame (INK4a/ARF) locus encoded proteins p16INK4a and p19ARF repress cyclin D1 transcription through distinct cis elements. *Cancer Res.* (2004) 64:4122–30. doi: 10.1158/0008-5472.CAN-03-2519

24. Seridi N, Hamidouche M, Belmessabih N, El Kennani S, Gagnon J, Martinez G, et al. Immortalization of primary sheep embryo kidney cells. *In Vitro Cell Dev Biol Anim.* (2021) 57:76–85. doi: 10.1007/s11626-020-00520-y

25. Takenouchi T, Iwamaru Y, Sato M, Yokoyama T, Shinagawa M, Kitani H. Establishment and characterization of SV40 large T antigen–immortalized cell lines derived from fetal bovine brain tissues after prolonged cryopreservation. *Cell Biol Int.* (2007) 31:57–64. doi: 10.1016/j.cellbi.2006.09.006

26. Muñoz–Gutiérrez JF, Schneider DA, Baszler TV, Greenlee JJ, Nicholson EM, Stanton JB. hTERT–immortalized ovine microglia propagate natural scrapie isolates. *Virus Res.* (2015) 198:35–43. doi: 10.1016/j.virusres.2014.10.028

27. Wu LA, Yuan G, Yang G, Ortiz–Gonzalez I, Yang W, Cui Y, et al. Immortalization and characterization of mouse floxed Bmp2/4 osteoblasts. *Biochem Biophys Res Commun.* (2009) 386:89–95. doi: 10.1016/j.bbrc.2009.05.144

28. Dahodwala H, Lee KH. The fickle CHO: a review of the causes, implications, and potential alleviation of the CHO cell line instability problem. *Curr Opin Biotechnol.* (2019) 60:128–37. doi: 10.1016/j.copbio.2019.01.011

29. Maqsood MI, Matin MM, Bahrami AR, Ghasroldasht MM. Immortality of cell lines: challenges and advantages of establishment. *Cell Biol Int.* (2013) 37:1038–45. doi: 10.1002/cbin.10137

30. Tsutsui T, Tanaka Y, Matsudo Y, Hasegawa K, Fujino T, Kodama S, et al. Extended lifespan and immortalization of human fibroblasts induced by X–ray irradiation. *Mol Carcinog.* (1997) 18:7–18. doi: 10.1002/(SICI)1098-2744(199701)18:1<7::AID-MC2>3.0.CO;2-F

31. Too C.K, Sierra–Rivera E, Oberley LW, Guernsey DL. Passage of X–ray–induced immortal, non–transformed phenotype by DNA–mediated transfection. *Cancer Lett.* (1995) 97:39–47. doi: 10.1016/0304-3835(95)03949-W

32. Namba M, Nishitani K, Fukushima F, Kimoto T. Multistep carcinogenesis of normal human fibroblasts. Human fibroblasts immortalized by repeated treatment with Co−60 gamma rays were transformed into tumorigenic cells with Ha–ras oncogenes. *Anticancer Res.* (1988) 8:947–58.

33. Marczynska B, Khoobyarian N, Chao TS, Tao M. Phorbol ester promotes growth and transformation of carcinogen–exposed nonhuman primate cells *in vitro*. *Anticancer Res.* (1991) 11:1711–7.

34. Kawaguchi T, Nomura K, Hirayama Y, Kitagawa T. Establishment and characterization of a chicken hepatocellular carcinoma cell line, LMH. *Cancer Res.* (1987) 47:4460–4.

35. Kitamura H, Gray TE, Jetten AM, Inayama Y, Nettesheim P. Enhanced growth potential of cultured rabbit tracheal epithelial cells following exposure to N–methyl–N'–nitro–N–nitrosoguanidine. *Jpn J Cancer Res.* (1993) 84:1113–9. doi: 10.1111/j.1349-7006.1993.tb02810.x

36. Manfredi JJ, Prives C. The transforming activity of simian virus 40 large tumor antigen. *Biochim Biophys Acta.* (1994) 1198:65–83. doi: 10.1016/0304-419X(94)90006-X

37. Bryan TM, Reddel RR. SV40–induced immortalization of human cells. *Crit Rev Oncog.* (1994) 5:331–57. doi: 10.1615/CritRevOncog.v5.i4.10

38. Moscoso I, Rodriguez–Barbosa JI, Barallobre–Barreiro J, Anon P, Domenech N. Immortalization of bone marrow–derived porcine mesenchymal stem cells and their differentiation into cells expressing cardiac phenotypic markers. *J Tissue Eng Regen Med.* (2012) 6:655–65. doi: 10.1002/term.469

39. Fu Y, Chen Z, Li C, Liu G. Establishment of a duck cell line susceptible to duck hepatitis virus type 1. *J Virol Methods.* (2012) 184:41–5. doi: 10.1016/j.jviromet.2012.05.004

40. Furukawa T, Duguid WP, Rosenberg L, Viallet J, Galloway DA, Tsao MS. Long–term culture and immortalization of epithelial cells from normal adult human pancreatic ducts transfected by the E6E7 gene of human papilloma virus 16. *Am J Pathol.* (1996) 148:1763–70.

41. Reznikoff CA, Belair C, Savelieva E, Zhai Y, Pfeifer K, Yeager T, et al. Long–term genome stability and minimal genotypic and phenotypic alterations in HPV16 E7–, but not E6–, immortalized human uroepithelial cells. *Genes Dev.* (1994) 8:2227–40. doi: 10.1101/gad.8.18.2227

42. Klingelhutz AJ, Foster SA, McDougall JK. Telomerase activation by the E6 gene product of human papillomavirus type 16. *Nature.* (1996) 380:79–82. doi: 10.1038/380079a0

43. Veldman T, Horikawa I, Barrett JC, Schlegel R. Transcriptional activation of the telomerase hTERT gene by human papillomavirus type 16 E6 oncoprotein. *J Virol.* (2001) 75:4467–72. doi: 10.1128/JVI.75.9.4467-4472.2001

44. Katakura Y, Alam S, Shirahata S. Immortalization by gene transfection. *Methods Cell Biol.* (1998) 57:69–91. doi: 10.1016/S0091-679X(08)61573-3

45. Boyer SN, Wazer DE, Band V. E7 protein of human papilloma virus−16 induces degradation of retinoblastoma protein through the ubiquitin–proteasome pathway. *Cancer Res.* (1996) 56:4620–4.

46. Sugimoto M, Ide T, Goto M, Furuichi Y. Reconsideration of senescence, immortalization and telomeres maintenance of Epstein–Barr virus–transformed human B–lymphoblastoid cell lines. *Mech Ageing Dev.* (1999) 107:51–60. doi: 10.1016/S0047-6374(98)00131-6

47. Greider CW, Blackburn EH. The telomeres terminal transferase of tetrahymena is a ribonucleoprotein enzyme with two kinds of primer specificity. *Cell.* (1987) 51:887–98. doi: 10.1016/0092-8674(87)90576-9

48. Kim NW, Piatyszek MA, Prowse KR, Harley CB, West MD, Ho PL, et al. Specific association of human telomerase activity with immortal cells and cancer. *Science.* (1994) 266:2011–5. doi: 10.1126/science.7605428

49. Bodnar AG, Ouellette M, Frolkis M, Holt SE, Chiu CP, Morin GB, et al. Extension of life–span by introduction of telomerase into normal human cells. *Science.* (1998) 279:349–52. doi: 10.1126/science.279.5349.349

50. Wang J, Xie LY, Allan S, Beach D, Hannon GJ. Myc activates telomerase. *Genes Dev.* (1998) 12:1769–74. doi: 10.1101/gad.12.12.1769

51. Vaziri H, Benchimol S. Reconstitution of telomerase activity in normal human cells leads to elongation of telomeres and extended replicative life span. *Curr Biol.* (1998) 8:279–82. doi: 10.1016/S0960-9822(98)70109-5

52. Halvorsen TL, Leibowitz G, Levine F. Telomerase activity is sufficient to allow transformed cells to escape from crisis. *Mol Cell Biol.* (1999) 19:1864–70. doi: 10.1128/MCB.19.3.1864

53. Ouellette MM, Aisner DL, Savre–Train I, Wright WE, Shay JW. Telomerase activity does not always imply telomeres maintenance. *Biochem Biophys Res Commun.* (1999) 254:795–803. doi: 10.1006/bbrc.1998.0114

54. Ouellette MM, McDaniel LD, Wright WE, Shay JW, Schultz RA. The establishment of telomerase–immortalized cell lines representing human chromosome instability syndromes. *Hum Mol Genet.* (2000) 9:403–11. doi: 10.1093/hmg/9.3.403

55. Simonsen JL, Rosada C, Serakinci N, Justesen J, Stenderup K, Rattan SI, et al. Telomerase expression extends the proliferative life–span and maintains the osteogenic potential of human bone marrow stromal cells. *Nat Biotechnol.* (2002) 20:592–6. doi: 10.1038/nbt0602-592

56. Mihara K, Imai C, Coustan–Smith E, Dome JS, Dominici M, Vanin E, et al. Development and functional characterization of human bone marrow mesenchymal cells immortalized by enforced expression of telomerase. *Br J Haematol.* (2003) 120:846–9. doi: 10.1046/j.1365-2141.2003.04217.x

57. Kawano Y, Kobune M, Yamaguchi M, Nakamura K, Ito Y, Sasaki K, et al. *Ex vivo* expansion of human umbilical cord hematopoietic progenitor cells using a coculture system with human telomerase catalytic subunit (hTERT)–transfected human stromal cells. *Blood.* (2003) 101:532–40. doi: 10.1182/blood-2002-04-1268

58. Wege H, Le HT, Chui MS, Liu L, Wu J, Giri R, et al. Telomerase reconstitution immortalizes human fetal hepatocytes without disrupting their differentiation potential. *Gastroenterology.* (2003) 124:432–44. doi: 10.1053/gast.2003.50064

59. Huang G, Zheng Q, Sun J, Guo C, Yang J, Chen R, et al. Stabilization of cellular properties and differentiation mutilpotential of human mesenchymal stem cells transduced with hTERT gene in a long–term culture. *J Cell Biochem.* (2008) 103:1256–69. doi: 10.1002/jcb.21502

60. Le QVC, Youk S, Choi M, Jeon H, Kim WI, Ho CS, et al. Development of an immortalized porcine fibroblast cell panel with different swine leukocyte antigen genotypes. *Front Genet.* (2022) 13:815328. doi: 10.3389/fgene.2022.815328

61. Cui H, Liang W, Wang D, Guo K, Zhang Y. Establishment and characterization of an immortalized porcine oral mucosal epithelial cell line as a cytopathogenic model for porcine circovirus 2 infection. *Front Cell Infect Microbiol.* (2019) 9:171. doi: 10.3389/fcimb.2019.00171

62. Cao H, Chu Y, Zhu H, Sun J, Pu Y, Gao Z, et al. Characterization of immortalized mesenchymal stem cells derived from foetal porcine pancreas. *Cell Prolif.* (2011) 44:19–32. doi: 10.1111/j.1365-2184.2010.00714.x

63. Kuruvilla L, Santhoshkumar TS, Kartha CC. Immortalization and characterization of porcine ventricular endocardial endothelial cells. *Endothelium.* (2007) 14:35–43. doi: 10.1080/10623320601177353

64. Hong HX, Zhang YM, Xu H, Su ZY, Sun P. Immortalization of swine umbilical vein endothelial cells with human telomerase reverse transcriptase. *Mol Cells.* (2007) 24:358–63.

65. Buser R, Montesano R, Garcia I, Dupraz P, Pepper MS. Bovine microvascular endothelial cells immortalized with human telomerase. *J Cell Biochem.* (2006) 98:267–86. doi: 10.1002/jcb.20715

66. Jin X, Lee JS, Kwak S, Lee SY, Jung JE, Kim TK, et al. Establishment and characterization of three immortal bovine muscular epithelial cell lines. *Mol Cells.* (2006) 21:29–33.

67. Zhang N, Li J, Zhong X, An X, Hou J. Reversible immortalization of sheep fetal fibroblast cells by tetracycline–inducible expression of human telomerase reverse transcriptase. *Biotechnol Lett.* (2016) 38:1261–8. doi: 10.1007/s10529-016-2103-6

68. Cui W, Wylie D, Aslam S, Dinnyes A, King T, Wilmut I, et al. Telomerase–immortalized sheep fibroblasts can be reprogrammed by nuclear transfer to undergo early development. *Biol Reprod.* (2003) 69:15–21. doi: 10.1095/biolreprod.102.013250

69. Bi CM, Zhang SQ, Zhang Y, Peng SY, Wang L, An ZX, et al. Immortalization of bovine germ line stem cells by c–myc and hTERT. *Anim Reprod Sci.* (2007) 100:371–8. doi: 10.1016/j.anireprosci.2006.10.017

70. Georgescu HI, Mendelow D, Evans CH. HIG−82: an established cell line from rabbit periarticular soft tissue, which retains the "activatable" phenotype. *In Vitro Cell Dev Biol.* (1988) 24:1015–22. doi: 10.1007/BF02620875

71. Takahashi K, Sawasaki Y, Hata J, Mukai K, Goto T. Spontaneous transformation and immortalization of human endothelial cells. *In Vitro Cell Dev Biol.* (1990) 26:265–74. doi: 10.1007/BF02624456

72. Castro–Muñozledo F. Development of a spontaneous permanent cell line of rabbit corneal epithelial cells that undergoes sequential stages of differentiation in cell culture. *J Cell Sci.* (1994) 107:2343–51. doi: 10.1242/jcs.107.8.2343

73. Kageyama T, Hayashi R, Hara S, Yoshikawa K, Ishikawa Y, Yamato M, et al. Spontaneous acquisition of infinite proliferative capacity by a rabbit corneal endothelial cell line with maintenance of phenotypic and physiological characteristics. *J Tissue Eng Regen Med.* (2017) 11:1057–64. doi: 10.1002/term.2005

74. Nachtigal M, Nagpal ML, Greenspan P, Nachtigal SA, Legrand A. Characterization of a continuous smooth muscle cell line derived from rabbit aorta. *In Vitro Cell Dev Biol.* (1989) 25:892–8. doi: 10.1007/BF02624001

75. Delia D, Fontanella E, Ferrario C, Chessa L, Mizutani S. DNA damage–induced cell–cycle phase regulation of p53 and p21waf1 in normal and ATM–defective cells. *Oncogene.* (2003) 22:7866–9. doi: 10.1038/sj.onc.1207086

76. Zhao C, Meng L, Hu H, Wang X, Shi F, Wang Y, et al. Spontaneously immortalised bovine mammary epithelial cells exhibit a distinct gene expression pattern from the breast cancer cells. *BMC Cell Biol.* (2010) 11:82. doi: 10.1186/1471-2121-11-82

77. Xie X, Pang M, Liang S, Yu L, Zhao Y, Ma K, et al. Establishment and characterization of a telomerase–immortalized canine bronchiolar epithelial cell line. *Appl Microbiol Biotechnol.* (2015) 99:9135–46. doi: 10.1007/s00253-015-6794-8

78. Ma GL, Qiao ZL, He D, Wang J, Kong YY, Xin XY, et al. Establishment of a low–tumorigenic MDCK cell line and study of differential molecular networks. *Biologicals.* (2020) 68:112–21. doi: 10.1016/j.biologicals.2020.07.003

79. Bailey KL, Cartwright SB, Patel NS, Remmers N, Lazenby AJ, Hollingsworth MA, et al. Porcine pancreatic ductal epithelial cells transformed with KRASG12D and SV40T are tumorigenic. *Sci Rep.* (2021) 11:13436. doi: 10.1038/s41598-021-92852-2

80. Kim D, Kim JY, Koh HS, Lee JP, Kim YT, Kang HJ, et al. Establishment and characterization of endothelial cell lines from the aorta of miniature pig for the study of xenotransplantation. *Cell Biol Int.* (2005) 29:638–46. doi: 10.1016/j.cellbi.2005.03.016

81. Callesen MM, Árnadóttir SS, Lyskjaer I, Ørntoft MW, Høyer S, Dagnaes–Hansen F, et al. A genetically inducible porcine model of intestinal cancer. *Mol Oncol.* (2017) 11:1616–29. doi: 10.1002/1878-0261.12136

82. Wang Q, Zhang X, Wang B, Bai G, Pan D, Yang P, et al. Immortalization of porcine hepatocytes with a α-1,3–galactosyltransferase knockout background. *Xenotransplantation.* (2020) 27:e12550. doi: 10.1111/xen.12550

83. Peng Y, Murr MM. Establishment of immortalized rat Kupffer cell lines. *Cytokine.* (2007) 37:185–91. doi: 10.1016/j.cyto.2007.03.003

84. MacDougall M, Mamaeva O, Lu C, Chen S. Establishment and characterization of immortalized mouse ameloblast–like cell lines. *Orthod Craniofac Res.* (2019) 22:134–41. doi: 10.1111/ocr.12313

85. Sakai Y, Miyake R, Shimizu T, Nakajima T, Sakakura T, Tomooka Y. A clonal stem cell line established from a mouse mammary placode with ability to generate functional mammary glands. *In Vitro Cell Dev Biol Anim.* (2019) 55:861–71. doi: 10.1007/s11626-019-00406-8

86. Kawasaki H, Ohama T, Hori M, Sato K. Establishment of mouse intestinal myofibroblast cell lines. *World J Gastroenterol.* (2013) 9:2629–37. doi: 10.3748/wjg.v19.i17.2629

87. Komine A, Abe M, Saeki T, Terakawa T, Uchida C, Uchida T. Establishment of adipose–derived mesenchymal stem cell lines from a p53–knockout mouse. *Biochem Biophys Res Commun.* (2012) 426:468–74. doi: 10.1016/j.bbrc.2012.08.094

88. Bartlett PF, Reid HH, Bailey KA, Bernard O. Immortalization of mouse neural precursor cells by the c–myc oncogene. *Proc Natl Acad Sci USA.* (1988) 85:3255–9. doi: 10.1073/pnas.85.9.3255

89. Orimoto A, Katayama M, Tani T, Ito K, Eitsuka T, Nakagawa K, et al. Primary and immortalized cell lines derived from the amami rabbit (*Pentalagus furnessi*) and evolutionally conserved cell cycle control with CDK4 and cyclin D1. *Biochem Biophys Res Commun.* (2020) 525:1046–53. doi: 10.1016/j.bbrc.2020.03.036

90. Thenet S, Benya PD, Demignot S, Feunteun J, Adolphe M. SV40–immortalization of rabbit articular chondrocytes: alteration of differentiated functions. *J Cell Physiol.* (1992) 150:158–67. doi: 10.1002/jcp.1041500121

91. Chen Y, Hu S, Wang M, Zhao B, Yang N, Li J, et al. Characterization and establishment of an immortalized rabbit melanocyte cell line using the SV40 large T antigen. *Int J Mol Sci.* (2019) 20:4874. doi: 10.3390/ijms20194874

92. Araki K, Ohashi Y, Sasabe T, Kinoshita S, Hayashi K, Yang XZ, et al. Immortalization of rabbit corneal epithelial cells by a recombinant SV40–adenovirus vector. *Invest Ophthalmol Vis Sci.* (1993) 34:2665–71.

93. Bai Y, Zhu C, Feng M, Pan B, Zhang S, Zhan X, et al. Establishment of A reversibly inducible porcine granulosa cell line. *Cells.* (2020) 9:156. doi: 10.3390/cells9010156

94. Zhang K, Li H, Dong S, Liu Y, Wang D, Liu H, et al. Establishment and evaluation of a PRRSV–sensitive porcine endometrial epithelial cell line by transfecting SV40 large T antigen. *BMC Vet Res.* (2019) 15:299. doi: 10.1186/s12917-019-2051-1

95. Zheng Y, Feng T, Zhang P, Lei P, Li F, Zeng W. Establishment of cell lines with porcine spermatogonial stem cell properties. *J Anim Sci Biotechnol.* (2020) 11:33. doi: 10.1186/s40104-020-00439-0

96. He S, Li Y, Chen Y, Zhu Y, Zhang X, Xia X, et al. Immortalization of pig fibroblast cells by transposon–mediated ectopic expression of porcine telomerase reverse transcriptase. *Cytotechnology.* (2016) 68:1435–45. doi: 10.1007/s10616-015-9903-8

97. Kuroda K, Kiyono T, Isogai E, Masuda M, Narita M, Okuno K, et al. Immortalization of fetal bovine colon epithelial cells by expression of human cyclin D1, mutant cyclin dependent kinase 4, and telomerase reverse transcriptase: an *in vitro* model for bacterial infection. *PLoS ONE.* (2015) 10:e0143473. doi: 10.1371/journal.pone.0143473

98. Pace MC, Chambliss KL, German Z, Yuhanna IS, Mendelsohn ME, Shaul PW. Establishment of an immortalized fetal intrapulmonary artery endothelial cell line. *Am J Physiol.* (1999) 277:L106–12. doi: 10.1152/ajplung.1999.277.1.L106

99. Da Silva Teixeira MF, Lambert V, Mselli–Lakahl L, Chettab A, Chebloune Y, Mornex JF. Immortalization of caprine fibroblasts permissive for replication of small ruminant lentiviruses. *Am J Vet Res.* (1997) 58:579–84.

100. Zhao R, Jin J, Sun X, Jin K, Wang M, Ahmed MF, et al. The establishment of clonally derived chicken embryonic fibroblast cell line (CSC) with high transfection efficiency and ability as a feeder cell. *J Cell Biochem.* (2018) 119:8841–50. doi: 10.1002/jcb.27137

101. Lee J, Foster DN, Bottje WG, Jang HM, Chandra YG, Gentles LE, et al. Establishment of an immortal chicken embryo liver–derived cell line. *Poult Sci.* (2013) 92:1604–12. doi: 10.3382/ps.2012-02582

102. Himly M, Foster DN, Bottoli I, Iacovoni JS, Vogt PK. The DF−1 chicken fibroblast cell line: transformation induced by diverse oncogenes and cell death resulting from infection by avian leukosis viruses. *Virology.* (1998) 248:295–304. doi: 10.1006/viro.1998.9290

103. Kawaguchi T, Nomura K, Hirayama Y, Kitagawa T. Establishment and characterization of a chicken hepatocellular carcinoma cell line, LMH. *Cancer Res.* (1987) 47:4460–4.

104. Wang W, Said A, Wang Y, Fu Q, Xiao Y, Lv S, et al. Establishment and characterization of duck embryo epithelial (DEE) cell line and its use as a new approach toward DHAV−1 propagation and vaccine development. *Virus Res.* (2016) 213:260–8. doi: 10.1016/j.virusres.2015.12.021

105. Wang W, Said A, Wang B, Qu G, Xu Q, Liu B, et al. Establishment and evaluation of the goose embryo epithelial (GEE) cell line as a new model for propagation of avian viruses. *PLoS ONE.* (2018) 13:e0193876. doi: 10.1371/journal.pone.0193876

106. Antin PB, Ordahl CP. Isolation and characterization of an avian myogenic cell line. *Dev Biol.* (1991) 143:111–21. doi: 10.1016/0012-1606(91)90058-B

107. Jaffredo T, Chestier A, Bachnou N, Dieterlen–Lièvre F. MC29–immortalized clonal avian heart cell lines can partially differentiate *in vitro*. *Exp Cell Res.* (1991) 192:481–91. doi: 10.1016/0014-4827(91)90067-5

108. Moscovici C, Moscovici MG, Jimenez H, Lai MM, Hayman MJ, Vogt PK. Continuous tissue culture cell lines derived from chemically induced tumors of Japanese quail. *Cell.* (1977) 11:95–103. doi: 10.1016/0092-8674(77)90320-8

109. Gionti E, Pontarelli G, Cancedda R. Avian myelocytomatosis virus immortalizes differentiated quail chondrocytes. *Proc Natl Acad Sci USA.* (1985) 82:2756–60. doi: 10.1073/pnas.82.9.2756

frontiers | Frontiers in Veterinary Science

TYPE Original Research
PUBLISHED 16 September 2022
DOI 10.3389/fvets.2022.999040

Check for updates

OPEN ACCESS

EDITED BY
Abdul Rasheed Baloch,
University of Karachi, Pakistan

REVIEWED BY
Takashi Ito,
Fukui Prefectural University, Japan
Fan Chen,
Universitätsmedizin
Greifswald, Germany
Xiaoge Yang,
Anqing Normal University, China

*CORRESPONDENCE
Junhong Gao
gaoxing2285@126.com

†These authors have contributed equally to this work

SPECIALTY SECTION
This article was submitted to Livestock Genomics, a section of the journal Frontiers in Veterinary Science

RECEIVED 20 July 2022
ACCEPTED 24 August 2022
PUBLISHED 16 September 2022

CITATION
Gao Y, Sun C, Gao T, Liu Z, Yang Z, Deng H, Fan P and Gao J (2022) Taurine ameliorates volatile organic compounds-induced cognitive impairment in young rats *via* suppressing oxidative stress, regulating neurotransmitter and activating NMDA receptor. *Front. Vet. Sci.* 9:999040. doi: 10.3389/fvets.2022.999040

COPYRIGHT
© 2022 Gao, Sun, Gao, Liu, Yang, Deng, Fan and Gao. This is an open-access article distributed under the terms of the Creative Commons Attribution License (CC BY). The use, distribution or reproduction in other forums is permitted, provided the original author(s) and the copyright owner(s) are credited and that the original publication in this journal is cited, in accordance with accepted academic practice. No use, distribution or reproduction is permitted which does not comply with these terms.

Taurine ameliorates volatile organic compounds-induced cognitive impairment in young rats *via* suppressing oxidative stress, regulating neurotransmitter and activating NMDA receptor

Yongchao Gao[1†], Chao Sun[2†], Ting Gao[1†], Zhiyong Liu[1], Zhao Yang[1], Hui Deng[1], Peng Fan[1] and Junhong Gao[1*]

[1]Toxicology Research Center, Institute for Hygiene of Ordnance Industry, Xi'an, China, [2]Xijing Hospital, The Fourth Military Medical University, Xi'an, China

Long-term exposure to volatile organic compounds (VOCs) in children leads to intellectual and cognitive impairment. Taurine is an essential nutritional amino acid for children, which can improve neurological development in children. However, the neuroprotective effect of taurine on VOCs-induced cognitive impairment in children remains unclear. The aim of this study was to investigate the neuroprotective effects of taurine on VOCs-induced cognitive impairment in young rats. The rats were nose-only exposed to VOCs for a period of 4 weeks to create a model of cognitive impairment, and 0.5% and 1% taurine in tap water were administered throughout the trial period, respectively. Our results showed that young rats adjusted the recovery of their physiological functions by voluntarily increasing the intake of taurine in tap water when exposed to excessive VOCs by inhalation. In addition, taurine enhanced grasp, shortened the latency period of escape, and improved the learning and memory function of young rats. Moreover, taurine decreased malondialdehyde (MDA), γ-aminobutyric acid (GABA), Aspartate aminotransferase (AST), Alanine aminotransferase (ALT), Urea, Creatinine (CREA) and injury biomarker level, enhanced superoxide dismutase (SOD), reduced glutathione (GSH) and glutamic acid (Glu) activities, up-regulated the protein expression of brain derived neurotrophic factor (BDNF) and N-Methyl-d-aspartate receptor 1 (NMDAR1) in model rats, and in most of cases 1% but not 0.5%, ameliorated the defects induced by VOCs. Collectively, these findings suggested that taurine protected against VOCs-induced cognitive-behavioral impairment in young rats through inhibiting oxidative stress and regulating neurotransmitter homeostasis. In addition, taurine were capable of restoring abilities of learning and memory in young rats exposed to VOCs by activating

the N-Methyl-d-aspartate (NMDA) receptor. The findings suggest taurine as a potential novel drug for the treatment of cognitive behavioral disorders in children.

KEYWORDS

taurine, volatile organic compounds, cognitive impairment, oxidative stress, neurotransmitter, NMDAR1

Introduction

With the wide and extensive application of new building materials and decorative materials, including coatings, adhesives, furniture, flooring, wallpaper, etc., will release a variety of volatile organic compounds (VOCs), which aggravates indoor air pollution. Because of the increasing concentration of indoor chemical compounds and the fact that most people spend the majority of their time inside, indoor air pollution has become a major public health concern (1). In humans, VOC exposure can cause negative health effects, for example, neurological reactions, behaving as weakness, loss of appetite, fatigue, disorientation, and nausea (2). In the VOCs series of compounds, some kinds of VOCs have strong toxicity, serious harm to human health. Benzene series and formaldehyde have been determined as class I carcinogen by the International Center for Research on Cancer (3). Indoor is the main place for human activities, and the indoor environment is closely related to the health of people (4). However, indoor air quality (IAQ) is a common problem in new residential buildings in China (5). With few precautions, inhalation and skin exposure to unhealthy levels of concentration are almost inevitable. VOCs are the main indoor air pollutants, of which benzene, toluene, xylene and formaldehyde are the more common indoor VOCs, including smoking, solvent use, renovation and household products, especially in the presence of new houses and furniture (6). VOCs tests were carried out on more than 7,000 residences in China in the last decade (nearly one-third were newly renovated) and found ubiquitous pollutants exceeding recommended concentrations, including particulate matter, formaldehyde, benzene and other VOCs and molds (7). Human exposure to VOCs includes direct contact through hands and other skin surfaces, as well as inhalation of gases and airborne particulate matter (8).

City dwellers typically spend more than 90% of their time indoors (9). As one of the specially sensitive groups, children are in an important stage of growth and development. They spend more time and volume of breath indoors than adults, and are more vulnerable to pollution than adults due to physiological conditions and other factors (10), so they are more sensitive to indoor environmental pollution. Epidemiological investigations have shown that VOCs exposure can cause neurological symptoms such as headaches and inattention (11). Previous animal studies have shown that VOCs has multi-target organ toxicity and can cause damage to multiple organs and systems in the body. Sub-chronic exposure of low-dose VOCs can damage the body shape and motor function of mice, as well as the learning and memory ability of mice (12). Acute inhalation exposure of high-dose formaldehyde can induce cognitive deficits in mice, causing damage to the hippocampal region and leading to learning and memory disorders (13). Benzenes such as toluene are also well-known neurotoxins (14). The adaptability of infant rats to such as adverse environment is weaker than that of adult rats (15), and the cognitive impairment is particularly serious. Mice's motor function, as well as learning and memory abilities, can be affected by subchronic exposure to low-dose VOCs (16). Recent studies have reported that variable age stages of animals show different amounts of oxidative stress in response to VOCs exposure, and infant rats have weaker adaptability to adverse environment than adults (15). Oxidative damage, altered expression of neurotransmitters and NMDA receptors may be the possible mechanisms of VOCs neurotoxicity (12). How to improve neurotoxicity and cognitive impairment caused by VOCs has become an important problem to be solved urgently. In terms of drug prevention and treatment, neurostimulants and hormone drugs such as amphetamine and dexamethasone have a certain protective effect on cognitive impairment, but their side effects are large and cannot be used as routine preventive drugs (17). Research on how to effectively reduce VOCs damage to brain tissue through dietary approach is of great significance for improving children's intelligence and cognitive ability.

Taurine (2-aminoetaurine), which is an amino acid that may be found in practically all animal tissues, is abundant in the nervous system. It is the only free amino acid second only to Glutamate. Its physiological functions include antioxidant, growth promotion, nervous, cardiovascular, immune and endocrine regulation (18, 19). Taurine has a variety of impacts on the central nervous system: Neuromodulators, neurotrophic agents and neuro protective agents can protect neurons in neuro-related diseases (20), improve fetal brain development (21). It can also significantly improve the cognitive impairment of young rats after prenatal stress (22). In animal studies, taurine has an age-dependent effect on overall cognitive development.

A study found that mice in the post-weaning group learned tasks faster than mice in the control group during the first four phases of adulthood (lifetime, pre-weaning, post-weaning, and control) (23). Taurine (dissolved in 1% and 2% tap water, respectively), ameliorates cognitive impairment and inhibits apoptosis of hippocampal neurons exposed to high Glucose in diabetic rats through the NGF-Akt/Bad pathway (24). In this study, the VOCs mixed inhalation exposure method was used to establish a model of cognitive function impairment in young rats. This method was consistent with the exposure environment of indoor VOCs pollution, in reality, and the protective effect of taurine on VOCs-induced cognitive function impairment was evaluated from the aspects of neuro behavior, oxidative stress, brain tissue morphology and related active factors. The underlying molecular mechanisms that may be involved in taurine's improvement of behavioral disorders were elucidated.

Materials and methods

Reagents and kits

Taurine (Food grade, Jiangsu Xinrui Biotechnology Co., Ltd. China), Formaldehyde, Benzene, Toluene, Xylene (Analytical purity, Chengdu Cologne Chemical Co., Ltd. China), Malondialdehyde (MDA), Reduced Glutathione (GSH), Superoxide dismutase (SOD), Catalase (CAT), Glutamic acid (Glu) Determination Kit (Nanjing Jiancheng Institute of Biological Engineering, China), Aspartate aminotransferase (AST), Alanine aminotransferase (ALT), Urea, Creatinine (CREA) Determination Kit (Beckman, USA), Rat Glial fibrillary acidic protein (GFAP), Myelin basic protein (MBP), Neurofilament light chain (NF-L), γ-aminobutyric acid (GABA) and Taurine (TAU) ELISA Kit (Shanghai Enzyme-Linked Biotechnology Co., Ltd. China), Anti-BDNF antibody (ab108319) (Abcam, Britain), Anti-NMDAR1 antibody (ab274377) (Abcam, Britain).

Animals

SD rats were purchased from Sibeifu (Beijing) Biotechnology Co., LTD., with the production license: SCXK (Beijing) 2019-0010. At the beginning of the infection, the animals were 4 weeks old, weighing 89.2 ± 9.1 g, and kept in the barrier system. The license was SYXK (Shaanxi) 2021-008. The ambient temperature was 22°C∼26°C, the relative humidity was 40–70%, and the light and shade were alternating with 12 h. The rats fed and drank freely. The experiment was followed the National Institutes of Health guide for the care and use of Laboratory animals (NIH Publications No. 8023, revised 1978) and approved by the Laboratory Animal Management and used Committee of the unit, approval number: IACUC202104.

Experimental design

Twenty-four healthy young SPF male SD rats were randomly divided into four groups of six rats in each group: control group (control), VOCs model group (VOCs), VOCs+0.5% taurine intervention group (VOCs+0.5% taurine) and VOCs+1%taurine intervention group (VOCs+1% taurine). VOCs, VOCs+0.5% taurine and VOCs+1% taurine groups were exposed to VOCs (Theoretical concentration of 5 mg/m^3 formaldehyde+5 mg/m^3 benzene+10 mg/m^3 toluene+10 mg/m^3 xylene) mixed liquid aerosol (25) by nose-only inhalation for 4 h/day, 5 day/week for a period of 28 days (4 weeks). The concentrations of formaldehyde and benzene series were dynamically monitored by pump formaldehyde detector and gas chromatography, respectively, to ensure that the actual concentration was consistent with the theoretical concentration. At the same time, the control group inhaled clean air with an inhalation exposure system for 28 days. The VOCs+0.5% taurine and VOCs+1% taurine groups were dissolved in tap water with 0.5% and 1% taurine, respectively. They were given tap water every day from the beginning of modeling to the end of modeling. Control and VOCs model group drank water normally. During the experiment, the body weight of the animals was measured every week, and the drinking volume of each cage (2 rats in 1 cage) was recorded daily by the scale on the drinking bottle, and the daily drinking volume of each rat was obtained after averaging.

Nose-only inhalation exposure

Four 20-port nose-only inhalation exposure devices are available at the facility (TSE Systems, Germany). Each inhalation exposure system consists of a nose-only inhalation exposure chamber, an aerosol generation system, and a test atmosphere monitor and control system. The test atmosphere was created by aerosolizing the test formulation, a mixture of VOCs in 5% formaldehyde, 5% benzene, 10% toluene, 10% xylene and 70% water with a nebulizer (TSE Systems, Germany). The total air flow was set to produce an air flow of approximately 1 L/min/exposure port. The concentrations of VOCs in the formulations were adjusted to control the aerosol concentrations. To ensure an oxygen concentration of at least 19%, mass flow controllers and a Daco monitoring and control system (TSE Systems, Germany) were used to control the input and exhaust air flows to and from the chamber (26).

The capacity of the nose-only inhalation exposure systems was validated prior to the *in vivo* inhalation exposure investigation. To verify that the concentrations in the aerosols were within 10% of the target concentrations, the parameters of test atmosphere in rat breathing zones were measured for 1 h per day for 3 days (simulated exposure). The concentrations of formaldehyde and benzene series were dynamically monitored

using a PGM620 pump-suction formaldehyde detector (RAE, USA) and GC-type gas chromatograph (Shimadzu, Japan).

Neurobehavioral test

After the 28-day inhalation exposure experiment, the rats were, firstly, tested for their grasping power using the rat and mouse gripping force tester (Shanghai Ruanxin, Inc. China), then the multi-condition behavioral system (TSE Systems, Germany) was used to test the rat's spontaneous activity in the open-field test, and finally the Morris The water maze (Anhui Zhenghua Biology, China) tests the learning and memory abilities of rats.

Grip strength test

After the inhalation exposure, the grasping force of each animal was measured. All experiments were conducted in triplicate for technical replication of each animal. The average value was taken as the grasping force value.

Open field test

All animals were acclimated in the behavioral testing room for 1 h before the open-field experiment (27). The multi-condition animal behavior system was used for testing, and the animals were placed in the open-field experimental box facing the wall of the experimental box, and after allowing them to adapt for 5 min, the activities of 5 min were recorded. After each animal experiment, the feces in the experimental box were cleaned up, sprayed with alcohol, and dried with a clean towel to continue the subsequent experiment.

Morris water maze test

MWM includes place navigation test and spatial probe test, according to Wang's team for specific test methods (12). The experimental period was 7 days. During the experiment, the animals were fed in the behavioral test room to adapt to the experimental environment. The animals were put into the pool from any quadrant on the 1st day of the experiment to swim for 2 min. Positioning and navigation experiment: a total of 5 days (days 2–6), training every day from 2 p.m. to 5 p.m. Before the training, put the platform in quadrant IV, put the animals into the pool from different quadrants facing the pool wall, and record the time when the animals climb onto the platform (escape latency); Space exploration experiment: on the 7th day, remove the platform before the experiment, put the animals into the pool from quadrant II, and record the residence time of the animals in the target quadrant (quadrant IV) and the times of crossing the platform position within 120's.

Detection of biomarkers of nerve injury and general biochemical parameters in rat serum

After the behavioral test, the rats were put into a CO_2 anesthesia box, and 40% CO_2 was introduced for about 2–5 min to achieve the anesthesia effect, and then blood was collected from the abdominal aorta. The collected blood was centrifuged at 3,000 rpm for 10 min, the upper serum was isolated. The contents of GFAP, MBP and NF-L in serum of animals in each group were determined by ELISA test, according to the instructions of rat GFAP, MBP and NF-L ELISA Kit (Shanghai enzyme linked Biotechnology Co., Ltd. China). In addition, the contents of AST, ALT, urea and CREA in serum of animals in each group were determined by automatic biochemical analyser (Beckman, USA).

Detection of oxidative stress and neurotransmitter level in rat brain tissue

The brain tissues of rats in each group were collected, and normal saline was added at 1:9 to make brain tissue homogenate, centrifuged at 1,000 rpm for 10 min, and the contents of SOD, CAT, GSH, MDA and Glu in the supernatant were determined. The SOD, CAT, GSH, MDA and Glu in the rat brain were detected using commercial kits obtained from Nanjing Jiancheng Bioengineering Research Institute (China) following the manufacturer's instructions. GABA levels in brain tissue were measured using an enzyme-linked immunosorbent assay. The detection was carried out according to the instructions of the rat GABA ELISA kit purchased by Shanghai Enzyme-Linked Biotechnology Co., Ltd. (China).

Detection of taurine content in rat serum, brain, liver and kidney tissue

In order to investigate the dose-dependent effects of taurine, the serum, brain, liver and kidney tissues of rats in each group were collected to detection of taurine content. Tissue samples were processed by adding normal saline at a ratio of 1:9 to make tissue homogenated, and centrifuged at 1,000 rpm for 10 min to obtain supernatant. The detection method was carried out according to the instruction of taurine (TAU) ELISA kit (Shanghai Enzyme-Linked Biotechnology Co., Ltd. China).

Histopathological observation

Whole-brain tissue sections of rats in each group ($n = 3$) were stained with H&E and Nissl staining. The brain tissue

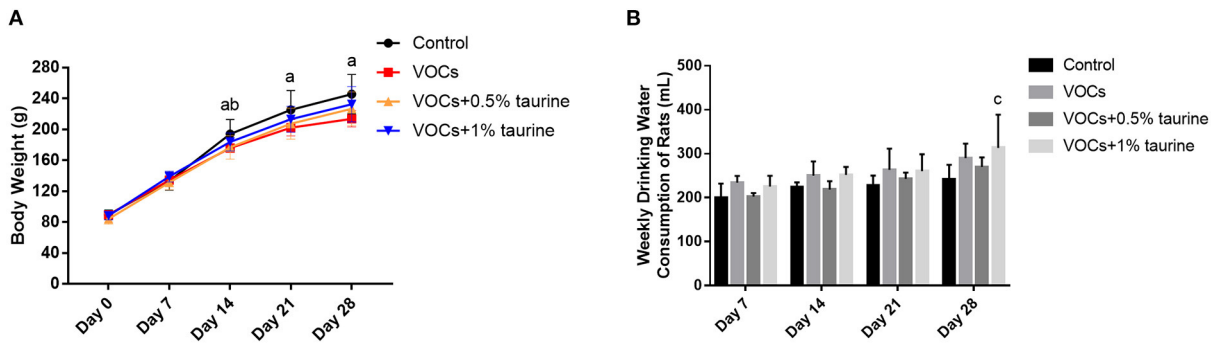

FIGURE 1
Effects of taurine on body weight and water intake of rats exposed to VOCs. **(A)** The body weight of the rats in each group during the experiment. **(B)** The water intake of the rats in each group during the experiment. Data are expressed as mean ± SD. ($n = 6$). a: $P < 0.05$, VOCs group vs. control group. b: $P < 0.05$, VOCs+0.5% taurine group vs. control group. c: $P < 0.05$, VOCs+1% taurine group vs. control group. d: $P < 0.05$, VOCs+0.5% taurine group vs. VOCs group. e: $P < 0.05$ VOCs+1% taurine group vs. VOCs group.

was fixed with neutral formalin solution and the paraffin embedded tissue was used to make 7 μm paraffin sections. Some sections were stained with hematoxylin and eosin dyes (Solarbio, China) for H&E staining, and the other sections were stained with methyl violet dyes and Nissl differentiation solution (Solarbio, China) for Nissl staining. Finally, the images were captured under a microscope (Leica, Germany) after being fully transparent in anhydrous ethanol to xylene and sealed in a neutral resin to observe morphological changes and analyze the number of living neurons in hippocampus (28).

Western blot analysis

The hippocampus was isolated from brains of each group which washed by 0.9% cold saline on a cold plate and stored at −80°C for detection, and the tissue was broken by adding lysate containing the protease inhibitor. Centrifuge at 12,000 r/min for 15 min at 4°C, take the supernatant, and use BCA kit for protein quantification. Mix the sample and 5× loading buffer thoroughly at a ratio of 1:4, and boil in a water bath at 100°C for 5 min. NMDAR1 (99 kDa), GAPDH (36 kDa), and BDNF (13 kDa) were separated by 15% SDS-PAGE electrophoresis, electrotransferred to 0.22 μm PVDF membrane, and blocked in 5% skim milk at room temperature for 2 h. The blocked membranes were incubated with primary antibody at a dilution of 1:2000 at 4°C overnight. Then the membranes were washed three times each in TBST buffer (TBS buffer containing 0.5% Tween-20) and incubated with 1:4000 diluted horseradish peroxidase-labeled secondary antibody at room temperature for 1 h.

After washing with TBST, the membrane was developed with ECL. Grayscale analysis was performed after taking pictures with a protein gel imaging system. Standard control was performed with GAPDH as an internal referred.

Statistical analysis

All data were subject to normal distribution and homogeneous variance. The MWM data were analyzed by repeated measurement analysis of variance. Significance of the other data was determined with one-way analysis of variance (ANOVA) followed by an LSD test for *post hoc* multiple comparisons. Inspection level $\alpha = 0.05$.

Results

Effects of taurine on body weight and water intake of rats exposed to VOCs

During inhalation exposure, the activities and diet of rats in each dose group were normal without death. The body weight and water intake of rats in each group during the experiment were shown in Figure 1. The results showed no significant difference in body weight between day 0 and 7 ($P > 0.05$). In day 14, the significantly lower body weight of rats was observed in VOCs group and VOCs+0.5% taurine group than that in control group ($P < 0.05$), whereas there was no significant difference between VOCs+1% taurine and control group ($P > 0.05$). On day 21 and 28, only the body weight of rats in VOCs group showed significant difference compared with control group ($P < 0.05$), but no significant difference was observed among other groups ($P > 0.05$, Figure 1A). From the 1st week to the 3rd week of the experiment, there was no difference in the water consumption of the rats in each group ($P > 0.05$), but

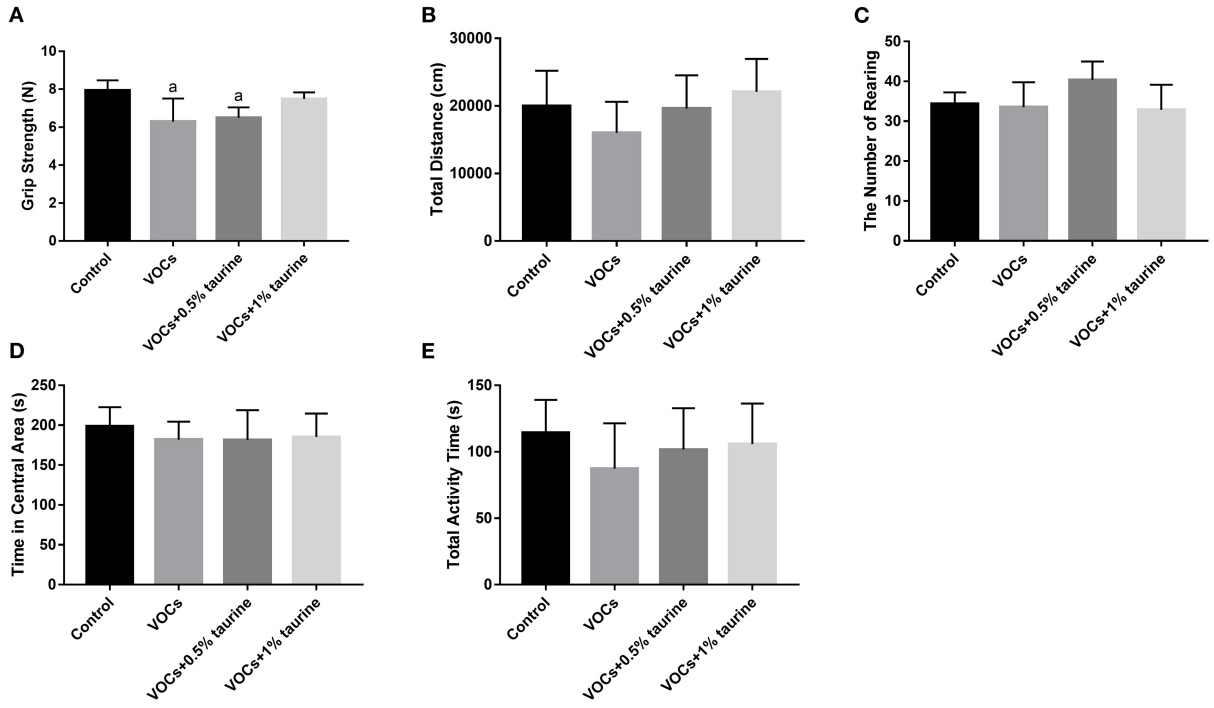

FIGURE 2
Effects of taurine on grasping strength, autonomous activity and exploration behavior of rats exposed to VOCs. **(A)** Grasping strength. **(B)** Total distance. **(C)** The number of rearing. **(D)** Time in central area. **(E)** Total activity time. Data are expressed as mean ± SD. ($n = 6$). a: $P < 0.05$ vs. control group. b: $P < 0.05$ vs. VOCs group. c: $P < 0.05$ vs. VOCs+0.5% taurine group.

in the 4th week, the water consumption of the rats in the VOCs+1% taurine group was higher than that in the control group ($P < 0.05$, Figure 1B).

Effects of taurine on grasping strength, autonomous activity and exploration behavior of rats exposed to VOCs

After VOCs exposure, the rats in each group were tested for grasping strength (Figure 2A). The results showed that the grasping strength of rats in VOCs and VOCs+0.5% taurine group decreased significantly, compared with control group ($P < 0.05$). It showed no significant difference in grasping force between the VOCs+1% taurine group and control group ($P > 0.05$). The results demonstrated that taurine reversed grasping strength of rats exposed to VOCs.

To figure out the effects of taurine on autonomous activity and exploring behavior in VOC-exposed rats, we did an open field test. As a result, no significant difference was showed in total distance, total activity time, time in central area and number of rearing of rats in each group ($P > 0.05$, Figures 2B–E). Compared with control group, the total distance and activity time of rats in VOCs group showed a downward trend, while taurine slightly recovered autonomous activity and exploration behavior.

Effects of taurine on learning and memory ability of rats exposed to VOCs

In the place navigation test, through repeated measurement analysis of variance of escape latency data, the results show that the escape latency has a downward trend with the experimental time, and the role of time factors does not vary with different groups, and the escape latency of each group is not the same as a whole (Figure 3A). The results according to one-way ANOVA indicated that there was no significant difference in the escape latency of rats in each group on the 1st day of the test ($P > 0.05$). On the 2nd day, the escape latency of the VOCs+1% taurine group was significantly lower than that of the control and VOCs groups ($P < 0.05$). On the 3rd day, the escape latency of rats in VOCs group was significantly higher than that in control group ($P < 0.05$), but no significant difference was shown among the other three groups ($P > 0.05$). On the fourth day, VOCs group showed the significantly higher escape latency of rats than that in control, VOCs+0.5% taurine and VOCs+1% taurine groups (P

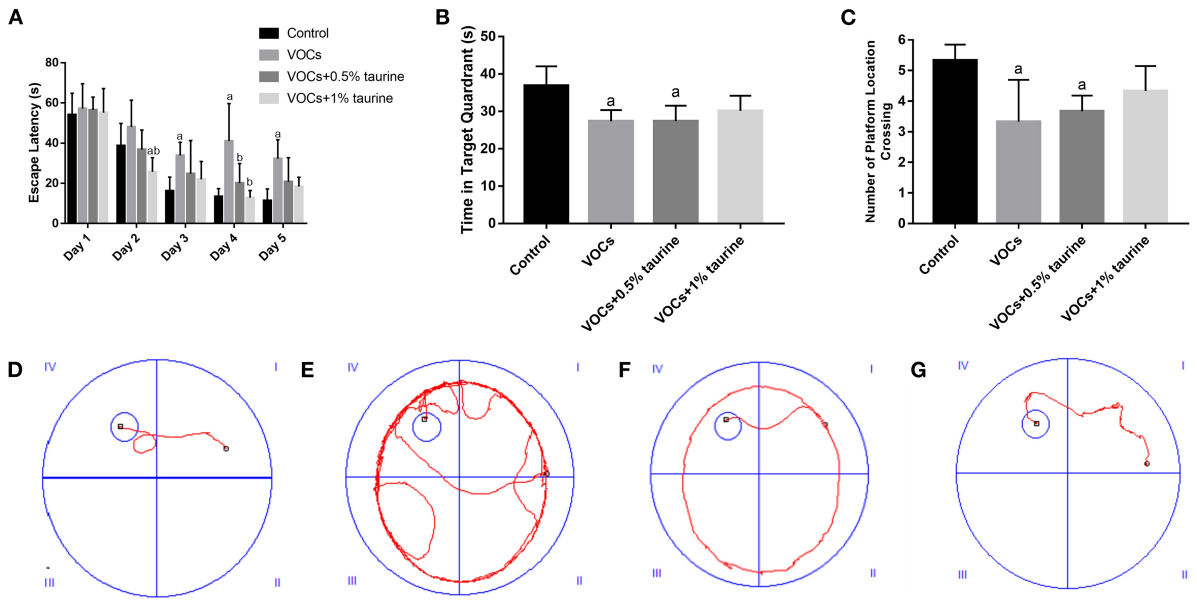

FIGURE 3
Effects of taurine on learning and memory of rats exposed to VOCs. **(A)** Escape latency. **(B)** Time in target quadrant. **(C)** Number of platform location crossing. **(D–G)** Movement tracks of rats in control group, VOCs group, VOCs+0.5% taurine group and VOCs+1% taurine group. Data are expressed as mean ± SD. ($n = 6$). a: $P < 0.05$ vs. control group. b: $P < 0.05$ vs. VOCs group. c: $P < 0.05$ vs. VOCs+0.5% taurine group.

< 0.05), and there was no significant difference among the other three groups ($P > 0.05$). On the 5th day, the escape latency of rats in VOCs group was significantly higher than that in control group ($P < 0.05$). There was no significant difference among the other three groups ($P > 0.05$).

The results of the spatial probe test were shown in Figures 3B,C. The time in target quadrant and the number of platform location crossing of VOCs group and VOCs+0.5% taurine group were significantly lower than that of the control group ($P < 0.05$). There was no significant difference between the VOCs+1% taurine group and control group ($P > 0.05$).

It showed the movement trajectories of rats in each group (Figures 3D–G). The control and VOCs+1% taurine groups have similar movement trajectories, and the rats can quickly locate the platform position. Compared with control group, the trajectories of VOCs and VOCs+0.5% taurine groups were significantly prolonged.

Effects of taurine on biomarkers of serum nerve injury and general biochemical parameters of rats exposed to VOCs

In Figures 4A–C, the contents of GFAP, MBP, and NF-L in VOCs group were significantly higher than those in control group ($P < 0.05$). There was no difference in the contents of GFAP and NF-L between VOCs group and VOCs+0.5% taurine group ($P > 0.05$). The contents of GFAP, MBP, and NF-L in serum of the VOCs+1% taurine group were not different from those in control group ($P > 0.05$), but lower than those in VOCs group ($P < 0.05$). Furthermore, we tested serum biochemical parameters that reflect liver and kidney function. The results showed that compared with control group, the serum urea, CREA, ALT and AST of VOCs group were significantly increased ($P < 0.05$, Figures 4D–G). The urea and ALT content in serum of rats in VOCs+0.5% taurine and VOCs+1% taurine groups were lower than that in VOCs group ($P < 0.05$, Figures 4D,F), and there was no significant difference compared to the control group ($P > 0.05$). Although the CREA and AST content of VOCs+0.5% taurine and VOCs+1% taurine groups were lower than that of VOCs group ($P < 0.05$), only VOCs+1% taurine group had no significant difference with the control group ($P > 0.05$, Figures 4E,G).

Effects of taurine on oxidative stress level in brain tissue of rats exposed to VOCs

To investigate whether taurine mitigated VOCs-induced lipid peroxidation damage, the antioxidant enzymes SOD, CAT, GSH and lipid peroxidation product MDA in the antioxidant

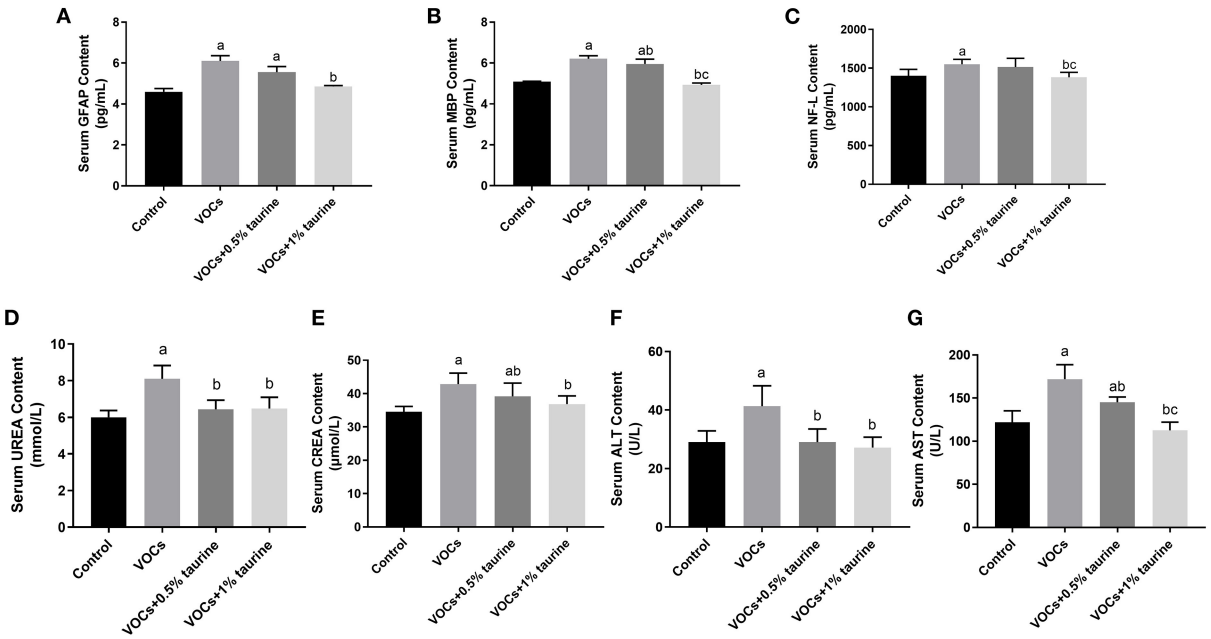

FIGURE 4
Effects of taurine on biomarkers of serum nerve injury and general biochemical parameters caused by VOCs in rats. **(A)** Contents of GFAP in rat serum. **(B)** Contents of MBP in rat serum. **(C)** Contents of NF-L in rat serum. **(D)** Contents of UREA in rat serum. **(E)** Contents of CREA in rat serum. **(F)** Contents of ALT in rat serum. **(G)** Contents of AST in rat serum. Data are expressed as mean ± SD. ($n = 6$). a: $P < 0.05$ vs. control group. b: $P < 0.05$ vs. VOCs group. c: $P < 0.05$ vs. VOCs+0.5% taurine group.

system were measured. The results were shown in Figure 5. Compared with control group, MDA was increased in VOCs group, while SOD, GSH and CAT activities were decreased ($P < 0.05$). The MDA content in brain tissues of rats in VOCs+0.5% taurine and VOCs+1% taurine groups was lower than that in VOCs group ($P < 0.05$), and there was no significant difference between VOCs+1% taurine and control groups ($P > 0.05$, Figure 5A). Rats in the VOCs+1% taurine group had higher SOD activity and GSH concentration in brain tissue than rats in the VOCs group ($P < 0.05$, Figures 5B,C). However, there was no significant difference in CAT activity between 1% taurine group and the VOCs group ($P > 0.05$, Figure 5D).

Effects of taurine on neurotransmitters in brain tissue of rats exposed to VOCs

The contents of Glu and GABA in rat brain tissues of each group were shown in Figure 6. Glu was found to be considerably lower in the VOCs and VOCs+0.5% taurine groups compared to the control group, but GABA concentration was significantly higher ($P < 0.05$). Glu was significant higher in the VOCs+1% taurine group compared to VOCs and VOCs+0.5% taurine groups ($P < 0.05$), and GABA was lower in the VOCs+1% taurine group ($P < 0.05$), but there was no significant difference with control group ($P > 0.05$).

Changes of taurine content in the serum, brain, liver, and kidney tissue of rats exposed to VOCs

We further examined taurine levels in serum, brain, liver and kidney tissues to investigate the dose-dependent effects of taurine. The results showed that there was no significant difference in serum taurine content of each group ($P > 0.05$, Figure 7A). However, taurine content in brain, liver and kidney of VOCs group was significantly lower than that of control group. Compared with VOCs and VOCs+0.5% taurine group, taurine content in these tissues was significantly increased in VOCs+1% taurine group ($P < 0.05$, Figures 7B–D).

Effects of taurine on the hippocampus of rats exposed to VOCs

The effects of taurine on VOCs-induced hippocampal neuron injury in rats were investigated by H&E and Nissl staining. Nissl staining showed that neurons in the hippocampus of control group (Figure 8A) were neatly arranged. In VOCs group (Figure 8B), nerve cells in the hippocampal area were scattered and stained slightly. After 0.5% and 1% taurine intervention (Figures 8C,D), the neurons showed

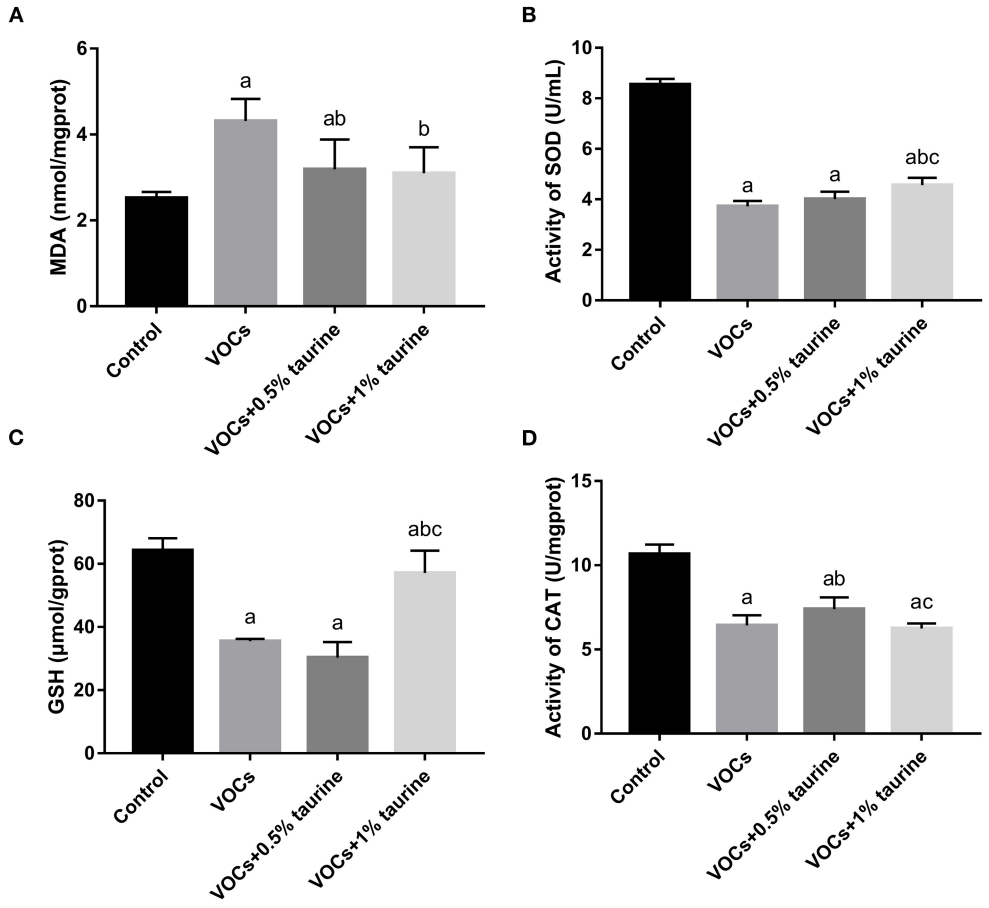

FIGURE 5
Effects of taurine on oxidative stress level in brain tissue of rats exposed to VOCs. **(A)** MDA content in brain tissue. **(B)** SOD activity in brain tissue. **(C)** GSH content in brain tissue. **(D)** CAT activity in brain tissue. Data are expressed as mean ± SD ($n = 6$). a: $P < 0.05$ vs. control group. b: $P < 0.05$ vs. VOCs group. c: $P < 0.05$ vs. VOCs+0.5% taurine group.

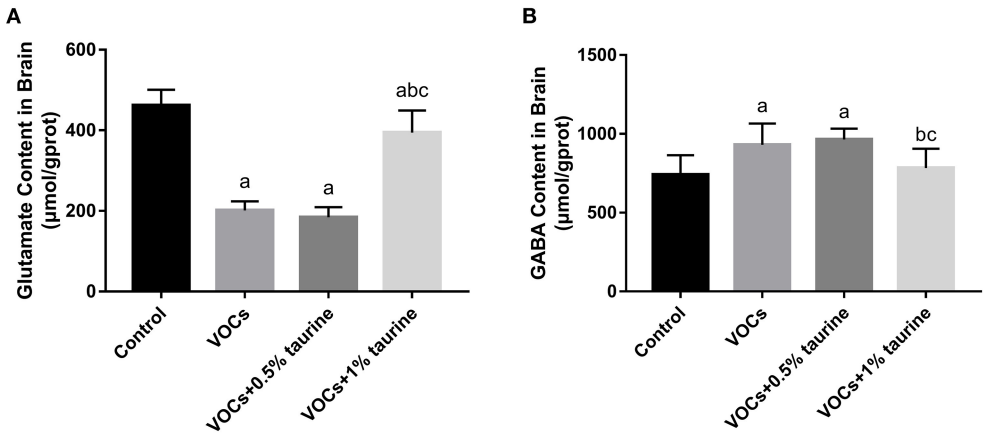

FIGURE 6
Effects of taurine on neurotransmitters in brain tissue of rats exposed to VOCs. **(A)** Glutamate content in brain tissue. **(B)** γ - aminobutyric acid content in brain tissue. Data are expressed as mean ± SD. ($n = 6$). a: $P < 0.05$ vs. control group. b: $P < 0.05$ vs. VOCs group. c: $P < 0.05$ vs. VOCs+0.5% taurine group.

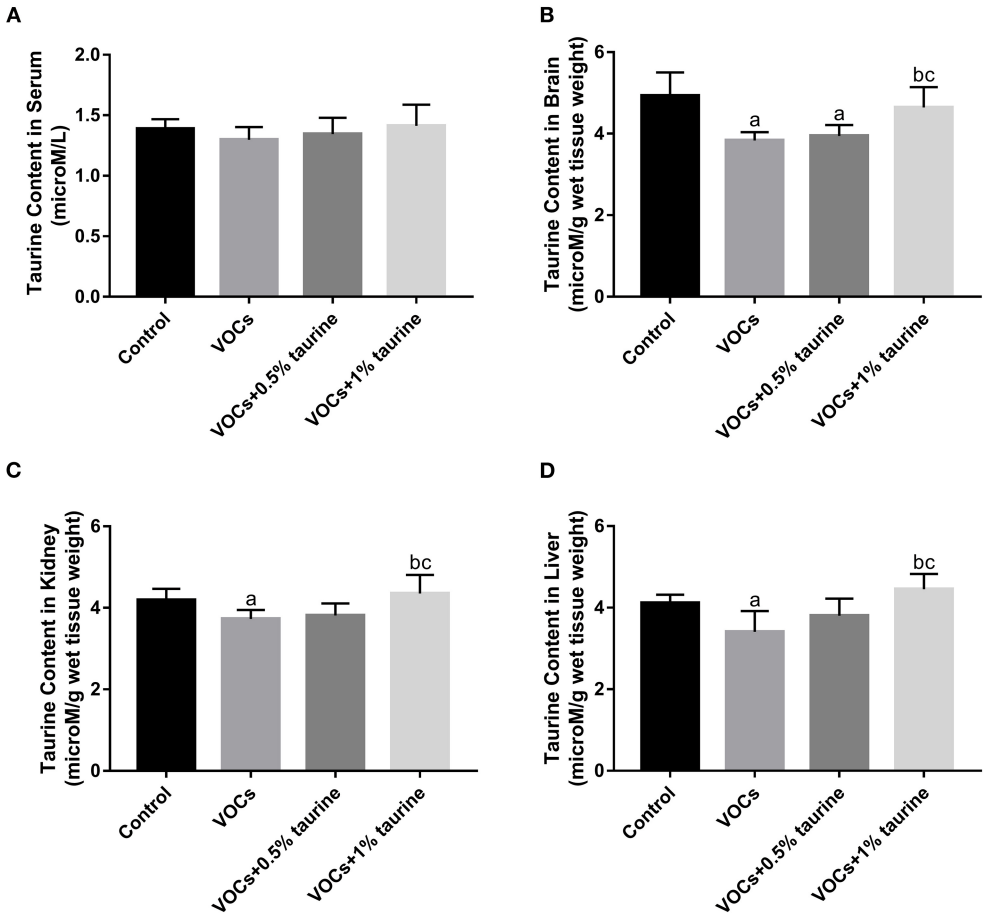

FIGURE 7
Changes of taurine content in the serum, brain, liver and kidney tissue of rats exposed to VOCs. **(A)** Taurine content in rat serum. **(B)** Taurine content in rat brain. **(C)** Taurine content in rat kidney. **(D)** Taurine content in rat liver. Data are expressed as mean ± SD. ($n = 6$). a: $P < 0.05$ vs. control group. b: $P < 0.05$ vs. VOCs group. c: $P < 0.05$ vs. VOCs+0.5% taurine group.

darker staining. H&E staining showed regular arrangement of cells in the hippocampus of rats in control group (Figure 8E). The number of neurons in the hippocampus of rats in VOCs group (Figure 8F) decreased and arranged irregularly. Taurine intervention improved hippocampal nerve injury in VOCs+0.5%taurine and VOCs+1%taurine groups (Figures 8G,H). Compared with VOCs group, the number of viable neurons in the hippocampal CA1 region of rats in VOCs+1%taurine group (Figure 8I) ($P < 0.05$) increased with regular arrangement.

Effects of taurine on BDNF and NMDAR1 protein expression in hippocampus of rats exposed to VOCs

The protein expressions of BDNF and NMDA receptor were evaluated using the western blotting technique to investigate the protective effects of taurine. Compared to the control group, BDNF expression was shown to be significantly lower in the VOCs group ($P < 0.05$, Figure 9). Treatment with 1% taurine significantly upregulated BDNF protein expression in VOCs-exposed rats ($P < 0.05$), while 0.5% taurine did not ($P > 0.05$, Figure 9B). The NMDAR1 protein expression level was found significantly decreased in VOCs and VOCs+0.5% taurine group ($P < 0.05$). Following 1% taurine treatment, there was a significant activation of NMDAR1 protein expression compared with the VOCs group ($P < 0.05$, Figure 9C).

Discussion

Taurine has antioxidant and neuroprotective properties (29, 30). Dietary supplementation of taurine has been recognized to improve neurological abnormalities and promote health in infants and children (31). It is particularly prevalent in the developing brain, where it regulates neural progenitor

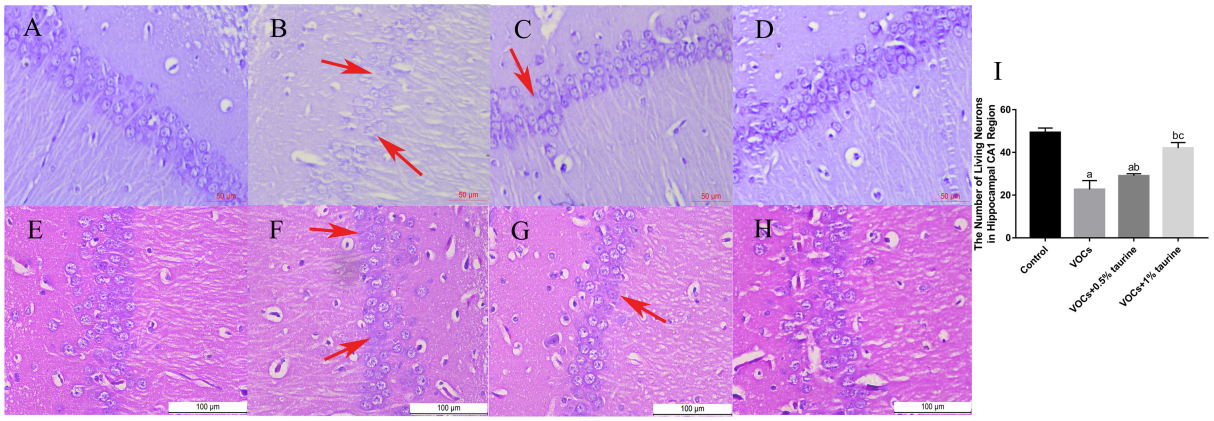

FIGURE 8
Effects of taurine on the hippocampus of rats exposed to VOCs. **(A)** control group (Nissl staining, ×400). **(B)** VOCs group (Nissl staining, ×400). **(C)** VOCs+0.5% taurine group (Nissl staining, ×400). **(D)** VOCs+1% taurine group (Nissl staining, ×400). **(E)** control group (H&E, ×400). **(F)** VOCs group (H&E, ×400). **(G)** VOCs+0.5% taurine group (H&E, ×400). **(H)** VOCs+1% taurine group (H&E, ×400). **(I)** The number of living neurons in hippocampal CA1 region. Data are expressed as mean ± SD. ($n = 3$). a: $P < 0.05$ vs. control group. b: $P < 0.05$ vs. VOCs group. c: $P < 0.05$ vs. VOCs+0.5% taurine group. The red arrow indicates damaged neuronal cells.

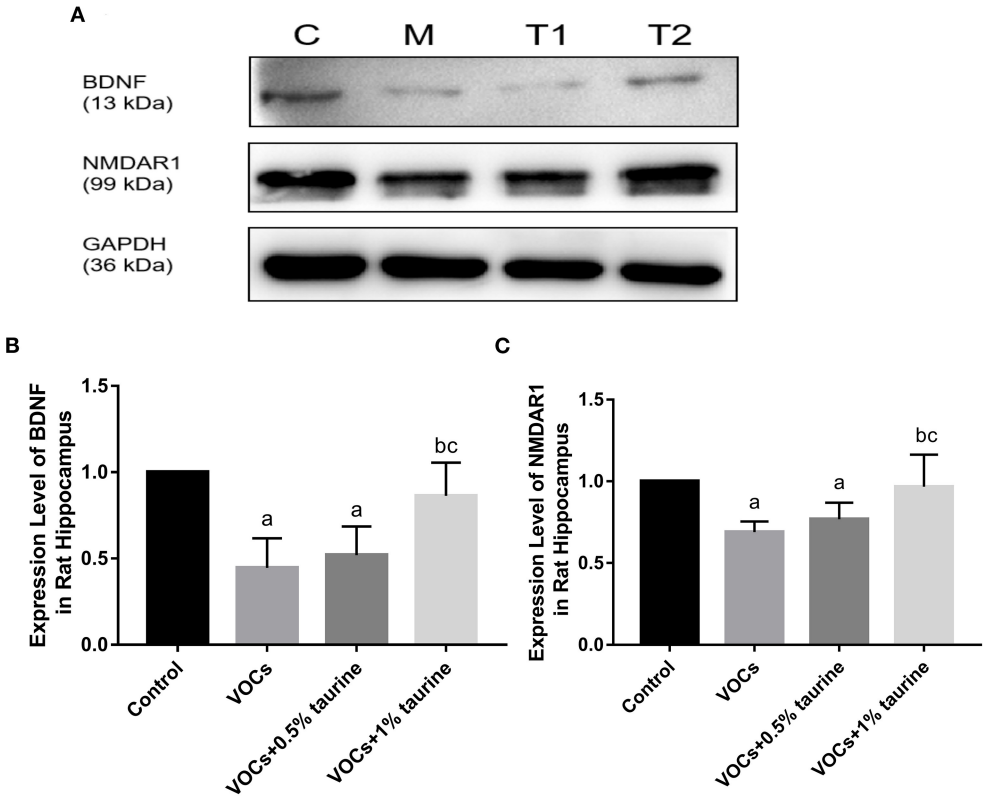

FIGURE 9
Effects of taurine on BDNF and NMDAR1 protein expression in hippocampus of rats exposed to VOCs. **(A)** Western blot analyses of BDNF and NMDAR1 proteins. GAPDH served as a loading control. **(B)** Western blots analysis showing the effect of taurine on BDNF protein expression level. **(C)** Western blots analysis showing the effect of taurine on NMDAR1 protein expression level. Data are expressed as mean ± SD. ($n = 3$). a: $P < 0.05$ vs. control group. b: $P < 0.05$ vs. VOCs group. c: $P < 0.05$ vs. VOCs+0.5% taurine group.

cell proliferation and synaptic formation throughout fetal and neonatal development (32). In this study, we used the formaldehyde, benzene, toluene, xylene mixture of liquid aerosols acting inhaled infected were cognitie impairment model is established, from the nerve behavior, nerve damage markers, oxidative stress and neurotransmitter protein expression etc. Comprehensive study of the taurine to improve the effectiveness of VOCs to her pups cognitie impairment. And we found that taurine protected against VOCs-induced cognitive-behavioral impairment in young rats through inhibiting oxidative stress and regulating neurotransmitter homeostasis. In addition, taurine were capable of restoring abilities of learning and memory in young rats exposed to VOCs by activating the NMDA receptor. This study confirmed the potential protective effect of taurine on VOCs-induced cognitive impairment in young rats, which is of great significance for taurine to improve children's intelligence and cognitive ability through dietary approach.

Animal body weight, food intake, and water consumption are all critical indicators of bodily system toxicity. The weight and food intake of rats in the model group dropped in varied degrees from 2 to 4 weeks after exposure, resulting in delayed weight gain, as compared to the blank control group. However, as compared to the blank control group, the 1% taurine intervention group's weight and food intake remained unchanged. We found that at week 4, the water intake of the 1% taurine intervention group was slightly higher than that of the control group. It was considered that the body could adjust its physiological function recovery by increasing the intake of taurine after exposure to VOCs and formaldehyde mixed inhalation.

Grasp control is closely related to the central nervous system, and is often used to study the neuromuscular function of rodents. Grasping change is an important evidence of motor neurotoxicity. Some scholars have found that subchronic low-dose VOCs exposure damages neuromuscular function in mice (12), which is consistent with our findings. In this experiment, the grasping force of rats in the model group was considerably lower than that of rats in the control group, showing that rats' neuromuscular function was harmed by subacute exposure to VOCs. However, the high-dose taurine intervention group and the control group had the same gripping force, indicating that a 1% taurine intervention can effectively restore the neuromuscular function loss caused by VOCs in rats. In our further study on spontaneous activity and the exploratory behavior, we found that activity time and distance of young rats in the model group were reduced to some extent compared with 1% taurine intervention group and control group. The results indicated that taurine could reverse spontaneous activity and exploration behavior in VOCs damaged rats, but the improvement effect was not significant. At present, a study conducted Morris water maze behavioral test on VOCs modeled animals and found that the escape latency of mice significantly increased and the residence time in the target quadrant decreased after acute or long-term inhalation of VOCs (12). The Morris Water Maze results of this study show that: Model group rats time find the platform, through the platform of the times, stay time in the target quadrant are lower than the control group, shows that VOCs subacute exposure affects the ability of learning and memory of rats, the water intake of taurine intervene and found that 1% taurine intervention group of rats and control rats trajectory is roughly same, can quickly find the platform position. In general, through the analysis of behavioral test results, taurine has a significant improvement effect on VOCs-induced cognitive behavioral damage in young rats.

Serum GFAP, MBP and NF-L are important biomarkers of nervous system injury, which are often used to determine the degree of nervous system injury. GFAP is an intermediate filament involved in astrocyte cytoskeleton construction and is also a central nervous expression protein (33). MBP is the main protein of myelin in central nervous system and is involved in myelin structural proteins (34). NF-L is mainly expressed in axon white matter and is the main component of cytoskeleton. Under normal physiological conditions, these three substances mainly exist in the central nervous system (35). When the nervous system is damaged, GFAP, MBP and NF-L can cross the blood-brain barrier and enter the blood, resulting in increased blood content. In this study, the levels of GFAP, MBP, and NF-L in the serum of rats in the VOCs model group were higher than in the control group, demonstrating that high-dose VOC exposure can cause nervous system injury in young rats. Meanwhile, we found that the abnormally elevated biomarkers of nerve damage in serum of rats in the 1% taurine intervention group could be restored to the normal level. However, the specific mechanism is unclear and needs further study. It has been reported that taurine has liver and kidney protective effects against the harmful effects of a variety of exogenous substances (36, 37). Meantime, VOCs may have toxicity not only in brain but in many other tissues, especially liver and kidney. Therefore, through further check general blood biochemical parameters, we found that the rats in the VOCs+1% taurine group showed significant recovery in serum AST, ALT, UREA and CREA compared with those in the VOCs model group, but not obvious by 0.5% taurine. We speculate that the effect of taurine in peripheral may partly contribute to the action of taurine against brain damage.

Taurine is a key modulator of homeostasis that has a number of roles in providing protection against oxidative stress. Taurine has been demonstrated to protect cultured cells, organs, and mammals from the harmful effects of oxidative stress caused by a wide range of chemicals, such as Arsenic, carbon tetrachloride, Nitrogen content, arsenide, Endosulfan, cisplatin, adriamycin, Streptozotocin, Bisphenol A, etc. Harmful consequences of oxidative stress (38, 39). According to *in vitro* and *in vivo* studies, taurine's neuroprotective potential is due to its antioxidant action in the brain (40). Studies on the

neuroprotective mechanism of taurine mainly focus on the activities of acetylcholinesterase and antioxidant enzyme, as well as scavenging oxygen-free radicals and enhancing antioxidant stress ability by preventing the increase of hydrogen peroxide and lipid peroxide levels in animal brain tissues caused by toxic and harmful substances (29, 41, 42). Therefore, we assessed the effect of taurine on VOCs-induced oxidative stress levels. The results found that exposure to MDA content in rats tissue levels of VOCs, endogenous antioxidant GSH content is reduced, this may be due to too many free radicals can't get the enzymes GSH antioxidant substances removal, cause lipid peroxidation, and thus the increase of lipid peroxidation products MDA, lipid peroxidation damage, Taurine treatment significantly prevented oxidative damage to the brain. Taurine was found to considerably reduce the lipid peroxidation damage caused by VOCs in this investigation. Taurine also enhanced the involvement of the antioxidant enzyme SOD in an attempt to combat VOCs-induced oxidative stress, but the effect was not obvious. In addition, histopathology showed that taurine significantly hindered the progression of brain tissue injury, and the effect was most obvious in the 1% taurine intervention group. This may be because the resistance of brain tissue to morphological injury is related to the restoration of antioxidant system.

Oxidative stress subsequently enhances proinflammatory factor release through activation of B cell activator (NF-κB pathway). Changes in the release of neurotransmitters such as Glutamate, neuropeptides, and growth factors are caused by high amounts of pro-inflammatory cytokines, resulting in neuroanxiety and depression (43). BDNF is an important neurotrophic factor that promotes neuronal development, differentiation, survival, and the creation of long-term memories. There is a large amount of evidence for the role of BDNF in the pathogenesis of behavioral disorders (44). It has been proved that by stimulating the PKA-CREB-BDNF signaling pathway *in vitro*, taurine can accelerate neural stem cell differentiation into neurons, raise the ratio of neurons to glial cells, and inhibit gliosis (45). The endocrine system and cerebral development are disrupted by hexabromocyclododecanes (HBCDs), which impairs cognitive function further. Taurine increases protein expression of BDNF and NGF, Significantly improved cognitive impairment caused by HBCDs in developing rats (46). This study also found that 1% taurine treatment can significantly improve VOCs-induced cognitive impairment in young rats by upregulating the protein expression of BDNF. In this VOCs model, we found that the endogenous taurine content in the brain, liver and kidney tissue were significantly reduced. Results showed that the taurine content in the brain, liver and kidney tissue was increased obviously after exogenous 1% taurine supplementation, and with the increase of taurine level, the taurine content in tissues increased in a dose-dependent effect. Therefore, it is believed that 1% taurine treatment may recover the change in taurine content in the brain, liver and kidney tissues and ameliorate the defects induced by VOCs, but not enough by 0.5%.

Central nervous system toxicity usually occurs in an imbalance between excitatory and inhibitory neurotransmitters. Neurotransmitters act as signaling molecules that carry signals from neurons to target cells and regulate a variety of biological processes and behaviors. Glu and GABA are typical neurotransmitters that are important for learning and memory (47). Past studies showed that a low Glu/GABA ratio can cause learning and memory problems (48, 49). The destruction of Glu and GABA balance may be an important pathway for impaired learning and memory (50). In this study, Glu content decreased and GABA content increased in rats brain tissue after VOCs exposure, suggesting that neurotransmitter homeostasis was disrupted and thus impaired learning and memory. Taurine significantly improved the VOCs-induced imbalance of Glu and GABA, suggesting that taurine could play a neuroprotective role by affecting the balance of Glu and GABA. The role of taurine in the central nervous system is largely determined by complex interactions in the Glu/GABA system and NMDA receptors (51). In vertebrate central nerves, ionic Glutamate receptors (iGluRs) are ligand-gated ion channels that mediate most excitatory neurotransmission. The key drivers of synaptic plasticity are NMDA receptors, which are major members of the iGluR family. They are commonly recognized as the main cellular matrix for learning and memory (52). NMDARl is a functional subunit of the NMDA receptor that is involved in synaptic plasticity, memory, and learning. Studies have shown that deletion of the NMDARl gene leads to deficits in social memory in CA3 pyramidal cells (53). Abnormal activation of extracellular NMDA receptor subunits may lead to elevated extracellular Glutamate levels and reduced reuptake, leading to neuronal damage (54). Studies have shown that short-term inhalation of high-dose VOCs mixtures affects learning and memory performance and expression of NMDA receptor subunits in mice (16). Taurine is a weak agonist of NMDA receptor (55). Taurine has been found to protect nervous system and cognitive function by activating GABAA receptors and NMDA receptors in animal models of lead poisoning (56). The expression of NMDAR1 protein in the hippocampus of rats in the VOCs group was shown to be lower in this study, which could be one of the fundamental mechanisms of VOCs affecting learning and memory. Taurine supplementation can considerably reduce the VOCs-induced reduction in NMDAR1 protein expression, improve rat learning and memory, and safeguard nervous system function.

Conclusion

In summary, this study demonstrated that 1% taurine treatment ameliorated cognitive impairment caused by VOCs in young rats. Taurine protects nerve injury by down-regulating

GFAP, MBP and NF-L levels in serum and up-regulating BDNF protein expression in brain tissue, thus improving neurobehavioral function. Further, taurine ameliorates lipid peroxidation damage in the nervous system by preventing the VOCs-induced elevation of MDA levels in rat brain tissue. In addition, taurine can restore learning and memory ability and neurological damage in young rats exposed to VOCs by regulating imbalance of Glu/GABA system and activating the NMDA receptor. This study demonstrates taurine as a potential novel drug for the treatment of cognitive behavioral disorders especially in children.

Data availability statement

The raw data supporting the conclusions of this article will be made available by the authors, without undue reservation.

Ethics statement

The animal study was reviewed and approved by Laboratory Animal Management and used Committee of the Institute for Hygiene of Ordnance Industry.

Author contributions

YG: Conceptualization, funding acquisition, methodology, and writing—original draft. CS: Supervision and writing and editing. TG: Methodology, data curation, and writing and editing. ZL: Investigation and formal analysis. ZY: Methodology and writing. HD and PF: Methodology. JG: Project administration. All authors contributed to the article and approved the submitted version.

Funding

This work was supported by grants from the Science and Technology Plan Project of Shaanxi Province (2021JQ-934).

Acknowledgments

The authors appreciate Dr. Xie Xuan (The Fourth Military Medical University) and Dr. Hu Lifang (Northwestern Polytechnical University) for their generous support on the polish of the paper.

Conflict of interest

The authors declare that the research was conducted in the absence of any commercial or financial relationships that could be construed as a potential conflict of interest.

Publisher's note

All claims expressed in this article are solely those of the authors and do not necessarily represent those of their affiliated organizations, or those of the publisher, the editors and the reviewers. Any product that may be evaluated in this article, or claim that may be made by its manufacturer, is not guaranteed or endorsed by the publisher.

References

1. Zhang Z-F, Zhang X, Zhang X, Liu L-Y, Li Y-F, Sun W. Indoor occurrence and health risk of formaldehyde, toluene, xylene and total volatile organic compounds derived from an extensive monitoring campaign in Harbin, a megacity of China. *Chemosphere.* (2020) 250:126324. doi: 10.1016/j.chemosphere.2020.126324

2. World Health Organization. *WHO Guidelines for Indoor Air quality: Selected Pollutants.* Copenhagen: WHO (2010).

3. Iarc Working Group On The Evaluation Of The Carcinogenic Risk Of Chemicals To Humans, Agenzia Internazionale Per La Ricerca Sul Cancro. *Chemical Agents and Related Occupations.* Lyon: International Agency For Research On Cancer (2012).

4. Tham KW. Indoor air quality and its effects on humans—A review of challenges and developments in the last 30 years. *Energy Build.* (2016) 130:637–50. doi: 10.1016/j.enbuild.2016.08.071

5. Chang T, Ren D, Shen Z, Huang Y, Sun J, Cao J, et al. Indoor air pollution levels in decorated residences and public places over Xi'an, China. *Aerosol Air Q Res.* (2017) 17:2197–205. doi: 10.4209/aaqr.2016.12.0542

6. Vardoulakis S, Giagloglou E, Steinle S, Davis A, Sleeuwenhoek A, Galea KS, et al. Indoor exposure to selected air pollutants in the home environment: a systematic review. *Int J Environ Res Public Health.* (2020) 17:e89772. doi: 10.3390/ijerph17238972

7. Ye W, Zhang X, Gao J, Cao G, Zhou X, Su X. Indoor air pollutants, ventilation rate determinants and potential control strategies in Chinese dwellings: A literature review. *Sci Total Environ.* (2017) 586:696–729. doi: 10.1016/j.scitotenv.2017.02.047

8. Liu X. Understanding semi-volatile organic compounds in indoor dust. *Indoor Built Environ.* (2022) 31:1420326X2110708. doi: 10.1177/1420326X211070859

9. Vardoulakis S, Kinney P. Grand challenges in sustainable cities and health. *Front Sustain Cities.* (2019) 1:e0007. doi: 10.3389/frsc.2019.00007

10. Bateson TF, Schwartz J. Children's response to air pollutants. *J Toxicol Environ Health Part A.* (2007) 71:238–43. doi: 10.1080/15287390701598234

11. Kilburn KH. Indoor. air effects after building renovation and in manufactured homes *Am J Med Sci.* (2000) 320:249–54. doi: 10.1016/S0002-9629(15)40835-3

12. Wang F, Li C, Liu W, Jin Y. Potential mechanisms of neurobehavioral disturbances in mice caused by sub-chronic exposure to low-dose VOCs. *Inhalation Toxicol.* (2014) 26:250–8. doi: 10.3109/08958378.2014.882447

13. Li F, Qin Y, Gong S, Zhang H, Ding S. Learning and memory impairment of mice caused by gaseous formaldehyde. *Environ Res.* (2020) 184:109318. doi: 10.1016/j.envres.2020.109318

14. Demir M, Cicek M, Eser N, Yoldaş A, Sisman T. Effects of acute toluene toxicity on different regions of rabbit brain. *Anal Cell Pathol.* (2017) 2017:1–6. doi: 10.1155/2017/2805370

15. Kum C, Sekkin S, Kiral F, Akar F. Effects of xylene and formaldehyde inhalations on renal oxidative stress and some serum biochemical parameters in rats. *Toxicol Indus Health.* (2007) 23:115–20. doi: 10.1177/0748233707078218

16. Yihe J, Chonglei L, Fan W, Wei L. Effects of exposure to VOCs on spatial learning and memory capacity and the expression of NMDA receptor in mice. *J Animal Vet Adv.* (2012) 11:3355–64. doi: 10.3923/javaa.2012.3355.3364

17. Maiti P, Singh SB, Muthuraju S, Veleri S, Ilavazhagan G. Hypobaric hypoxia damages the hippocampal pyramidal neurons in the rat brain. *Brain Res.* (2007) 1175:1–9. doi: 10.1016/j.brainres.2007.06.106

18. Ochoa-de la Paz L, Zenteno E, Gulias-Cañizo R, Quiroz-Mercado H. Taurine and GABA neurotransmitter receptors, a relationship with therapeutic potential? *Exp Rev Neurotherap.* (2019) 19:289–91. doi: 10.1080/14737175.2019.1593827

19. Murakami S. Role of taurine in the pathogenesis of obesity. *Mol Nutr Food Res.* (2015) 59:1353–63. doi: 10.1002/mnfr.201500067

20. Kumari N, Prentice H, Wu J-Y. Taurine and its neuroprotective role. *Adv Experi Med Biol.* (2013) 775:19–27. doi: 10.1007/978-1-4614-6130-2_2

21. Liu J, Wang H-W, Liu F, Wang X-F. Antenatal taurine improves neuronal regeneration in fetal rats with intrauterine growth restriction by inhibiting the Rho-ROCK signal pathway. *Metab Brain Dis.* (2014) 30:67–73. doi: 10.1007/s11011-014-9572-x

22. Jia N, Sun Q, Su Q, Dang S, Chen G. Taurine promotes cognitive function in prenatally stressed juvenile rats via activating the Akt-CREB-PGC1α pathway. *Redox Biol.* (2016) 10:179–90. doi: 10.1016/j.redox.2016.10.004

23. Suge R, Hosoe N, Furube M, Yamamoto T, Hirayama A, Hirano S, et al. Specific timing of taurine supplementation affects learning ability in mice. *Life Sci.* (2007) 81:1228–34. doi: 10.1016/j.lfs.2007.08.028

24. Wu P, Shi X, Luo M, Li K, Zhang M, Ma J, et al. Taurine inhibits neuron apoptosis in hippocampus of diabetic rats and high glucose exposed HT-22 cells via the NGF-Akt/Bad pathway. *Amino Acids.* (2019) 52:87–102. doi: 10.1007/s00726-019-02810-6

25. Wang F, Li C, Liu W, Jin Y. Effect of exposure to volatile organic compounds (VOCs) on airway inflammatory response in mice. *J Toxicol Sci.* (2012) 37:739–48. doi: 10.2131/jts.37.739

26. Oecd, Ocde. *Test No. 412: Subacute Inhalation Toxicity: 28-Day Study*. Oecd Publishing. (2018).

27. Kuniishi H, Ichisaka S, Yamamoto M, Ikubo N, Matsuda S, Futora E, et al. Early deprivation increases high-leaning behavior, a novel anxiety-like behavior, in the open field test in rats. *Neurosci Res.* (2017) 123:27–35. doi: 10.1016/j.neures.2017.04.012

28. Wang J, Yue B, Zhang X, Guo X, Sun Z, Niu R. Effect of exercise on microglial activation and transcriptome of hippocampus in fluorosis mice. *Sci Total Environ.* (2021) 760:143376. doi: 10.1016/j.scitotenv.2020.143376

29. Rossato RC, Granato AEC, Moraes CDG de O, Salles GN, Soares CP. Neuroprotective effects of taurine on SH-SY5Y cells under hydrocortisone induced stress. *Res Soc Dev.* (2021) 10:e55510918426. doi: 10.33448/rsd-v10i9.18426

30. Franscescon F, Müller TE, Bertoncello KT, Rosemberg DB. Neuroprotective role of taurine on MK-801-induced memory impairment and hyperlocomotion in zebrafish. *Neurochem Int.* (2020) 135:104710. doi: 10.1016/j.neuint.2020.104710

31. Wu G. Important roles of dietary taurine, creatine, carnosine, anserine and 4-hydroxyproline in human nutrition and health. *Amino Acids.* (2020) 52:329–60. doi: 10.1007/s00726-020-02823-6

32. Tochitani S. Functions of maternally-derived taurine in fetal and neonatal brain development. *Adv Experi Med Biol.* (2017) 1:17–25. doi: 10.1007/978-94-024-1079-2_2

33. Korley FK, Nikolian VC, Williams AM, Dennahy IS, Weykamp M, Alam HB. Valproic acid treatment decreases serum glial fibrillary acidic protein and neurofilament light chain levels in swine subjected to traumatic brain injury. *J Neurotrauma.* (2018) 35:1185–91. doi: 10.1089/neu.2017.5581

34. Agoston DV, Shutes-David A, Peskind ER. Biofluid biomarkers of traumatic brain injury. *Brain Injury.* (2017) 31:1195–203. doi: 10.1080/02699052.2017.1357836

35. Brureau A, Blanchard-Bregeon V, Pech C, Hamon S, Chaillou P, Guillemot J-C, et al. NF-L in cerebrospinal fluid and serum is a biomarker of neuronal damage in an inducible mouse model of neurodegeneration. *Neurobiol Dis.* (2017) 104:73–84. doi: 10.1016/j.nbd.2017.04.007

36. Jamshidzadeh A, Heidari R, Abasvali M, Zarei M, Ommati MM, Abdoli N, et al. Taurine treatment preserves brain and liver mitochondrial function in a rat model of fulminant hepatic failure and hyperammonemia. *Biomed Pharmacother.* (2017) 86:514–20. doi: 10.1016/j.biopha.2016.11.095

37. Junichi A, Schaffer SW, Takashi I. *Taurine 7*. New York, NY: Springer (2009).

38. Surai PF, Earle-Payne K, Kidd MT. Taurine as a natural antioxidant: from direct antioxidant effects to protective action in various toxicological models. *Antioxidants.* (2021) 10:1876. doi: 10.3390/antiox10121876

39. Baliou S, Adamaki M, Ioannou P, Pappa A, Panayiotidis M, Spandidos D, et al. Protective role of taurine against oxidative stress (Review). *Mol Med Rep.* (2021) 24:e12242. doi: 10.3892/mmr.2021.12242

40. Wu G-F, Ren S, Tang R-Y, Xu C, Zhou J-Q, Lin S-M, et al. Antidepressant effect of taurine in chronic unpredictable mild stress-induced depressive rats. *Sci Rep.* (2017) 7:4989. doi: 10.1038/s41598-017-05051-3

41. Adedara IA, Abolaji AO, Idris UF, Olabiyi BF, Onibiyo EM, Ojuade TD, et al. Neuroprotective influence of taurine on fluoride-induced biochemical and behavioral deficits in rats. *Chemico-Biol Interact.* (2017) 261:1–10. doi: 10.1016/j.cbi.2016.11.011

42. Zhou J, Li Y, Yan G, Bu Q, Lv L, Yang Y, et al. Protective role of taurine against morphine-induced neurotoxicity in C6 cells via inhibition of oxidative stress. *Neurotoxicity Res.* (2011) 20:334–42. doi: 10.1007/s12640-011-9247-x

43. Felger JC, Lotrich FE. Inflammatory cytokines in depression: Neurobiological mechanisms and therapeutic implications. *Neuroscience.* (2013) 246:199–229. doi: 10.1016/j.neuroscience.2013.04.060

44. Jangra A, Sriram CS, Dwivedi S, Gurjar SS, Hussain MI, Borah P, et al. Sodium phenylbutyrate and edaravone abrogate chronic restraint stress-induced behavioral deficits: implication of oxido-nitrosative, endoplasmic reticulum stress cascade, and neuroinflammation. *Cell Mol Neurobiol.* (2016) 37:65–81. doi: 10.1007/s10571-016-0344-5

45. Fang Q, Liu J, Chen L, Chen Q, Ke J, Zhang J, et al. Taurine improves the differentiation of neural stem cells in fetal rats with intrauterine growth restriction via activation of the PKA-CREB-BDNF signaling pathway. *Metabolic Brain Dis.* (2021) 36:969–81. doi: 10.1007/s11011-021-00672-0

46. Zhang X, Wang X, Zhang J, Pan X, Jiang J, Li Y. Effects of taurine on alterations of neurobehavior and neurodevelopment key proteins expression in infant rats by exposure to hexabromocyclododecane. *Adv Experi Med Biol.* (2017) 975:119–30. doi: 10.1007/978-94-024-1079-2_11

47. Wideman CE, Jardine KH, Winters BD. Involvement of classical neurotransmitter systems in memory reconsolidation: Focus on destabilization. *Neurobiol Learn Memory.* (2018) 156:68–79. doi: 10.1016/j.nlm.2018.11.001

48. Matsuyama S, Taniguchi T, Kadoyama K, Matsumoto A. Long-term potentiation-like facilitation through GABAA receptor blockade in the mouse dentate gyrus *in vivo*. *NeuroReport.* (2008) 19:1809–13. doi: 10.1097/WNR.0b013e328319ab94

49. Luo J, Min S, Wei K, Li P, Dong J, Liu Y. Propofol protects against impairment of learning-memory and imbalance of hippocampal Glu/GABA induced by electroconvulsive shock in depressed rats. *J Anesthesia.* (2011) 25:657–65. doi: 10.1007/s00540-011-1199-z

50. Zhang H, Kuang H, Luo Y, Liu S, Meng L, Pang Q, et al. Low-dose bisphenol A exposure impairs learning and memory ability with alterations of neuromorphology and neurotransmitters in rats. *Sci Total Environ.* (2019) 697:134036. doi: 10.1016/j.scitotenv.2019.134036

51. Schaffer S, Kim HW. Effects and mechanisms of taurine as a therapeutic agent. *Biomol Therap.* (2018) 26:225–41. doi: 10.4062/biomolther.2017.251

52. Stroebel D, Mony L, Paoletti P. Glycine agonism in ionotropic glutamate receptors. *Neuropharmacology.* (2021) 193:108631. doi: 10.1016/j.neuropharm.2021.108631

53. Chiang M-C, Huang AJY, Wintzer ME, Ohshima T, McHugh TJ. A role for CA3 in social recognition memory. *Behav Brain Res.* (2018) 354:22–30. doi: 10.1016/j.bbr.2018.01.019

54. Engin AB, Engin A. Nanoparticles and neurotoxicity: Dual response of glutamatergic receptors. *Nanoneuroprot Nanoneurotoxicol.* (2019) 245:281–303. doi: 10.1016/bs.pbr.2019.03.005

55. Chan CY, Sun HS, Shah SM, Agovic MS, Ho I, Friedman E, et al. Direct interaction of taurine with the NMDA glutamate receptor subtype via multiple mechanisms. *Adv Experi Med Biol.* (2013) 775:45–52. doi: 10.1007/978-1-4614-6130-2_4

56. Neuwirth LS, Volpe NP, Corwin C, Ng S, Madan N, Ferraro AM, et al. Taurine recovery of learning deficits induced by developmental Pb2+ exposure. *Adv Experi Med Biol.* (2017) 975:39–55. doi: 10.1007/978-94-024-1079-2_4

frontiers | Frontiers in Veterinary Science

TYPE Original Research
PUBLISHED 23 September 2022
DOI 10.3389/fvets.2022.1008497

Check for updates

OPEN ACCESS

EDITED BY
Abdul Rasheed Baloch,
University of Karachi, Pakistan

REVIEWED BY
Saqib Umer,
University of Agriculture,
Faisalabad, Pakistan
Kaiyuan Ji,
Anhui Agricultural University, China

*CORRESPONDENCE
Ying Yu
yuying@cau.edu.cn

†These authors have contributed equally to this work

SPECIALTY SECTION
This article was submitted to Livestock Genomics, a section of the journal Frontiers in Veterinary Science

RECEIVED 31 July 2022
ACCEPTED 26 August 2022
PUBLISHED 23 September 2022

CITATION
Khan MZ, Dari G, Khan A and Yu Y (2022) Genetic polymorphisms of *TRAPPC9* and *CD4* genes and their association with milk production and mastitis resistance phenotypic traits in Chinese Holstein.
Front. Vet. Sci. 9:1008497.
doi: 10.3389/fvets.2022.1008497

COPYRIGHT
© 2022 Khan, Dari, Khan and Yu. This is an open-access article distributed under the terms of the Creative Commons Attribution License (CC BY). The use, distribution or reproduction in other forums is permitted, provided the original author(s) and the copyright owner(s) are credited and that the original publication in this journal is cited, in accordance with accepted academic practice. No use, distribution or reproduction is permitted which does not comply with these terms.

Genetic polymorphisms of *TRAPPC9* and *CD4* genes and their association with milk production and mastitis resistance phenotypic traits in Chinese Holstein

Muhammad Zahoor Khan[1,2†], Gerile Dari[1†], Adnan Khan[3] and Ying Yu[1*]

[1]Key Laboratory of Animal Genetics, Breeding, and Reproduction, Ministry of Agriculture and National Engineering Laboratory for Animal Breeding, College of Animal Science and Technology, China Agricultural University, Beijing, China, [2]Faculty of Veterinary and Animal Sciences, Department of Animal Breeding and Genetics, The University of Agriculture, Dera Ismail Khan, Pakistan, [3]Genome Analysis Laboratory of the Ministry of Agriculture, Agricultural Genomics Institute at Shenzhen, Chinese Academy of Agricultural Sciences, Shenzhen, China

The present study was designed to evaluate the association of polymorphisms in bovine *trafficking protein particle complex subunit 9* (*TRAPPC9)* and *cluster of differentiation 4* (*CD4)* genes with milk production and mastitis resistance phenotypic traits in a different cattle population. Three single nucleotide polymorphisms (SNPs) (SNP1 Position: Chr14:2484891, SNP2 (rs110017379), SNP3 Position: Chr14:2525852) in bovine *TRAPPC9* and one SNP (Position: Chr5:104010752) in *CD4* were screened through Chinese Cow's SNPs Chip-I (CCSC-I) and genotyped in a population of 312 Chinese Holsteins (156: Mastitis, 156: Healthy). The results were analyzed using the general linear model in SAS 9.4. Our analysis revealed that milk protein percentage, somatic cell count (SCC), somatic cell score (SCS), serum cytokines interleukin 6 (IL-6) and interferon-gamma (IFN-γ) were significantly ($P < 0.05$) associated with at least one or more identified SNPs of *TRAPPC9* and *CD4* genes. Furthermore, the expression status of SNPs in CD4 and *TRAPPC9* genes were verified through RT-qPCR. The expression analysis showed that genotypes GG in SNP3 of *TRAPPC9* and TT genotype in SNP4 of *CD4* showed higher expression level compared to other genotypes. The GG genotype in SNP2 and TT genotype in SNP3 of *TRAPPC9* were associated with higher bovine milk SCC and lower IL6. Altogether, our findings suggested that the SNPs of *TRAPPC9* and *CD4* genes could be useful genetic markers in selection for milk protein improvement and mastitis resistance phenotypic traits in dairy cattle. The CCSC-I used in current study is proposed to be validate in different and large population of dairy cattle not only in China but also in other countries. Moreover, our analyses recommended that besides SCC and SCS, the association of genetic markers could also be considered with the serum cytokines (IL-6, IFN-γ) while selecting genetically mastitis resistance dairy cattle.

KEYWORDS

Chinese Holstein, milk protein, mastitis, SNP, CD4, *TRAPPC9*

Introduction

Bovine mastitis is the inflammation of udder tissues with a marked decrease in milk quantity and quality in dairy cattle (1, 2). Bovine mastitis is one of the most costly diseases affecting dairy cattle's health and welfare globally (3, 4). This disease caused around $2 billion in losses to the US dairy industry annually (5). Because of mammary gland inflammation, the polymorphonuclear leukocytes from blood rush toward the site and results in a marked increase in milk's somatic cells content (6).

The somatic cell count (SCC) and somatic cell score (SCS) are the key indicators for susceptibility and resistance of a cow to mastitis (7–10). Due to the positive genetic correlation (0.4–0.8) between mastitis and SCC or SCS (11, 12), the strategy to minimize the risk of this disease by selecting dairy cattle against higher SCS is a worthy approach. However, the SCC and SCS are not constant and are influenced by many environmental factors (13, 14); therefore, in current research, we targeted serum cytokines (IL-6 and IFN-γ) in combination with SCC and SCS as mastitis resistance phenotypic traits.

Cytokines have dual nature, i.e., either activate or repress the inflammatory response and thus play a vital role in mastitis development (15). In addition, the increased levels of IFN-γ, IL-6 and IL-17 have been documented in acute mastitis (16). Consistently, a study showed that the detection of IL-6 in milk indicated subclinical mastitis earlier than SCC (17). Although the mentioned phenotypic traits are good indicators of mastitis, however, due to low heritability, mastitis resistance will yet be a challenge for animal breeders (18). Therefore, the association of mastitis resistance phenotypic traits with a polymorphism in genes is the research of interest in the modern dairy industry for control of mastitis.

The researchers rely on a marker-assisted selection strategy for mastitis resistance (19, 20). The candidate gene approach, which takes in account of SNPs in the genes that are associated with these traits, is a widely used method to control mastitis (19). Being quantitative traits, mastitis and milk production traits are controlled by many genes (21). The *TRAPPC9* and *CD4* are the key genes that play an important role in developing innate immunity and milk production traits.

The *TRAPPC9* gene, residing on bovine chromosome 14 is the vital member of the nuclear factor kappa B (NF-κB) family which has an essential role in inflammation and innate immunity (22–24). The elevated level of *TRAPPC9* gene enhances the activity of NF-κB signaling during mastitis development in dairy cattle (22). The associations of polymorphisms in *CD4* and *TRAPPC9* genes with milk production and mastitis resistance traits have been documented in previous reports (2, 25–27). Similarly, our in our previous study by using transcriptomic screening, we reported that *TRAPPC9* gene was significantly associated with milk SCC and bovine mastitis susceptibility (28). Recently, a study have reported the association of *TRAPPC9* gene with milk fat and immunity in Ayrshire and Jersey dairy cattle (29). In addition, the increase in milk CD4+ T cells was documented to be correlated with non-specific mastitis which suggested their link with low bacterial shedding (30).

Keeping in view the importance of these two immunity-associated genes (*TRAPPC9, CD4*); we selected three polymorphisms (SNP1 Position: Chr14:2484891, SNP2 (rs110017379), SNP3 Position: Chr14:2525852) in bovine *TRAPPC9* and one SNP (Position: Chr5:104010752) in *CD4* from our previous studies and validate them in a new and large Chinese Holstein population. For this purpose, these SNPs in *TRAPPC9* and *CD4* genes were detected by a new technique, i.e., Chinese Cow's SNPs Chip-I (CCSC-I) and genotyped in a different and a bit larger Chinese Holsteins population to explore their association with mastitis resistance and milk production phenotypic traits.

Materials and methods

Ethical statement

All animal procedures were performed according to the regulation approved by the ethical committee of the College of Animal Science and Technology, China Agriculture University, Beijing, PR China [Permission number: DK996]. All the data was collected from China Agriculture University dairy farm and no consent was needed from farmers.

Sample size and collection

We randomly selected a total of 312 Chinese Holstein cows (156: Mastitis, 156: Healthy) in parities ranging 1–3 from a single dairy farm in Beijing China. In addition, based on SCC level, the cows were confirmed as mastatic (cattle with SCC higher than 200,000/ml) or healthy (cattle with SCC lower than 200,000/ml). The blood samples were collected from the caudal vein of all the selected population of Chinese Holsteins in 9 mL of 3 tubes including one each for DNA extraction (EDTA coated tube), RNA extraction, and serum isolation (non-EDTA tube). For serum isolation, the blood samples were placed at room temperature for 30 min to enable blood coagulation and then centrifuged at 3,000 rpm for 10 min to separate serum. The serum samples were stored at 4°C and sent to the Beijing Huaying Biological Technology Research Institute within 24 h to detect the concentration of IL-6 and IFN-γ. The milk SCC data were obtained from the Beijing Jinyindao Dairy Farm data record section, while SCS was calculated using the formula: SCS = log2 (SCC / 100,000) + 3.

DNA extraction, SNP identification and genotyping

Genomic DNA was isolated from blood samples of 312 Chinese Holstein using Tiangen Blood DNA Kit (Tiangen Biotech Co., China) following the manufacturer's instructions. The quantity and quality of DNA were measured using NanoDrop ND-2000c Spectrophotometer (Thermo Scientific, Chelmsford, MA, USA) and gel electrophoresis. After confirmation of quality and quantity, all the DNA samples were sent to Capital Bio Technology Co., Ltd, Beijing, China, for identification of SNPs and genotyping with Chinese Cow's SNPs Chip-I. The selected SNPs in *TRAPPC9* and *CD4* genes were genotyped in the different and bit large population of 312 Chinese Holstein.

RNA isolation and purification

Total RNA extraction from the Holstein cattle's white blood cells was carried out through the standard TRIzol method (Invitrogen, Carlsbad, CA, USA) following the manufacturer's protocols. RNase-Free DNase Set (QIAGEN) was used to purify RNA and to ensure genomic DNA elimination. The quantity and quality of RNA were measured by using a NanoDropTM ND-2000c Spectrophotometer (Thermo Scientific, Inc.), and the integrity of RNA was monitored on 1% agarose gel.

Reverse transcription and primer design

According to the manufacturer's instructions, reverse transcription was performed using PrimeScript 1st Strand cDNA Synthesis kit (TaKaRa, Dalian, China). The PCR primers for the bovine *CD4, TRAPPC9*, and a housekeeping gene *GAPDH* (glyceraldehyde-3-phosphate dehydrogenase) were designed by Primer-Blast on NCBI and synthesized by Beijing Genomics Institute Tech, based on the golden rules for real-time reverse transcription PCR (RT-PCR). The amplification efficiency of these primer pairs was tested by RT-qPCR initially, and the mRNA expression of the two genes was normalized against the housekeeping gene *GAPDH* by the cDNA in the corresponding samples. Three pairs of primers designed for *GAPDH, TRAPPC9,* and *CD4* are given in Table 1. For mRNA expression analysis, four samples for each SNP were run in triplicate.

TABLE 1 Detail of PCR primers of qRT-PCR used in the study.

Primers	Sequence of primers
CD4	F: 5'-CCACTGGGACCTGAGGTGTC-3'
	R: 5'-GCATCACCACACCAATTCA-3'
TRAPPC9	F: 5'-CTGCTCCGCTCGGTGAATGAC-3'
	R:5'- CGTTCTCTGCCTTGACTGTG-3'
GAPDH	F: 5'-CCCTGAGACAAGATGGTGAAG-3'
	R:5'-CATGTAGTGAAGGTCAATGAAG-3'

Gene expression analysis by RT-QPCR

Real-time quantitative polymerase chain reaction (RT-qPCR) was performed to determine *TRAPPC9* and *CD4* genes expression levels. The reactions were performed in a total volume of 20 μL containing 2 μL cDNA, 1 μL each primer, 10 μL SYBR Green Master Mix (Roche, Penzberg, Germany), 6 μL nuclease-free water using the following amplification condition: 94°C for 10 min, followed by 44 cycles of 94°C for 15 s, 60°C for 10 s, 72°C for 10 s, and 72°C for 30 s. Fluorescence signals were collected at 60°C step. Mean was consequential from the two repeats for each sample. Light Cycler 480 RT-PCR system was used to perform amplification, detection and data analyses.

Statistical analysis

The allele and genotype frequencies were tested for deviations from proportions of Hardy–Weinberg equilibrium (HWE) by using Chi-square test ($\chi 2$). The association analysis of SNPs in *TRAPPC9* and *CD4* with milk production and mastitis-related traits were carried out by the least-squares method as applied in the GLM procedure of SAS (SAS Institute Inc., Cary, NC, USA) according to the following linear model.

$$P_{ijkn=}\mu + f_{i+}p_{j+}snp_{k+}e_{ijkn}$$

where P_{ijkn} indicates mastitis traits (SCC, SCS or serum concentration of cytokine IL-6 and IFN-γ) or milk production traits (fat percentage or protein percentage), μ is overall mean, f_i is the fixed effect of the farm, p_j is the fixed effect of parity, snp_k is the fixed effect of genotype, e_{ijkn} is the random residual error.

The estimated genotype effects were further divided into additive effect (A) and dominant effect (D). The additive effect was the mean deviation of two homozygous genotypes (Formula 1), and the dominant influence was calculated by the deviation of the heterozygous genotype from the mean of two homozygous genotypes (Formula 2) (31).

$$A = (AA - BB)/2 \text{ (Formula 1)}$$

$$D = AB - (AA + BB)/2 \text{ (Formula 2)}$$

Where, AA, AB and BB were least square means of genotype AA, AB and BB, respectively.

Student *t*-test was performed for RT-qPCR analyses for the comparison of mRNA expression levels of different genotypes of SNPs in the two genes (*TRAPPC9* and *CD4*).

Results

The SNPs information, identification and genotyping

Three SNPs in *TRAPPC9* and one SNP from *CD4* gene were screened through CCSC-I (10) and genotyped in a total of 312 (156: Mastitis, 156: Healthy) Chinese Holstein population. It was found that except the SNP1, all SNPs' allele and genotypic frequencies were in Hardy–Weinberg equilibrium ($P > 0.05$). The observations, genotypic and allelic frequencies and values of Chi-square test (χ^2) of the selected SNPs in the present study are summarized in Table 2.

Association of mutations in TRAPPC9 and CD4 genes with milk production and mastitis resistance phenotypic traits

The association of three SNPs in *TRAPPC9* was evaluated with milk production and mastitis resistance traits. Our findings illustrated that SNP1 was significantly associated with milk protein, the SNP2 at position A/G 2607583 linked notably with SCS ($P < 0.05$), whereas the SNP3 (T/G 2525852) with SCC, SCS, and serum cytokine IL-6 ($P < 0.05$). Additionally, the association analysis revealed that the SNP in the *CD4* gene (104010752C/T) did not show any link with milk production traits, however, revealed a significant association with IFN-γ and IL-6 ($P < 0.05$). Finally, the association analysis showed that the genotypes GG in SNP3 and homozygous TT (SNP4) were significantly associated with low SCC, SCS and a higher level of IL-6 (Table 3). Similarly, the analyses revealed that genotypes TT (SNP3) and CC (SNP4) were associated with low IL-6 and high SCC level, which make the dairy cattle more vulnerable to the mastitis development.

Additive and dominant effect of polymorphism in *TRAPPC9* and CD4 genes on milk production and mastitis resistance phenotypic traits

The additive and dominant effect of SNPs in *CD4* and *TRAPPC9* genes are summarized in Table 4. The current association analysis for the additive and dominant effect of polymorphisms (SNP1, SNP2, SNP3and SNP4) revealed that dominant effect of SNP1 is significantly ($P < 0.05$) associated with milk protein, whereas SNP3 showed a significant additive effect on SCC, SCS and IL-6 ($P < 0.05$). Similarly, the additive effect of SNP2 was significantly associated with SCS and the SNP4 in *CD4* was correlated with IFN-γ and IL-6 ($P < 0.05$) (Table 4).

The MRNA relative expression assays of genotypes of SNPs in *TRAPPC9* and CD4 genes

The expression level of mutations in the *TRAPPC9* and *CD4* genes was measured by real-time quantitative PCR. The analysis showed that the relative mRNA expression of AA genotype in SNP2 had higher expression compared to GG and AG genotypes in the *TRAPPC9* gene. Similarly, the GG genotype in SNP3 in *TRAPPC9* demonstrated significantly higher expression than TG genotype in the given Chinese Holsteins dairy cattle population (Figure 1A, $P < 0.05$). Moreover, the genotype TT's mRNA expression level was comparatively higher than CC and CT genotypes in the SNP4 of *CD4* gene (Figure 1B).

Discussion

Recently, single nucleotide polymorphisms in many genes have been found to be associated with milk production and mastitis resistance traits suggesting that these variants could be used as potential genetic markers in modern breeding schemes for the improvement of production and increasing resistance to mastitis. In the present study, the polymorphisms in *TRAPPC9* and *CD4* genes that cause variation in the economic and health traits (milk production and mastitis resistance phenotypic traits) were selected from our previous studies and analyzed for validation in a new and larger population by using CCSC-I. To our knowledge, this is the first study in which we practically applied CCSC-I in mastitis resistance research. Bovine SNP Chip's application was previously used by Mullen and his co-workers in 2013 for dairy and beef production research (32). Similarly, a research study has also reported that SNP Chip is a cost and time-effective approach for implementing genomic selection in livestock (33). Keeping in view the importance of the SNP Chip from various published studies we used this technique in the present study to validate the role of the significant variants from our previous studies in *CD4* and *TRAPPC9* genes for production and mastitis resistance traits. Our research team reported in previous studies that SNPs at position 2484891 C/T, 2525852 T/G and 2607583 A/G in *TRAPPC9* were associated with milk protein and fat percentages (34). In contrast, polymorphism at position 2525852 T/G (*TRAPPC9*) did not show any link with milk contents (35). Furthermore, the mutation (2607583 A/G) was noticed to be associated with SCS, while the SNPs at position 2484891 C/T, and 2525852 T/G were linked to IL-6 and IFN-γ, respectively, however no correlation of 2607583 A/G in *TRAPPC9* gene was found with SCC, SCS and serum cytokines (IL-6 and IFN-γ) (36). In comparison, we found that the SNP (2484891 C/T) was linked to protein percentage, whereas the polymorphisms 2525852 T/G and 2607583 A/G were associated with IL-6,

TABLE 2 The information of single nucleotide polymorphisms and their Allelic and genotypic frequencies in *TRAPPC9* and *CD4* genes.

SNP (Gene)	Mutation	Reference	Position	Genotypes	Allelic frequency	Genotypic frequency
SNP1	C-T/Exon2	Novel	Chr14:2484891	CC(303)	0.974277	C(0.98)
(TRAPPC9)				CT(3)	0.009646	T(0.02)
				TC(5)	0.016077	
SNP2	A/G	rs110017379	Chr14: 2607583	AA(122)	0.391026	A(0.62)
(TRAPPC9)				AG(144)	0.461538	G(0.38)
				GG (46)	0.147436	
SNP3	T-G/Intron6	Novel	Chr14:2525852	TT(64)	0.205128	T(0.46)
(TRAPPC9)				TG(158)	0.50641	G(0.54)
				GG(90)	0.288462	
SNP4	C/T Promoter	Novel	Chr5:104010752	CC(148)	0.48	C(0.70)
(CD4)				CT(141)	0.45	T(0.30)
				TT(23)	0.07	

TABLE 3 Association of SNPs in *TRAPPC9* and *CD4* genes on SCC, SCS, milk production, and serum cytokines traits in Chinese Holsteins.

SNP	Genotype	Fat (%)	Protein (%)	IL-6	IFN-γ	SCC	SCS
SNP1	CC(303)	4.09 ± 0.05	2.93 ± 0.15	67.19 ± 1.43	96.43 ± 1.12	330.98 ± 39.93	2.60 ± 0.15
(*TRAPPC9*)	CT(3)	4.43 ± 0.53	3.82 ± 0.18	57.58 ± 16.83	107.23 ± 13.22	40.66 ± 400.05	1.69 ± 1.46
	TC(5)	4.44 ± 0.41	2.91 ± 0.15	77.18 ± 11.90	100.71 ± 9.35	162.2 ± 309.87	2.80 ± 1.13
	P-value	0.57	**< 0.0001*****	0.59	0.65	0.67	0.81
SNP2	AA(122)	4.08 ± 0.08	3.05 ± 0.03	70.03 ± 2.23	95.28 ± 1.75	219.87 ± 62.23	2.08 ± 0.23
(*TRAPPC9*)	AG(144)	4.12 ± 0.07	3.06 ± 0.02	65.62 ± 2.08	98.65 ± 1.64	375.36 ± 57.68	2.87 ± 0.21
	GG (46)	4.08 ± 0.13	3.04 ± 0.05	64.70 ± 2.66	94.21 ± 2.88	444.8 ± 101.34	3.05 ± 0.37
	P-value	0.89	0.87	0.26	0.24	0.08	**0.01****
SNP3	TT(64)	4.16 ± 0.12	3.04 ± 0.04	65.08 ± 3.09	96.78 ± 2.44	515.68 ± 85.52	2.91 ± 0.31
(*TRAPPC9*)	TG(158)	4.14 ± 0.07	3.08 ± 0.03	64.85 ± 1.96	97.88 ± 1.55	316.07 ± 54.50	2.83 ± 0.20
	GG(90)	4.99 ± 0.10	3.03 ± 0.04	72.96 ± 2.59	94.43 ± 2.05	201.79 ± 74.52	1.92 ± 0.26
	P-value	0.41	0.48	**0.03****	0.41	**0.02****	**0.01****
SNP4	CC(148)	4.07 ± 0.08	3.07 ± 0.03	63.14 ± 2.01	98.33 ± 1.59	294.85 ± 56.97	2.79 ± 0.21
(*CD4*)	CT(141)	4.12 ± 0.08	3.03 ± 0.03	68.64 ± 2.02	96.53 ± 1.62	376.8 ± 58.98	2.51 ± 0.21
	TT(23)	4.19 ± 0.19	3.15 ± 0.02	85.32 ± 5.17	86.18 ± 4.14	195.26 ± 144.03	1.75 ± 0.52
	P-value	0.82	0.23	**0.0003*****	**0.02****	0.39	0.17

P-value is the significance level from analyses of the association of SNPs with milk production, SCC, SCS, and serum cytokines traits in Chinese Holsteins (***$P < 0.001$; **$P < 0.01$; *$P < 0.05$).

SCS, SCC, and SCS, respectively. Moreover, the mutation at point C104010752T was significantly correlated to milk SCC in Chinese Holsteins (26) and mutation at point g.13598C>T was linked to milk yield, protein and SCS (27). Importantly, in the new dairy population, our results further revealed the noteworthy correlation of SNP (C104010752T) with IL-6 and IFN-γ instead of SCC and SCS ($P < 0.05$). Based on our current findings, we reported that the SNPs in *TRAPPC9* and *CD4* genes show pleiotropic ability; however, it is also possible that the documented polymorphisms in the current study and our previous research might be influenced by population size and environmental factors.

Within an SNP, allele combinations and genotypes exert a critical role in the regulation of any traits. In the current study, we found that the homozygous GG genotype in SNP3 (*TRAPPC9*) and TT genotype in SNP4 (*CD4*) were associated with a higher level of IL-6 and a low level of SCC. These findings suggested that the mentioned genotypes (GG and TT) are linked with mastitis resistance and should be considered as potential markers while selecting genetically mastitis resistance cattle. Finally, the primary functional validation of SNPs in *TRAPPC9* and *CD4* genes were verified through RT-qPCR. Similar trends for all the genotypes in SNPs (*TRAPPC9* and *CD4*) that were found for their association with serum cytokines and mastitis

TABLE 4 Genetic effect of SNPs in *TRAPPC9* and *CD4* genes on milk production, mastitis resistance and serum cytokine traits in Chinese Holstein.

SNPs	Effect	Fat %	Protein %	IL-6	IFN-γ	SCC	SCS
SNP1	A	−0.18 ± 0.21	0.07 ± 0.07	−4.99 ± 5.99	−2.14 ± 4.71	84.39 ± 156.21	−0.09 ± 0.57
	P-value	0.39	0.35	0.41	0.64	0.58	0.86
	D	0.16 ± 0.56	1.15 ± 0.20	−14.61 ± 17.87	8.67 ± 14.03	−205.92 ± 429.46	−1.009 ± 1.57
	P-value	0.78	**<0.0001*****	0.41	0.53	0.68	0.52
SNP2	A	0.00 ± 0.08	0.003 ± 0.03	2.66 ± 2.14	0.54 ± 1.69	−112.45 ± 59.45	−0.48 ± 0.22
	P-value	0.99	0.91	0.21	0.75	0.06	**0.02****
	D	0.04 ± 0.11	0.02 ± 0.04	−1.74 ± 2.99	3.91 ± 2.35	46.83 ± 82.83	0.30 ± 0.30
	P-value	0.66	0.61	0.56	0.99	0.61	0.32
SNP3	A	0.08 ± 0.08	0.01 ± 0.03	−3.94 ± 2.01	1.17 ± 1.59	156.95 ± 56.06	0.50 ± 0.20
	P-value	0.26	0.86	**0.05***	0.46	**0.005*****	**0.02****
	D	0.07 ± 0.10	0.05 ± 0.04	−4.17 ± 2.81	2.29 ± 2.22	−42.66 ± 78.26	0.42 ± 0.29
	P-value	0.53	0.25	0.13	0.31	0.58	0.14
SNP4	A	−0.06 ± 0.10	−0.04 ± 0.04	−11.08 ± 2.77	6.07 ± 2.21	49.79 ± 77.44	0.52 ± 0.28
	P-value	0.58	0.31	**<0.0001*****	**0.006*****	0.52	0.06
	D	−0.01 ± 0.13	−0.082 ± 0.048	−5.59 ± 3.43	4.27 ± 2.75	131.74 ± 96.98	0.25 ± 0.35
	P-value	0.92	0.08	0.104	0.12	0.17	0.49

A means additive effect, D means dominant effect, single asterisk (*) shows that the additive and dominance effect of the locus is significant ($P < 0.05$), while ***$P < 0.001$ and **$P < 0.01$ demonstrate that the additive and dominance effect of the locus is highly significant.

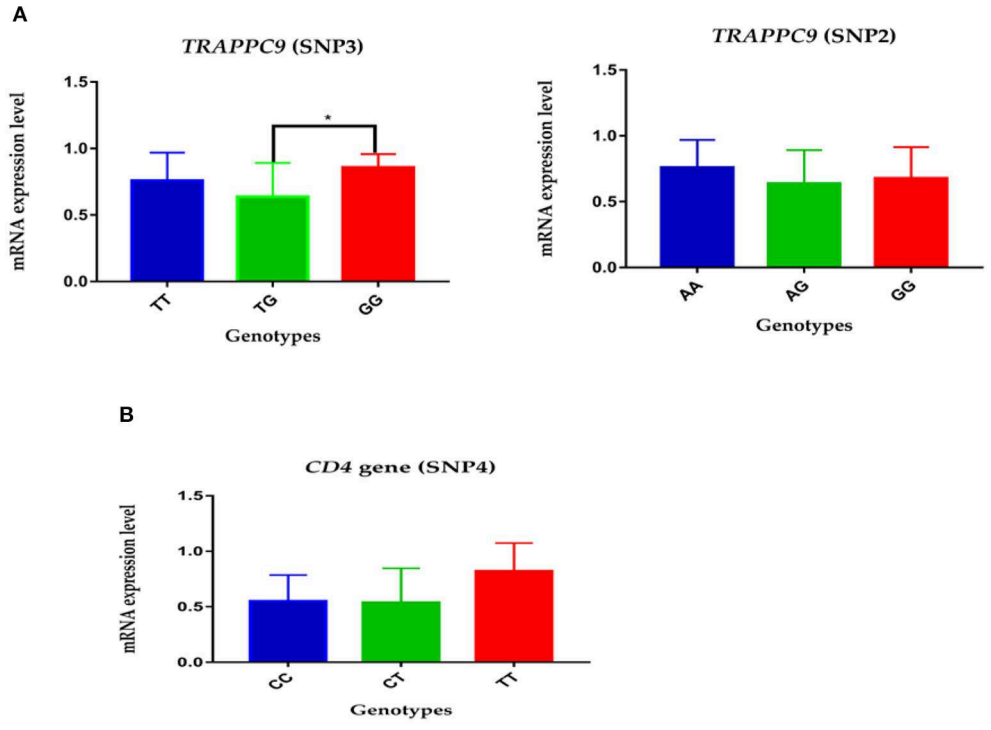

FIGURE 1
The relative mRNA expression level of polymorphisms in *TRAPPC9* and *CD4* gene: **(A)** The expression level of genotypes in SNP2 and SNP3 of *TRAPPC9:* the GG genotype show significantly higher relative mRNA expression than TG in SNP3; however, no significant difference was reported among the three genotypes of SNP2. **(B)** The relative genotypes expression of SNP4 in *CD4* gene: the TT genotype showed comparatively higher relative mRNA expression than CT and CC.

resistance phenotypic traits were also reported in expression analysis. In relation to the association of the genetic variants to the specific mastitis resistance phenotypic trait and the level of significance documented in our previous studies, there were some differences in the present study's findings and in the previous studies, which still need further validation in large and different population of Chinese Holsteins.

In general, the present study using a newly designed CCSC-I for genotyping to validate the association of SNPs in *TRAPPC9* and *CD4* genes with milk production and mastitis resistance traits. Although we reported the significant link of the selected SNPs in *TRAPPC9* and *CD4* genes milk production and mastitis resistance phenotypic traits, however, we recommend further in-depth studies to test the documented reported SNPs of *TRAPPC9* and *CD4* in a large Chinese Holstein population as well as in other different dairy breeds from various regions of the world by using our newly designed CCSC-I for the validation of its capability to improve milk production and mastitis resistance in dairy cattle.

Conclusions

Overall, the present study validated the three SNPs of *TRAPPC9* and *one* SNP of *CD4* in a large and different Chinese Holstein population by using our newly designed CCSC-I. The results verify that the documented SNPs in both genes (*TRAPPC9* and *CD4)* could be considered as powerful genetic markers against bovine mastitis resistance. The targeted SNPs in the *TRAPPC9* gene might be used as a marker for improved milk protein percentage as well. The study proposed that the CCSC-I could also be validated in more large dairy cattle population not only in China but also in other countries across the globe. Additionally, the upshot of a study infers that not only SCS and SCC but IL-6 and IFN-γ association can be establish with genetic markers while selecting genetically mastitis resistance dairy cattle.

Data availability statement

The original contributions presented in the study are included in the article/supplementary material, further inquiries can be directed to the corresponding author/s.

Ethics statement

The animal study was reviewed and approved by the Ethical Committee of the College of Animal Science and Technology, China Agriculture University, Beijing, PR China [Permission number: DK996].

Author contributions

Conceptualization and methodology: MK and YY. Validation: MK. Resources: MK and GD. Writing—original draft preparation: MK. Writing—review and editing: MK, AK, YY, and GD. Supervision: YY. All authors have read and agreed to the published version of the manuscript.

Funding

This article was financially supported by the National Key R&D Program of China (2021YFD1200900, 2021YFD1200903), NSFC-PSF Joint Project (31961143009), Beijing Dairy Industry Innovation Team (BAIC06), China Agriculture Research System of MOF and MARA, Beijing Natural Science Foundation (6182021), and the Program for Changjiang Scholar and Innovation Research Team in University (IRT-15R62).The funders had no role in study design, data collection, and analysis, decision to publish, or preparation of the manuscript.

Conflict of interest

The authors declare that the research was conducted in the absence of any commercial or financial relationships that could be construed as a potential conflict of interest.

Publisher's note

All claims expressed in this article are solely those of the authors and do not necessarily represent those of their affiliated organizations, or those of the publisher, the editors and the reviewers. Any product that may be evaluated in this article, or claim that may be made by its manufacturer, is not guaranteed or endorsed by the publisher.

References

1. Gomes, F, Henriques M. Control of bovine mastitis: old and recent therapeutic approaches. *Curr Microbiol.* (2016) 72:377–82. doi: 10.1007/s00284-015-0958-8

2. Usman T, Ying Y, Zhai L, Chao L, Wang X, Wang Y. Association of CD4 SNPs with a fat percentage of Holstein cattle. *Genet Mol Res.* (2016) 15:gmr.15038697. doi: 10.4238/gmr.15038697

3. Rainard P, Cunha P, Gilbert FB. Innate and adaptive immunity synergize to trigger inflammation in the mammary gland. *PLoS ONE.* (2016) 11:e0154172. doi: 10.1371/journal.pone.0154172

4. Whelehan JC, Meade GK, Eckersall DP, Young, JF, O'Farrelly C. Experimental *Staphylococcus aureus* infection of the mammary gland induce region-specific changes in innate immune gene expression. *Vet Immunol Immunopathol.* (2011) 140:181–9. doi: 10.1016/j.vetimm.2010.11.013

5. Sordillo LM, Streicher KL. Mammary gland immunity and mastitis susceptibility. *J Mammary Gland Biol Neoplasia.* (2002) 7:135–46. doi: 10.1023/A:1020347818725

6. Lafi SQ. Use of somatic cell counts and California Mastitis Test results from udder halves milk samples to detect subclinical intramammary infection in Awassi sheep. *Small Ruminant Res.* (2006) 62:83–6. doi: 10.1016/j.smallrumres.2005.07.035

7. Usman, T, Yachun W, Chao, L, Wang X. Association study of single nucleotide polymorphisms in JAK2 and STAT5B genes and their differential mRNA expression with mastitis susceptibility in Chinese Holstein cattle. *Animal Genet.* (2015) 46:371–380. doi: 10.1111/age.12306

8. Gernand E, König S. Random regression test-day model for clinical mastitis: genetic parameters, model comparison, and correlations with indicator traits. *J Dairy Sci.* (2014) 97:3953–63. doi: 10.3168/jds.2013-7830

9. Wang X, Zhong J, Gao Y, Ju Z, Huang J. A SNP in intron 8 of CD46 causes a novel transcript associated with mastitis in Holsteins. *BMC Genomics.* (2014) 15:630. doi: 10.1186/1471-2164-15-630

10. Khan M, Wang D, Liu L, Usman T, Wen H, Zhang R, et al. Significant genetic effects of JAK2 and DGAT1 mutations on milk fat content and mastitis resistance in Holsteins. *J Dairy Res.* (2019) 86:388–93. doi: 10.1017/S0022029919000682

11. Hu HC, Wang HM, Li JB, Wang CF, Lai SJ, Li LQ, et al. Genetic polymorphism of the Nramp1 gene and correlation with mastitis in Holstein cattle. *Yi Chuan.* (2009) 31:57–62. doi: 10.3724/SP.J.1005.2009.00057

12. Rupp R, Bergonier D, Dion S, Hygonenq CM, Aurel RM, Christèle R, et al. Response to somatic cell count-based selection for mastitis resistance in a divergent selection experiment sheep. *J Dairy Sci.* (2009) 92:1203–19. doi: 10.3168/jds.2008-1435

13. Van G, Green LE, Guzmán D, Esparza H, Tadich N. Risk factors for bulk *milk somatic cell counts* and total bacterial *counts* in smallholder dairy farms in the 10th region of Chile. *Prevent Vet Med.* (2005) 67:1–17. doi: 10.1016/j.prevetmed.2004.10.002

14. Reyes J, Sanchez J, Stryhn H, Ortiz T, Olivera M, Keefe GP. *Influence* of milking method, disinfection and herd management practices on bulk tank *milk somatic cell counts* in tropical dairy herds in Colombia. *Vet J.* (2017) 220:34–39. doi: 10.1016/j.tvjl.2016.12.011

15. Bonifati C, Ameglio F. Cytokines in psoriasis. *Int J Dermatol.* (1999) 38:241–51. doi: 10.1046/j.1365-4362.1999.00622.x

16. Sakemi Y, Tamura Y, Hagiwara K. Interleukin-6 in quarter milk as a further prediction marker for bovine subclinical mastitis. *J Dairy Sci.* (2011) 78:118–21. doi: 10.1017/S0022029910000828

17. Fontanesi L, Calo DG, Galimberti G., Negrini R., Marino R., Nardone A., et al., Russo V. A candidate gene association study for nine economically important traits in Italian Holstein cattle. *Animal Genet.* (2014) 45:576–80. doi: 10.1111/age.12164

18. Hinchs D, Bennewitz J, Stamer E, Junge W, Kalm E, Thaller G. Genetic analysis of mastitis data with different models. *J Dairy Sci.* (2011) 94:471–8. doi: 10.3168/jds.2010-3374

19. Wiggans GR, Vanraden PM, Cooper TA. The genomic evaluation system in the United States: past, present, future. *J Dairy Sci.* (2011) 94:3202–11. doi: 10.3168/jds.2010-3866

20. García-Ruiz A, Cole JB, VanRaden PM, Wiggans GR, Ruiz-López FJ, Van CP. Changes in genetic selection differentials and generation intervals in US Holstein dairy cattle as a result of genomic selection. *Proc Natl Acad Sci* **US***A.* (2016) 113:E3995–4004. doi: 10.1073/pnas.1519061113

21. Sender G, Agnieszka K, Adrianna P, Karima G, Jolanta O. Genetic basis of mastitis resistance in dairy cattle –a review. *Annals of Animal Science.* (2013) 13:663– 673. doi: 10.2478/aoas-2013-0043

22. Khan MZ, Khan A, Xiao J, Ma J, Ma Y, Chen T, et al. Z. Overview of research development on the role of NF-κB signaling in mastitis. *Animals*. (2020) 10:1625. doi: 10.3390/ani10091625

23. Denis-Donini S, Dellarole A, Crociara P, Maria TF, Valeria B, Giorgia Q, et al. Impaired adult neurogenesis associated with short-term memory defects in NF-kappaB p50-deficient mice. *J Neurosci.* (2008) 28:3911–9. doi: 10.1523/JNEUROSCI.0148-08.2008

24. Oeckinghaus A, Matthew SH, Sankar G. Crosstalk in NF-kappaB signaling pathways. *Nat Immunol.* (2011) 12:695–708. doi: 10.1038/ni.2065

25. Wang X, Ma P, Liu J, Zhang Q, Zhang Y, Ding X, et al. Genome-wide association study in Chinese Holstein cows reveals two candidate genes for somatic cell score as an indicator for mastitis susceptibility. *BMC Genetics.* (2015) 16:16–111. doi: 10.1186/s12863-015-0263-3

26. Usman T, Yachun W, Minyan S, Xiao W., Yichun D, Chao L, et al. Novel polymorphisms in bovine CD4 and LAG-3 genes associated with somatic cell counts of clinical mastitis cows. *Genetics Mol Res.* (2017) 16:gmr16039859. doi: 10.4238/gmr16039859

27. He Y, Qin C, Peipei M, Yachun W, Qin Z, Dongxiao S, et al. Association of bovine CD4 and STAT5b single nucleotide polymorphisms with somatic cell scores and milk production traits in Chinese Holsteins. *J Dairy Res.* (2011) 78:242–9. doi: 10.1017/S0022029911000148

28. Wang D, Liu L, Augustino S, Duan T, Hall TJ, MacHugh DE, et al. Identification of novel molecular markers of mastitis caused by *Staphylococcus aureus* using gene expression profiling in two consecutive generations of Chinese Holstein dairy cattle. *J Animal Sci Biotechnol.* (2020) 11:1–17. doi: 10.1186/s40104-020-00494-7

29. Freitas PHF, Oliveira HR, Silva FF, Fleming A, Schenkel FS, Miglior LF, et al. Time-dependent genetic parameters and single-step genome-wide association analyses for predicted milk fatty acid composition in Ayrshire and Jersey dairy cattle. *J Dairy Sci.* (2020) 103:5263–9. doi: 10.3168/jds.2019-17820

30. Souza FN, Blagitz MG, Batista CF, Takano PV. Immune response in nonspecific mastitis: What can it tell us? *J Dairy Sci.* (2020) 103:5376–86. doi: 10.3168/jds.2019-17022

31. Falconer DS, Mackay TFC. *Introduction to Quantitative Genetics (4th ed.)*. Longman. (1995).

32. Mullen PM, McClure CM, Kearney FJ, Waters MS, Weld R, Flynn P, et al. Development of a custom SNP chip for dairy and beef cattle breeding, parentage and research. *Interbull Bulletin.* (2013) 47:23–25.

33. Berry DP, McClure MC, Mullen MP. Within- and across-breed imputation of high-density genotypes in dairy and beef cattle from medium- and low-density genotypes. *J Animal Breed Genet.* (2013) 131:165–72. doi: 10.1111/jbg.12067

34. Feng W, Dong Y, Xiao W, Liu C, Wang X, Wang Y, et al. The genetic effect of TRAPPC9 on mastitis resistance to *S. aureus* in dairy cows. *Acta Veterin Zootecn Sina*. (2016) 47:276–83. https://www.cabdirect.org/cabdirect/abstract/20163110701

35. Dong Y, Liu C, Xiao W, Wang Y, Zhang Y, Sun D, et al. Confirming the genetic effect of Bovine TRAPPC9 on milk production traits based on Post-GWAS strategies. *Acta Veterin Zootecn Sina*. (2015) 46:60–8. https://www.cabdirect.org/cabdirect/abstract/20153108958

36. Dong, Y, Yu Y. *Genetic Effect Analysis and Preliminary Confirmation of Anti-Mastitis Related Gene TRAPPC9*. Thesis submitted to China Agricultural University, Beijing, China (2014).

frontiers | Frontiers in Veterinary Science

TYPE Original Research
PUBLISHED 14 October 2022
DOI 10.3389/fvets.2022.1036495

Check for updates

OPEN ACCESS

EDITED BY
Abdul Rasheed Baloch,
University of Karachi, Pakistan

REVIEWED BY
Effrosyni Fatira,
University of Las Palmas de Gran Canaria, Spain
Xiaoge Yang,
Anqing Normal University, China

*CORRESPONDENCE
Xuan Xie
xiexuan1991@hotmail.com

SPECIALTY SECTION
This article was submitted to Livestock Genomics, a section of the journal Frontiers in Veterinary Science

RECEIVED 04 September 2022
ACCEPTED 26 September 2022
PUBLISHED 14 October 2022

CITATION
Xie X, Franěk R, Pšenička M, Chen F and Kašpar V (2022) Optimization of *in vitro* culture conditions of common carp germ cells for purpose of surrogate production. *Front. Vet. Sci.* 9:1036495. doi: 10.3389/fvets.2022.1036495

COPYRIGHT
© 2022 Xie, Franěk, Pšenička, Chen and Kašpar. This is an open-access article distributed under the terms of the Creative Commons Attribution License (CC BY). The use, distribution or reproduction in other forums is permitted, provided the original author(s) and the copyright owner(s) are credited and that the original publication in this journal is cited, in accordance with accepted academic practice. No use, distribution or reproduction is permitted which does not comply with these terms.

Optimization of *in vitro* culture conditions of common carp germ cells for purpose of surrogate production

Xuan Xie[1,2]*, Roman Franěk[2,3], Martin Pšenička[2], Fan Chen[4] and Vojtech Kašpar[2]

[1]Department of Gynecology & Obstetrics, Xijing Hospital of Airforce Military Medical University, Xi'an, China, [2]Research Institute of Fish Culture and Hydrobiology, South Bohemian Research Center of Aquaculture and Biodiversity of Hydrocenoses, Faculty of Fisheries and Protection of Waters, University of South Bohemia in Ceské Budějovice, Ceské Budějovice, Czechia, [3]Department of Genetics, The Silberman Institute, The Hebrew University of Jerusalem, Jerusalem, Israel, [4]Department of Neurosurgery, Tangdu Hospital of Fourth Military Medical University, Xi'an, China

Common carp (*Cyprinus carpio*) is the fourth most-produced fish species in aquaculture and frequently used model species with significant effort invested in development of biotechnological applications. In present study, we attempted to establish an *in vitro* germ cell culture condition for short term cell culture, which could facilitate further applications such as surrogacy or gene manipulation. Basal media and different types of feeder cells were investigated to optimize carp germ cell culture condition to favor maintenance of mitotic proliferation. Results indicated that germ cells cultured with hESC media and RTG2 cell line as feeder possessed significantly higher proliferation and survival rate compared to that cultured with StemPro media and Sertoli cell line as feeder. In addition, we compared two dissection strategies to compare risk of cell culture contamination and body cavity was open from dorsal part or from ventral part. As a result, carp open from the dorsal side can minimize the risk of contamination. In summary, this is the first study to optimize the cultivation of germ cells in common carp. This opens up new opportunities for the application of specific techniques in the breeding of those species with high commercial value and frequent use as a model fish. Results obtained in this study are important for implementation of new strategies in common carp breeding, conservation of genetic resources, restoration of lines or development of clonal and isogenic carp lines.

KEYWORDS

common carp, germ cell, germ cell culture, Sertoli cell, feeder cell

Introduction

Common carp (*Cyprinus carpio*) is the fourth most cultured fish species in aquaculture, with production reaching 4,411,900 metric tons in 2019 (FAO Fisheries Statistics). This species is reared both in Europe and Asia, with significant effort invested in establishing breeding programs (1–3) or programs for conservation of

genetic resources (4, 5). Genetic resource preservation resulted in development of *in vitro* conservation strategies for sperm (6, 7), germ cells (8), and development of surrogate production technology (9). Common carp is not only a species of commercial interest, but popular model species as recognized by OECD guidelines. Although cryopreservation protocols have been established to provide ways for restoration of developed breeds, utilization of cryopreserved milt has not reached commercial levels for production and breeding programs. Unfortunately, ovarian follicles have been damaged after cryopreservation (10, 11). Thus, surrogate production based on transplantation of carp germ cells into the body cavity of goldfish (*Carassius auratus*) shows promising results, providing a possibility for conservation of the female lineage.

Fish germ cells have the unique ability to self-renew as well as to differentiate into other germ cell stages. Both type A spermatogonia and oogonia show high sexual plasticity even after maturation of the donor (12). This specific attribute allows them to be used for biotechnological applications, specific breeding strategies, or to support the conservation of genetic resources (13). Germ cells cultured *in vitro* can be transplanted when populations are declining, or when limited numbers of germ cells are obtained from suitable or available donors. As well, this technology is available when stem cell purification shows low efficacy, or when cells are damaged by enzymatic dissociation. In recent years, *in vitro* culture of germ cells was established for some model species, including zebrafish (*Danio rerio*) (14), medaka (*Oryzias latipes*) (15), rainbow trout (*Oncorhynchus mykiss*) (16), or sturgeon *spp*. (*Acipenser spp.*) (17). Therefore, in present study, we aimed to establish *in vitro* culture conditions of carp germ cells using different types of culture medium and to investigate whether feeder cells are essential for carp germ cell proliferation.

Materials and methods

Animal ethics statement

Experiments were conducted at the Genetic Fisheries Center, Faculty of Fisheries and Protection of Waters (FFPW) in Vodnany, Czech Republic. The facility is authorized to perform the described manipulations and to perform experiments on animals (Act no. 246/1992 Coll., ref. number 16OZ19179/2016–17214). The methodological protocol of the current study was approved by the expert committee of the Institutional Animal Care and Use Committee of the FFPW, according to the law on the protection of animals against cruelty (reference number: MSMT-6406/119/2). The study did not involve endangered or protected species. Authors of the study hold certificates of professional competence for designing experiments and experimental projects under Section 15d (3) of Act no. 246/1992 Coll. on the Protection of Animals against Cruelty.

Fish disinfection and dissection

Common carp used for present study were cultivated at the Faculty of Fisheries and Protection of Waters, University of South Bohemia. Gonads were collected from 6 to 9 month old carp (length ranged from 15 to 20 cm and total weight ranged from 0.15 to 0.20 kg). Carp were anesthetized by 0.05% 3-aminobenzoic acid ethyl ester methanesulfonate-222 (MS-222, Sigma, USA) until no gill movements where observed and there was no response to a tail pinch. Fish were bleed by cutting the gills and then the whole body was disinfected with 70% ethanol for 1 min and briefly dried on a paper towel. Based on previous germ cell transplantation studies, and to avoid contamination, we opened the fishes body cavity from the dorsal and ventral side, respectively. In brief, carp were cut from the dorsal side with a longitudinal cut using sterile scalpels and forceps, and the body cavity was open from dorsal side. On the other hand, we cut fish along belly from ventral side, exposed abdominal cavity and remove gut. In total, 30 carp were dissected by each of these methods. Gonads were gently collected by forceps. Each gonad was washed twice with phosphate-buffered saline (PBS; Gibco) containing 50 μg/mL ampicillin, 200 U/mL penicillin, 20 μg/mL streptomycin (all from Sigma-Aldrich, pH 8.0) in petri dishes.

Testicular cell preparation

Dissociation of carp testicular cells was performed according to Xie et al. (17). Gonads were washed in PBS and minced into ∼1 mm^3 aliquots. Next, pieces of tissue were dissociated by 0.25% trypsin (Gibco) with 0.05% fetal bovine serum (FBS) and 40 U/mL DNase I (Sigma-Aldrich) in PBS at 24 °C for 2 h. The digestion was stopped by L-15 medium supplemented with 20% (v/v) fetal bovine serum (FBS), filtered through a 40 μm pore-size nylon screen and centrifuged at 300 g. The cell pellet was resuspended in PBS.

Germ cell enrichment and culture condition optimization

After digestion, spermatozoa were eliminated by Ficoll-Paque PLUS density gradient media (GE Healthcare). Gradient separation was performed by centrifugation at 500 g for 30 min at room temperature. Enriched cells were seeded in a 6-well plate at a concentration of 1,200 cells/mm^2. Cells were cultured at 21°C without CO_2. After 4–5 days of culture, germ cells were enriched by differential plating and re-seeded on feeder cells at a

TABLE 1 Components of cell culture medium.

Components	Medium	
Basal media	hESC	Stempro-34
Fetal bovine serum (10%)	+	+
Bovine serum albumin (2.50%)	+	+
2-mercaptoethanol (55 μm)	+	+
Basic fibroblast growth factor (bFGF, 10 ng/mL)	+	+
Glial cell line-derived neurotrophic factor (GDNF, 25 ng/mL)	+	+
leukemia inhibitory factor (LIF, 25 ng/mL)	+	+
Ascorbic acid (50 μm)	+	+
Chemically defined lipid concentrate (0.10%)	+	+
hESC supplement (2%)	+	+
Carp serum (1%)	+	+
non-essential amino acids (NEAA, 1%)	+	+
B-27 (1x)	+	+
Penicillin (50 μg/mL)	+	+
Ampicillin (50 μg/mL)	+	+
Streptomycin (50 μg/mL)	+	+

concentration of 800 cells/mm^2 in a 48-well plate. Components of culture medium are showed in Table 1. To remove somatic cells and to enrich germ cells, differential plating was performed for every passage.

Feeder cell preparation

In present study, RTG-2 and sertoli cell line were utilized as feeder cells. RTG-2 was purchased from ATCC (Summit Pharmaceuticals International, Tokyo, Japan) and maintained according to the instructions, while the sertoli cell line was derived from rainbow trout and maintained >50 passages (18). To use these cell lines as feeder cells for germ cell culture, proliferation activity was inhibited by treatment with 10 μg/mL mitomycin C for 6 h and cells were seeded onto 0.1% gelatin-coated plates at a concentration of 1200 cells/mm^2 in a 48-well plate.

Germ cell proliferation assay

To detect germ cell proliferation, a EdU incorporation assay was performed by adding 10 μM EdU (Sigma-Aldrich, USA) to the culture medium during the final 24 h of culture. EdU staining and 4,6-diamidino-2- phenylindole (DAPI) staining were performed with EdU Cell Proliferation Kit for Imaging (BCK-EdU647, baseclick, Germany) according to kit instructions. Then the cells were incubated 1 h at room temperature with DDX4 (vasa) rabbit polyclonal antibody (dilution 1:300, final concentration 1.8 μg/mL, GTX116575, GeneTex) and exposed for 1 h with secondary antibody anti-rabbit IgG–fluorescein isothiocyanate (FITC; F0382, Sigma, dilution 1:50) followed by staining with DAPI (3 ng/mL). The ratios of vasa-EdU-positive cells/total cells were calculated. Cell proliferation assays with EdU were performed at 7, 14, 21, and 28 days of culture at 21°C.

Histology

The maturational stage of each testis was determined using histological techniques. Testicular tissue from donor common carp was fixed overnight in Bouin's fixative and processed for paraffin sectioning and stained with Masson trichrome stain. Histological sections were photographed using a microscope with mounted camera (Olympus BX61).

Statistical analyses

The results were expressed as a ratio against control as mean ± SEM. Significance was determined with two-way analysis of variance (ANOVA) followed by Tukey's tests. Alpha was set at 0.05.

Results

Dissection of donor carp specimens

In present study, two dissection strategies were applied to avoid contamination of common carp gonads and 30 individuals were dissected in each group (Figure 1). Results showed that 24 out of 30 fish were contaminated when the body cavity was approached from ventral side. However, when the body cavity was open from the dorsal side, only 2 out of 30 fish showed signs of contamination.

Optimalization of basal culture condition of carp germ cells

According to histological observation, testes contained type A spermatogonia, type B spermatogonia, spermatocytes, and few developing spermatids (Figure 1). We identified an optimal culture medium for carp germ cells by comparing two different basal culture media. Enriched carp germ cells were cultured in two different types of medium (Table 1) and the number of germ cells were monitored on after 7, 14, 21, and 28 days of incubation. Two-way ANOVA, using quantity of germ cells as the dependent variable, and media and feeder cells as main effects, revealed significant variation ($p < 0.001$) in

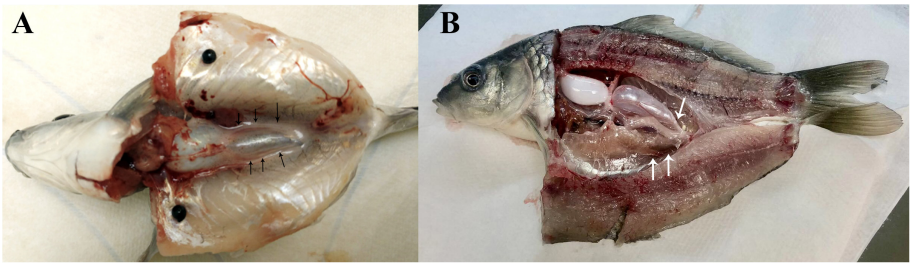

FIGURE 1
Common carp dissection illustration. **(A)** Carp dissected from ventral side. **(B)** Carp dissected from dorsal part. Gonads are indicated by arrowheads.

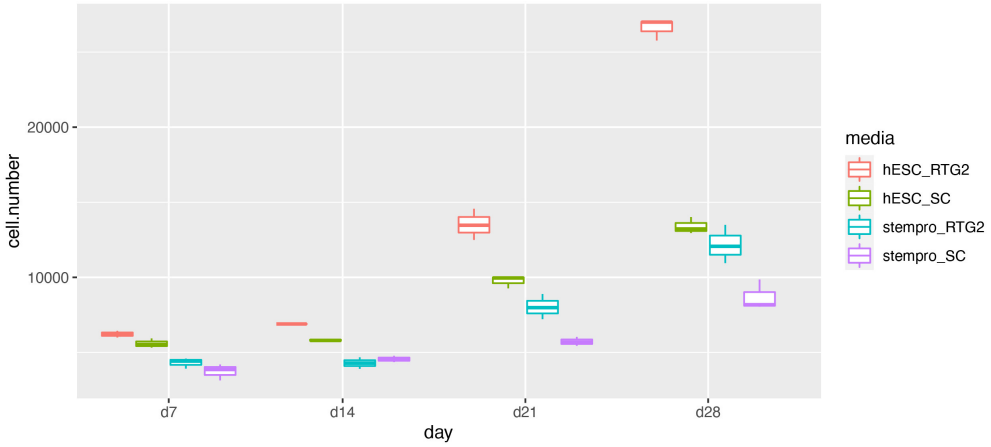

FIGURE 2
Effects of somatic cells on mitotic activity of common carp germ cells. The figure shows mean ± SEM ($n = 3$) of total germ cell number under hESC and stempro media with RTG2 and Sertoli cell line (SC). Cell number was count on days 7, 14, 21 and 28 of culture. Data are shown as the mean ± SEM ($n = 3$).

the proliferation of germ cells for both factors (Figure 2). In addition, there was a significant interaction between media and feeder cell types ($P = 0.049 < 0.05$). For groups with hESC and StemPro media, significantly greater proliferation was shown in those cultured with hESC media. The most significant increase of germ cells was observed with hESC culture medium and RTG2 feeder. Germ cell propagation was observed throughout the 28 day test period. Cells cultured with RTG2 formed clumps and expanded, whereas cells lost their shape and turned apoptotic when cultured with Sertoli cells (Figure 3A).

In this study, we also assessed whether Sertoli and RTG2 cell lines could serve as feeder cells to improve germ cell proliferation. After 2 weeks, newborn cells cultured with the RTG2 cell line were detected through EdU assays, indicating that cells cultured with the RTG2 cell line had better proliferation activity (Figure 3B). After 2 months, we still could observe germ cell clumps according to vasa antibody immunocytochemistry (Figure 3C).

Discussion

The gut of common carp carries symbiotic bacteria. Thus, removing gut contents during germ cell processing may release bacteria into the body cavity, which can contaminate germ cell cultures (19). To address this issue, we have compared two methods to dissect and open the body cavity of common carp. Our results revealed that dissection of fish from the dorsal part enabled us to avoid contamination.

A combination of internal and extrinsic mechanisms control fish germ stem cell survival, self-renewal, and differentiation (20–22). Somatic cells, particularly sertoli cells, assist in germ cell development and provide growth factors that positively affect germ cell proliferation and destiny. Germ cells

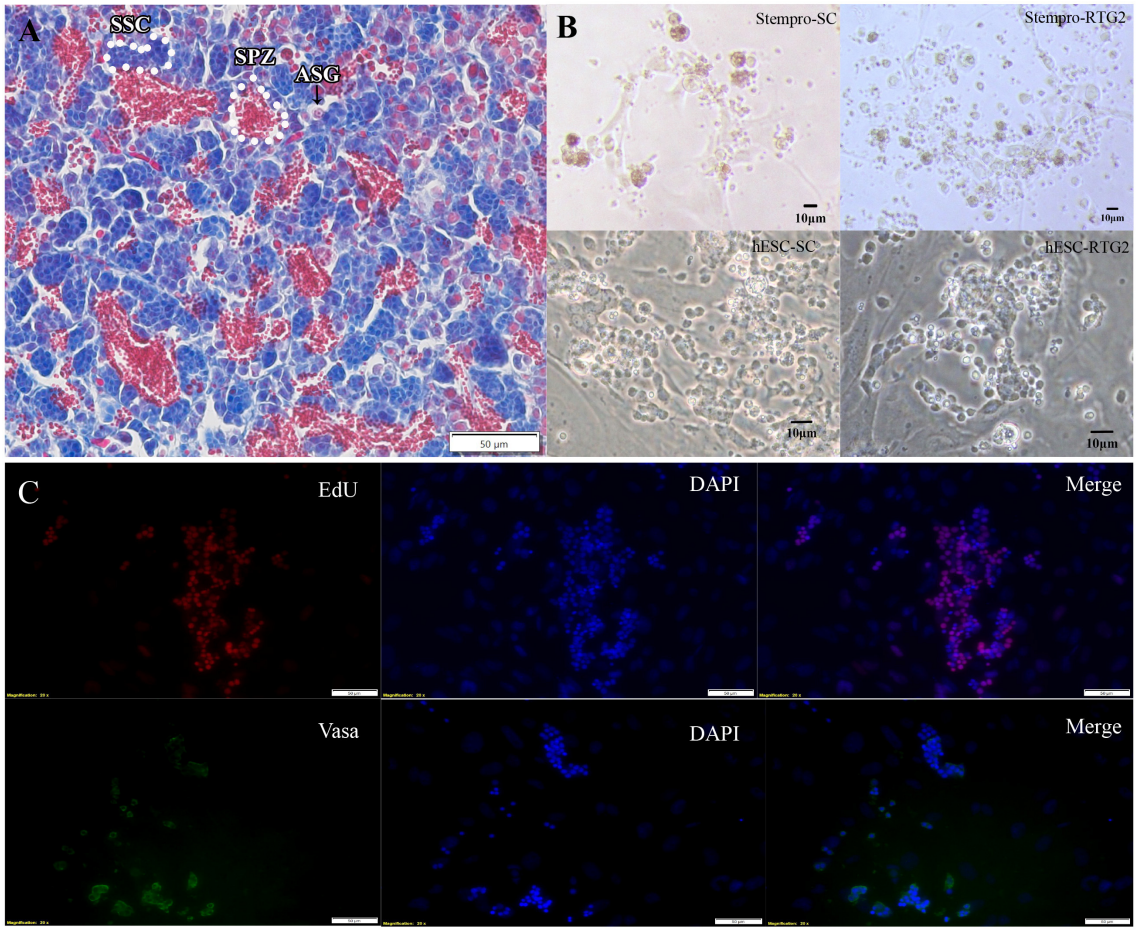

FIGURE 3
(A) Histological observation of common carp gonads. Various germ cell populations are indicated by arrowhead or white broken lines. **(B)** Morphology of cells cultured under different condition. **(C)** Immunocytochemistry of cultured cells at day 14. hESC-SC, hESC medium with Sertoli cells; hESC-RTG2, hESC medium with RTG2 cells; stempro-SC, stempro medium with Sertoli cells; stempro-RTG2, stempro medium with RTG2 cells. Less differentiated germ cells are blue, more differentiated are red, some spermatozoa are in the lumens already.

are capable of autonomously controlling the differentiation pattern. For germ stem cell proliferation and differentiation, as well to start meiosis, gonadal somatic cells must produce growth factors (23, 24). Therefore, in present study, we investigated whether RTG2 and Sertoli cell lines can work as feeder cells to support germ cell proliferation. Our results indicated that in comparison with Sertoli cells, RTG2 could significantly improve carp germ cell growth. In addition, it turned out that germ cells performed better proliferation rate when it cultured with hESC media than stempro- 34 media. Applications of hESC were also reported in germ cell culture of human (25) and rainbow trout (18). It probably indicated that compared with stempro- 34 media, stempro hESC media are more capable of domestication of germ cells.

During fish spermatogenesis, germ cell survival and development depend on constant close contact with Sertoli cells (26). Sertoli cell are involved in the regulation of spermatogonial stem cell self-renewal and differentiation by secreting growth factors. In zebrafish, Igf3 is expressed in Sertoli cells and promotes differentiation and proliferation by activating β-catenin signaling in the germ cells. Amh, a member of the TGF-β (transforming growth factor-beta) superfamily produced by Sertoli cells, exerts an inhibitory role on spermatogonial self-renewal and germ cell differentiation in the zebrafish testes. In addition, GDNF has been proven in many fishes produced by Sertoli cells plays an important role in SSC self-renewal (27).

Interestingly, when RTG2 was used as feeder cells they could promote more germ cell propagation than Sertoli cells. Especially during the later stages of culture, the growth rate

of germ cells decreased when cultured with Sertoli cells. This phenomenon was probably because the Sertoli cell line utilized in this study was derived from rainbow trout. Gdnf is not produced as an autocrine SSC niche factor in rainbow trout testes, unlike in mammals, as evidenced by the fact that it is expressed in germ cells from spermatogonia to spermatocytes but not in Sertoli cells (28). To overcome this issue, extra human recombined GDNF was supplemented in culture medium. However, germ cell proliferation rate did not remain as expected. It will be of interest decipher differences in growth factors secreted by RTG2 and Sertoli cell lines in the future. Moreover, germ cell transplantation is expected to be applied to investigate the germ cell stemness after prolonged culture.

In conclusion, a short-term carp germ cell *in vitro* culture condition has been established by optimizing the dissection method, basal culture mediums, and types of feeder cells. To date, cells could be maintained > 2 months, which is suitable for several research applications. This is the first report of successful *in vitro* germ cell culture in common carp, species important for aquaculture production as well as important model species in basic and applied science. Development of successful *in vitro* germ cell culture enables number of applications in surrogate production such as development and effective production of isogenic fish lines or production, restoration of lines or breeds from few available individuals or development of lines based on reported superior genotypes. In the future, it could be of interest to prolong carp germ cell proliferation and to investigate their cell capacity by transplantation.

Data availability statement

The raw data supporting the conclusions of this article will be made available by the authors, without undue reservation.

Ethics statement

The animal study was reviewed and approved by Institutional Animal Care and Use Committee of the FFPW.

Author contributions

Conceptualization, supervision, and validation: XX and VK. Data curation and formal analysis: XX, VK, and RF. Funding acquisition and investigation: VK and MP. Methodology: XX, RF, MP, and VK. Project administration: VK. Resources: XX and RF. Visualization and writing—original draft: XX, VK, and FC. Writing—review and editing: all authors. All authors contributed to the article and approved the submitted version.

Funding

This work was supported by National Agriculture Agency project number QK1910428, Czech Science Foundation project 22-01781O and 22-31141J, by the Ministry of Education, Youth and Sports of the Czech Republic and project Biodiversity (CZ.02.1.01/0.0/0.0/16_025/0007370). This project has received funding from the European Union's Horizon 2020 Research and Innovation Programme under grant agreement and No. 871108 (AQUAEXCEL3.0). This output reflects only the authors' view and the European Union cannot be held responsible for any use that may be made of the information contained therein.

Acknowledgments

We thank all members of the Laboratory of Germ Cells and Laboratory of Molecular, Cellular and Quantitative Genetics, Faculty of Fisheries and Protection of Waters, University of South Bohemia in Ceske Budejovice for their support. Especially we acknowledge Dr. Veronika Piačková for experimental material support. We deeply thank Dr. Ian Butts for his help of English editing.

Conflict of interest

The authors declare that the research was conducted in the absence of any commercial or financial relationships that could be construed as a potential conflict of interest.

Publisher's note

All claims expressed in this article are solely those of the authors and do not necessarily represent those of their affiliated organizations, or those of the publisher, the editors and the reviewers. Any product that may be evaluated in this article, or claim that may be made by its manufacturer, is not guaranteed or endorsed by the publisher.

References

1. Hulata G. A review of genetic-improvement of the common carp (Cyprinus carpio L.) and other cyprinids by crossbreeding. hybridization and selection. *Aquaculture*. (1995) 129:143–55. doi: 10.1016/0044-8486(94)00244-I

2. Kocour M, Mauger S, Rodina M, Gela D, Linhart O, Vandeputte M. et al. Heritability estimates for processing and quality traits in common carp (Cyprinus carpio L.) using a molecular pedigree. *Aquaculture*. (2007) 270:43–50. doi: 10.1016/j.aquaculture.2007.03.001

3. Prchal M, Bugeon J, Vandeputte M, Kause A, Vergnet A, Zhao J, et al. Potential for genetic improvement of the main slaughter yields in common carp with in vivo morphological predictors. Front *Genet*. (2018) 9:283. doi: 10.3389/fgene.2018.00283

4. Flajšhans M, Linhart O, Šlechtová V, Šlechta V. Genetic resources of commercially important fish species in the Czech Republic: present state and future strategy. *Aquaculture*. (1999) 173:471–83. doi: 10.1016/S0044-8486(98)00477-3

5. Flajšhans M, Kocour M, Rodina M, Boryshpolets S, Kašpar V, Hulák M, et al. On-farm conservation of fish genetic resources and testing of performance traits. In. *World Aquaculture Society Conference AQUA 2012*. Prague: Prague Congress Centre. (2012). p. 356.

6. Linhart O, Rodina M, Cosson J. Cryopreservation of sperm in common carp Cyprinus carpio: sperm motility and hatching success of embryos. *Cryobiology*. (2000) 41:241–50. doi: 10.1006/cryo.2000.2284

7. Horváth A, Miskolczi E, Mihálffy S, Osz K, Szabó K, Urbányi B, et al. Cryopreservation of common carp (Cyprinus carpio) sperm in 1.2 and 5 ml straws and occurrence of haploids among larvae produced with cryopreserved sperm. *Cryobiology*. (2007) 54:251–57. doi: 10.1016/j.cryobiol.2007.02.003

8. Franěk R, Tichopád T, Steinbach C, Xie X, Lujić J, Marinović Z, et al. Preservation of female genetic resources of common carp through oogonial stem cell manipulation. *Cryobiology*. (2019) 87:78–85. doi: 10.1016/j.cryobiol.2019.01.016

9. Franěk R, Kašpar V, Shah MA, Gela D, Pšenička M. Production of common carp donor-derived offspring from goldfish surrogates. *Aquaculture*. (2021) 534:736252. doi: 10.1016/j.aquaculture.2020.736252

10. Anil S, Rawson D, Zhang T. Development of molecular markers for zebrafish (Danio rerio) ovarian follicle growth assessment following in-vitro culture in cryopreservation studies. *Cryobiology*. (2018) 83:75–83. doi: 10.1016/j.cryobiol.2018.05.004

11. Tsai S, Rawson DM, Zhang T. Development of *in vitro* culture method for early stage zebrafish (Danio rerio) ovarian follicles for use in cryopreservation studies. *Theriogenology*. (2010) 74:290–303. doi: 10.1016/j.theriogenology.2010.02.013

12. Okutsu T, Suzuki K, Takeuchi Y, Takeuchi T, Yoshizaki G. Testicular germ cells can colonize sexually undifferentiated embryonic gonad and produce functional eggs in fish. *Proc Natl Acad Sci U S A*. (2006) 103:2725–9. doi: 10.1073/pnas.0509218103

13. Jin YH, Robledo D, Hickey JM, McGrew MJ. Surrogate broodstock to enhance biotechnology research and applications in aquaculture. *Biotechnol Adv*. (2021) 49:107756. doi: 10.1016/j.biotechadv.2021.107756

14. Sakai N. *In vitro* male germ cell cultures of zebrafish. *Methods*. (2006) 39:239–45. doi: 10.1016/j.ymeth.2005.12.008

15. Hong Y, Liu T, Zhao H, Xu H, Wang W, Liu R, et al. Establishment of a normal medakafish spermatogonial cell line capable of sperm production *in vitro*. *Proc Natl Acad Sci USA*. (2004) 101:8011–6. doi: 10.1073/pnas.0308668101

16. Shikina S, Yoshizaki G. Improved *in vitro* culture conditions to enhance the survival, mitotic activity, and transplantability of rainbow trout type A spermatogonia. *Biol Reprod*. (2010) 83:268–76. doi: 10.1095/biolreprod.109.082123

17. Xie X, Li P, Pšenička M, Ye H, Steinbach C, Li C. Optimization of *in vitro* culture conditions of sturgeon germ cells for purpose of surrogate production. *Animals*. (2019) 9:106. doi: 10.3390/ani9030106

18. Iwasaki-Takahashi Y, Shikina S, Watanabe M, Banba A, Yagisawa M, Takahashi K, et al. Production of functional eggs and sperm from *in vitro*-expanded type A spermatogonia in rainbow trout. *Commun Biol*. (2020) 3:308. doi: 10.1038/s42003-020-1025-y

19. Su S, Jing X, Zhang C, Hou Y, Li Z, Yang X., et al. Interaction between the intestinal microbial community and transcriptome profile in common carp (Cyprinus Carpio L). *Front Microbiol*. (2021) 12:659602. doi: 10.3389/fmicb.2021.659602

20. Schulz RW, de França LR, Lareyre JJ, Le Gac F, Chiarini-Garcia H, Nobrega RH. *Spermatogenesis in Fish. Gen Comp Endocrinol*. (2010) 165:390–411. doi: 10.1016/j.ygcen.2009.02.013

21. Skaar KS, Nobrega RH, Magaraki A, Olsen LC, Schulz RW, Male R, et al. Proteolytically activated, recombinant anti-müllerian hormone inhibits androgen secretion, proliferation, and differentiation of spermatogonia in adult zebrafish testis organ cultures. *Endocrinology*. (2011) 152:3527–40. doi: 10.1210/en.2010-1469

22. Miura T, Chiemi M, Kohei Y. Spermatogenesis in the Japanese Eel. In: *Eel Biology*. London: Springer. (2003). p. 319–29.

23. Ohta H, Yomogida K, Dohmae K, Nishimune Y. Regulation of proliferation and differentiation in spermatogonial stem cells: the role of c-Kit and its ligand SCF. *Development*. (2000) 27:2125–131. doi: 10.1242/dev.127.10.2125

24. Vincent S, Segretain D, Nishikawa S, Nishikawa SI, Sage J, Cuzin F, et al. Stage-Specific expression of the kit receptor and its ligand (KL) during Male gametogenesis in the mouse: a kit-KL interaction critical for meiosis. *Development*. (1998) 125:4585–93. doi: 10.1242/dev.125.22.4585

25. Conrad S, Hossein A, Maryam H, Mikael K, Michael B, Jörg H, Markus R. Differential gene expression profiling of enriched human spermatogonia after short- and long-term culture. editor, Irma Virant-Klun. *BioMed Res International*. Histon: The Company of Biologists. (2014). p. 138350.

26. França Luiz R, Rafael H, Nóbrega Roberto DVS, Morais Luiz H, De Castro A, Rüdiger W, et al. *Sertoli cell structure and function in anamniote vertebrates*. In: *Sertoli Cell Biology*. Amsterdam: Elsevier. (2015). p. 385–407.

27. Meng X, Lindahl M, Hyvönen ME, Parvinen M, de Rooij DG, Hess MW, et al. Regulation of Cell Fate Decision of Undifferentiated Spermatogonia by GDNF. *Science*. (2000) 287:1489–93. doi: 10.1126/science.287.5457.1489

28. Nakajima S, Hayashi M, Kouguchi T, Yamaguchi K, Miwa M, Yoshizaki G. Expression patterns of Gdnf and Gfrα1 in rainbow trout testis. *Gene Expr Patterns*. (2014) 14:111–20. doi: 10.1016/j.gep.2014.01.006

frontiers | Frontiers in Veterinary Science

TYPE Original Research
PUBLISHED 26 October 2022
DOI 10.3389/fvets.2022.1012276

Check for updates

OPEN ACCESS

EDITED BY
Nelida Rodriguez-Osorio,
Universidad de la República, Uruguay

REVIEWED BY
Mauricio Corredor,
University of Antioquia, Colombia
Wuzi Dong,
Northwest A&F University, China

*CORRESPONDENCE
Jie Tang
yaya184@xab.ac.cn

SPECIALTY SECTION
This article was submitted to Livestock Genomics, a section of the journal Frontiers in Veterinary Science

RECEIVED 05 August 2022
ACCEPTED 05 October 2022
PUBLISHED 26 October 2022

CITATION
Tang J, Suo L, Li F, Yang C, Bian K and Wang Y (2022) ITRAQ-based quantitative proteomics analysis of forest musk deer with pneumonia. *Front. Vet. Sci.* 9:1012276. doi: 10.3389/fvets.2022.1012276

COPYRIGHT
© 2022 Tang, Suo, Li, Yang, Bian and Wang. This is an open-access article distributed under the terms of the Creative Commons Attribution License (CC BY). The use, distribution or reproduction in other forums is permitted, provided the original author(s) and the copyright owner(s) are credited and that the original publication in this journal is cited, in accordance with accepted academic practice. No use, distribution or reproduction is permitted which does not comply with these terms.

ITRAQ-based quantitative proteomics analysis of forest musk deer with pneumonia

Jie Tang*, Lijuan Suo, Feiran Li, Chao Yang, Kun Bian and Yan Wang

Shaanxi Key Laboratory for Animal Conservation, Shaanxi Institute of Zoology, Xi'an, China

Pneumonia can seriously threaten the life of forest musk deer (FMD, an endangered species). To gain a comprehensive understanding of pneumonia pathogenesis in FMD, iTRAQ-based proteomics analysis was performed in diseased (Pne group) lung tissues of FMD that died of pneumonia and normal lung tissues (Ctrl group) of FMD that died from fighting against each other. Results showed that 355 proteins were differentially expressed (fold change $\geq$ 1.2 and adjusted *P*-value$<$ 0.05) in Pne vs. Ctrl. GO/KEGG annotation and enrichment analyses showed that dysregulated proteins might play vital roles in bacterial infection and immunity. Given the close association between bacterial infection and pneumonia, 32 dysregulated proteins related to *Staphylococcus aureus* infection, bacterial invasion of epithelial cells, and pathogenic *Escherichia coli* infection were screened out. Among these 32 proteins, 13 proteins were mapped to the bovine genome. Given the close phylogenetic relationships of FMD and bovine, the protein-protein interaction networks of the above-mentioned 13 proteins were constructed by the String database. Based on the node degree analysis, 5 potential key proteins related to pneumonia-related bacterial infection in FMD were filtered out. Moreover, 85 dysregulated proteins related to the immune system process were identified given the tight connection between immune dysregulation and pneumonia pathogenesis. Additionally, 12 proteins that might function as crucial players in pneumonia-related immune response in FMD were screened out using the same experimental strategies described above. In conclusion, some vital proteins, biological processes, and pathways in pneumonia development were identified in FMD.

KEYWORDS

forest musk deer, pneumonia, proteomics, bacterium, immunity

Introduction

Forest musk deer (FMD, *Moschus berezovskii*) is a type of mammal that mainly lives in the alpine forests in China and Vietnam (1, 2). The populations of FMD are sharply declined since the 1950s due to habitat destruction/degradation and massive hunting for their musk (Moschus) (3, 4). Musk is the dried secretion from the musk sac gland of male musk deer, such as *Moschus berezovskii Flerov*, *Moschus moschiferus Linnaeus*, and *Moschus sifanicus Przewalski* (5, 6). Musk is a superior component in perfume and

is believed to have potential therapeutic values for multiple diseases such as cancers, strokes, and heart diseases in the traditional Asian medicine industry (6, 7). This species has been listed in the First-Class National Protected Animal List of China and is protected under the Chinese Wild Animal Protection Law (4, 8). Moreover, FMD is the major species of musk deer that can be reared artificially in special farms under the support of the Chinese government, which contributes to the growth of the population, reduction of poaching behaviors, and better utilization of FMD resources (9, 10).

The increase in the population of FMD is also limited by some fatal diseases including pneumonia (11–13). Pneumonia can be caused by multiple pathogens including bacteria (14–16). However, previous research on pneumonia mainly focused on the isolation, identification, and genome analysis of pathogens in FMD (12, 17, 18). To reduce the risk and harm of pneumonia for the health and life of FMD, it is imperative to have an in-depth insight into the molecular mechanisms underlying pneumonia development and identify key molecules or pathways related to pneumonia pathogenesis.

Recently, mass spectrometry (MS)-based proteomics has attracted much attention from researchers because proteins are responsible for most biological functions and proteomics can simultaneously capture and quantify thousands of proteins rather than RNAs in a cost-effective manner (19, 20). Isobaric tag for relative and absolute quantification (iTRAQ), an isotope labeling strategy, has been widely used in proteomics studies needing relative quantification due to the multiple advantages such as multiplexing capacity, reproducibility, easy operation, and flexibility (21–23). The combination of iTRAQ and MS-based proteomics technologies and bioinformatics analytical methods have emerged as a powerful strategy for identifying vital proteins related to disease pathogenesis, comprehensively understanding protein roles and basic biological functions, and deciphering complicated molecular mechanisms underlying disease development in multiple animals (24–26).

However, to our knowledge, there is no proteomics data to explore the pathogenesis of pneumonia in FMD to date. To build up a general and comprehensive understanding of pneumonia pathogenesis, the iTRAQ-based LC-MS/MS technique was used to explore the proteomics alterations in diseased lung tissues of FMD that died of pneumonia than in normal lung tissues of FMD died from fighting against each other. Moreover, some genes/proteins, biological processes, and signaling pathways that might play vital roles in pneumonia progression were screened out based on differential expression, annotation, enrichment, and protein-protein interaction analysis.

Materials and methods

Animal samples

Forest musk deer are reared in the Shaanxi Institute of Zoology (China). The Animal breeding area (34.210832°N, 106.902117°E) is located in Fengxian, Southwest of BaoJi City, Shaanxi Province, China, a region of Qinling mountain at an altitude of 1,500 m. Diseased lung tissues were obtained from 3 adult FMD (2♂1♀, 4.5 years old) that died of pneumonia. Normal lung tissues were obtained from 3 adult FMD (♂, 3.5 years old) that died from fighting against each other. Tissue samples with a weight of no <200 mg were stored at −80°C. The study was approved by the Academic Committee of Shaanxi Institute of Zoology with Ethical Approval No.: 20210327001.

Histological analysis

The tissues mentioned above were fixed in a PBS buffered formaldehyde solution for 48 h. After routine dehydration and transparency, sectioned at a thickness of 4 μm and stained with Eosin Staining Kit (Beyotime, Shanghai, China) following the protocols of the manufacturer, and examined by light microscopy.

ITRAQ-based proteomics analysis

ITRAQ-based proteomics analysis was performed as previously described (27, 28). The detailed experimental procedures of proteomics analysis including sample preparation, iTRAQ labeling and fractionation, LC-MS/MS analysis, and data analysis were shown in Supplementary file 1. Briefly, tissue samples were ground to a fine powder in liquid nitrogen and then lysed using the protein lysis buffer [7M Urea/4% SDS/2M Thiourea/40 mM Tris-HCl (pH 8.5)] supplemented with 2 mM EDTA and 1mM phenylmethylsulfonyl fluoride. Samples were labeled using the iTRAQ Reagent-8 plex Multiplex Kit (SCIEX, Framingham, MA, USA) according to the protocols of the manufacturer, in which only 6 channels were used in our project. The information of sample-corresponding channels was shown in Table 1. Pne and Ctrl groups represented diseased and normal lung tissue groups, respectively. LC-MS/MS analysis was carried out on TripleTOF 5600+ mass spectrometry (SCIEX) coupled with an EksigentnanoLC system (SCIEX). Raw data analysis was performed using the Protein Pilot Software (version 4.5, SCIEX). The raw MS/MS file data were searched against the PR1-19060015_pep. fasta (containing 24,352 sequences). Proteins were regarded to be significantly

TABLE 1 Sample-corresponding iTRAQ channels.

Sample groups	Sample label	Channel
Disease-1	Pne_1	113
Disease-2	Pne_2	114
Disease-3	Pne_3	117
Normal-1	Ctrl_1	118
Normal-2	Ctrl_2	119
Normal-3	Ctrl_3	121

differentially expressed when fold-change $\geq$ 1.2 and adjusted P-value $<$ 0.05.

Bioinformatics and annotations

To determine the biological and functional properties of all the identified proteins, the identified protein sequences were mapped with those in the Swiss-Prot database using BLASTP. In addition, a homology search was performed for the differentially expressed protein sequences using a localized NCBI blastp program against the NCBI non-redundant protein (NR) animal database. Moreover, the GO and KEGG annotation information of matched proteins was extracted. GO and KEGG pathway enrichment analysis was performed using the hypergeometric test. GO and KEGG pathway terms were considered to be significantly enriched at a P-value $<$ 0.05. Protein-protein interaction (PPI) networks were constructed using the STRING database (version: 11.5) (https://cn.string-db.org/).

qRT-PCR analysis for gene expression

Ten mRNAs were randomly selected for expression analysis by qRT-PCR to validate the data. The primer sequences are listed in Table 2. The GAPDH gene was used as the internal control. The total RNA was extracted from the Lung tissues with the RNAiso plus reagent (Takara, Dalian, China) following the manufacturer's protocols. The qRT-PCR was performed using SYBR Premix ExTaq (TaKaRa, Dalian, China) and a Thermal Cycler CFX96 Real Time-PCR detection system (Bio-Rad, Hercules, CA, USA) with the following parameters: 95 °C for 60 s; 40 cycles at 95 °C for 15 s; 60 °C for 30 s; and 72 °C 10 s. The concentration and purity of total RNA were measured using a GE Nanovue™ Spectrophotometer (GE Health care Biosciences, Pittsburgh, USA). cDNA was synthesized using the SYBR Prime Script™ RT Master Mix (Perfect Real Time) Kit (Takara, Dalian, China). The relative expression of each gene was calculated with the 2−ΔΔCt method. There were three biological sample replicates, and each biological sample replicates included three technical replicates.

Results

Histological observation of lung tissue

Histological analysis showed that the alveolar cavity has inflammatory cell exudates and the alveolar wall capillary hyperemia in the pneumonia group (Figures 1C,D). Numerous broken neutrophils were exuded from the alveolar cavity and obvious bleeding was noticed in the pneumonia group (Figures 1E,F). And, the most notable pathological changes were interstitial pneumonia and hemorrhagic pneumonia in the pneumonia group (Figures 1G,H). Moreover, red blood cell, inflammatory cell, and fibrin exudate were present in the alveolar lumen, and the lung interstitium was widened in the pneumonia group (Figures 1G,H).

Identification of differentially expressed proteins

In our proteomics analysis, 355 proteins (169 down-regulated and 186 up-regulated) were found to be differentially expressed (up-regulated ratio $\geq$ 1.2 or down-regulated ratio $\leq$ 0.83; adjusted P-value $<$ 0.05) in the diseased lung tissues of FMDs who died of pneumonia compared to the normal lung tissue group (Figure 2; Supplementary Table 1). The volcano plot of differentially expressed proteins was shown in Figure 2. Among these differentially expressed proteins, 158 proteins were annotated in the bovine Swiss-Prot database.

GO and KEGG annotation analysis of differentially expressed proteins

To screen out key proteins related to the pathogenesis of pneumonia, the sequences of differentially expressed proteins were compared against the NCBI NR database using the NCBI-BLAST. These differentially expressed proteins were also annotated by comparisons against the GO and KEGG databases. Based on the principle of sequence similarity, proteins with similar sequences have similar functions. GO annotation analysis revealed that most of the down-regulated and up-regulated proteins were involved in the regulation of biological processes such as cellular process, metabolic process, biological regulation, response to stimulus, and cellular component organization or biogenesis (Figure 3A; Supplementary Table 2). Also, many differentially expressed proteins were implicated in the immune system process, death, locomotion, cell proliferation, biological adhesion, and growth (Figure 3A; Supplementary Table 2). Moreover, KEGG pathway annotation analysis showed that most up-regulated and down-regulated proteins played crucial roles in the pathways related to focal adhesion, phagosome, microbial metabolism

TABLE 2 Primers used in quantitative real-time PCR analysis.

Target gene	Primer	Sequence (5'to3')
GAPDH	GAPDH-F	GGCACAGTCAAGGCAGAGAAC
	GAPDH-R	TACTCCGCACCAGCATCACC
Galectin-9	Galectin-9 F	CGGTTTGAAGAAGGCGGGTATG
	Galectin-9 R	AGATGGCGTTGAATTGGTAGAAGG
Coronin-1A	CORO1A-F	CACTTTGGATGAGGAGCAGAA
	CORO1A-R	TGGCTGGCTGTCCAAATAC
Annexin A6	ANXA6-F	AATGACACCTCTGGCGAATAC
	ANXA6-R	ACTGCACTAAGTTCCCACATC
Protein S100-A10	S100A10-F	TGCCGTCTCAAATGGAACA
	S100A10-R	TCCATGAGTACTCTCAGGTCTT
Moesin	MSN -F	AGAAGAGGTGGCAAGAATACAC
	MSN -R	TTCCAGGATGTCTGGCTCTA
Envoplakin	EVPL -F	TTCCAGGATGTCTGGCTCTA
	EVPL -R	GTAGGTTCTTGCACTCCCTATG
Platelet endothelialcell adhesion molecule	PECAM1-F	GAGTATGAGGTGTGGGTGAAAG
	PECAM1-R	CTGGGACAGAACAGTTGACTAC
Integrin beta-1	ITGB1-F	AGGCCACTGTTCATGTTGTAG
	ITGB1-R	CAGCAATGCAAGGCCAATAAG
CD177	CD177-F	CTACTGAACCTACCCAAGACAAG
	CD177-R	GCAGAGGTGATGTTGATGAGTA
Collectin-12	COLEC12-F	CAACTCAGAACTCTCCACCTTC
	COLEC12-R	TGGCCAAAGCGGAGTTATT

in diverse environments, leukocyte transendothelial migration, bacterial invasion of epithelial cells, endocytosis, *Staphylococcus aureus* infection, and pathogenic *Escherichia coli* infection (Supplementary Tables 3, 4). The statistics of the top 20 KEGG pathways of up-regulated and down-regulated proteins were shown in Figure 3B.

GO and KEGG enrichment analysis of differentially expressed proteins

GO enrichment analysis showed that differentially expressed proteins were significantly enriched in biological processes such as acute-phase response, leukocyte adhesion, leukocyte migration, phagocytosis, regulation of tumor necrosis factor biosynthetic process, defense response to Gram-negative bacterium, regulation of locomotion, receptor-mediated endocytosis, cell structure disassembly during apoptosis, defense response to fungus (Supplementary Table 5). The top 20 GO biological process terms that were significantly enriched by differentially expressed genes were displayed in Figure 4A. KEGG enrichment analysis disclosed that differentially expressed proteins were significantly enriched in pathways related to *Staphylococcus aureus* infection, focal adhesion, complement and coagulation cascades, phagosome, antigen processing and presentation, bacterial invasion of epithelial cells, and pathogenic *Escherichia coli* infection (Supplementary Table 6). The top 20 KEGG pathways that were significantly enriched by the differentially expressed proteins were shown in Figure 4B.

Screening and PPI network construction of dysregulated proteins related to bacterial infection

Both KEGG annotation and enrichment outcomes suggested that pathways related to *Staphylococcus aureus* infection, bacterial invasion of epithelial cells, and pathogenic *Escherichia coli* infection might play vital roles in pneumonia progression. Given the close association between bacterial infection and pneumonia pathogenesis, dysregulated proteins in the above-mentioned pathways were filtered out based on KEGG annotation analysis. The information on these proteins was shown in Supplementary Table 7. As presented in Supplementary Table 7, 13 (9 down-regulated and 4 up-regulated), 14 (7 down-regulated and 7 up-regulated), or 12 (4 down-regulated and 8 up-regulated) differentially expressed proteins were identified to be implicated in *Staphylococcus*

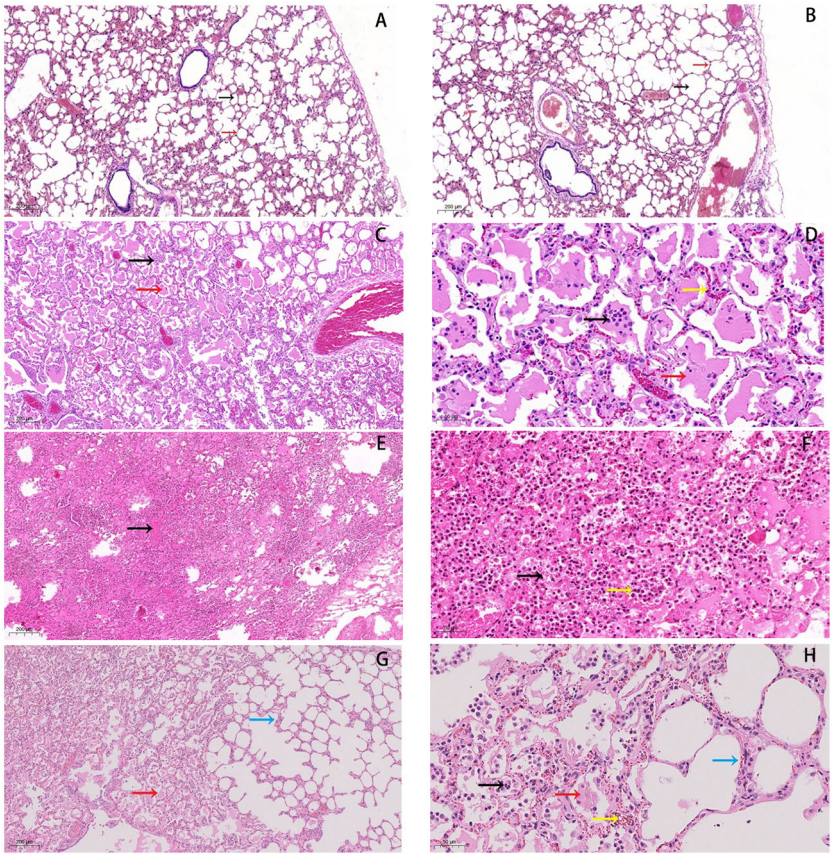

FIGURE 1
Histopathological changes in lungs of forest musk deer. **(A,B)** normal lung tissue in the control group, HE staining of normal tissues was performed (5×). The black arrow indicates the alveolar cavity, the red arrow points to the alveolar wall. **(C,D)** Inflammatory cells (black arrow) and exudate can be seen in the alveolar cavity (red arrow), and the capillaries in the alveolar wall are hyperemic (yellow arrow). **(E,F)** Numerous broken neutrophils (yellow arrow) exuded from the alveolar cavity, bleeding obvious (black arrow). **(G,H)** Red blood cell (yellow arrow), inflammatory cell (black arrow) and fibrin exudates (red arrow) present in alveolar lumen, and lung interstitium is widened (blue arrow). Bars: **(B,D,F,H)** 50 μm, Bars: **(A,C,E,G)** 200 μm, (magnification, 5.0×, 20.0×).

aureus infection, bacterial invasion of epithelial cells, or pathogenic *Escherichia coli* infection, respectively. The above-mentioned differentially expressed proteins related to bacterial infection (total number: 32) were integrated into Supplementary Table 8. The STRING database has been widely used to construct the PPI network and identify hub proteins in previous studies (29, 30). Prior phylogenetic tree analysis showed that FMD was a member of the suborder Ruminantia and order Artiodactyla with close phylogenetic relationships with four members of the family Bovidae (sheep, yak, cattle, and Tibetan antelope) (31). Also, a recent study showed that most FMD unigenes that were identified by *de novo* assembly of heart and musk gland transcriptomes were homologous with bovine genes (32). Given the close phylogenetic relationships of FMD and bovine, the PPI networks of filtered proteins were constructed based on the information of the organism species Bos taurus (bovine). Among filtered 32 differentially expressed proteins related to bacterial infection, 13 proteins were annotated in the bovine Swiss-Prot database (Supplementary Table 8). The PPI networks of the 13 proteins were constructed and displayed in Figure 4 (organism: Bos taurus, combined interaction score $\geq$ 0.4) (the solitary proteins had been removed from the network). The detailed interaction information of these 13 proteins was shown in Supplementary Table 9. The node degrees (number of interacted proteins) of proteins in the PPI networks (Figure 5) were exhibited in Supplementary Table 10. The node degree can be used to identify hub proteins in the PPI networks (33, 34). Results suggested that 5 proteins with greater node degrees [*i.e.* catenin beta-1 (CTNNB1), integrin beta-1 (ITGB1), catenin alpha-1 (CTNNA1), dynamin-2 (DNM2), Keratin, type I cytoskeletal 19 (KRT19)] might function as crucial players in pneumonia-related bacterial infection in FMD.

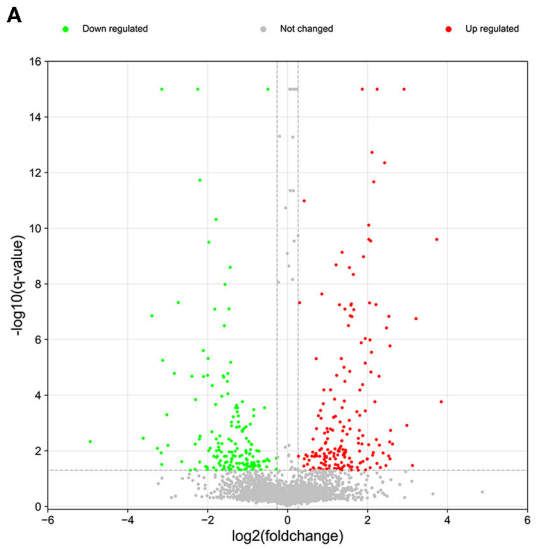

FIGURE 2
The volcano plot of differentially expressed and unchanged proteins. Red dots represent the up-regulated proteins and green dots denote the down-regulated proteins.

Screening and PPI network construction of dysregulated proteins related to immunity

It has been reported that the pathogenesis of pneumonia is closely linked with the dysfunction of the immune system (35, 36). In this project, 53 down-regulated and 32 up-regulated proteins that were implicated in the immune system process were screened out based on the GO annotation analysis. These 85 proteins related to the immune system process were shown in Supplementary Table 11. Among these 85 proteins, 49 proteins that were mapped to the bovine genome were screened out (Supplementary Table 11). Next, the PPI networks of these 49 proteins were established and presented in Figure 6 (organism: Bos taurus, combined interaction score $\geq$ 0.4) (the solitary proteins have been removed from the network). The detailed protein-protein interaction information and node degrees of the above-mentioned 49 proteins in the PPI networks were displayed in Supplementary Tables 12, 13, respectively. The outcomes suggested that CTNNB1, ITGB1, Annexin A5 (ANXA5), calreticulin (CALR), prothrombin (F2), matrix metalloproteinase-9 (MMP9), platelet endothelial cell adhesion molecule (PECAM1), thrombospondin-1 (THBS1), heat shock protein HSP 90-beta (HSP90AB1), endoplasmin (HSP90B1), integrin alpha-3 (ITGA3), and moesin (MSN) might be the hub proteins in the PPI networks because they had greater node degrees. In other words, these proteins might play vital roles in the immune response related to pneumonia in FMD.

Validation of differentially expressed proteins by qRT-PCR analysis

The expression patterns determined by qRT-PCR were consistent with those obtained by iTRAQ, with 90% agreement between the qRT-PCR and iTRAQ results (Figure 7). This result indicated that the differential proteomic analysis outcomes in this study were reliable.

Discussion

In this project, a total of 355 differentially expressed (up-regulated ratio $\geq$ 1.2 or down-regulated ratio $\leq$ 0.83; adjusted *P*-value $<$ 0.05) proteins were identified in the diseased lung tissues of FMDs who died of pneumonia vs. the normal group. Among these dysregulated proteins, 158 proteins were mapped to the bovine genome.

Moreover, KEGG pathway annotation analysis showed that 9 pathways (i.e., metabolic pathways, focal adhesion, pathways in cancer, regulation of actin cytoskeleton, amoebiasis, microbial metabolism in diverse environments, tight junction, leukocyte transendothelial migration, bacterial invasion of epithelial cells) were shared in the top 20 KEGG pathways of up-regulated and down-regulated proteins. Among the 46 metabolic pathways-related proteins (28 up-regulated and 18 down-regulated), alpha-enolase (ENO1), neutrophil gelatinase-associated lipocalin (LCN2), and Acetyl-CoA acetyltransferase (ACAT1) have been found to be related to pathogens-induced pneumonia. For instance, ENO1 facilitated lipopolysaccharide (LPS)-driven monocyte recruitment to the acutely inflamed lung, and ENO1 was highly expressed in blood monocyte cell surface and alveolar mononuclear cells of patients with pneumonia (37). LCN2 had a potential protective effect against *Escherichia coli*-induced pneumonia (38). LCN2 knockout notably improved the susceptibility of mice to *Acinetobacter baumannii pneumonia* (39). LCN2 hindered the clearance of *pneumococcal pneumonia* and exacerbated pneumococcal pneumonia in mice and humans (40). ACAT1 expression was notably increased in THP-1-derived macrophages following the infection of *Chlamydia pneumonia* (41). The inhibition of ACAT1 weakened pulmonary inflammation and inhibited macrophage activation in bleomycin-induced acute lung injury (42). Among the 27 focal adhesion-related dysregulated proteins (18 up-regulated and 9 down-regulated), thrombospondin-1 (THBS1) and caveolin-1 (CAV1) have been reported to be associated with pneumonia. For example, THBS1 loss promoted the clearance of lung *Klebsiella pneumonia*, decreased lung inflammation burden, and enhanced the innate immune responses against *Klebsiella pneumonia* infection (43). CAV1 depletion reduced mouse survival rate, enhanced bacterial burdens, facilitated bacterial dissemination, and potentiated pro-inflammatory responses in mice infected with *Klebsiella*

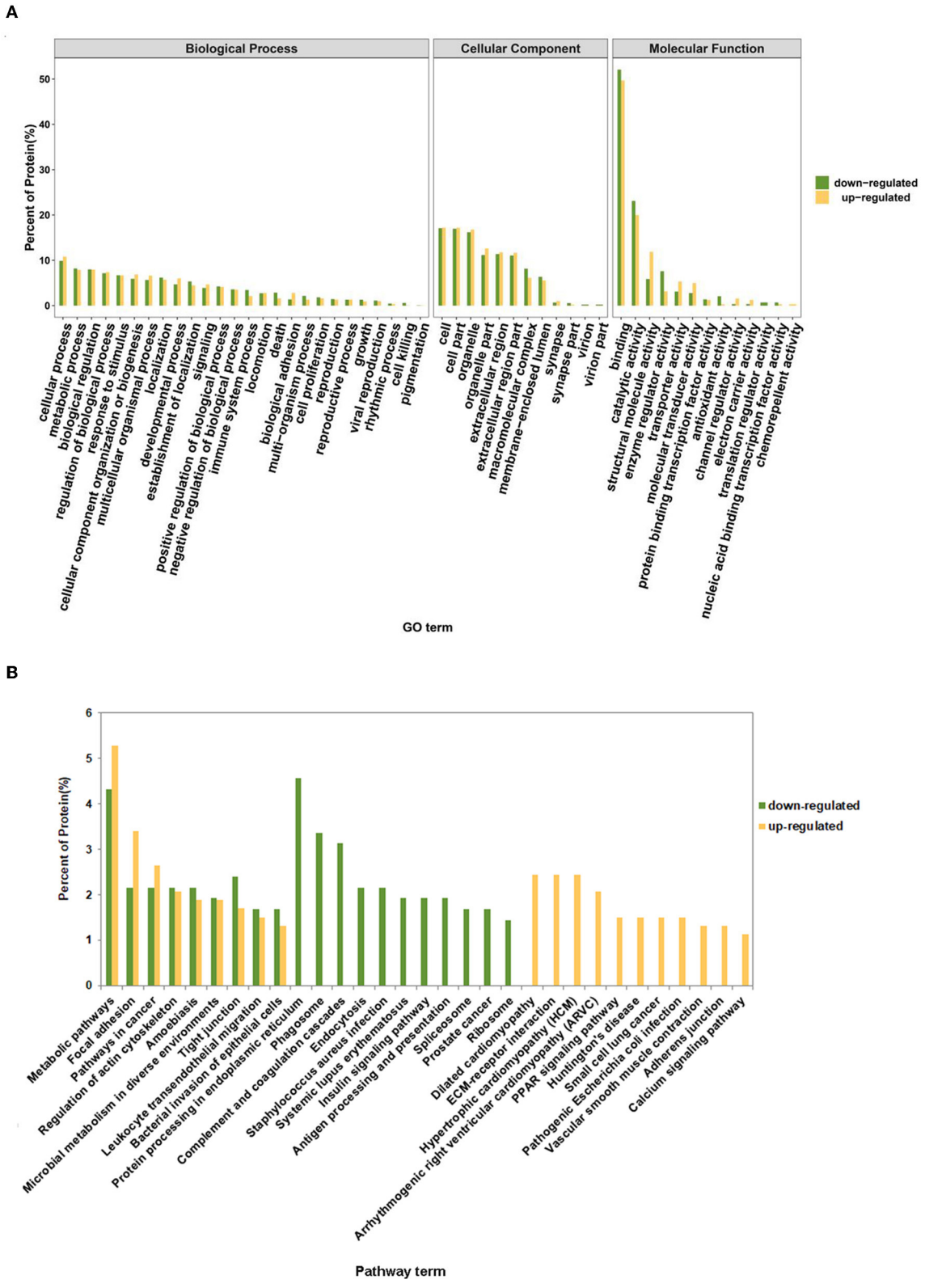

FIGURE 3
GO and KEGG annotation analysis of up-regulated and down-regulated proteins. **(A)** The percentage of up-regulated and down-regulated proteins in each GO term. **(B)** The percentage of up-regulated and down-regulated proteins in the top 20 annotated KEGG pathway terms.

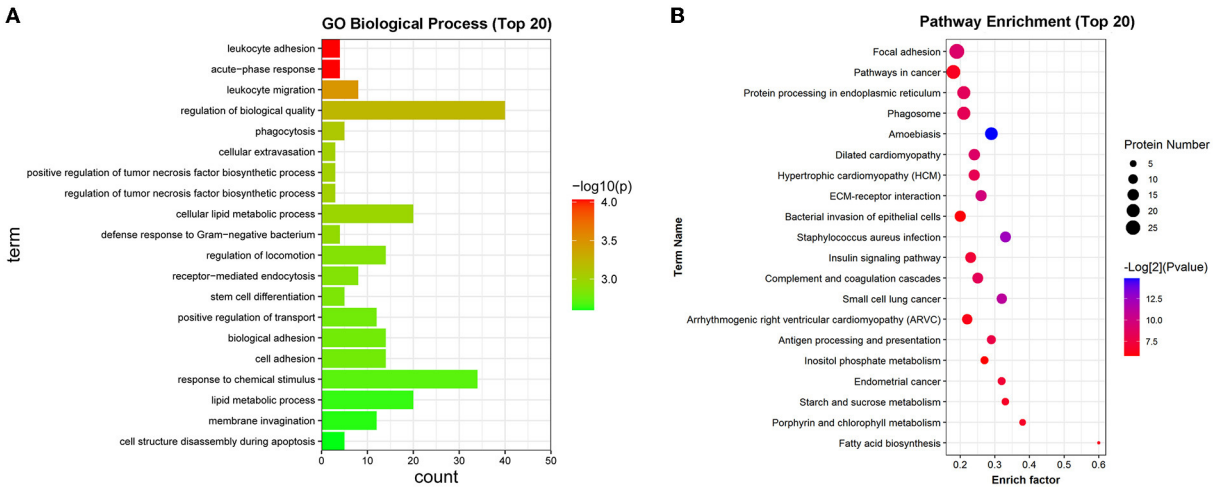

FIGURE 4
GO and KEGG enrichment analysis of differentially expressed proteins. **(A)** The top 20 GO biological process terms that were significantly enriched by the differentially expressed proteins. **(B)** The top 20 KEGG pathways that were significantly enriched by the differentially expressed proteins.

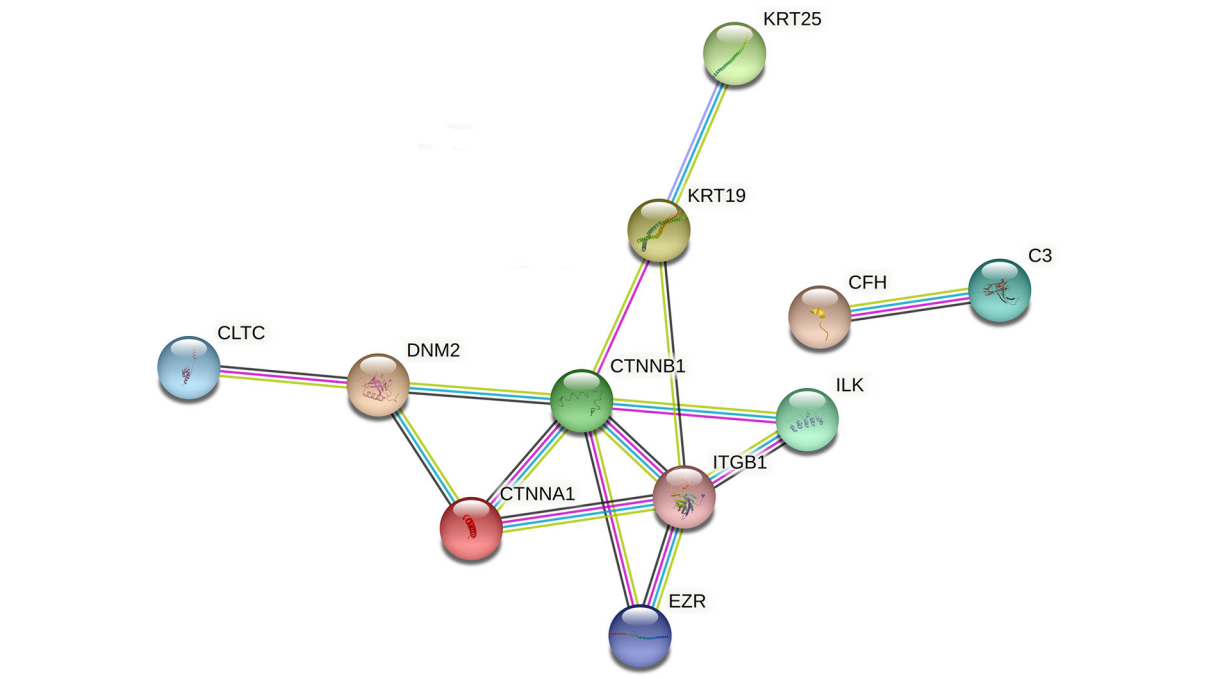

FIGURE 5
The PPI networks of differentially expressed proteins (species: bovine) related to bacterial infection. The darkturquoise and pink lines represented the interactions that were identified from curated databases and experimentally determined, respectively. The green, red, and blue lines represented the predicted interactions based on gene neighborhood, gene fusions, and gene co-occurrence relationships, respectively. The yellow-green, black, and purple lines denoted the potential interactions that were identified by textmining, co-expression, and protein homology. The full names of proteins in this figure were shown as follows: C3, complement C3; CFH, complement factor H, KRT19, keratin, type I cytoskeletal 19; KRT25, keratin, type I cytoskeletal 25; DNM2: dynamin-2; ILK: integrin-linked protein kinase; CLTC, clathrin heavy chain 1; CTNNA1, catenin alpha-1; ITGB1, integrin beta-1; CTNNB1, catenin beta-1; BCAM, basal cell adhesion molecule; TUBA4A, tubulin alpha-4A chain; EZR, ezrin.

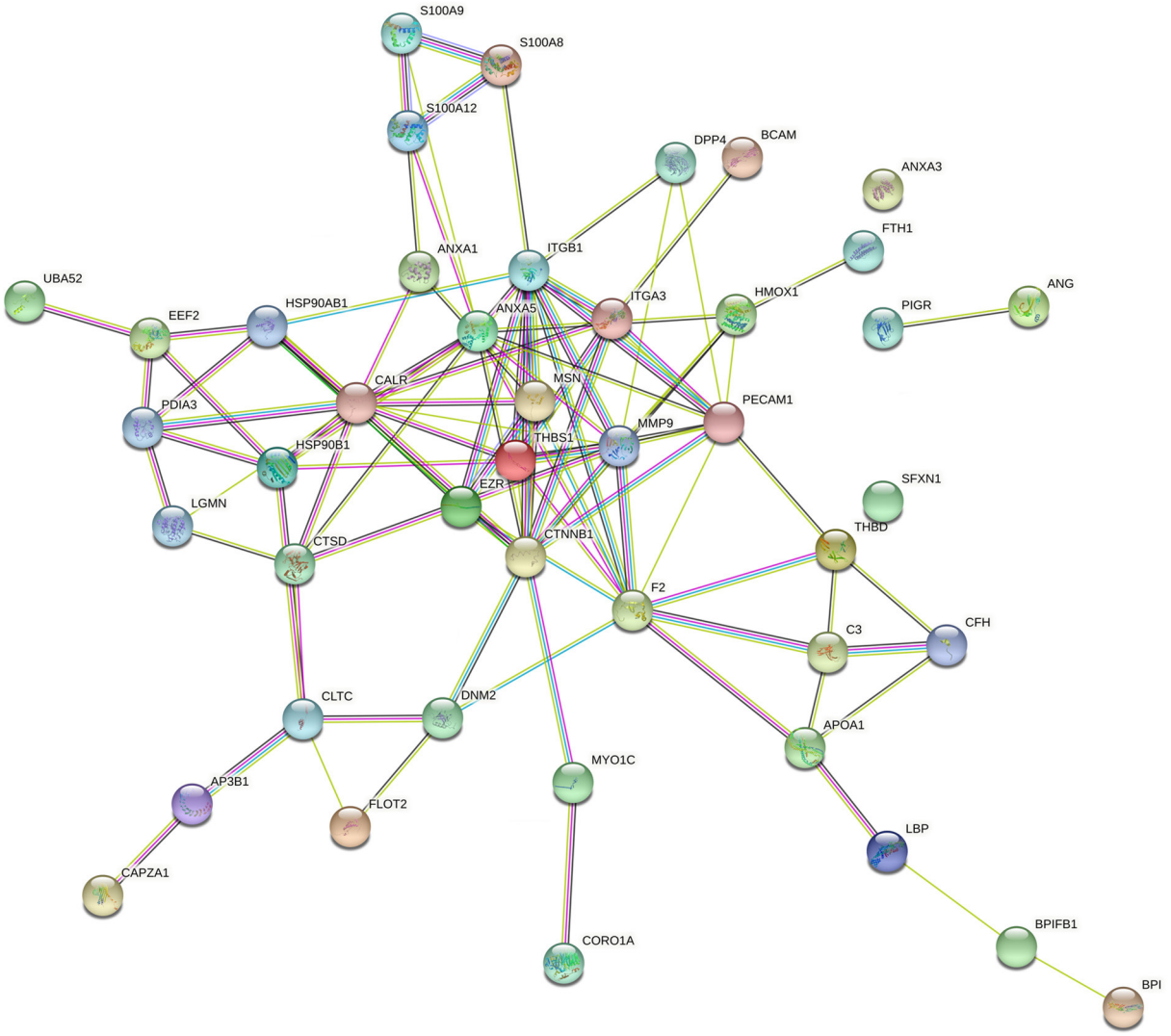

FIGURE 6
The PPI networks of differentially expressed proteins (species: bovine) related to immunity. The full names of the proteins in this figure were presented as below: CALR, calreticulin; LGALS9, galectin-9; C3, complement C3; EPB42, protein 4.2; HSP90B1, endoplasmin; CORO1A, coronin-1A; ANXA1, annexin A1; MMP9, matrix metalloproteinase-9; AP3B1,AP-3 complex subunit beta-1; BPI, bactericidal permeability-increasing protein; THBS1, thrombospondin-1; ANG1, angiogenin-1; S100A12, protein S100-A12; LBP, lipopolysaccharide-binding protein; ANXA5, annexin A5; S100A8, protein S100-A8; S100A9, protein S100-A9; HSP90AB1, heat shock protein HSP 90-beta; DHX9,ATP-dependent RNA helicase A; CAPZA1, f-actin-capping protein subunit alpha-1; GPI, glucose-6-phosphate isomerase; CLTC, clathrin heavy chain 1; DNM2,dynamin-2;F2, prothrombin; THBD, thrombomodulin (fragment); CFH, complement factor H; EEF2, elongation factor 2; BPIFB1, BPI fold-containing family B member 1; PDIA3, protein disulfide-isomerase A3; FLOT2, flotillin-2; UBA52, ubiquitin-60S ribosomal protein L40; MSN, moesin; PIGR, polymeric immunoglobulin receptor; ITGB1, integrin beta-1; LGMN, legumain; COLEC12, collectin-12; CTNNB1, catenin beta-1; SFXN1, sideroflexin-1; BCAM, basal cell adhesion molecule; HMOX1, heme oxygenase 1; ANXA3, annexin A3; MYO1C, unconventional myosin-Ic; CTSD, cathepsin D; APOA1, apolipoprotein A-I; DPP4, dipeptidyl peptidase 4; ITGA3, integrin alpha-3; EZR, ezrin; PECAM1, platelet endothelial cell adhesion molecule; FTH1, ferritin heavy chain.

pneumonia (44). In other words, CAV1 enhanced the resistance of mice to *Klebsiella pneumonia* infection (44). Among 20 proteins related to the regulation of actin cytoskeleton, Rho guanine nucleotide exchange factor 1 (Arhgef1) and myosin light chain kinase (MYLK) have been demonstrated to be related to lung inflammation. For instance, Brown et al. demonstrated that Arhgef1 knockout mice presented decreased airway hyperreactivity and lung inflammation (45). The intravenous injection of MYLK peptide inhibitor reduced lipopolysaccharide-induced lung inflammation in mice (46). Also, 19 (9 down-regulated and 10 up-regulated) and 23 (9 down-regulated and 14 up-regulated) dysregulated proteins in the pneumonia group vs. the control group were identified to be implicated in the amoebiasis and cancer pathways, respectively.

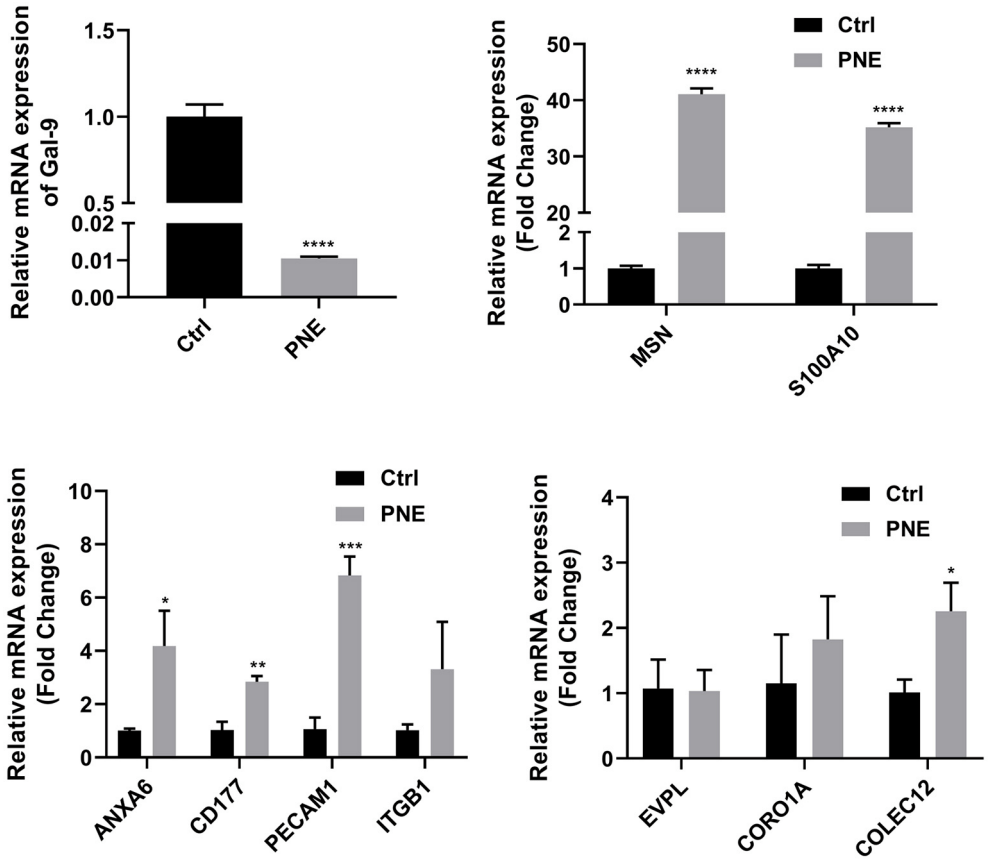

FIGURE 7
Quantitative RT-PCR analyses of gene expression in normal and diseased tissues. Quantitative expression patterns of genes, which was calculated based on Ct value normalized against the housekeeping GAPDH gene. The *, **, and *** symbols indicate the *P*-value < 0.05, *P*-value < 0.01, and *P*-value < 0.001 respectively.

As mentioned above, the amoebiasis and cancer pathways were shared in the top 10 KEGG pathways of up-regulated and down-regulated proteins. Although amoebiasis and cancer might be irrelevant or not the study's subject, we supposed that the immunology activity for pneumonia had the same or like response activity in amoebiasis and cancer due to the central roles of pneumonia-induced dysregulated proteins in amoebiasis and cancer. Also, prior studies of some proteins related to amoebiasis and cancer preliminarily validated our speculation. For example, among amoebiasis pathway-related proteins, integrin beta-2 (ITGB2), heat shock protein beta-1 (HSPB1), LCN2, leukocyte elastase inhibitor (SERPINB1), laminin subunit alpha-4 (LAMA4), and fibronectin (FN1) have been found to be correlated with immunity. Wang et al. demonstrated that ITGB2 depletion in combination with CXCR7 and PDGFB knockdown markedly suppressed *Chlamydia pneumonia* entry into human cells (47). Also, ITGB2 has been identified as an immune-related gene (48, 49). HSPB1 inhibitor J2 reduced lung inflammation (50). Epinephelus coioides HSPB1 was a negative regulator in Singapore grouper iridovirus (SGIV)-induced innate immune response and apoptosis (51). LCN2 not only plays a vital role in antibacterial infection but also functions as a crucial player in the immune response to pathogenic inflammatory stimuli (52, 53). SERPINB1 loss increased the susceptibility of mice to pulmonary bacterial and viral infections (54, 55). Also, SERPINB1 controlled neutrophil survival and homeostatic expansion of IL-17+ γδ and CD4+ Th17 cells (56, 57). LAMA4 deficient mice presented impaired recruitment of neutrophils, monocytes, and lymphocytes to inflammatory loci relative to wild-type mice (58). FN1 also has been found to be involved in the regulation of innate immune response and to be correlated with immune infiltrates in cancers (59–61). Among the cancer-related proteins, signal transducer and activator of transcription 3 (STAT3) has been well documented to be inflammation and immunity (62–64). Also, STAT3 served as a positive regulator of pneumonia induced by influenza virus H1N1 (65), *Agiostrongylus cantonensis* (66), and *Mycoplasma pneumonia* (67). Combined with these data, we supposed that dysregulated proteins related to amoebiasis and cancer might also function

as crucial players in pneumonia, immune, and inflammation, suggesting the same or like immune response activity between pneumonia and amoebiasis or cancer.

Both KEGG pathway annotation and enrichment analyses showed that dysregulated proteins played vital roles in pathways related to bacterial infection (e.g., bacterial invasion of epithelial cells, *Staphylococcus aureus* infection, and pathogenic *Escherichia coli* infection) and immunity (focal adhesion, phagosome, and complement and coagulation cascades), suggesting that pathways related to bacterial infection and immunity might be closely linked with the development of pneumonia in FMD. Moreover, it has been reported that bacteria including *Staphylococcus aureus* and *Escherichia coli* are common risk factors for pneumonia in FMD (11, 12, 17, 68). Moreover, multiple bacterial pathogens, such as *Leclercia spp.*, *Stenotrophononas maltophila*, *Staphylococcus aureus*, and *Staphylococcus sciur*, have been identified in bovine pneumonia (69, 70). Thus, differentially expressed proteins in the pathways of *Staphylococcus aureus* infection, bacterial invasion of epithelial cells, and pathogenic *Escherichia coli* infection were screened out. After integration, a total of 32 dysregulated proteins were identified to be implicated in bacterial infection. Among these 32 proteins, 13 proteins, whose sequences were aligned onto the bovine genome, were screened out for further exploration given the close genetic relationships between FMD and bovine. Based on the PPI and node degree analyses of these 13 proteins, we supposed that 5 proteins (CTNNB1, ITGB1, CTNNA1, DNM2, and KRT19) might play crucial roles in bacteria-related pneumonia in FMD. CTNNB1 (protein name: β-catenin) and CTNNA1 are two vital players in the Wnt signaling pathway (71, 72). Wnt/β-catenin signaling has been reported to be a target of bacterial virulence factors (73) and a vital player in lung development and lung diseases (74–77). Additionally, Chen et al. demonstrated that morusin could mitigate mycoplasma pneumonia by inhibiting the Wnt/β-catenin signaling pathway in mice lung tissues (78). ITGB1, also named β1-integrin, hindered bacterial clearance and facilitated bacterial infection in cystic fibrosis airway cells and cystic fibrosis mice (79).

Given the close correlation between immune system dysfunction and pneumonia development, 85 differentially expressed proteins (53 down-regulated and 32 up-regulated) that were implicated in the immune system process were filtered out based on GO annotation analysis. Among these 85 proteins, the sequences of 49 proteins were mapped to the bovine genome. PPI and node degree analysis of these 49 proteins suggested that CTNNB1, ITGB1, ANXA5, CALR, F2, MMP9, PECAM1, THBS1, HSP90AB1, HSP90B1, ITGA3, and MSN might be the hub proteins in the pneumonia-related immune responses in FMD. Some of these proteins have been found to be implicated in pneumonia, lung inflammation, and lung injury. For instance, CALR blockade alleviated acute lung injury (ALI), reduced pro-inflammatory cytokine expression, and inhibited neutrophil and T cell infiltration in bronchoalveolar lavage and lung tissues in lipopolysaccharide (LPS)-induced ALI mouse model (80). MMP9 loss facilitated pulmonary cell death and aggravated lung injury in an interleukin-1β (IL-1β)-induced lung injury mouse model (81). MMP9 acted as a potentially protective factor against *Streptococcus pneumonia* infection (82, 83). PECAM1, an endothelial cell adhesion molecule, played a potentially protective role in lung injury and acute respiratory distress syndrome (84, 85). THBS1 also has been found to be implicated in the pathogenesis of gram-positive bacteria and the development of lung injury (86, 87). For instance, THBS1 loss reduced mouse survival rate, increased lung bacterial burden and lung microvascular permeability, impaired host defense against *Pseudomonas aeruginosa* (*P. aeruginosa*), and potentiated inflammatory injury during *P. aeruginosa* acute intrapulmonary infection (87), while *P. aeruginosa* is a common pathogen of pneumonia in FMD (17). HSP90B1 depletion reduced the phagocytic capacity of macrophages against *Klebsiella pneumonia* (*K. pneumonia)* (a common gram-negative bacteria that can cause pneumonia) and inhibited pro-inflammatory mediator release in alveolar and peritoneal macrophages treated with LPS derived from *K. pneumonia* or heat-killed *K. pneumonia* (88). Moreover, HSP90B1 loss in macrophages led to the increase of mouse lung K. pneumonia loads and are duction in mouse survival rate during *K. pneumonia* (88). CTNNA1 and CTNNB1 are two members of the catenin family (89). Multiple members of catenin family including CTNNA1 and CTNNB1 have been identified to be implicated in immune responses (90–92). For example, CTNNB1 activation enhanced the inflammatory activity of alveolar macrophages and facilitated acute host morbidity in a murine influenza pneumonia model (93). Integrins are crucial players in cell development, cell adhesion, pathogen clearance, inflammation, and immune responses (35, 36). ITGB1 and ITGA3 are two integrin family subunits (94, 95). It has been reported that ITGB1 mediated the entry of coronavirus severe acute respiratory syndrome coronavirus-2 (SARS-CoV-2) (96) and the conditional depletion of ITGB1 in type 2 alveolar epithelial cells could trigger emphysema, epithelial dysfunction, increased efferocytosis and pulmonary macrophage infiltration, and widespread lung inflammation in mice (97). Also, Li et al. suggested that ITGA3 was implicated in the infiltration of 6 immune cells (i.e., B cells, CD8 T cells, CD4 T cells, macrophages, neutrophils, and dendritic cells) in breast cancer (98).

Conclusions

Taken together, our proteomics analysis revealed that 355 proteins were differentially expressed in diseased lung tissues of FMD that died of pneumonia compared to the normal

control group. KEGG annotation and enrichment analysis showed that these dysregulated proteins mainly be associated with bacterial infection and immunity. Moreover, we further screened out the dysregulated proteins related to bacterial infection ($n = 32$) and immunity ($n = 85$). Some key proteins in pneumonia-related bacterial infection and immunity were identified based on PPI and node degree analyses in the FMD. This is the first study to investigate the lung proteomics alterations caused by pneumonia in FMD, which can deepen our understanding of the molecular mechanisms of pneumonia in this rare species. Additionally, the identification of some pathways and proteins that might play vital roles in pneumonia development might contribute to the better management of pneumonia and reduction of mortality rate in FMD. However, only 6 FMD with 3 FMD in each group were used due to the rareness of this species and the difficulty in the acquisition of their organs.

Data availability statement

The datasets presented in this study can be found in online repositories. The names of the repository/repositories and accession number(s) can be found in the article/Supplementary material. The mass spectrometry proteomics data have been deposited via the iProX partner repository (https://www.iprox.cn/page/home.html) with the dataset identifier PXD031240.

Author contributions

JT conceived this study, designed, and supervised the experiments. LS, FL, CY, and KB performed the experiments, conducted data analysis, prepared figures and tables. JT wrote the manuscript. YW modified the manuscript. All authors reviewed and approved the manuscript.

Funding

This research was supported by Science and Technology Program of Shaanxi Academy of Science, China (Program No. 2021K-37) and Shaanxi Province Forestry Science and Technology Innovation Plan (SXLK2021-0222).

Acknowledgments

We would like to express our gratitude to all those who have helped us during the writing of this thesis. Also, we appreciate the Wuhan GeneCreate Biological Engineering Co., Ltd. for Proteomics sequencing.

Conflict of interest

The authors declare that the research was conducted in the absence of any commercial or financial relationships that could be construed as a potential conflict of interest.

Publisher's note

All claims expressed in this article are solely those of the authors and do not necessarily represent those of their affiliated organizations, or those of the publisher, the editors and the reviewers. Any product that may be evaluated in this article, or claim that may be made by its manufacturer, is not guaranteed or endorsed by the publisher.

Supplementary material

The Supplementary Material for this article can be found online at: https://www.frontiersin.org/articles/10.3389/fvets.2022.1012276/full#supplementary-material

References

1. Wang Y, Harris R. Moschus berezovskii. *The IUCN Red List of Threatened Species*. 2015:e.T13894A103431781. (2015). doi: 10.2305/IUCN.UK.2015-4.RLTS.T13894A61976926.en

2. Jie H, Zhang P, Xu Z, Mishra SK, Lei M, Zeng D, et al. microRNA and other small RNA sequence profiling across six tissues of Chinese forest musk deer (*Moschus berezovskii*). *Biomed Res Int.* (2019) 2019:4370704. doi: 10.1155/2019/4370704

3. Jie H, Zheng CL, Wang JM, Feng XL, Zeng DJ, Zhao GJ. [Research progress on molecular genetics of forest musk deer]. *Zhongguo Zhong Yao Za Zhi.* (2015) 40:4319–23.

4. Yang Q, Meng X, Xia L, Feng Z. Conservation status and causes of decline of musk deer (Moschus spp.) in China. *Biol Conserv.* (2003) 109:333–42. doi: 10.1016/S0006-3207(02)00159-3

5. Lv S, Lei Z, Yan G, Shah SA, Ahmed S, Sun T. Chemical compositions and pharmacological activities of natural musk (Moschus) and artificial musk: a review. *J Ethnopharmacol.* (2022) 284:114799. doi: 10.1016/j.jep.2021.114799

6. Liu K, Xie L, Deng M, Zhang X, Luo J, Li X. Zoology, chemical composition, pharmacology, quality control and future perspective of Musk (Moschus): a review. *Chin Med.* (2021) 16:46. doi: 10.1186/s13020-021-00457-8

7. Wang J, Xing H, Qin X, Ren Q, Yang J, Li L. Pharmacological effects and mechanisms of muscone. *J Ethnopharmacol.* (2020) 262:113120. doi: 10.1016/j.jep.2020.113120

8. Guan T-L, Zeng B, Peng Q-K, Yue B-S, Zou F-D. Microsatellite analysis of the genetic structure of captive forest musk deer populations and its implication for conservation. *Biochem Syst Ecol.* (2009) 37:166–73. doi: 10.1016/j.bse.2009.04.001

9. Xiuxiang M, Caiquan Z, Jinchu H, Cao L, Zhibin M, Jinchao F, et al. Musk deer farming in China. *Anim Sci.* (2006) 82:1–6. doi: 10.1079/ASC200516

10. He L. Li L-h, Wang W-x, Liu G, Liu S-q, Liu W-h, et al. Welfare of farmed musk deer: changes in the biological characteristics of musk deer in farming environments. *Appl Anim Behav Sci.* (2014) 156:1–5. doi: 10.1016/j.applanim.2014.03.011

11. Qiao J, Wu X, Su L. A review of mainly affected on musk-deer diseases: purulent, respiratory system and parasitic diseases. *J Econ Anim.* (2009) 13:104–7.

12. Tian Q, Zhou X, Cheng J, Luo Y, Dai L, Zhao W, et al. Genome sequence of lung pathogenic Escherichia coli O78, a chimeric strain isolated from pneumonia forest musk deer. *Genes Genomics.* (2017) 39:805–15. doi: 10.1007/s13258-017-0545-4

13. Zhao W, Yu D, Cheng JG, Luo Y, Wang Y, Yao XP, et al. Affinity of Streptococcal G protein to forest musk deer (Moschus berezovskii) serum immunoglobulin G. *J Wildl Dis.* (2020) 56:684–6. doi: 10.7589/2019-09-223

14. Yan M, Yan Q, Yang G. The mass diseases of captive musk deer. *J Econ Anim.* (2016) 20:112–7. doi: 10.13326/j.jea.2016.112

15. Luo Y, Kang J, Cheng J, Zou L, Li B, Wang C, et al. Physicochemical properties of musk deer pneumonia and purulent disease viruses. *Animal Husbandry and Feed Science.* (2010) 2:37–40. doi: 10.19578/j.cnki.ahfs.2010.05.014

16. Karikalan M, Ram H, Pathak S, Banerjee PS, Chandra MS, Pawdeand AM, et al. Pneumonia due to protostrongylid lung worms in wild himalayan bluesheep (Pseudoisnayaur). *Indian J Vet Pathol.* (2020) 44:181–3. doi: 10.5958/0973-970X.2020.00036.X

17. Zhao W, Ren Z, Luo Y. Metagenomics analysis of the gut microbiome in healthy and bacterial pneumonia forest musk deer. *Genes Genomics.* (2021) 43:43–53. doi: 10.1007/s13258-020-01029-0

18. Zhao W, Tian Q, Luo Y, Wang Y, Yang ZX, Yao XP, et al. Isolation, identification, and genome analysis of lung pathogenic klebsiella pneumoniae (LPKP) in forest musk deer. *J Zoo Wildl Med.* (2017) 48:1039–48. doi: 10.1638/2016-0241.1

19. McArdle AJ, Menikou S. What is proteomics? *Arch Dis Child Educ Pract Ed.* (2021) 106:178–81. doi: 10.1136/archdischild-2019-317434

20. Noor Z, Ahn SB, Baker MS, Ranganathan S, Mohamedali A. Mass spectrometry-based protein identification in proteomics-a review. *Brief Bioinform.* (2021) 22:1620–38. doi: 10.1093/bib/bbz163

21. Evans C, Noirel J, Ow SY, Salim M, Pereira-Medrano AG, Couto N, et al. An insight into iTRAQ: where do we stand now? *Anal Bioanal Chem.* (2012) 404:1011–27. doi: 10.1007/s00216-012-5918-6

22. Rauniyar N, Yates JR 3rd. Isobaric labeling-based relative quantification in shotgun proteomics. *J Proteome Res.* (2014) 13:5293–309. doi: 10.1021/pr500880b

23. Chen X, Sun Y, Zhang T, Shu L, Roepstorff P, Yang F. Quantitative proteomics using isobaric labeling: a practical guide. *Genomics Proteomics Bioinformatics.* (2022) 19:689–706. doi: 10.1016/j.gpb.2021.08.012

24. Li Y, Guo T, Wang X, Ni W, Hu R, Cui Y, et al. ITRAQ-based quantitative proteomics reveals the proteome profiles of MDBK cells infected with bovine viral diarrhea virus. *Virol J.* (2021) 18:119. doi: 10.1186/s12985-021-01592-2

25. Miller I, de Almeida AM, Eckersall PD. Across the great divide: proteomics becoming an essential tool for animal and veterinary sciences. *J Proteomics.* (2021) 241:104225. doi: 10.1016/j.jprot.2021.104225

26. Zhang Z, Yu J, Wang P, Lin L, Liu R, Zeng R, et al. iTRAQ-based proteomic profiling reveals protein alterations after traumatic brain injury and supports thyroxine as a potential treatment. *Mol Brain.* (2021) 14:25. doi: 10.1186/s13041-021-00739-0

27. Bian J, Liang M, Ding S, Wang L, Ni W, Xiong S, et al. iTRAQ-based high-throughput proteomics analysis reveals alterations of plasma proteins in patients infected with human bocavirus. *PLoS ONE.* (2019) 14:e0225261. doi: 10.1371/journal.pone.0225261

28. Tang J, Yu Y, Zheng H, Yin L, Sun M, Wang W, et al. ITRAQ-based quantitative proteomic analysis of Cynops orientalis limb regeneration. *BMC Genomics.* (2017) 18:750. doi: 10.1186/s12864-017-4125-4

29. Szklarczyk D, Gable AL, Lyon D, Junge A, Wyder S, Huerta-Cepas J, et al. STRING v11: protein-protein association networks with increased coverage, supporting functional discovery in genome-wide experimental datasets. *Nucleic Acids Res.* (2019) 47:D607–13. doi: 10.1093/nar/gky1131

30. Szklarczyk D, Gable AL, Nastou KC, Lyon D, Kirsch R, Pyysalo S, et al. The STRING database in 2021: customizable protein-protein networks, and functional characterization of user-uploaded gene/measurement sets. *Nucleic Acids Res.* (2021) 49:D605–d612. doi: 10.1093/nar/gkaa1074

31. Fan Z, Li W, Jin J, Cui K, Yan C, Peng C, et al. The draft genome sequence of forest musk deer (Moschus berezovskii). *GigaScience.* (2018) 7:giy038. doi: 10.1093/gigascience/giy038

32. Xu Z, Jie H, Chen B, Gaur U, Wu N, Gao J, et al. Illumina-based de novo transcriptome sequencing and analysis of Chinese forest musk deer. *J Genet.* (2017) 96:1033–40. doi: 10.1007/s12041-017-0872-x

33. Fox AD, Hescott BJ, Blumer AC, Slonim DK. Connectedness of PPI network neighborhoods identifies regulatory hub proteins. *Bioinformatics.* (2011) 27:1135–42. doi: 10.1093/bioinformatics/btr099

34. Vallabhajosyula RR, Chakravarti D, Lutfeali S, Ray A, Raval A. Identifying hubs in protein interaction networks. *PLoS ONE.* (2009) 4:e5344. doi: 10.1371/journal.pone.0005344

35. Quinton LJ, Walkey AJ, Mizgerd JP. Integrative physiology of pneumonia. *Physiol Rev.* (2018) 98:1417–64. doi: 10.1152/physrev.00032.2017

36. Mizgerd JP. Pathogenesis of severe pneumonia: advances and knowledge gaps. *Curr Opin Pulm Med.* (2017) 23:193–7. doi: 10.1097/MCP.0000000000000365

37. Wygrecka M, Marsh LM, Morty RE, Henneke I, Guenther A, Lohmeyer J, et al. Enolase-1 promotes plasminogen-mediated recruitment of monocytes to the acutely inflamed lung. *Blood.* (2009) 113:5588–98. doi: 10.1182/blood-2008-08-170837

38. Wu H, Santoni-Rugiu E, Ralfkiaer E, Porse BT, Moser C, Høiby N, et al. Lipocalin 2 is protective against E. coli pneumonia. *Respir Res.* (2010) 11:96. doi: 10.1186/1465-9921-11-96

39. Sheldon JR, Himmel LE, Kunkle DE, Monteith AJ, Maloney KN, Skaar EP. Lipocalin-2 is an essential component of the innate immune response to Acinetobacter baumannii infection. *PLoS Pathog.* (2022) 18:e1010809. doi: 10.1371/journal.ppat.1010809

40. Warszawska JM, Gawish R, Sharif O, Sigel S, Doninger B, Lakovits K, et al. Lipocalin 2 deactivates macrophages and worsens pneumococcal pneumonia outcomes. *J Clin Invest.* (2013) 123:3363–72. doi: 10.1172/JCI67911

41. Liu W, He P, Cheng B, Mei CL, Wang YF, Wan JJ. Chlamydia pneumoniae disturbs cholesterol homeostasis in human THP-1 macrophages via JNK-PPARγ dependent signal transduction pathways. *Microbes Infect.* (2010) 12:1226–35. doi: 10.1016/j.micinf.2010.09.004

42. Stevenson ER, Wilkinson ML, Abramova E, Guo C, Gow AJ. Intratracheal administration of Acyl Coenzyme A Acyltransferase-1 inhibitor K-604 reduces pulmonary inflammation following bleomycin-induced lung injury. *J Pharmacol Exp Ther.* (2022) 382:356–65. doi: 10.1124/jpet.122.001284

43. Zhao Y, Olonisakin TF, Xiong Z, Hulver M, Sayeed S, Yu MT, et al. Thrombospondin-1 restrains neutrophil granule serine protease function and regulates the innate immune response during Klebsiella pneumoniae infection. *Mucosal Immunol.* (2015) 8:896–905. doi: 10.1038/mi.2014.120

44. Guo Q, Shen N, Yuan K, Li J, Wu H, Zeng Y, et al. 3rd, Bansal AK, Singh BB, Gao H Caveolin-1 plays a critical role in host immunity against Klebsiella pneumoniae by regulating STAT5 and Akt activity. *Eur J Immunol.* (2012) 42:1500–11. doi: 10.1002/eji.201142051

45. Brown JP, Taube C, Miyahara N, Koya T, Pelanda R, Gelfand EW, et al. Arhgef1 is required by T cells for the development of airway hyperreactivity and inflammation. *Am J Respir Crit Care Med.* (2007) 176:10–9. doi: 10.1164/rccm.200702-270OC

46. Mirzapoiazova T, Moitra J, Moreno-Vinasco L, Sammani S, Turner JR, Chiang ET, et al. Non-muscle myosin light chain kinase isoform is a viable molecular target in acute inflammatory lung injury. *Am J Respir Cell Mol Biol.* (2011) 44:40–52. doi: 10.1165/rcmb.2009-0197OC

47. Wang A, Johnston SC, Chou J, Dean D. A systemic network for Chlamydia pneumoniae entry into human cells. *J Bacteriol.* (2010) 192:2809–15. doi: 10.1128/JB.01462-09

48. Wei J, Huang XJ, Huang Y, Xiong MY, Yao XY, Huang ZN Li SN, et al. Key immune-related gene ITGB2 as a prognostic signature for acute myeloid leukemia. *Ann Transl Med.* (2021) 9:1386. doi: 10.21037/atm-21-3641

49. Altorki T, Muller W, Brass A, Cruickshank S. The role of β(2) integrin in dendritic cell migration during infection. *BMC Immunol.* (2021) 22:2. doi: 10.1186/s12865-020-00394-5

50. Oh A, Jeon S, Jeong MG, Kim HK, Kang J, Lee YS, et al. HSPB1 inhibitor J2 attenuates lung inflammation through direct modulation of Ym1 production and paracrine signaling. *Biomed Pharmacother.* (2021) 143:112225. doi: 10.1016/j.biopha.2021.112225

51. Li PH, Cai YJ, Zhu XL, Yang JD, Yang SQ, Huang W, et al. Epinephelus coioides Hsp27 negatively regulates innate immune response and apoptosis induced by Singapore grouper iridovirus (SGIV) infection. *Fish Shellfish Immunol.* (2022) 120:470–80. doi: 10.1016/j.fsi.2021.12.016

52. Guardado S, Ojeda-Juárez D, Kaul M, Nordgren TM. Comprehensive review of lipocalin 2-mediated effects in lung inflammation. *Am J Physiol Lung Cell Mol Physiol.* (2021) 321:L726–l733. doi: 10.1152/ajplung.00080.2021

53. Xiao X, Yeoh BS, Vijay-Kumar M. Lipocalin 2: An Emerging Player in Iron Homeostasis and Inflammation. *Annu Rev Nutr.* (2017) 37:103–30. doi: 10.1146/annurev-nutr-071816-064559

54. Benarafa C, Priebe GP Remold-O'Donnell E. The neutrophil serine protease inhibitor serpinb1 preserves lung defense functions in Pseudomonas aeruginosa infection. *J Exp Med.* (2007) 204:1901–9. doi: 10.1084/jem.20070494

55. Farley K, Stolley JM, Zhao P, Cooley J, Remold-O'Donnell E. A serpinB1 regulatory mechanism is essential for restricting neutrophil extracellular trap generation. *J Immunol.* (2012) 189:4574–81. doi: 10.4049/jimmunol.1201167

56. Zhao P, Hou L, Farley K, Sundrud MS, Remold-O'Donnell E. SerpinB1 regulates homeostatic expansion of IL-17+ γδ and CD4+ Th17 cells. *J Leukoc Biol.* (2014) 95:521–30. doi: 10.1189/jlb.0613331

57. Benarafa C, LeCuyer TE, Baumann M, Stolley JM, Cremona TP. Remold-O'Donnell E: SerpinB1 protects the mature neutrophil reserve in the bone marrow. *J Leukoc Biol.* (2011) 90:21–9. doi: 10.1189/jlb.0810461

58. Kenne E, Soehnlein O, Genové G, Rotzius P, Eriksson EE, Lindbom L. Immune cell recruitment to inflammatory loci is impaired in mice deficient in basement membrane protein laminin alpha4. *J Leukoc Biol.* (2010) 88:523–8. doi: 10.1189/jlb.0110043

59. Zheng M, Ambesi A, McKeown-Longo PJ. Role of TLR4 receptor complex in the regulation of the innate immune response by fibronectin. *Cells.* (2020) 9:216. doi: 10.3390/cells9010216

60. Kelsh R, You R, Horzempa C, Zheng M, McKeown-Longo PJ. Regulation of the innate immune response by fibronectin: synergism between the III-1 and EDA domains. *PLoS ONE.* (2014) 9:e102974. doi: 10.1371/journal.pone.0102974

61. Zhang XX, Luo JH, Wu LQ. FN1 overexpression is correlated with unfavorable prognosis and immune infiltrates in breast cancer. *Front Genet.* (2022) 13:913659. doi: 10.3389/fgene.2022.913659

62. Wang Y, Shen Y, Wang S, Shen Q, Zhou X. The role of STAT3 in leading the crosstalk between human cancers and the immune system. *Cancer Lett.* (2018) 415:117–28. doi: 10.1016/j.canlet.2017.12.003

63. Chen W, Dai X, Chen Y, Tian F, Zhang Y, Zhang Q, et al. Significance of STAT3 in immune infiltration and drug response in cancer. *Biomolecules.* (2020) 10:834. doi: 10.3390/biom10060834

64. Hu YS, Han X, Liu XH. STAT3: a potential drug target for tumor and inflammation. *Curr Top Med Chem.* (2019) 19:1305–17. doi: 10.2174/1568026619666190620145052

65. Guo L, Wang Q, Zhang D. MicroRNA-4485 ameliorates severe influenza pneumonia via inhibition of the STAT3/PI3K/AKT signaling pathway. *Oncol Lett.* (2020) 20:215. doi: 10.3892/ol.2020.12078

66. Zhou H, Lu Y, Wei H, Chen Y, Limpanon Y, Dekumyoy P, et al. Stat3/IL-6 signaling mediates sustained pneumonia induced by Agiostrongylus cantonensis. *PLoS Negl Trop Dis.* (2022) 16:e0010461. doi: 10.1371/journal.pntd.0010461

67. Chen Y, Dong S, Tian L, Chen H, Chen J, He C. Combination of azithromycin and methylprednisolone alleviates Mycoplasma pneumoniae induced pneumonia by regulating miR-499a-5p/STAT3 axis. *Exp Ther Med.* (2022) 24:578. doi: 10.3892/etm.2022.11515

68. Shaukat A, Hanif S, Shaukat I, Shukat R, Rajput SA, Jiang K, et al. Upregulated-gene expression of pro-inflammatory cytokines, oxidative stress and apoptotic markers through inflammatory, oxidative and apoptosis mediated signaling pathways in Bovine Pneumonia. *Microb Pathog.* (2021) 155:104935. doi: 10.1016/j.micpath.2021.104935

69. Choudhary M, Choudhary BK, Chandra Ghosh R, Bhoyar S, Chaudhari S, Barbuddhe SB. Cultivable microbiota and pulmonary lesions in polymicrobial bovine pneumonia. *Microb Pathog.* (2019) 134:103577. doi: 10.1016/j.micpath.2019.103577

70. Panciera RJ, Confer AW. Pathogenesis and pathology of bovine pneumonia. *Vet Clin North Am Food Anim Pract.* (2010) 26:191–214. doi: 10.1016/j.cvfa.2010.04.001

71. van der Wal T, van Amerongen R. Walking the tight wire between cell adhesion and WNT signalling: a balancing act for β-catenin. *Open Biol.* (2020) 10:200267. doi: 10.1098/rsob.200267

72. Jesinghaus M, Konukiewitz B, Foersch S, Stenzinger A, Steiger K. Appendiceal goblet cell carcinoids and adenocarcinomas ex-goblet cell carcinoid are genetically distinct from primary colorectal-type adenocarcinoma of the appendix. *Mod Pathol.* (2018) 31:829–39. doi: 10.1038/modpathol.2017.184

73. Silva-García O, Valdez-Alarcón JJ, Baizabal-Aguirre VM. Wnt/β-catenin signaling as a molecular target by pathogenic bacteria. *Front Immunol.* (2019) 10:2135. doi: 10.3389/fimmu.2019.02135

74. Hussain M, Xu C, Lu M, Wu X, Tang L, Wu X. Wnt/β-catenin signaling links embryonic lung development and asthmatic airway remodeling. *Biochim Biophys Acta Mol Basis Dis.* (2017) 1863:3226–42. doi: 10.1016/j.bbadis.2017.08.031

75. Raslan AA, Yoon JK. WNT signaling in lung repair and regeneration. *Mol Cells.* (2020) 43:774–83. doi: 10.14348/molcells.2020.0059

76. Baarsma HA, Königshoff M. 'WNT-er is coming': WNT signalling in chronic lung diseases. *Thorax.* (2017) 72:746–59. doi: 10.1136/thoraxjnl-2016-209753

77. Königshoff M, Eickelberg O. WNT signaling in lung disease: a failure or a regeneration signal? *Am J Respir Cell Mol Biol.* (2010) 42:21–31. doi: 10.1165/rcmb.2008-0485TR

78. Chen C, Wang J, Chen J, Zhou L, Wang H, Chen J, et al. Morusin alleviates mycoplasma pneumonia via the inhibition of Wnt/β-catenin and NF-κB signaling. *Biosci Rep.* (2019) 39:BSR20190190. doi: 10.1042/BSR20190190

79. Grassmé H, Henry B, Ziobro R, Becker KA, Riethmüller J, Gardner A, et al. β1-integrin accumulates in cystic fibrosis luminal airway epithelial membranes and decreases sphingosine, promoting bacterial infections. *Cell Host Microbe.* (2017) 21:707–18.e708. doi: 10.1016/j.chom.2017.05.001

80. Jiang Z, Chen Z, Hu L, Qiu L, Zhu L. Calreticulin blockade attenuates murine acute lung injury by inducing polarization of M2 subtype macrophages. *Front Immunol.* (2020) 11:11. doi: 10.3389/fimmu.2020.00011

81. Lukkarinen H, Hogmalm A, Lappalainen U, Bry K. Matrix metalloproteinase-9 deficiency worsens lung injury in a model of bronchopulmonary dysplasia. *Am J Respir Cell Mol Biol.* (2009) 41:59–68. doi: 10.1165/rcmb.2008-0179OC

82. Böttcher T, Spreer A, Azeh I, Nau R, Gerber J. Matrix metalloproteinase-9 deficiency impairs host defense mechanisms against Streptococcus pneumoniae in a mouse model of bacterial meningitis. *Neurosci Lett.* (2003) 338:201–4. doi: 10.1016/S0304-3940(02)01406-4

83. Hong JS, Greenlee KJ, Pitchumani R, Lee SH, Song LZ, Shan M, et al. Dual protective mechanisms of matrix metalloproteinases 2 and 9 in immune defense against Streptococcus pneumoniae. *J Immunol.* (2011) 186:6427–36. doi: 10.4049/jimmunol.1003449

84. Villar J, Zhang H, Slutsky AS. Lung repair and regeneration in ARDS: role of PECAM1 and Wnt signaling. *Chest.* (2019) 155:587–94. doi: 10.1016/j.chest.2018.10.022

85. Shi J, Hu CL, Gao YF, Liao XX, Xu H. The relationship between platelet endothelial cell adhesion molecule-1 and paraquat-induced lung injury in rabbits. *World J Emerg Med.* (2012) 3:60–4. doi: 10.5847/wjem.j.issn.1920-8642.2012.01.011

86. Binsker U, Kohler TP, Hammerschmidt S. Contribution of human Thrombospondin-1 to the pathogenesis of gram-positive bacteria. *J Innate Immun.* (2019) 11:303–15. doi: 10.1159/000496033

87. Qu Y, Olonisakin T, Bain W, Zupetic J, Brown R, Hulver M, et al. Thrombospondin-1 protects against pathogen-induced lung injury by limiting extracellular matrix proteolysis. *JCI Insight.* (2018) 3:e96914. doi: 10.1172/jci.insight.96914

88. Anas AA, de Vos AF, Hoogendijk AJ, van Lieshout MH, van Heijst JW, Florquin S, et al. Endoplasmic reticulum chaperone gp96 in macrophages is essential for protective immunity during Gram-negative pneumonia. *J Pathol.* (2016) 238:74–84. doi: 10.1002/path.4637

89. Smith A, Bourdeau I, Wang J, Bondy CA. Expression of Catenin family members CTNNA1, CTNNA2, CTNNB1 and JUP in the primate prefrontal cortex and hippocampus. *Brain Res Mol Brain Res.* (2005) 135:225–31. doi: 10.1016/j.molbrainres.2004.12.025

90. Chignalia AZ, Vogel SM, Reynolds AB, Mehta D, Dull RO, Minshall RD, et al. p120-catenin expressed in alveolar type II cells is essential for the regulation of lung innate immune response. *Am J Pathol.* (2015) 185:1251–63. doi: 10.1016/j.ajpath.2015.01.022

91. Pai SG, Carneiro BA, Mota JM, Costa R, Leite CA, Barroso-Sousa R, et al. Wnt/beta-catenin pathway: modulating anticancer immune response. *J Hematol Oncol.* (2017) 10:101. doi: 10.1186/s13045-017-0471-6

92. Tong J, Ji X, Zhang H, Xiong B, Cui D, Jiang L. The analysis of the ubiquitylomic responses to streptococcus agalactiae infection in bovine mammary gland epithelial cells. *J Inflamm Res.* (2022) 15:4331–43. doi: 10.2147/JIR.S368779

93. Zhu B, Wu Y, Huang S, Zhang R, Son YM, Li C, et al. Uncoupling of macrophage inflammation from self-renewal modulates host recovery from respiratory viral infection. *Immunity.* (2021) 54:1200–18.e1209. doi: 10.1016/j.immuni.2021.04.001

94. Liu M, Zhang Y, Yang J, Cui X, Zhou Z, Zhan H, et al. ZIP4 Increases expression of transcription factor ZEB1 to promote integrin α3β1 signaling and inhibit expression of the gemcitabine transporter ENT1 in pancreatic cancer cells. *Gastroenterology*. (2020) 158:679–92.e671. doi: 10.1053/j.gastro.2019.10.038

95. Mautone L, Ferravante C, Tortora A, Tarallo R, Giurato G, Weisz A, et al. Higher integrin Alpha 3 beta1 expression in papillary thyroid cancer is associated with worst outcome. *Cancers*. (2021) 13:2937. doi: 10.3390/cancers13122937

96. Zhang Y, Shang L, Zhang J, Liu Y, Jin C, Zhao Y, et al. An antibody-based proximity labeling map reveals mechanisms of SARS-CoV-2 inhibition of antiviral immunity. *Cell Chem Biol*. (2022) 29:5–18.e16. doi: 10.1016/j.chembiol.2021.10.008

97. Plosa EJ, Benjamin JT, Sucre JM, Gulleman PM, Gleaves LA, Han W, et al. β1 Integrin regulates adult lung alveolar epithelial cell inflammation. *JCI Insight*. (2020) 5:129259. doi: 10.1172/jci.insight.129259

98. Li Y, Li F, Bai X, Li Y, Ni C, Zhao X, et al. ITGA3 is associated with immune cell infiltration and serves as a favorable prognostic biomarker for breast cancer. *Front Oncol*. (2021) 11:658547. doi: 10.3389/fonc.2021.658547

frontiers | Frontiers in Veterinary Science

TYPE Original Research
PUBLISHED 09 November 2022
DOI 10.3389/fvets.2022.1014286

Check for updates

OPEN ACCESS

EDITED BY
Abdul Rasheed Baloch,
University of Karachi, Pakistan

REVIEWED BY
Ali Raza Jahejo,
Shanxi Agricultural University, China
Paolo Zambonelli,
University of Bologna, Italy

*CORRESPONDENCE
Linsen Zan
zanlinsen@163.com

†These authors have contributed equally to this work

SPECIALTY SECTION
This article was submitted to Livestock Genomics, a section of the journal Frontiers in Veterinary Science

RECEIVED 08 August 2022
ACCEPTED 16 September 2022
PUBLISHED 09 November 2022

CITATION
Wang X, Wang J, Raza SHA, Deng J, Ma J, Qu X, Yu S, Zhang D, Alshammari AM, Almohaimeed HM and Zan L (2022) Identification of the hub genes related to adipose tissue metabolism of bovine. *Front. Vet. Sci.* 9:1014286. doi: 10.3389/fvets.2022.1014286

COPYRIGHT
© 2022 Wang, Wang, Raza, Deng, Ma, Qu, Yu, Zhang, Alshammari, Almohaimeed and Zan. This is an open-access article distributed under the terms of the Creative Commons Attribution License (CC BY). The use, distribution or reproduction in other forums is permitted, provided the original author(s) and the copyright owner(s) are credited and that the original publication in this journal is cited, in accordance with accepted academic practice. No use, distribution or reproduction is permitted which does not comply with these terms.

Identification of the hub genes related to adipose tissue metabolism of bovine

Xiaohui Wang[1†], Jianfang Wang[1†], Sayed Haidar Abbas Raza[1], Jiahan Deng[1], Jing Ma[1], Xiaopeng Qu[1], Shengchen Yu[1], Dianqi Zhang[1], Ahmed Mohajja Alshammari[2], Hailah M. Almohaimeed[3] and Linsen Zan[1,4*]

[1]College of Animal Science and Technology, Northwest A&F University, Xianyang, China, [2]Department of Biology, College of Science, University of Hail, Ha'il, Saudi Arabia, [3]Department of Basic Science, College of Medicine, Princess Nourah Bint Abdulrahman University, Riyadh, Saudi Arabia, [4]National Beef Cattle Improvement Center, Northwest A&F University, Xianyang, China

Due to the demand for high-quality animal protein, there has been consistent interest in how to obtain more high-quality beef. As well-known, the adipose content of beef has a close connection with the taste and quality of beef, and cattle with different energy or protein diet have corresponding effects on the lipid metabolism of beef. Thus, we performed weighted gene co-expression network analysis (WGCNA) with subcutaneous adipose genes from Norwegian red heifers fed different diets to identify hub genes regulating bovine lipid metabolism. For this purpose, the RNA sequencing data of subcutaneous adipose tissue of 12-month-old Norwegian red heifers ($n = 48$) with different energy or protein levels were selected from the GEO database, and 7,630 genes with the largest variation were selected for WGCNA analysis. Then, three modules were selected as hub genes candidate modules according to the correlation between modules and phenotypes, including pink, magenta and grey60 modules. GO and KEGG enrichment analysis showed that genes were related to metabolism, and participated in Rap, MAPK, AMPK, VEGF signaling pathways, and so forth. Combined gene interaction network analysis using Cytoscape software, eight hub genes of lipid metabolism were identified, including *TIA1, LOC516108, SNAPC4, CPSF2, ZNF574, CLASRP, MED15* and *U2AF2*. Further, the expression levels of hub genes in the cattle tissue were also measured to verify the results, and we found hub genes in higher expression in muscle and adipose tissue in adult cattle. In summary, we predicted the key genes of lipid metabolism in the subcutaneous adipose tissue that were affected by the intake of various energy diets to find the hub genes that coordinate lipid metabolism, which provide a theoretical basis for regulating beef quality.

KEYWORDS

different diets, WGCNA, lipid metabolism, energy metabolism, hub genes

Introduction

Because the worldwide demand for meat products is consistently increasing (1, 2), how to produce high-quality beef has always been a topic of concern among scholars (3). RNA sequencing has widely been used in animals to mine potential regulatory molecules for many years. For instance, using this approach, researchers have identified several pathways by which KLF6 is involved in lipid metabolism (4). Studies have indicated that the variation of the energy and protein levels in feed (5), and the change in the energy and protein intake ratio (6) have a non-negligible regulatory influence on cattle growth and development, production performance, metabolic level, immune function, and reproductive capacity. Meanwhile, the content and distribution of adipose tissue which plays a role in the metabolism of meat is an important factor affecting the taste and quality of beef (7, 8). A study demonstrated that feeding a high-energy diet effectively increased fat deposition in fattening cattle (9). However, monotonous performance and phenotypic changes have prevented us from understanding the molecular mechanistic effects of different energy and protein intakes on beef-related metabolism (10). At present, the complex molecular regulatory mechanism of bovine subcutaneous adipose tissue is not clear (11). Scholars at home and abroad have predicted many key signaling pathways and regulatory genes regulating bovine lipid metabolism through molecular biology and bioinformatics analysis and other research methods (12–14).

Weighted gene co-expression network analysis (WGCNA) is currently the preferred algorithm for calculating the correlation between genes and phenotypes (15). Based on high-throughput RNA sequencing data, it relies on the R software package (16) for data analysis, constructs a cluster tree portraying different gene modules, integrates genes with the same biological function into one module systematically (17). The gene expression patterns within the module are comparable (18), when they are associated with phenotypes and participate in the same biological process (19). To sum up, it is suitable for analyzing complex regulatory mechanisms. At present, in the research of livestock and poultry, researchers mainly forecast the regulatory network of important economic traits (20), the molecular regulatory mechanism of disease occurrence (21), and the associated network between the phenotype of livestock and the internal molecular regulatory mechanism by incorporating other bioinformatics analysis tools (22, 23). Therefore, it is viable to employ WGCNA to explore hub genes and metabolic processes that alter fat deposition. At present, some results have been moderately reported in pigs (24), chickens (25), cattle (26), and other animals (27).

Here, the association analysis between subcutaneous adipose tissue genes of Norwegian red heifers fed on different energy diets was conducted to predict the hub metabolic regulatory genes of subcutaneous adipose tissue. Qinchuan beef cattle were used as the molecular research objects to verify the generality of this result, which provide a theoretical basis for regulating the metabolism of subcutaneous adipose tissue and improving beef quality.

Materials and methods

Sample collection and processing

Tissues from the heart, liver, spleen, lung, kidney, subcutaneous fat, and muscle from a healthy adult cattle and newborn calf were collected after slaughter, frozen immediately with liquid nitrogen, and stored at −80°C. The samples in this study were collected from healthy Qinchuan beef cattle with consistent growth and bred at the National Beef Cattle Improvement Center of Northwest Agriculture and Forestry University (Yangling, China).

Data collection and collation

The reads count matrix of transcriptome data of each sample used in this study were obtained from GSE79347 dataset (https://www.ncbi.nlm.nih.gov/geo/query/acc.cgi?acc=GSE79347). The datasets respectively were from two types of Norwegian red heifers (high-yielding dairy group, hmy; normal milk producing group, lcm) fed with four kinds of feeds, including high energy high protein (HEHP), high energy low protein (HELP), low energy high protein (LEHP), and low energy low protein (LELP). Six biological replicates were taken from each treatment group, with a total of 48 samples.

The raw data were converted into standard fastq format through SRA tools (version 2.8.1) software, Then the quality control and preprocessing of the data were carried out using the FastQC (version 0.11.9) (https://www.bioinformatics.babraham.ac.uk/projects/fastqc/). For downstream WGCNA analysis, we first extracted the protein-coding gene-set according to gene annotation information from Ensembl database (https://asia.ensembl.org/index.html). Then, the FPKM (Fragments Per Kilobase of exon model per Million mapped fragments) value of each gene was calculated according to the reads count, which aims to normalize the gene expression.

Weighted gene co-expression network construction

The weighted co-expression network was constructed by the WGCNA package in R Studio (28, 29). The gene expression level, first, was calculated based on the raw counts of each sample to construct a gene expression matrix of 48 samples according to FPKM (Fragments per Kilobase of transcript per million) which

is a standardized measurement of transcription abundance. The top 75% (30) genes with the largest variation were selected by the gene expression level to construct a correlation matrix. Then we chose the soft threshold β that best fits the scale-free network to obtain the scale-free adjacency matrix which was computed into a Topological Overlap Matrix (TOM). We constructed a hierarchical clustering tree according to the corresponding dissimilarity (1-TOM), the minimum number threshold of genes in each module was set to 50, to identify modules by merging co-expression similarity genes. In addition, similar modules were merged based on the dissimilarity of module eigengenes with a threshold less than 0.20 (31). Finally, Pearson correlation analysis was performed between modular characteristic genes (ME) and lipid metabolism. The results of the correlation and significance levels of module eigengenes (MEs) with phenotypes were displayed by the R software package ggplot2, and the gene significance (GS) and module membership (MM) values were exported.

Functional annotation of module genes and screening of hub genes

The Pearson correlation coefficient greater than 0.3 and $p < 0.05$ were used as thresholds to select modules for GO function annotation and Kyoto Encyclopedia of Genes and Genomes (KEGG) pathway enrichment analysis. The online tool g:Profiler (https://biit.cs.ut.ee/gprofiler/) was used for GO function annotation with default parameters (32). There were three categories of GO annotation: biological process (BP), cellular component (CC), and molecular function (MF). The results were consistent with a $p < 0.05$ arranged in ascending order of p-value, and the top 5 of the obtained results were displayed. The module genes of KEGG pathway enrichment analysis were implemented by KOBAS (http://kobas.cbi.pku.edu.cn/genelist/) with default parameters (33) and screening condition for significant enrichment according to $p < 0.05$.

The higher the GS value, the greater the correlation between this gene and this phenotype is; the higher the MM value is, the greater the contribution of this characteristic gene to this module; the gene with the highest GS and MM values in the module is regarded as a hub gene. Therefore, the intramodular key genes were chosen based on $|GS| > 0.2$, $|MM| > 0.9$ with a $p < 0.05$ (34). The interaction network between key genes obtained through weighted gene co-expression network analysis and its target genes were arranged in descending order of weight, and the top 200 (35) genes were selected and imported into Cytoscape_V3.8.2 software (36) to select hub genes.

Quantitative real-time PCR analysis

After processing the beef tissues, we used RNAiso Plus Kit (Trizol, Takara, Beijing, China) to extract the total RNA from the beef heart, liver, spleen, lung, kidney, muscle, and adipose tissues. The cDNA was obtained by reverse transcription kit (PrimeScript^{TM} RT reagent Kit with gDNA Ewraser, Takara, Beijing, China). The DNA and CDS region sequences of hub genes were downloaded from the NCBI database for primer design. Then, the designed primer sequences were uploaded to BLAST (https://blast.ncbi.nlm.nih.gov/Blast.cgi) for specificity test. Primer sequences are shown in Table 1. The relative expression levels of hub genes in adult cattle heart, liver, spleen, lung, kidney, muscle, and adipose tissue were measured, and the expression levels of hub genes in the adult cattle and the newborn calves' adipose tissue were compared. Quantitative real-time PCR were performed using the PerfectStart Green qPCR SuperMix kit (TransGen Biotech, Beijing, China), and the results were obtained. It should be noted that three biological replicates and technical replicates were performed for all experiments. SPSS 25 (37) and Graphpad Prism 9 (38) softwares were used for difference significance analysis and mapping, respectively.

TABLE 1 The hub genes' quantitative PCR primer sequences.

Genes		Primer sequences(5′-3′)	Annealing temperature
β-actin	F:	ATCGGCAATGAGCGGTTC	60°C
	R:	CGTGTTGGCGTAGAGGTC	60°C
TIA1	F:	GGATACAGCCGGAAATGATCCA	60°C
	R:	TGTGTGCTGACAACGGTACT	60°C
LOC516108	F:	GCTGTAGGGCGGAAGATGTG	60°C
	R:	AGCCTCCTGTCCAGAGACATA	60°C
SNAPC4	F:	CTTCAAGCAGTTGCCAAGTATG	60°C
	R:	CCAACGCCGTATTTTTCTATC	60°C
CPSF2	F:	CGCTTTGGGGCAGGACTTAT	60°C
	R:	ATAAATTCCTTCTGGGCGGGG	60°C
CLASRP	F:	GAAGAAGGCATCCATCGGCTACAC	60°C
	R:	GCATCCTGACGAAGTCGCCATC	60°C
ZNF574	F:	TACCGCAAAGCAGAAGAGG	60°C
	R:	ACCTCGGTCACCACCTCAGT	60°C
MED15	F:	ACGTTTCGGGGCAGGAGA	60°C
	R:	TCTTGGCCTTCAGGAACACG	60°C
U2AF2	F:	GTCTCGCGCAGCCTTCTTA	60°C
	R:	GAGAGGAAACGGAGAAGGGC	60°C

Statistical analysis

The relative expression levels of different quantitative real-time PCR data were analyzed by the $2^{-\Delta\Delta Ct}$ method. All experiments were performed in triplicate. The results were expressed as mean ± standard error of the mean (SEM). Statistical analyzes were performed with SPSS 25 (37) and Graphpad Prism 9 (38). Differences between groups were

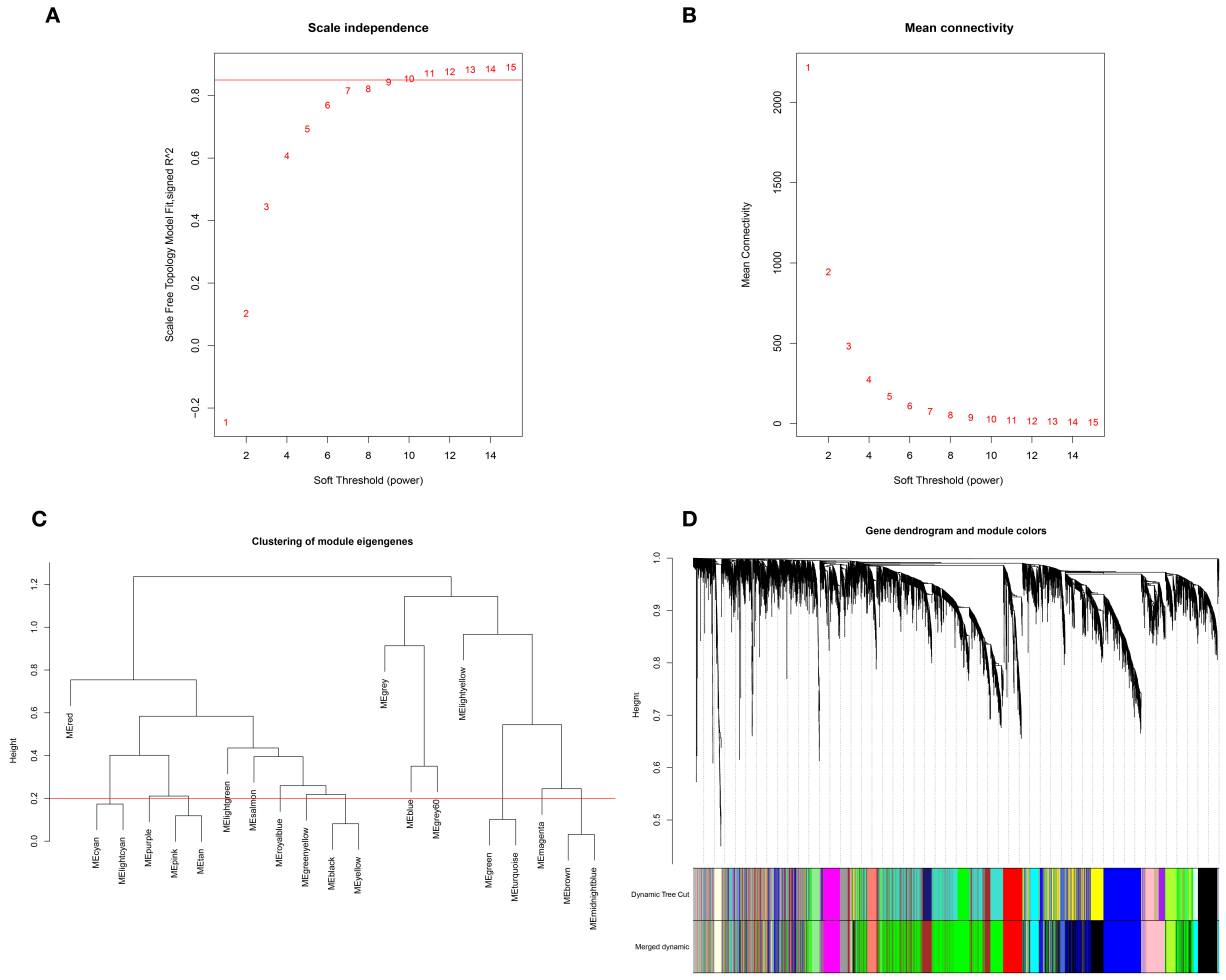

FIGURE 1
Identify soft thresholds and filter modules. **(A)** Scale-free topology fit index. **(B)** Mean connectivity of different soft-thresholding power. **(C)** The cluster dendrogram of gene modules eigengenes. **(D)** The gene clustering dendrogram.

calculated by Analysis of Variance (ANOVA) methods and significance was indicated by lowercase letters or asterisks. $^{*}p < 0.05$, significant; $^{**}p < 0.01$, moderately significant; $^{***}p < 0.001$, highly significant; and $^{****}p < 0.0001$, extremely significant.

Results

Construction of weighted gene co-expression network

A total of 7,630 genes, which was the largest variation, were obtained for subsequent analysis. There was no outlier in the samples through 48 samples drawn with a hierarchical clustering tree. First, the soft threshold was filtered. When the soft threshold $\beta = 10$ in this test, the scale-free network fitting index (R^2) was greater than 0.85 (Figure 1A) and the average connectivity approached 0 (Figure 1B), which conforms to the characteristics of a scale-free network. Then, by merging similar modules with the dynamic hybrid-cutting method and setting the MEDissThres cutting line to 0.20, light cyan was merged with cyan, yellow was merged with black, turquoise was merged with green, midnight-blue was merged with brown, and tan and purple were merged with pink (Figure 1C). Finally, there were 15 modules with different colors, blue, grey60, red, cyan, pink, light-green, salmon, royal blue, black, green-yellow, light-yellow, magenta, brown, green, and grey (Figure 1D). The number of genes in the different modules had a large variation, from 85 genes in the royal-blue module to 1954 in the green module (Supplementary Table S1).

Identification of candidate modules

As shown in Figure 2, there were three modules among 15 modules whose filter condition $| R | > 0.3$ ($p < 0.05$) were

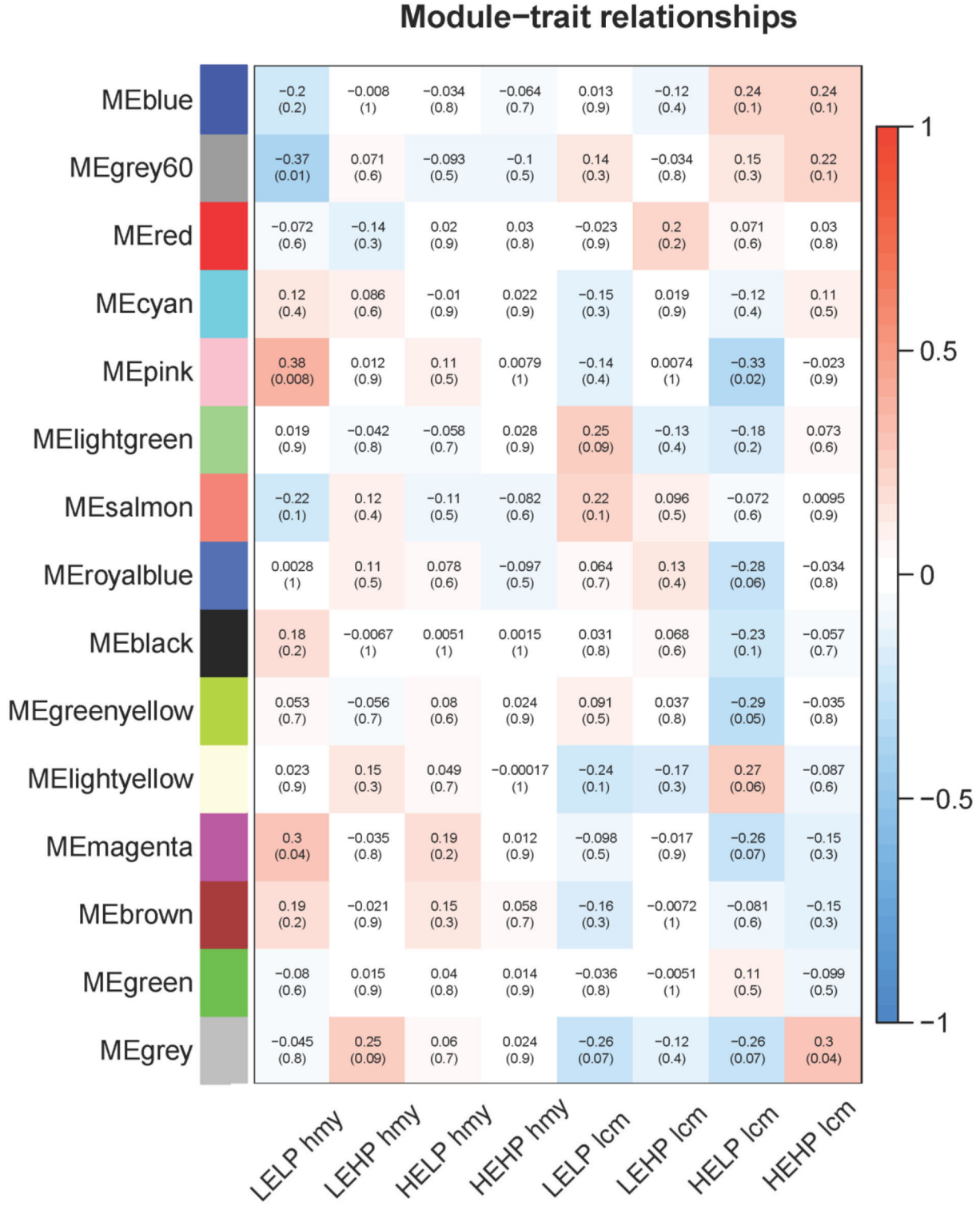

FIGURE 2
Relationship between modules and different feeding methods. The numbers on the top of the block represent the correlation and the *p*-value on the bottom. The horizontal axis represents the different feeding methods, and the vertical axis represents the eigenvector of each module. Red means positive correlation, and blue means negative correlation.

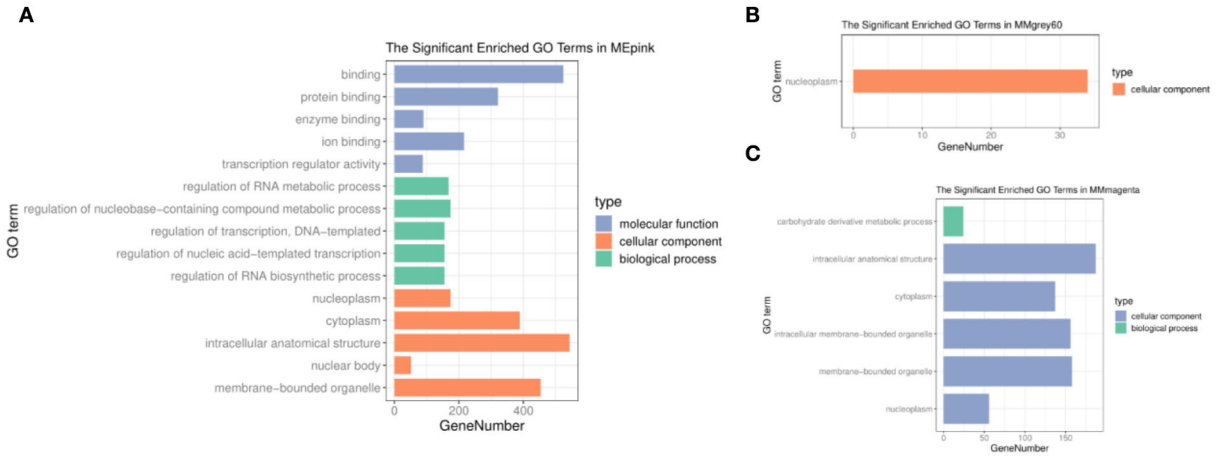

FIGURE 3
GO enrichment analysis. **(A)** Pink module. **(B)** Grey60 module. **(C)** Magenta module.

selected as key genes candidate modules, including the grey60 module, pink module, and magenta module. The grey60 module ($R = -0.37$, $p = 0.01$) significantly negatively correlated with low energy and low protein diets. Conversely, the pink module ($R = 0.38$, $p = 0.008$) significantly correlated with low energy and low protein diets, as well as significantly negatively associated with high energy and low protein diets ($R = -0.33$, $p = 0.02$). The magenta module ($R = 0.3$, $p = 0.04$) was significantly positively related to low energy and low protein diets. According to the analysis results, the different energy intakes of Norwegian red heifers had a significant impact on their gene expression. Therefore, these three modules were screened as lipid metabolism-related modules for subsequent functional analysis and identification of hub regulatory genes.

Functional enrichment analysis of three modules

To understand the molecular functions and biological pathways of genes in co-expression modules closely correlated with different feeding methods, the genes of three modules were executed to GO and KEGG enrichment analyzes above. Among the GO terms (Supplementary Table S2), the pink module genes were mainly used as nucleoplasm, cytoplasmic, and organelle components that participated in the regulation of the RNA metabolic process, regulation of nucleobase compound metabolic process, regulation of transcription, regulation of nucleic acid–templated transcription, and regulation of RNA biosynthetic process (Figure 3A). The cellular component of the grey60 module genes was significantly enriched in the nucleoplasm (Figure 3B). Moreover, the biological processes of the magenta module were closely related to carbohydrate derivative metabolic processes (Figure 3C).

The KEGG enrichment results of the pink module showed that the pathways, such as Rap1, MAPK, Notch, VEGF, IL-17, GnRH signaling pathway, and beta-alanine metabolism were related to different energy intakes (Figure 4A). Additionally, the pancreatic secretion, glycerophospholipid metabolism, Rap1, and MAPK signaling pathway were enriched in the grey60 module (Figure 4B) and the thermogenesis process, insulin resistance process, non-alcoholic fatty liver disease (NAFLD), oxidative phosphorylation, pyrimidine metabolism, insulin signaling pathway, adipocytokine signaling pathway, AMPK signaling pathway, metabolic pathways, and VEGF signaling pathway were enriched in the magenta module and were closely associated with low energy and low protein diets (Figure 4C). The complete results are shown in Supplementary Table S3.

Hub genes associated with lipid metabolism

To identify hub genes, $|\,GS\,| > 0.2$, $|\,MM\,| > 0.9$, and weighted $p < 0.05$ were used as the identification criteria in grey60, pink, and magenta modules (Supplementary Table S4). The *TIA1* gene in the grey60 module (Figure 5A) and the *LOC516108* gene in the magenta module (Figure 5B) met the requirements, which were exported to Cytoscape to construct a network of relationships between genes. The pink module had more genes, so the top 200 genes were selected according to weight, calculated, and visualized using the Cytohubba tab in Cytoscape (Figure 5C). The results showed that *TIA1*, *LOC516108*, *SNAPC4*, *CPSF2*, *ZNF574*, *CLASRP*, *MED15*, and *U2AF2* were hub genes.

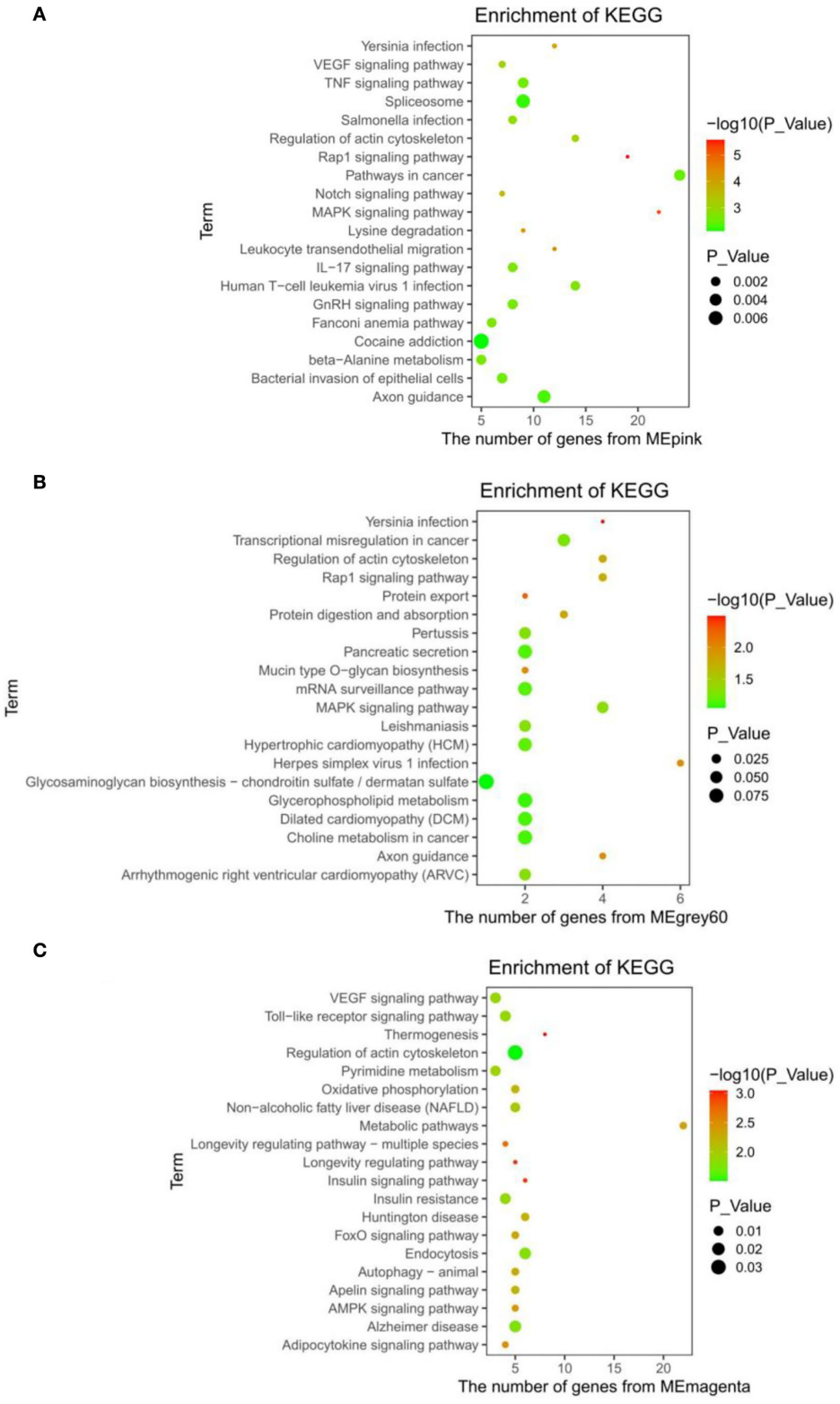

FIGURE 4
KEGG enrichment results. **(A)** Pink module. **(B)** Grey60 module. **(C)** Magenta module.

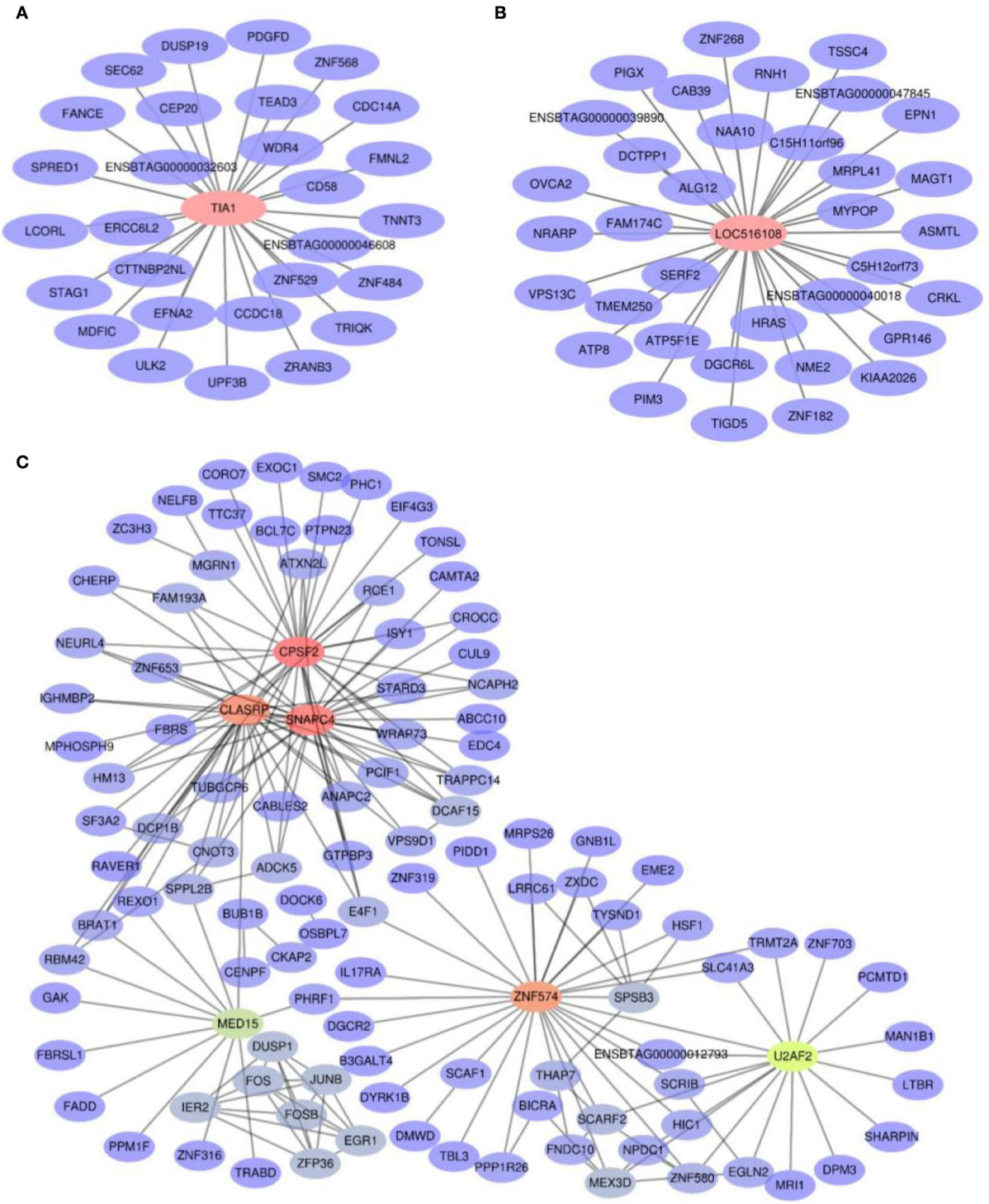

FIGURE 5
Co-expression network diagram of the interaction between hub genes and their target genes. **(A)** Grey60 module. **(B)** Magenta module. **(C)** Pink module.

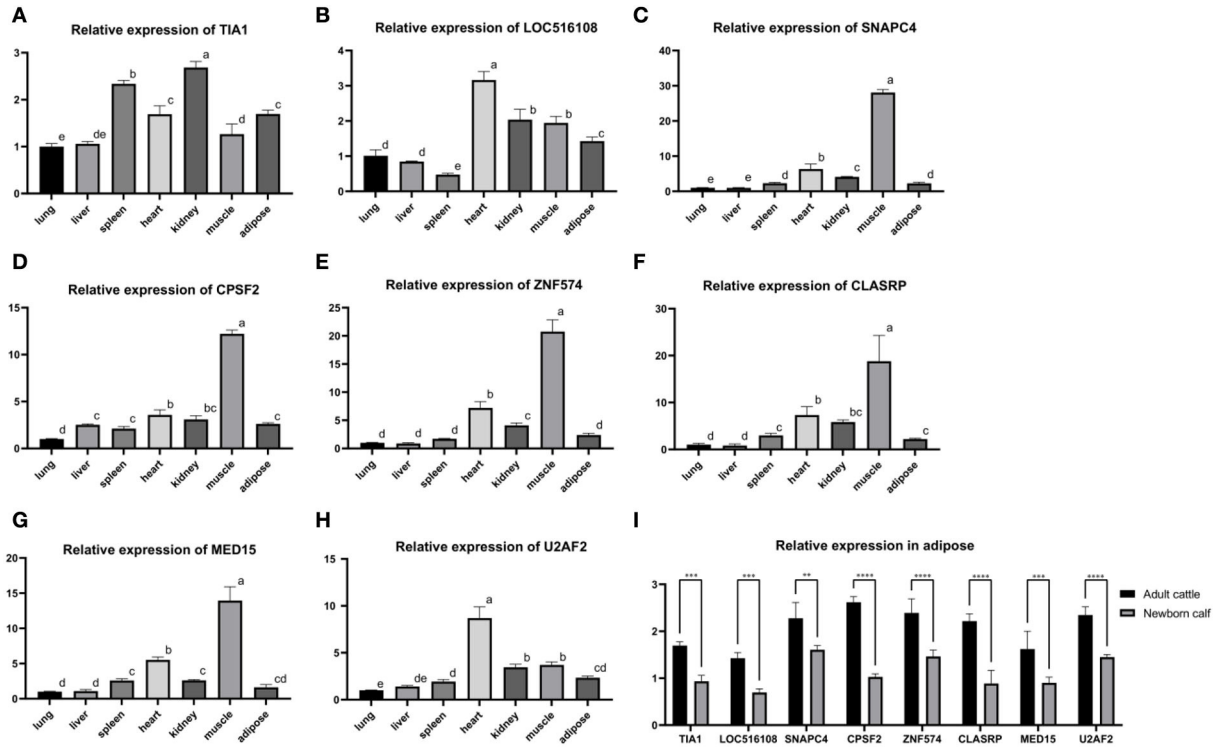

FIGURE 6
The tissue expression profile of 8 hub genes. **(A)** Tissue expression profile of *TIA1*. **(B)** Tissue expression profile of *LOC516108*. **(C)** Tissue expression profile of *SNAPC4*. **(D)** Tissue expression profile of *CPSF2*. **(E)** Tissue expression profile of *ZNF574*. **(F)** Tissue expression profile of *CLASRP*. **(G)** Tissue expression profile of *MED15*. **(H)** Tissue expression profile of *U2AF2*. Superscript letters indicate mean significant difference ($p < 0.05$). Values with superscript letters indicate a mean significant difference ($p < 0.05$). **(I)** Relative expression of adult cattle and newborn calf in adipose. *Denotes significance according to ANOVA methods, *$p < 0.05$, **$p < 0.01$, ***$p < 0.001$, and ****$p < 0.0001$.

Expression analysis of hub genes

RNA was extracted from the heart, liver, spleen, lung, kidney, muscle, and adipose tissue of the adult cattle and the adipose tissue of newborn calves, and reversely transcribed into cDNA. The primers of eight hub genes were combined with the tissue cDNA by PerfectStart Green qPCR SuperMix kit to determine the relative expression levels. The tissue expression profile showed that the relative expression level of eight hub genes was higher in adipose tissue as energy storage and muscle tissue as a metabolic organ (Figures 6A–H). At the same time, the expression level in adipose tissue of adult cattle was significantly higher than the expression level in adipose tissue of newborn calves (Figure 6I).

Discussion

In this research, bioinformatics analysis techniques were used to correlate the metabolic gene expression levels of subcutaneous adipose tissue of Norwegian red heifers with various energy and protein diets, and to predict the regulated lipid metabolism hub genes and biological processes linked with energy intake. The results indicated that different energy intakes were involved in the metabolic process of the subcutaneous adipose tissue of Norwegian red heifers, while different protein intakes did not significantly affect the metabolic process, which was consistent with the results of previous studies; but intergene regulatory network and hub genes were not identified in previous studies (39). Consequently, we eventually identified eight hub genes in three modules that regulate subcutaneous adipose tissue metabolism by weighted gene co-expression network analysis, laying a foundation for further understanding the regulatory mechanism of diverse energy intake on subcutaneous adipose tissue metabolism.

Enrichment analysis results of three modules

GO functional annotation and KEGG enrichment analysis were carried out on the three selected modules, and the

GO results showed that all 138 genes of the grey60 module were used as components of cellular nucleoplasm, and studies showed that part of the eukaryotic ribosome synthesis is carried out in nucleoplasm, resulting in huge energy consumption (40). Chromosome rearrangement in the nucleoplasm is also associated with carbohydrate intake (41), and energy intake may affect the biological processes in the nucleoplasm, thus affecting the expression of genes in the nucleoplasm. In addition, genes significantly associated with low energy and low protein in the grey60 module were primarily enriched in Rap1, MAPK, pancreatic secretion, glycerophospholipid metabolism, and so on. Studies have shown that the Rap1 signaling pathway controls systemic metabolism in the hypothalamus (42), regulates metabolic processes inside and outside the nucleus (43), and regulates energy dissipation processes such as plasma membrane transport signal transduction, endocytosis, exocytosis and cell membrane fusion (44). It has also been found to regulate the glucose metabolism process in mice, which can improve blood glucose and diabetes (45), and Rap1 protein is also an activator of MAPK signaling (46). MAPK signaling pathway is believed to play an important role in the regulation of insulin secretion and type II diabetes mellitus (T2DM) (47), and the secretion dose of insulin controls the lipid accumulation of precursor adipocytes and regulates the metabolism of adipose tissues (48). Besides, the MAPK signaling pathway was also found to be negatively regulated by TREM-2 in diet-induced diabetic mice (49), and genes enriched in the MAPK signaling pathway were shown to be related to lipid metabolism in mice (50). Because the main function of the pancreas is to secrete lipase (51), and the content of hydrolyzed fat of secreted pancreatic lipase accounts for more than 80% of the total diet (52), the pancreatic secretion process was markedly influenced. When mice were fed with various energy diets, the glycerophospholipid metabolism pathway was substantially distinct between low-energy and high-energy experimental groups (53), which was consistent with the results of this research. Therefore, GO and KEGG results revealed that genes in the grey60 module related to low energy and low protein diets were predominantly used as nucleoplasm components to regulate the adipose metabolism pathway.

In the GO results of the pink module, genes were mainly involved in RNA metabolism, regulation of nucleobase compound metabolic process, regulation of transcription, and regulation of nucleic acid-templated transcription as nucleoplasm, cytoplasmic, and organelle components. The KEGG analysis demonstrated that the module genes were mostly enriched in Rap1, MAPK, Notch, VEGF, IL-17, and GnRH signaling pathways. Rap1 and MAPK signaling pathways were also the main gene enrichment pathways in the grey60 module, which further confirms the importance of these two pathways for energy metabolism. Notch signaling was activated in mice fed a high-energy diet (54), and KCTD10 has also been recognized as an upstream regulator of Notch signaling to regulate brown fat thermogenesis and whole-body metabolism (55). Studies have also found that the VEGF signaling pathway is regulated by calcium dobesilate (CAD) to alleviate diabetes in mice with high energy diet (56), and gene encoding cyclooxygenase 2(COX2) regulates glucose and lipid metabolism by regulating VEGF signaling pathway in mice with obesity caused by high energy diet (57). Besides, studies have discovered that IL-17 and Azgp1 interact with each other to alter lipid metabolism in mice with a high-energy diet (58). Finally, gonadotropin has been found to be too low in rabbits on a high-energy diet (59), and metabolic pathways regulate the gonadotropin signaling pathway by affecting the hypothalamus have also been confirmed (60). In conclusion, the pink module is still closely associated with specific energy metabolism.

For the GO annotation, magenta module genes are mainly involved in carbohydrate metabolism as nucleoplasm, cytoplasm, and organelles, as well as KEGG, showed that genes in the module were enriched in thermogenesis, oxidative phosphorylation, pyrimidine metabolism, insulin signaling pathway, adipocytokine signaling pathway, AMPK signaling pathway, metabolic pathways, and VEGF signaling pathway. In the clinical study, 28 people were put on a low-energy diet, and the blood analysis of the patients indicated that a low-energy diet involved carbohydrate metabolism and insulin secretion (61). Insulin secretion and AMPK signaling pathway were also considerably modified after 14 weeks of high and low-energy diets in mice (62) in the magenta module. In previous studies, carbohydrate metabolism in adipose tissue was altered when mice were fed diets with different energy levels (63), and modulation of energy levels in the rat diet was also found to result in shifts in AMPK and insulin signaling (64). Likewise, in previous studies, 3-month-old mice were treated with high-energy and low-energy diets for 72 h, respectively, and both treatments involved the insulin secretion process and VEGF signaling pathway (65). All these results prompted us to further evaluate the relationship between genes and changes in energy metabolism.

Hub genes in three modules

Under the low-energy and low-protein diets, genes were down-regulated in the grey60 module. The *TIA1*, as the hub gene in the module, shuttled in the nucleus and was responsible for gene transcription and pre-mRNA splicing (66). In addition, the *TIA1* as an RNA-binding protein performed a role in translational regulation in the cytoplasm (67, 68), which is closely related to biological processes such as cell proliferation and apoptosis (69), immunity, and inflammation (70). At the same time, the *TIA1* gene has also been proven to be the core regulatory gene of RNA metabolism (71) and involved in a variety of cellular metabolic processes (72). It was identified that deletion of the *TIA1* gene in mice was comparable to mice

under starvation conditions, leading to upregulation of *Plin4*, *Pnpla2*, *Pnpla7,* and other genes (73), which are responsible for lipid droplet generation (74, 75), free fatty acid supply (76), regulation of energy metabolism, and lipid metabolism (77). The downstream gene regulated by *TIA1* and *PDGFD* is also a newly identified adipokine (78) which is down-regulated during adipogenesis in humans and mice (79), consistent with the results of this analysis.

Genes in the pink module are positively correlated with low-energy and low-protein diets, and negatively correlated with high-energy and low-protein diets. Among the hub genes, *SNAPC4* is related to pancreatic development (80), and the functions of the pancreas are secreting digestive enzymes and hormones to coordinate the digestion and absorption of nutrients and energy metabolism (81, 82). The *BUB1B*, as their downstream target gene, is co-regulated by *SNAPC4*, the recognition-specific polyadenylation signaling gene (83, 84), is co-regulated by *SNAPC4*, *CPSF2* and the RNA splicing gene (85). The *CLASRP* and its expression fluctuated in the lungs of 16-week-old mice on a high-energy diet (86, 87). Moreover, the down-regulation of *BUB1B* gene expression was also determined after 72 h of OE33P cells in a high-fat medium (88). Down-regulation of *IL17RA*, a downstream gene of *ZNF574* (the hub gene in the pink module), was found to reduce the side effects of obesity in mice fed with high energy diet for 9 weeks (89). As a key factor in the lipid regulation (90), *MED15* converts saturated fatty acids into unsaturated fatty acids to regulate lipid metabolism (91). Its downstream target gene *FADD* has also been convinced to be a key factor in glucose and lipid metabolism (92). In addition, mice, after 15 weeks of high-energy feeding, were found with down-regulated *FADD* and were not as obese as wild-type mice (93), which confirmed that the body may affect metabolism through down-regulation of *FADD* and decrease the impact of obesity. The *U2AF2*, the last hub gene in the pink module, binds to the *U2AF1* (94) and regulates translation through RNA in the cytoplasm (95, 96). Down-regulation of its downstream gene *EGLN2* was found to ameliorate metabolic problems in mice fed a 12-week high-energy diet (97).

LOC516108, the hub gene in the magenta module, is a protein-encoding gene, and its regulated *CAB39* was found to be a direct target of microRNA-451 in adipocytes (98). After 20 weeks of high-energy feeding, microRNA-451 was down-regulated and *CAB39* expression was also altered in mice compared with the control group (99). The *ATP8* downstream of the hub gene principally affects mitochondrial function (100), and has been identified to regulate insulin secretion and glucose metabolism of pancreatic β-cells in high-fat diet mice (101). Other studies have found that *HRAS* is up-regulated in low-fat diet mice (102), which is also the gene downstream of *LOC516108*, mainly blocks fat generation and regulates energy metabolism (103, 104).

To further verify the reliability of the results, real-time quantitative analysis of eight hub genes was performed in the heart, liver, spleen, lung, kidney, muscle, and adipose tissue of healthy adult cattle and newborn calves. Compared to the eight hub genes in the relative expression of the adult cattle group, we found that the relative expression quantity was elevated in the adipose tissue of energy storage and muscle tissue as a metabolic organ. When adult cattle and calf adipose tissues were compared, the relative expression levels of the eight hub genes were considerably higher in adult cattle than in newborn calves and were two to three times higher numerically. These results suggest that the above eight hub genes can turn on the homeostatic regulation of the metabolism of substances in the body by adjusting the external feeding method. However, the regulatory mechanism of their metabolism *in vivo* is still unclear and needs to be further explored.

Conclusions

In summary, we explored the effects of distinct energy and protein feeding methods on the changes of the entire transcriptome of cattle and screened out three related modules (grey60, pink, and magenta modules) by constructing a weighted co-expression network. They were related to the nucleoplasm, cytoplasmic, and organelle components, and participated in Rap1, MAPK, AMPK signaling pathways, and so on. Furthermore, we identified eight hub genes from these three modules, namely TIA1, LOC516108, SNAPC4, CPSF2, CLASRP, ZNF574, MED15, and U2AF2, which were all related to metabolic regulation. Our findings systematically elucidated the biological processes and important regulators closely related to subcutaneous adipose tissue metabolism, which would contribute to a better understanding of molecular mechanisms in the subcutaneous adipose tissue metabolism and provide useful reference information for molecular breeding of cattle.

Data availability statement

The original contributions presented in the study are included in the article/Supplementary materials, further inquiries can be directed to the corresponding author/s.

Ethics statement

The procedures for animal handling for experiments were approved by the Committee of Experimental Animal Management at Northwest Agriculture and Forestry University, China (protocol number: NWAFUCAST2018-168). Moreover, all applicable rules and regulation of the organization and government were followed regarding the ethical use of experimental animals. Written informed consent was obtained

from the owners for the participation of their animals in this study.

Author contributions

XW: conceptualization, investigation, data curation, and manuscript—original draft and revised. JW: conceptualization, investigation, and manuscript–revised. LZ: conceptualization, validation, writing—review and editing, funding acquisition, project administration, and supervision. SR: conceptualization, validation, and manuscript—review and editing. AA, HA, JD, and JM: validation, part of the data analysis and processing, and search for data and literature. XQ and SY: methodology and animal testing. DZ: methodology and use of analysis software. All authors have read and agreed to the published version of the manuscript.

Funding

This research was funded by the National Key Research and Development Program of China National Natural Science Foundation of China (31972994), National Beef and Yak Industrial Technology System (CARS-37), Key Research and Development Program of Shaanxi Province (2022NY-050 and 2022ZDLNY01-01), and Special Project for the Central Government to Guide Local Science and Technology Development (2060404-51301).

Conflict of interest

The authors declare that the research was conducted in the absence of any commercial or financial relationships that could be construed as a potential conflict of interest.

Publisher's note

All claims expressed in this article are solely those of the authors and do not necessarily represent those of their affiliated organizations, or those of the publisher, the editors and the reviewers. Any product that may be evaluated in this article, or claim that may be made by its manufacturer, is not guaranteed or endorsed by the publisher.

Supplementary material

The Supplementary Material for this article can be found online at: https://www.frontiersin.org/articles/10.3389/fvets.2022.1014286/full#supplementary-material

References

1. Brester GW, Marsh JM, Plain RL. International red meat trade. *Vet Clin North Am.* (2003) 19:493–518. doi: 10.1016/S0749-0720(03)00024-0

2. Churchward-Venne TA, Pinckaers PJM, van Loon JJA, van Loon LJC. Consideration of insects as a source of dietary protein for human consumption. *Nutr Rev.* (2017) 75:1035–45. doi: 10.1093/nutrit/nux057

3. Greenwood PL. Review: an overview of beef production from pasture and feedlot globally, as demand for beef and the need for sustainable practices increase. *Animal.* (2021) 15:100295. doi: 10.1016/j.animal.2021.100295

4. Raza SHA, Khan R, Cheng G, Long F, Bing S, Easa AA, et al. RNA-Seq reveals the potential molecular mechanisms of bovine KLF6 gene in the regulation of adipogenesis. *Int J Biol Macromol.* (2022) 195:198–206. doi: 10.1016/j.ijbiomac.2021.11.202

5. Salami SA, O'Grady MN, Luciano G, Priolo A, McGee M, Moloney AP, et al. Fatty acid composition, shelf-life and eating quality of beef from steers fed corn or wheat dried distillers' grains with solubles in a concentrate supplement to grass silage. *Meat Sci.* (2021) 173:108381. doi: 10.1016/j.meatsci.2020.108381

6. Dong LF, Zhang WB, Zhang NF, Tu Y, Diao QY. Feeding different dietary protein to energy ratios to Holstein heifers: effects on growth performance, blood metabolites and rumen fermentation parameters. *J Anim Physiol Anim Nutr (Berl).* (2017) 101:30–7. doi: 10.1111/jpn.12493

7. Daley CA, Abbott A, Doyle PS, Nader GA, Larson S. A review of fatty acid profiles and antioxidant content in grass-fed and grain-fed beef. *Nutr J.* (2010) 9:10. doi: 10.1186/1475-2891-9-10

8. Gruffat D, Bauchart D, Thomas A, Parafita E, Durand D. Fatty acid composition and oxidation in beef muscles as affected by ageing times and cooking methods. *Food Chem.* (2021) 343:128476. doi: 10.1016/j.foodchem.2020.128476

9. Bravo-Lamas L, Barron LJR, Farmer L, Aldai N. Fatty acid composition of intramuscular fat and odour-active compounds of lamb commercialized in northern Spain. *Meat Sci.* (2018) 139:231–8. doi: 10.1016/j.meatsci.2018.02.006

10. Silva-Vignato B, Coutinho LL, Poleti MD, Cesar ASM, Moncau CT, Regitano LCA, et al. Gene co-expression networks associated with carcass traits reveal new pathways for muscle and fat deposition in Nelore cattle. *BMC Genom.* (2019) 20:32. doi: 10.1186/s12864-018-5345-y

11. Pan C, Yang C, Wang S, Ma Y. Identifying key genes and functionally enriched pathways of diverse adipose tissue types in cattle. *Front Genet.* (2022) 13:790690. doi: 10.3389/fgene.2022.790690

12. Yu H, Zhao Z, Yu X, Li J, Lu C, Yang R. Bovine lipid metabolism related gene GPAM: molecular characterization, function identification, and association analysis with fat deposition traits. *Gene.* (2017) 609:31. doi: 10.1016/j.gene.2017.01.031

13. Junjvlieke Z, Khan R, Mei C, Cheng G, Wang S, Raza SHA, et al. Effect of ELOVL6 on the lipid metabolism of bovine adipocytes. *Genomics.* (2020) 112:2282–90. doi: 10.1016/j.ygeno.2019.12.024

14. Kajdasz A, Warzych E, Derebecka N, Madeja ZE, Lechniak D, Wesoly J, et al. Lipid stores and lipid metabolism associated gene expression in porcine and bovine parthenogenetic embryos revealed by fluorescent staining and RNA-seq. *Int J Mol Sci.* (2020) 21:6488. doi: 10.3390/ijms21186488

15. Zhao W, Langfelder P, Fuller T, Dong J, Li A, Hovarth S. Weighted gene coexpression network analysis: state of the art. *J Biopharm Stat.* (2010) 20:281–300. doi: 10.1080/10543400903572753

16. Langfelder P, Horvath S. WGCNA: an R package for weighted correlation network analysis. *BMC Bioinform.* (2008) 9:559. doi: 10.1186/1471-2105-9-559

17. Gong Y, Zhang Y, Li B, Xiao Y, Zeng Q, Xu K, et al. Insight into liver lncRNA and mRNA profiling at four developmental stages in ningxiang pig. *Biology.* (2021) 10:310. doi: 10.3390/biology10040310

18. Xiang Y, Zhang C-Q, Huang K. Predicting glioblastoma prognosis networks using weighted gene co-expression network analysis on TCGA data. *BMC Bioinform.* (2012) 13:S12. doi: 10.1186/1471-2105-13-S2-S12

19. Gong Y, He J, Li B, Xiao Y, Zeng Q, Xu K, et al. Integrated analysis of lncRNA and mRNA in subcutaneous adipose tissue of ningxiang pig. *Biology.* (2021) 10:726. doi: 10.3390/biology10080726

20. Oliveira GB, Regitano LCA, Cesar ASM, Reecy JM, Degaki KY, Poleti MD, et al. Integrative analysis of microRNAs and mRNAs revealed regulation of composition and metabolism in Nelore cattle. *BMC Genomics.* (2018) 19:126. doi: 10.1186/s12864-018-4514-3

21. Sheybani N, Bakhtiarizadeh MR, Salehi A. An integrated analysis of mRNAs, lncRNAs, and miRNAs based on weighted gene co-expression network analysis involved in bovine endometritis. *Sci Rep.* (2021) 11:18050. doi: 10.1038/s41598-021-97319-y

22. Sun H-Z, Srithayakumar V, Jiminez J, Jin W, Hosseini A, Raszek M, et al. Longitudinal blood transcriptomic analysis to identify molecular regulatory patterns of bovine respiratory disease in beef cattle. *Genomics.* (2020) 112:3968–77. doi: 10.1016/j.ygeno.2020.07.014

23. Yang C, Han L, Li P, Ding Y, Zhu Y, Huang Z, et al. Characterization and duodenal transcriptome analysis of chinese beef cattle with divergent feed efficiency using RNA-Seq. *Front Genet.* (2021) 12:741878. doi: 10.3389/fgene.2021.741878

24. Zhao X, Liu H, Pan Y, Liu Y, Zhang F, Ao H, et al. Identification of potential candidate genes from co-expression module analysis during preadipocyte differentiation in landrace pig. *Front Genet.* (2022) 12:753725. doi: 10.3389/fgene.2021.753725

25. Xing K, Liu H, Zhang F, Liu Y, Shi Y, Ding X, et al. Identification of key genes affecting porcine fat deposition based on co-expression network analysis of weighted genes. *J Anim Sci Biotechnol.* (2021) 12:100. doi: 10.1186/s40104-021-00616-9

26. Gao Z, Ding R, Zhai X, Wang Y, Chen Y, Yang C-X, et al. Common gene modules identified for chicken adiposity by network construction and comparison. *Front Genet.* (2020) 11:537. doi: 10.3389/fgene.2020.00537

27. Velotta JP, Jones J, Wolf CJ, Cheviron ZA. Transcriptomic plasticity in brown adipose tissue contributes to an enhanced capacity for nonshivering thermogenesis in deer mice. *Mol Ecol.* (2016) 25:13661. doi: 10.1111/mec.13661

28. Santos AJF, Dos Ferreira JM, Baptista F, Alexandrino B, Silva MAG, Da, et al. Statistical analysis between 2006 and 2019 and forecast of rabies in cattle from 2020 to 2022 in Tocantins State (Brazil), by using the R Studio software. *Epidemiol Infect.* (2022) 150:1–19. doi: 10.1017/S0950268822000553

29. Shedlock CJ, Stumpo KA. Data parsing in mass spectrometry imaging using R Studio and Cardinal: a tutorial. *J Mass Spectrom Adv Clin Lab.* (2022) 23:58–70. doi: 10.1016/j.jmsacl.2021.12.007

30. de Lima AO, Koltes JE, Diniz WJS, de Oliveira PSN, Cesar ASM, Tizioto PC, et al. Potential biomarkers for feed efficiency-related traits in nelore cattle identified by co-expression network and integrative genomics analyses. *Front Genet.* (2020) 11:189. doi: 10.3389/fgene.2020.00189

31. Bao Q, Zhang X, Bao P, Liang C, Guo X, Chu M, et al. Using weighted gene co-expression network analysis (WGCNA) to identify the hub genes related to hypoxic adaptation in yak (Bos grunniens). *Genes Genomics.* (2021) 43:1231–46. doi: 10.1007/s13258-021-01137-5

32. Zhao X, Zhang L, Wang J, Zhang M, Song Z, Ni B, et al. Identification of key biomarkers and immune infiltration in systemic lupus erythematosus by integrated bioinformatics analysis. *J Transl Med.* (2021) 19:35. doi: 10.1186/s12967-020-02698-x

33. Song WQ, Gu WQ, Qian YB, Ma X, Mao YJ, Liu WJ. Identification of long non-coding RNA involved in osteogenic differentiation from mesenchymal stem cells using RNA-Seq data. *Genet Mol Res.* (2015) 14:18268–79. doi: 10.4238/2015.December.23.14

34. Wang J, Sui J, Mao C, Li X, Chen X, Liang C, et al. Identification of key pathways and genes related to the development of hair follicle cycle in cashmere goats. *Genes.* (2021) 12:180. doi: 10.3390/genes12020180

35. Zhang X, Bao P, Ye N, Zhou X, Zhang Y, Liang C, et al. Identification of the key genes associated with the yak hair follicle cycle. *Genes.* (2021) 13:32. doi: 10.3390/genes13010032

36. Shannon P, Markiel A, Ozier O, Baliga NS, Wang JT, Ramage D, et al. Cytoscape: a software environment for integrated models of biomolecular interaction networks. *Genome Res.* (2003) 13:2498–504. doi: 10.1101/gr.1239303

37. Ren X, Chen X, Ji Y, Li L, Li Y, Qin C, et al. Upregulation of KIF20A promotes tumor proliferation and invasion in renal clear cell carcinoma and is associated with adverse clinical outcome. *Aging.* (2020) 12:25878–94. doi: 10.18632/aging.202153

38. Chen X, Raza SHA, Ma X, Wang J, Wang X, Liang C, et al. Bovine pre-adipocyte adipogenesis is regulated by bta-miR-150 through mTOR signaling. *Front Genet.* (2021) 12:636550. doi: 10.3389/fgene.2021.636550

39. Wærp HKL, Waters SM, McCabe MS, Cormican P, Salte R. RNA-seq analysis of bovine adipose tissue in heifers fed diets differing in energy and protein content. *PLoS ONE.* (2018) 13:e0201284. doi: 10.1371/journal.pone.0201284

40. Peña C, Hurt E, Panse VG. Eukaryotic ribosome assembly, transport and quality control. *Nat Struct Mol Biol.* (2017) 24:689–99. doi: 10.1038/nsmb.3454

41. Benassi-Evans B, Clifton PM, Noakes M, Keogh JB, Fenech M. High protein-high red meat versus high carbohydrate weight loss diets do not differ in effect on genome stability and cell death in lymphocytes of overweight men. *Mutagenesis.* (2009) 24:271–7. doi: 10.1093/mutage/gep006

42. Kaneko K, Xu P, Cordonier EL, Chen SS, Ng A, Xu Y, et al. Neuronal rap1 regulates energy balance, glucose homeostasis, and leptin actions. *Cell Rep.* (2016) 16:3003–15. doi: 10.1016/j.celrep.2016.08.039

43. Wong KHK, Cai Y, Ying F, Chen X, Vanhoutte PM, Tang EHC. Deletion of Rap1 disrupts redox balance and impairs endothelium-dependent relaxations. *J Mol Cell Cardiol.* (2018) 115:1–9. doi: 10.1016/j.yjmcc.2017.12.009

44. Jaśkiewicz A, Pajak B, Orzechowski A. The many faces of Rap1 GTPase. *Int J Mol Sci.* (2018) 19:2848. doi: 10.3390/ijms19102848

45. Kaneko K, Lin, H.-Y., Fu Y, Saha PK, De la Puente-Gomez AB, et al. Rap1 in the VMH regulates glucose homeostasis. *JCI Insight.* (2021) 6:e142545. doi: 10.1172/jci.insight.142545

46. Shah S, Brock EJ, Ji K, Mattingly RR. Ras and Rap1: a tale of two GTPases. *Semin Cancer Biol.* (2019) 54:29–39. doi: 10.1016/j.semcancer.2018.03.005

47. Cui X, Qian D-W, Jiang S, Shang E-X, Zhu Z-H, Duan J-A. Scutellariae radix and coptidis rhizoma improve glucose and lipid metabolism in T2DM Rats via regulation of the metabolic profiling and MAPK/PI3K/Akt signaling pathway. *Int J Mol Sci.* (2018) 19:3634. doi: 10.3390/ijms19113634

48. Baumgard LH, Hausman GJ, Sanz Fernandez MV. Insulin: pancreatic secretion and adipocyte regulation. *Domest Anim Endocrinol.* (2016) 54:76–84. doi: 10.1016/j.domaniend.2015.07.001

49. Zhang J, Liu Y, Zheng Y, Luo Y, Du Y, Zhao Y, et al. TREM-2-p38 MAPK signaling regulates neuroinflammation during chronic cerebral hypoperfusion combined with diabetes mellitus. *J Neuroinflammation.* (2020) 17:2. doi: 10.1186/s12974-019-1688-9

50. Wang Z, Zhu M, Wang M, Gao Y, Zhang C, Liu S, et al. Integrated multiomic analysis reveals the high-fat diet induced activation of the MAPK signaling and inflammation associated metabolic cascades via histone modification in adipose tissues. *Front Genet.* (2021) 12:650863. doi: 10.3389/fgene.2021.650863

51. Krogdahl Å. Digestion and absorption of lipids in poultry. *J Nutr.* (1985) 115:675–85. doi: 10.1093/jn/115.5.675

52. Bialecka-Florjanczyk E, Fabiszewska AU, Krzyczkowska J, Kurylowicz A. Synthetic and natural lipase inhibitors. *Mini Rev n Med Chem.* (2018) 18:672–83. doi: 10.2174/1389557516666160630123356

53. Cai H, Wen Z, Meng K, Yang P. Metabolomic signatures for liver tissue and cecum contents in high-fat diet-induced obese mice based on UHPLC-Q-TOF/MS. *Nutr Metab.* (2021) 18:69. doi: 10.1186/s12986-021-00595-8

54. Lin QQ, Zhao J, Zheng CG, Chun J. Roles of Notch signaling pathway and endothelial-mesenchymal transition in vascular endothelial dysfunction and atherosclerosis. *Eur Rev Med Pharmacol Sci.* (2018) 22:6485–91. doi: 10.26355/eurrev_201810_16062

55. Ye M, Luo L, Guo Q, Su T, Cheng P, Huang Y. KCTD10 regulates brown adipose tissue thermogenesis and metabolic function via Notch signaling. *J Endocrinol.* (2022) 252:155–66. doi: 10.1530/JOE-21-0016

56. Wang Y, Lu Y, Tang C, Xue M, Li X, Chang Y, et al. Calcium dobesilate restores autophagy by inhibiting the VEGF/PI3K/AKT/mTOR signaling pathway. *Front Pharmacol.* (2019) 10:886. doi: 10.3389/fphar.2019.00886

57. Fu P, Zhu R, Jia J, Hu Y, Wu C, Cieszczyk P, et al. Aerobic exercise promotes the functions of brown adipose tissue in obese mice via a mechanism involving COX2 in the VEGF signaling pathway. *Nutr Metab.* (2021) 18:56. doi: 10.1186/s12986-021-00581-0

58. Na HS, Kwon J-E, Lee SH, Jhun J, Kim S-M, Kim S-Y, et al. Th17 and IL-17 cause acceleration of inflammation and fat loss by inducing α2-Glycoprotein 1

(AZGP1), in rheumatoid arthritis with high-fat diet. *Am J Pathol.* (2017) 187:1049–58. doi: 10.1016/j.ajpath.2016.12.023

59. Morelli A, Sarchielli E, Comeglio P, Filippi S, Vignozzi L, Marini M, et al. Metabolic syndrome induces inflammation and impairs gonadotropin-releasing hormone neurons in the preoptic area of the hypothalamus in rabbits. *Mol Cell Endocrinol.* (2014) 382:107–19. doi: 10.1016/j.mce.2013.09.017

60. Sánchez-Garrido MA, Ruiz-Pino F, Manfredi-Lozano M, Leon S, Heras V, Castellano JM, et al. Metabolic and gonadotropic impact of sequential obesogenic insults in the female: influence of the loss of ovarian secretion. *Endocrinology.* (2015) 156:2984–98. doi: 10.1210/en.2014-1951

61. Wang L-L, Wang Q, Hong Y, Ojo O, Jiang Q, Hou Y-Y, et al. The effect of low-carbohydrate diet on glycemic control in patients with type 2 diabetes mellitus. *Nutrients.* (2018) 10:661. doi: 10.3390/nu10060661

62. Nybacka S, Simrén M, Störsrud S, Törnblom H, Winkvist A, Lindqvist HM. Changes in serum and urinary metabolomic profile after a dietary intervention in patients with irritable bowel syndrome. *PLoS ONE.* (2021) 16:e0257331. doi: 10.1371/journal.pone.0257331

63. Hoevenaars FPM, Keijer J, Herreman L, Palm I, Hegeman MA, Swarts HJM, et al. Adipose tissue metabolism and inflammation are differently affected by weight loss in obese mice due to either a high-fat diet restriction or change to a low-fat diet. *Genes Nutr.* (2014) 9:391. doi: 10.1007/s12263-014-0391-9

64. Pataky MW, Arias EB, Wang H, Zheng X, Cartee GD. Exercise effects on γ3-AMPK activity, phosphorylation of Akt2 and AS160, and insulin-stimulated glucose uptake in insulin-resistant rat skeletal muscle. *J Appl Physiol.* (2020) 128:410–21. doi: 10.1152/japplphysiol.00428.2019

65. Miller CN, Morton HP, Cooney PT, Winters TG, Ramseur KR, Rayalam S, et al. Acute exposure to high-fat diets increases hepatic expression of genes related to cell repair and remodeling in female rats. *Nutr Res.* (2014) 34:85–93. doi: 10.1016/j.nutres.2013.10.010

66. Pihlajamäki J, Boes T, Kim EY, Dearie F, Kim BW, Schroeder J. Thyroid hormone-related regulation of gene expression in human fatty liver. *J Clin Endocrinol Metab.* (2009) 94:521–3529. doi: 10.1210/jc.2009-0212

67. Byres LP, Mufteev M, Yuki KE, Wei W, Piekna A, Wilson MD, et al. Identification of TIA1 mRNA targets during human neuronal development. *Mol Biol Rep.* (2021) 48:6349–61. doi: 10.1007/s11033-021-06634-0

68. Jiang L, Ash PEA, Maziuk BF, Ballance HI, Boudeau S, Abdullatif A, et al. TIA1 regulates the generation and response to toxic tau oligomers. *Acta Neuropathol.* (2019) 137:259–77. doi: 10.1007/s00401-018-1937-5

69. LeBlang CJ, Medalla M, Nicoletti NW, Hays EC, Zhao J, Shattuck J, et al. Reduction of the RNA binding protein TIA1 exacerbates neuroinflammation in tauopathy. *Front Neurosci.* (2020) 14:285. doi: 10.3389/fnins.2020.00285

70. Rayman JB, Hijazi J, Li X, Kedersha N, Anderson PJ, Kandel ER. Genetic perturbation of TIA1 reveals a physiological role in fear memory. *Cell Rep.* (2019) 26:2970–83.e4. doi: 10.1016/j.celrep.2019.02.048

71. Mackenzie IR, Nicholson AM, Sarkar M, Messing J, Purice MD, Pottier C, et al. TIA1 mutations in amyotrophic lateral sclerosis and frontotemporal dementia promote phase separation and alter stress granule dynamics. *Neuron.* (2017) 95:808–16.e9. doi: 10.1016/j.neuron.2017.07.025

72. Huang S, Liu N, Li H, Zhao J, Su L, Zhang Y, et al. TIA1 interacts with annexin A7 in regulating vascular endothelial cell autophagy. *Int J Biochem Cell Biol.* (2014) 57:115–22. doi: 10.1016/j.biocel.2014.10.015

73. Heck MV, Azizov M, Stehning T, Walter M, Kedersha N, Auburger G. Dysregulated expression of lipid storage and membrane dynamics factors in Tia1 knockout mouse nervous tissue. *Neurogenetics.* (2014) 15:135–44. doi: 10.1007/s10048-014-0397-x

74. Sirois I, Aguilar-Mahecha A, Lafleur J, Fowler E, Vu V, Scriver M, et al. A unique morphological phenotype in chemoresistant triple-negative breast cancer reveals metabolic reprogramming and PLIN4 expression as a molecular vulnerability. *Mol Cancer Res.* (2019) 17:2492–507. doi: 10.1158/1541-7786.MCR-19-0264

75. Chen W, Chang B, Wu X, Li L, Sleeman M, Chan L. Inactivation of Plin4 downregulates Plin5 and reduces cardiac lipid accumulation in mice. *Am J Physiol Endocrinol Metab.* (2013) 304:E770–9. doi: 10.1152/ajpendo.00523.2012

76. Haemmerle G, Moustafa T, Woelkart G, Büttner S, Schmidt A, van de Weijer T, et al. ATGL-mediated fat catabolism regulates cardiac mitochondrial function via PPAR-α and PGC-1. *Nat Med.* (2011) 17:1076–85. doi: 10.1038/nm.2439

77. Heier C, Kien B, Huang F, Eichmann TO, Xie H, Zechner R, et al. The phospholipase PNPLA7 functions as a lysophosphatidylcholine hydrolase and interacts with lipid droplets through its catalytic domain. *J Biol Chem.* (2017) 292:19087–98. doi: 10.1074/jbc.M117.792978

78. Cheng Y-W, Zhang Z-B, Lan B-D, Lin J-R, Chen X-H, Kong L-R, et al. PDGF-D activation by macrophage-derived uPA promotes AngII-induced cardiac remodeling in obese mice. *J Exp Med.* (2021) 218:e20210252. doi: 10.1084/jem.20210252

79. Dong K, Yang M, Han J, Ma Q, Han J, Song Z, et al. Genomic analysis of worldwide sheep breeds reveals PDGFD as a major target of fat-tail selection in sheep. *BMC Genomics.* (2020) 21:800. doi: 10.1186/s12864-020-07210-9

80. Voz ML, Coppieters W, Manfroid I, Baudhuin A, Von Berg V, Charlier C, et al. Fast homozygosity mapping and identification of a zebrafish ENU-induced mutation by whole-genome sequencing. *PLoS ONE.* (2012) 7:e34671. doi: 10.1371/journal.pone.0034671

81. Rasmussen HH. Nutrition in chronic pancreatitis. *World J Gastroenterol.* (2013) 19:7267. doi: 10.3748/wjg.v19.i42.7267

82. Matafome P, Eickhoff H, Letra L, Seiça R. Neuroendocrinology of adipose tissue and gut–brain axis. *Adv Neurobiol.* (2017) 19:49–70. doi: 10.1007/978-3-319-63260-5_3

83. Nilubol N, Boufraqech M, Zhang L, Kebebew E. Loss of CPSF2 expression is associated with increased thyroid cancer cellular invasion and cancer stem cell population, and more aggressive disease. *J Clin Endocrinol Metab.* (2014) 99:E1173–82. doi: 10.1210/jc.2013-4140

84. Hinske LC, Galante PAF, Limbeck E, Möhnle P, Parmigiani RB, Ohno-Machado L, et al. Alternative polyadenylation allows differential negative feedback of human miRNA miR-579 on Its host gene ZFR. *PLoS ONE.* (2015) 10:e0121507. doi: 10.1371/journal.pone.0121507

85. Michael AB, Ashby C, Wardell C, Boyle EM, Ortiz M, Flynt E, et al. Differential RNA splicing as a potentially important driver mechanism in multiple myeloma. *Haematologica.* (2020) 106:736–45. doi: 10.3324/haematol.2019.235424

86. Jiao CY, Feng QC, Li CX, Wang D, Han S, Zhang YD, et al. BUB1B promotes extrahepatic cholangiocarcinoma progression via JNK/c-Jun pathways. *Cell Death Dis.* (2021) 12:63. doi: 10.1038/s41419-020-03234-x

87. Kim EJ, Oh HY, Heo H-S, Hong JE, Jung S-J, Lee KW, et al. Biological features of core networks that result from a high-fat diet in hepatic and pulmonary tissues in mammary tumour-bearing, obesity-resistant mice. *Br J Nutr.* (2013) 110:241–55. doi: 10.1017/S0007114512004965

88. Mongan AM, Lynam-Lennon N, Casey R, Maher S, Pidgeon G, Reynolds JV, et al. Visceral obesity stimulates anaphase bridge formation and spindle assembly checkpoint dysregulation in radioresistant oesophageal adenocarcinoma. *Clin Transl Oncol.* (2016) 18:632–40. doi: 10.1007/s12094-015-1411-y

89. Pérez MM, Martins LMS, Dias MS, Pereira CA, Leite JA, Gonçalves ECS, et al. Interleukin-17/interleukin-17 receptor axis elicits intestinal neutrophil migration, restrains gut dysbiosis and lipopolysaccharide translocation in high-fat diet-induced metabolic syndrome model. *Immunology.* (2019) 156:339–55. doi: 10.1111/imm.13028

90. Yang F, Vought BW, Satterlee JS, Walker AK, Jim Sun Z-Y, Watts JL, et al. An ARC/Mediator subunit required for SREBP control of cholesterol and lipid homeostasis. *Nature.* (2006) 442:700–4. doi: 10.1038/nature04942

91. Lee D, An SWA, Jung Y, Yamaoka Y, Ryu Y, Goh GYS, et al. MDT-15/MED15 permits longevity at low temperature via enhancing lipidostasis and proteostasis. *PLoS Biol.* (2019) 17:e3000415. doi: 10.1371/journal.pbio.3000415

92. Zhuang H, Gan Z, Jiang W, Zhang X, Hua Z-C. Functional specific roles of FADD: comparative proteomic analyses from knockout cell lines. *Mol Biosyst.* (2013) 9:2063–78. doi: 10.1039/C3MB70023B

93. Zhuang H, Wang X, Zha D, Gan Z, Cai F, Du P, et al. FADD is a key regulator of lipid metabolism. *EMBO Mol Med.* (2016) 8:895–918. doi: 10.15252/emmm.201505924

94. Parra M, Booth BW, Weiszmann R, Yee B, Yeo GW, Brown JB, et al. An important class of intron retention events in human erythroblasts is regulated by cryptic exons proposed to function as splicing decoys. *RNA.* (2018) 24:1255–65. doi: 10.1261/rna.066951.118

95. Akef A, McGraw K, Cappell SD, Larson DR. Ribosome biogenesis is a downstream effector of the oncogenic U2AF1-S34F mutation. *PLoS Biol.* (2020) 18:e3000920. doi: 10.1371/journal.pbio.3000920

96. Palangat M, Anastasakis DG, Fei DL, Lindblad KE, Bradley R, Hourigan CS, et al. The splicing factor U2AF1 contributes to cancer progression through a noncanonical role in translation regulation. *Genes Dev.* (2019) 33:482–97. doi: 10.1101/gad.319590.118

97. Thomas A, Belaidi E, Aron-Wisnewsky J, van der Zon GC, Levy P, Clement K, et al. Hypoxia-inducible factor prolyl hydroxylase 1 (PHD1), deficiency promotes hepatic steatosis and liver-specific insulin resistance in mice. *Sci Rep.* (2016) 6:24618. doi: 10.1038/srep24618

98. Hur W, Lee JH, Kim SW, Kim J-H, Bae SH, Kim M, et al. Downregulation of microRNA-451 in non-alcoholic steatohepatitis inhibits fatty acid-induced proinflammatory cytokine production through the AMPK/AKT pathway. *Int J Biochem Cell Biol.* (2015) 64:265–76. doi: 10.1016/j.biocel.2015.04.016

99. Kuwabara Y, Horie T, Baba O, Watanabe S, Nishiga M, Usami S, et al. MicroRNA-451 exacerbates lipotoxicity in cardiac myocytes and high-fat diet-induced cardiac hypertrophy in mice through suppression of the LKB1/AMPK pathway. *Circ Res.* (2015) 116:279–88. doi: 10.1161/CIRCRESAHA.116.304707

100. Boominathan A, Vanhoozer S, Basisty N, Powers K, Crampton AL, Wang X, et al. Stable nuclear expression of ATP8 and ATP6 genes rescues a mtDNA Complex V null mutant. *Nucleic Acids Res.* (2016) 44:gkw756. doi: 10.1093/nar/gkw756

101. Weiss H, Wester-Rosenloef L, Koch C, Koch F, Baltrusch S, Tiedge M, et al. The mitochondrial atp8 mutation induces mitochondrial ROS generation, secretory dysfunction, and β-cell mass adaptation in conplastic B6-mtFVB mice. *Endocrinology.* (2012) 153:4666–76. doi: 10.1210/en.2012-1296

102. Park J-C, Jeong W-J, Seo SH, Choi K-Y. WDR76 mediates obesity and hepatic steatosis via HRas destabilization. *Sci Rep.* (2019) 9:19676. doi: 10.1038/s41598-019-56211-6

103. Oba D, Inoue S, Miyagawa-Tomita S, Nakashima Y, Niihori T, Yamaguchi S, et al. Mice with an oncogenic HRAS mutation are resistant to high-fat diet-induced obesity and exhibit impaired hepatic energy homeostasis. *EBioMedicine.* (2018) 27:138–50. doi: 10.1016/j.ebiom.2017.11.029

104. Burgoyne JR, Haeussler DJ, Kumar V, Ji Y, Pimental DR, Zee RS, et al. Oxidation of HRas cysteine thiols by metabolic stress prevents palmitoylation in vivo and contributes to endothelial cell apoptosis. *FASEB J.* (2012) 26:832–41. doi: 10.1096/fj.11-189415

frontiers | Frontiers in Veterinary Science

TYPE Review
PUBLISHED 10 November 2022
DOI 10.3389/fvets.2022.1032983

Check for updates

OPEN ACCESS

EDITED BY
Abdul Rasheed Baloch,
University of Karachi, Pakistan

REVIEWED BY
Zheng Chen,
Jiangxi Agricultural University, China
Luca D. Bertzbach,
Leibniz Institute of Virology (LIV), Germany

*CORRESPONDENCE
Ibrar Muhammad Khan
ibrar.pesh@gmail.com
Yong Liu
liuyong@fynu.edu.cn

SPECIALTY SECTION
This article was submitted to Livestock Genomics, a section of the journal Frontiers in Veterinary Science

RECEIVED 31 August 2022
ACCEPTED 28 October 2022
PUBLISHED 10 November 2022

CITATION
Gul H, Habib G, Khan IM, Rahman SU, Khan NM, Wang H, Khan NU and Liu Y (2022) Genetic resilience in chickens against bacterial, viral and protozoal pathogens. *Front. Vet. Sci.* 9:1032983. doi: 10.3389/fvets.2022.1032983

COPYRIGHT
© 2022 Gul, Habib, Khan, Rahman, Khan, Wang, Khan and Liu. This is an open-access article distributed under the terms of the Creative Commons Attribution License (CC BY). The use, distribution or reproduction in other forums is permitted, provided the original author(s) and the copyright owner(s) are credited and that the original publication in this journal is cited, in accordance with accepted academic practice. No use, distribution or reproduction is permitted which does not comply with these terms.

Genetic resilience in chickens against bacterial, viral and protozoal pathogens

Haji Gul[1,2], Gul Habib[3], Ibrar Muhammad Khan[1]*, Sajid Ur Rahman[4,5], Nazir Muhammad Khan[6], Hongcheng Wang[1], Najeeb Ullah Khan[7] and Yong Liu[1]*

[1]Anhui Province Key Laboratory of Embryo Development and Reproduction Regulation, Anhui Province Key Laboratory of Environmental Hormone and Reproduction, School of Biological and Food Engineering, Fuyang Normal University, Fuyang, China, [2]College of Animal Science and Technology, Anhui Agricultural University, Hefei, China, [3]Department of Microbiology, Abbottabad University of Science and Technology, Abbottabad, Pakistan, [4]Department of Food Science and Engineering, School of Agriculture and Biology, Shanghai Jiao Tong University, Shanghai, China, [5]Key Laboratory of Animal Parasitology of Ministry of Agriculture, Laboratory of Quality and Safety Risk Assessment for Animal Products on Biohazards (Shanghai) of Ministry of Agriculture, Shanghai Veterinary Research Institute, Chinese Academy of Agricultural Sciences, Shanghai, China, [6]Department of Zoology, University of Science and Technology, Bannu, Pakistan, [7]Institute of Biotechnology and Genetic Engineering, The University of Agriculture, Peshawar, Pakistan

The genome contributes to the uniqueness of an individual breed, and enables distinctive characteristics to be passed from one generation to the next. The allelic heterogeneity of a certain breed results in a different response to a pathogen with different genomic expression. Disease resistance in chicken is a polygenic trait that involves different genes that confer resistance against pathogens. Such resistance also involves major histocompatibility (MHC) molecules, immunoglobulins, cytokines, interleukins, T and B cells, and CD4+ and CD8+ T lymphocytes, which are involved in host protection. The MHC is associated with antigen presentation, antibody production, and cytokine stimulation, which highlight its role in disease resistance. The natural resistance-associated macrophage protein 1 (Nramp-1), interferon (IFN), myxovirus-resistance gene, myeloid differentiation primary response 88 (MyD88), receptor-interacting serine/threonine kinase 2 (RIP2), and heterophile cells are involved in disease resistance and susceptibility of chicken. Studies related to disease resistance genetics, epigenetics, and quantitative trait loci would enable the identification of resistance markers and the development of disease resistance breeds. Microbial infections are responsible for significant outbreaks and have blighted the poultry industry. Breeding disease-resistant chicken strains may be helpful in tackling pathogens and increasing the current understanding on host genetics in the fight against communicable diseases. Advanced technologies, such as the CRISPR/Cas9 system, whole genome sequencing, RNA sequencing, and high-density single nucleotide polymorphism (SNP) genotyping, aid the development of resistant breeds, which would significantly decrease the use of antibiotics and vaccination in poultry. In this review, we aimed to reveal the recent genetic basis of infection and genomic modification that increase resistance against different pathogens in chickens.

KEYWORDS

chicken MHC, genetics, SNPs, non-coding RNAs, pathogens, infectious diseases, novel technology

Introduction

The breeding of chicks with polygenic resistance is the top priority of poultry farmers as these chickens may tolerate challenging environments without losing their productivity. The poultry industry is susceptible to bacterial, viral, and protozoal pathogens that cause several infectious diseases and reduce growth yield, productivity, and profit. Prophylactic measures, such as vaccination, antibiotics, disinfectants, and culling, are used to control infections in poultry (1). However, current vaccines lack cross-protection against multiple strains of each virus. Furthermore, the mutagenicity of viruses has led to the emergence of highly virulent strains (2). To counter emerging pathogens, a genetically resistant breed should be developed to prevent outbreaks, enable sustained economic viability, and retain consumer confidence in poultry products. By rearing genetically disease-resistant flocks, a breed that can withstand infectious diseases and pathogens owing to its unique genetic modifications, can be obtained (1, 3, 4).

Many disease-resistant genes, including MHC, chicken interleukin 1beta converting enzyme 1 (Caspase1), inducible nitric oxide synthase, IFN, Nramp-1, myxovirus-resistance gene, and toll-like receptor (TLR) genes, play a role in the active immune system of chickens (4, 5). The immune system varies among different hosts, which exhibit different responses to immune cells, such as T and B cells, antibody production, phagocytosis, and lymphocyte proliferation that protect the host from pathogen damage (3). The communication network of immune cells consists of T and B cell receptors, MHC, antibodies, and cytokines that are involved in antigen processing of the effector cells, and play a pivotal role in resistance and susceptibility against bacterial, viral, and parasitic diseases (3, 5). For instance, the Athens Canadian Random Bred strain, which is the oldest pedigreed meat-type chicken existing since the 1950's, has a more stable immune response and disease-resistant phenotype than modern-day broilers (6).

Based on genomic analysis, phosphoinositide-3-kinase–protein kinase B, Janus kinase/signal transducers and activators of transcription (JAK/STAT), nuclear factor kappa B (NF-κB), IL-1β, and IL-6 mRNA are highly expressed in Athens Canadian Random Bred compared to modern broiler (6). In our previous work, immunoglobulin lambda light chain precursor, Ig-gamma (clone-36 chicken), *P01875*, and *PIT-54* genes were identified to be involved in immune response during embryogenesis (7). In a subsequent study, dietary ellagic acid was found to significantly increase antioxidant and antibacterial activities in layers and improve bird health status (8). Importantly, breeding with new technologies improves poultry productivity and enhances disease resistance traits. For example, the livestock-breeding program produced nematode-resistant sheep (9). Similarly, birds resistant to lymphoid leucosis and Marek's disease (10), mastitis-resistant cattle (11), immunocompetent pigs (12), bird flu-resistant chickens (13), Trypanosoma resistant cows (14), porcine reproductive and respiratory syndrome virus-resistant pigs (15), and prion protein-resistant sheep and goat (16, 17) have been developed.

As poultry products are globally consumed on a large scale, there has been substantial interest in generating disease-resistant chicken. Here, we aimed to discuss the genetic responses of chickens to bacterial, viral, and protozoal pathogens, and summarize recent advancements in the generation of pathogen-resistant chickens *via* gene expression modulation using the CRISPR/Cas system (clustered regularly interspaced short palindromic repeat/Cas9), RNA interference (RNAi), and viral vectors. Finally, we highlighted some candidate genes that are involved in various biological pathways and may contribute to the resistance of chickens against the diseases.

Genetic roles in host resistance and susceptibility

The MHC gene is widely evaluated in chickens to identify differences in their resistance and susceptibility to certain pathogens and infectious diseases. MHC class I, II, III, and IV molecules are unique and distinct between species, leading to a differential MHC response among individuals (3). Chickens have few MHC genes with different haplotypes involved in the development of resistance against bacterial, viral, and protozoal pathogens. For instance, MHC haplotype B19 is associated with susceptibility, while B2 and B21 are involved in resistance (18). MHC-dependent resistance and susceptibility rely on peptide-binding specificity. For example, chicken-affected cells expressing MHC-I haplotype, which binds to the Rous sarcoma virus src peptide targeted by cytotoxic CD8+ T cells, are resistant to Rous sarcoma virus (19). In susceptible chickens, the MHC haplotype does not bind with viral peptides, and chickens are infested by the virus. For instance, the MHC class I haplotypes do not bind to the antigenic peptides of Marek's disease virus (MDV), resulting in chickens remaining susceptible (19). The chicken MHC haplotype has a regulatory effect on immune cells resistant to the Rous sarcoma virus and exhibit enhanced natural killer cell activity (20). In a recent study, the MHC haplotypes B15 and B21 homozygotes led to the lowest MDV-induced tumorigenesis and lymphoma formation in VALO specific pathogen-free chickens, demonstrating that MHC conferred resistance to oncogenic herpesviruses (21). Notably, the MHC-peptide complexes engaged T cell receptors (TCRs) that recognize antigens on MHC molecules with the cooperation of CD4+ or CD8+ coreceptors and activate T cells (22). Each T cell has a unique TCR that recognizes and binds with the antigenic peptide on the infected cell surface. The antigen peptides are derived from intracellular pathogens, such as viruses and bacteria, and are displayed at the cell surface by MHC for immune clearance (23). Viruses, such as the avian leucosis virus, have six subgroups, with

subgroup J causing severe outbreaks in China. The avian leucosis virus subgroup J receptor is a sodium/hydrogen exchanger 1, which is edited on chicken somatic cell lines that are resistant to avian leucosis virus *in vitro* (24). Avian influenza virus replication is facilitated by the acidic leucine-rich nuclear phosphoprotein-32A (ANP32A) protein in chicken and waterfowl. An *in vitro* study revealed that the deletion of a minor region of chicken ANP32A stops the replication of the avian influenza virus (25). Although such studies have increased our understanding of the genetic roles, a functional study of edited ANP32A and sodium/hydrogen exchanger 1 gene has not been performed *in vivo* and edited chicken has hitherto been developed.

Generally, increasing poultry resistance to infectious pathogens *via* gene modification is an ideal approach for the development of transgenic livestock. In particular, resistance to diseases originates from the interplay of numerous genes. For example, the mouse fibroblast cell lines are resistant to influenza virus owing to the autosomal dominant Mx1 allele of the murine Mx gene (26). The introduction of the Mx1 gene in mice lacking the Mx1 allele leads to influenza-resistant mice (27) whereas transfer of the same gene in swine does not result in viral-resistant pigs (28). The overexpression of pathogen anti-receptor proteins blocks viral attachment and penetration, and alters the host receptor genes that prevent viral attachment and enhanced resistance against diseases (29). Transgenic chickens express a recombinant avian leukosis envelope protein, which inhibits the corresponding subgroup of avian leukosis virus attachment (30). Similarly, transgenic sheep express the Maedi-visna virus envelope protein and display resistance *via* the prevention of virus adhesion to host cells (31). Collectively, the observed immune responses of chicken against viral, protozoal, and bacterial agents are pathogen-specific, and are closely linked to expression changes in MHC, Nramp-1, RIP2, MyD88, IFN, interleukin, MX1, TLR4, antibodies, and immune cells that govern antibacterial and antiviral states (Figure 1).

Genetic resilience and viral pathogens

Viral diseases cause more outbreaks, reduce growth performance and productivity, and cause immunosuppression in poultry (3). Marek's disease, a well-known viral disease, is caused by MDV. Marek's disease is a lymphotropic disease in chickens and the MDV targets all avian species, causing symptoms such as paralysis, loose watery stool, lymphomas, wasting, and immunosuppression. The poultry response to Marek's disease is the activation of MHC molecules and cytokines that give resistance to MDV (22). Other genes that confer resistance to MDV include *GH1*, *SCA2*, *IRG1*, *CD79B*, *PTPN3*, *LY6E*, and *SMOC1* (32). Another important virus is influenza, a zoonotic virus that causes avian flu. Genes, such as interferon-inducible transmembrane, a retinoic acid-inducible gene I, and MX1 gene polymorphisms are reported to be associated with susceptibilities to avian influenza in chickens and ducks (33, 34). Newcastle disease virus widely infects chickens. Newcastle Disease is characterized by ruffled feathers of chicken, and respiratory, neurological, hyperthermia, and listlessness complications in affected chickens (35). Potential genes, such as *IFNα*, *IFN-γ*, *DDX-1*, *MHC-1*, and *IL-6*, were identified in chicken embryos infected with Newcastle disease virus. These important genes have an antiviral function and induce TLR-mediated activation of macrophages and dendritic cells in response to viruses (36). Newcastle disease virus-infected Fayoumis birds were found to have lower expression of EIF2B5, EIF2S3, EIF2B4, and EIF2S3 than Leghorn's infected lines. Such results indicate that different genetic lines display different expression of host translation initiation factor-2 associated genes, which might contribute to their differential resistance to Newcastle disease virus (37). In a study conducted in Ghana, three Ghanaian local chicken ecotype responses to the lentogenic and velogenic strains of Newcastle disease virus assessed. Based on the findings, resistance to Newcastle disease virus was identified to be caused by an individual's chicken genetic makeup and not by the chicken ecotype (38). The genes, MHC-B locus, *LEI0070*, *ADL0146*, *LEI0104*, *ADL0320*, and *ADL0304*, are associated with a direct response of antibody titer against Newcastle disease virus in chickens (39). Wang et al. (40) revealed that the hemoglobin family genes, functional involvement of oxygen transportation and circulation, and cell adhesion molecule signaling pathway play significant roles in disease resistance to AIV infection in chickens. The influenza H5N1 strain was inoculated into genetically resistant and susceptible Ri chicken native to Vietnam. The resistant chicken displayed a group of genes, *MX1*, *TLR3*, *STAT1*, *IRF7*, *IFN*, and cytokines, which are found in H5N1 strain-resistant chickens (41). Avian Leukosis virus infection is highly receptor-specific and the Leukosis virus subtype A uses specific membrane proteins, such as Tva receptors for binding, CAR1 receptors for avian Leukosis virus subtypes B & D attachment, and SEAR receptors for Avian Leukosis virus subtype E, which is encoded by tumor virus genes (42). These chicken breeds express certain receptors on their cell surface, such as Tva and CAR1, and are susceptible to the corresponding avian Leukosis virus subtype (42, 43). Chickens resistant to infectious bronchitis, Newcastle disease, Marek's disease, coccidiosis, and salmonellosis had high production of IFN-γ, which validated the enhanced production of Th1 and cytotoxic T cells (44). By examining fowl Adenovirus serotype 4 infection, which causes hepatitis hydropericardium syndrome in poultry, Xiang et al. (45) revealed that the expression levels of IL-6, IL-1β, IFN-α, JAK, and STAT were significantly high after viral infection. In summary, during infection, the host induces changes in gene expression that confer transient or long-lasting protection against pathogens. Exploring why, when, which, and how a host reprograms its genome against infectious pathogens is an

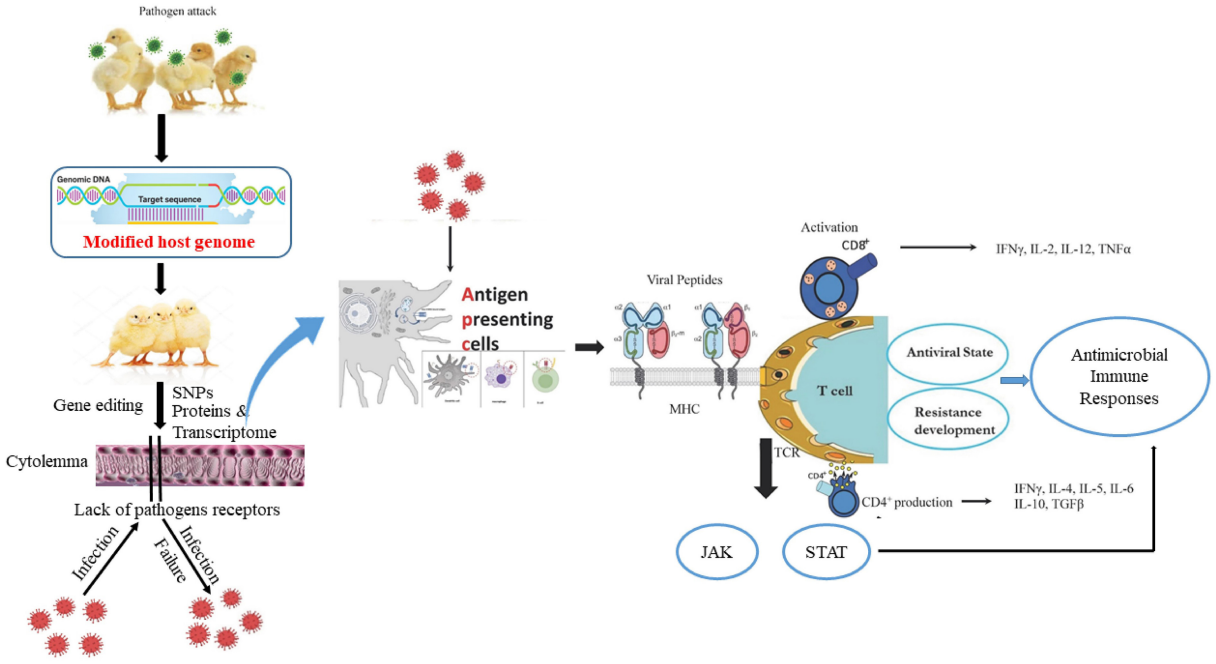

FIGURE 1
The host edited-genome and active immune responses of chicken during pathogen attack. Usually, chicken antigen presenting cells (dendritic cell, macrophage, B cell) engulf, digest, and present pathogen antigen on the cell surface in conjunction with an MHC molecule. The MHC/peptide complex stimulates the TCR and activates CD4+ and CD8+ cells. Accordingly, cytokines are produced, cell-signaling pathways such as JAK/STAT are activated, and a disease resistance state is developed inside the chicken that counters the pathogen virulence.

exciting research topic that can reveal the amplitude of virulence and its genetics.

Genetic resilience and autoimmune diseases

The TCR exhibits polymorphism that creates high diversity and differences in disease response by T cells (38). The TCR diversity is due to gene rearrangement where different segments, including variable (V), diversity (D), and joining (J) segments of the TCR gene, randomly recombine, and genes for the α, β, γ, and δ chains are formed (46). Although chickens have few V, D, and J genes that limit TCR diversity, TCR heterodimers can be created. For example, the TCR heterodimers of the α and β chains are the αβ T cells distinguished by the V region of the β-chain that causes Vβ1+ (TCR 2) and Vβ2+ (TCR 3) with functional multiplicity (47). TCR defects in chicken are associated with susceptibility to autoimmune diseases. In fact, the TCR defects in scleroderma disease cause low CD4+ cells and non-specific T cell response in chicken (48). Moreover, autoimmune thyroiditis disease is prevented by the depletion of CD4+ cells, highlighting the involvement of the TCR Vβ1 gene (49). Coccidiosis-resistant chicken lines have a high number of CD4+ cells whereas susceptible chickens have a high number of CD8+ cells (50). Moreover, a low number of CD8+ was detected in turkeys infected with Newcastle disease virus, *Pasteurella multocida*, and *Erysipelothrix rhusiopathiae* (50) whereas a high number of CD8+ cells was found in amyloidosis-resistant chickens compared to susceptible chickens (51). Altogether, the amount of CD4+ and CD8+ in resistant or susceptible birds does not align with a particular disease or pathogen in poultry, which might be due to the polymorphism of CD8+ and CD4+. CD4+ cells exhibit resistance toward non-intracellular while CD8+ cells exhibit toward intracellular pathogens that direct differential immune responses against a pathogen (52, 53). In conjunction with cellular immunity, humoral immunity plays a very key role in resistance to diseases. Immunoglobulin genes produce antibodies, and chickens with high antibody production display resistance against microbes, such as *Mycoplasma gallisepticum*, *Escherichia coli*, Newcastle disease virus, and *Salmonella enteritidis* relative to low antibody producers (54, 55). Chicks that are high antibody producers have numerous CD4+ and type II helper T lymphocytes (Th2), whereas low antibody producers have numerous CD8+ cells and type I helper T lymphocytes (Th1) that improve their resistance against pathogens (56, 57). The Th1 cytokines include IFN-γ, IL-2, and IL-12 whereas the Th2 cytokines include IL-4, IL-5, IL-6, and IL-10, which stimulate cell-mediated and

antibody responses, respectively (58). Altogether, variations exist in cellular and humoral immune responses in different chicken breeds, and high expression of cytokines leads to a higher immunocompetence of the host.

Genetic resilience and bacterial pathogens

Bacterial invasiveness in chickens depends on the species, severity, and virulence of the pathogen. The predominant bacterial pathogens affecting poultry are *Escherichia coli*, *Campylobacter jejuni*, *Clostridium perfringens*, Mycoplasma, and *Salmonella spp*. In contrast, *Erysipelothrix rhusiopathiae*, Gallibacterium anatis, *Pasteurella multocida*, *Riemerella anatipestifer*, *Avibacterium paragallinarum*, *Ornitobacterium rhinotracheale*, and *Bordetella avium* are infrequently detected (59, 60). The most devastating bacteria in terms of yield in the poultry industry belong to the genus, *Salmonella*, and include the species, *S. enterica* and *S. bongori*, that easily infect the newly hatched chicks and cause a decline in growth, egg production, and hatchability in chickens (61). To counter salmonellosis, prophylactic measures, such as antibiotics, vaccination, and disease management, are insufficient in poultry flock surveillance (62). Accordingly, the importance of resistant-chickens has increased, and the development of disease-resistant traits through genetic improvement has become more significant. Chicken MHC I, MHC II, Nramp-1, heterophils, IFN γ, and interleukins are involved in Salmonella-specific antibody responses and lead to resistance to salmonellosis (63). In a previous study, heterophils from chicken resistant to *S. enteritidis* had a higher level of cytokine mRNA than heterophils isolated from susceptible chickens (64). The mRNA level of interleukins and IFN γ increased in resistant chicks relative to that in chickens susceptible to salmonellosis (65). IFN γ plays a significant role in the eradication of Salmonella carriers and persistence state (66). The genes, *Nramp-1* and *Nramp-2*, are the macrophage proteins expressed in heterophils and leukocytes that facilitate *S. enteritidis* phagocytosis in resistant chicks (67). Other genes, such as transforming growth factor B4 (*TGFB4*) and *Sal1*, are involved in controlling Salmonella and other bacterial loads in the spleen, and have been linked to increasing genetic resistance against *S. enteritidis* (68). In a recent study, Beijing-You and Cobb chicks were orally challenged with *S. typhimurium*, which revealed robust responses of natural killer-cell-mediated-cytotoxicity, phagosomes, cytokines, MHC, and antibody production in Beijing-You chicken, ultimately indicating the greater resistance of Beijing-You breed to *S. typhimurium* (69). The chicken RIP2 pathway plays a significant role in resistance against avian pathogenic *E. coli* infection. *E. coli* infection promotes RIP2 expression and inhibits cell viability, whereas knockdown of RIP2 restores cell viability and represses the apoptosis of chicken HD11 cells. Nuclear factor I B increases the expression of RIP2, reduces cell viability, and accelerates *E. coli*-induced apoptosis, confirming that RIP2 supported *E. coli* proliferation in chicken cells (70). *Mycoplasma gallisepticum* infects the lungs of chickens and causes chronic respiratory disease. Glycyrrhizic acid is a herb that has anti-inflammatory, anti-microbial, and antioxidant activities and inhibits *M. gallisepticum* infection by suppressing the expression of matrix metalloproteinases through the JNK (c-Jun N-terminal kinase) and p38 pathways and inhibiting the expression of virulence genes of *M. gallisepticum* (71). *Campylobacter jejuni* infections are prevalent in poultry and colonize the intestine of birds. The bird's response to *C. jejuni* is similar to Salmonella infection, and high expression levels of cytokines, T and B cells, and antibodies are detected in *C. jejuni*-resistant birds relative to susceptible birds (72), except quantitative trait loci localization, which is located in different chromosomes (73). Breeder selection of traits that correlate with enhanced resistance against pathogens is highly desirable, and can be determined *via* extensive immunogenetics research. Therefore, screening host genome for disease-resistance genes and pathways in chickens can pave the way for the development of immunocompetent chickens.

Genetic resilience and protozoans

The next important etiological agents that cause infectious diseases in chicken are protozoal parasites, including *Eimeria tenella*, *Ascaridia galli*, and *Histomonas meleagridis*. The protozoan, *H. meleagridis*, causes blackhead disease or histomoniasis (74); *E. tenella* causes coccidiosis in chickens (75); and *A. galli* infects chickens and turkeys and causes stunted growth and enteritis (76). Pathogen-specific immune responses occur against parasitic infections in chicken. For instance, the myeloid leukemia factor 2 gene help in resistance to Eimeria (77), and the *IFNG* gene is associated with *Ascaridia* resistance in poultry (78). Moreover, the MHC haplotypes protect the jungle fowl from coccidian (79) and chicken lines from *Ascaridia* infections (80). Other genes, such as TGFβ 2-TGFβ 4, Caspase-1, inhibitor of apoptosis protein1, prosaposin, inducible nitric oxide production, IL-2, immunoglobulin light chain, and tumor necrosis factor-related apoptosis-inducing ligand, have been relatively less explored in protozoan resistance, but can improve the disease resistance traits in poultry.

Yang et al. (81) discovered that butyrate, forskolin, and lactose compounds synergistically increase the expression of multiple host defense peptides, improve the survival of chickens, and reduce the colonization of *Eimeria maxima* and *Clostridium perfringens*. A list of candidate genes in poultry that exhibit important functional activities in animals, but have not been explored for disease resistance in chickens, is provided in Table 1.

TABLE 1 The key genes are involved in the infectious diseases of chickens.

Gene ID	Gene symbol	Gene name	Access code	Study type	Function	Location	Reference
396241	*TF*	*Transferrin*	NM_205304.2	*In vitro*	Iron-binding glycoprotein and involved in anti-microbial activities, against Marek's disease	*chromosome: 9*	(7, 82)
416928	*IGLL1*	*Immunoglobulin lambda-like polypeptide 1*	NM_001278545.1	*In vivo*	Antibacterial properties against *Streptococcus mutans*	*chromosome: 15*	(83)
100543636	*LOC100543636*	*Ovoinhibitor*	XM_010719004.3	*In vitro*	Antibacterial activities during embryo developments	*chromosome: 15*	(7, 84)
424533	*VTG2*	*Vitellogenin 2*	NM_001031276.2	*In vivo*	Transfer of nutrients for developing embryo and reduce intestinal oxidative stress	*chromosome: 8*	(7, 85)
418974	*VMO1*	*Vitelline membrane outer layer 1*	NM_001167761.2	*In vivo*	Diagnostic marker of ovarian cancer in hen	*chromosome: 1*	(86)
395364	*PIT54*	*PIT54 protein*	NM_207180.2	*In vivo*	Hemoglobin-binding protein of plasma in chicken which has antioxidant activity	*chromosome: 31*	(87)
420897	*OVALY*	*Ovalbumin-related protein Y*	NM_001031001.1	*In vitro and In vivo*	Ovalbumin has antioxidant and radical scavenging activities	*chromosome: 2*	(88, 89)
396393	*EX-FABP*	*Extracellular fatty acid-binding protein*	NM_205422.2	*In vitro*	Function as an antibacterial siderophore binding lipocalin	*chromosome: 17*	(90)
395722	*CLU*	*Clusterin*	NM_001396177.1	*In vivo*	Serve as a marker for follicular atresia and involve in developmental phases of follicles	*chromosome: 3*	(91)
396384	*IRF1*	*Interferon regulatory factor 1*	NM_205415.2	*In vitro*	Inhibits the replication of avian influenza virus and Newcastle disease virus	*chromosome: 13*	(92)
769014	*TLR2*	*Toll like receptor 2*	NM_001161650.3	*In vivo*	Immunity and resistance to bacterial infection	*chromosome: 4*	(93)
395764	*CASP1*	*Caspase 1*	XM_015295935.4	*In vitro and In vivo*	Involved in apoptosis, necrosis, mitophagy, and autophagy	*chromosome: 19*	(94–96)
418300	*ZYX*	*Zyxin*	NM_001004386.2	*In vivo*	Zyxin is a candidate gene potentially associated with increased resistance to experimental avian coccidiosis.	*chromosome: 1*	(97)
396260	*AVD*	*Avidin*	NM_205320.2	*In vitro*	Antimicrobial activity	*chromosome: Z*	(98, 99)
418812	*ACOD1*	*Aconitate decarboxylase 1*	NM_001030821.2	*In vivo*	Antimicrobial activity	*chromosome: 1*	(100)

(Continued)

TABLE 1 (Continued)

Gene ID	Gene symbol	Gene name	Access code	Study type	Function	Location	Reference
374125	*LITAF*	*Lipopolysaccharide induced TNF factor*	NM_204267.2	*In vitro and In vivo*	Initiates the activation of caspases and kinase protein signaling of the cell death pathway and has antimicrobial activity	*chromosome: 14*	(101)
395283	*TRAIL-LIKE*	*TNF-related apoptosis inducing ligand-like*	XM_015278184.4	*In vitro and In vivo*	It declines the autoimmune response by suppressing cell cycle progression.	*chromosome: 4*	(102)
420963	*PTPN3*	*Protein tyrosine phosphatase, non-receptor type 3*	XM_419047.8	*In vivo*	Involved in immune suppression disease.	*chromosome: 2*	(103)
378897	*THY1*	*Thy-1 cell surface antigen*	NM_204381.3	*In vitro*	Involved in chicken Marek disease.	*chromosome: 24*	(104)
768688	*SMOC1*	*SPARC related modular calcium binding 1*	XM_015287582.4	*In vivo*	Enhanced endothelial cell proliferation and angiogenesis.	*chromosome: 5*	(105)
422993	*LOC422993*	*Interferon-induced transmembrane protein 3-like*	NM_001350059.2	*In vivo*	Highly expressed in response to avian Tembusu virus infection	*chromosome: 5*	(106)

SNP-dependent resistance and susceptibility in chickens

SNP is the nucleotide sequence variation that occurs at a single position in DNA fragments and is extensively used as a molecular marker in genetic studies. The roles of SNPs are largely associated with production traits in chicken. SNPs have been detected in follicle-stimulating hormone, prolactin receptor, dopamine receptor 2, low-density lipoprotein receptor-related protein, and luteinizing hormone receptors, with characteristic changes in duck and chicken (107, 108). For instance, the follicle-stimulating hormone regulates reproductive activities in birds, and the SNP detected in the follicle-stimulating hormone is linked to the reproductive traits of chickens (109). Two key SNPs, A227G and C320T, were identified in the Muscovy duck follicle-stimulating hormone gene that improve egg production traits (110). Ye et al. (111) revealed two SNPs in the insulin-like growth factor 2 gene and 11 SNPs in dopamine receptor 2 that are linked with egg-laying traits (111). In a recent study, the polymorphism of the DMA gene, a member of the non-classical MHC class II gene, was associated with disease resistance traits in broiler chickens. Four SNPs linked to seven haplotype formations were found, with haplotypes 1 and 5 associated with high immunoglobulin yolk concentration and ND antibody level, respectively (112). The SNPs detected in the carboxypeptidase Q and leucine-rich repeat transmembrane neuronal 4 gene regions resulted in a decrease in pulmonary hypertension syndrome and greater innate ascites resistance in chicken offspring (113). Mountford et al. (2) correlated SNPs with resistance and susceptibility to MDV, infectious bursal disease virus, avian influenza virus, and infectious bronchitis virus. These researchers detected 10 SNPs that were involved in the resistance to MDV and 8 SNPs associated with the susceptibility to infectious bursal disease virus. Recently, IL10Rβ SNP resulted in an R318K amino acid substitution that was involved in the enhanced regulation of the type III interferon pathway that reduced bursal damage in infectious bursal disease virus-infected birds (114). A previous study revealed the same SNP involvement in increased susceptibility to MDV (115). Thus, IFN response can vary for viruses owing to viral mutagenicity and strain diversity. As a result, viruses can block the IFN responses. Nramp-1, Sal-1, and Tnc are the genes involved in resistance to *Mycobacterium*, *Salmonella*, and *Leishmania* infections (116). In chicken, Nramp-1 polymorphism is correlated with susceptibility to salmonellosis. Frequent sequence variations were detected in this gene that conferred resistance differences in chicken (4, 117). MyD88

polymorphism is associated with *S. pullorum* susceptibility in chickens and has a favorable effect on vulnerability to *S. pullorum* infection (118). These recently identified SNPs are associated with disease-resistance genotypes that can help in the identification of new genes and their roles in eradicating infectious diseases.

Non-coding RNA resistance in chicken

Non-coding RNAs are biological molecules involved in epigenetic regulation and disease resistance (119). There are different classes of non-coding RNAs, such as circular RNAs, small interfering RNAs, long non-coding RNAs (LncRNAs), microRNAs, and transfer RNAs, that play important roles in avian immunity and cell development. Among these classes of RNAs, LncRNAs, circular RNAs, and microRNAs are called regulatory RNAs that mediate gene expression in different hosts (120). LncRNAs are longer than 200 nucleotides and are known as signaling molecules that interact with mRNA, miRNA, DNA, and proteins, thereby regulating various processes, such as apoptosis, tumor cell invasion, RNA transcription, and host resistance to pathogen infection (121, 122). Based on recent studies, lncRNAs regulate vitamins A and D during bacterial and fungal infections and activate immune responses during chicken leukemia virus infection (123). Specialized lncRNAs that reduce the production of inflammatory cytokines, such as IL-6, IL-8, and TNF-α, were identified in response to *E. tenella* infection in chickens (124). An important ERL lncRNA acts as an antisense transcript of MDV carcinogen, is expressed during the lytic and lysogenic phases of viral infection, and inhibits the expression of MDV miRNAs (125, 126). The lncRNA, GLAMD3, cis-regulates the gga-miR-223 expression that targets IGF1R (insulin-like growth factor 1 receptor), which regulates Marek's disease lymphoma (127). Another important lncRNA, linc-stab1, regulates the Marek's disease resistance gene, SATB1, which is also involved in cell-mediated immunity for termination of MDV-infected cells (128).

Several studies revealed the roles of circRNAs in avian leukosis virus infection. Furthermore, differentially-expressed circRNAs were detected in infected organs. circRNAs are involved in T and B-cell activation (129), and Jak-STAT pathway regulation (130). In contrast to lncRNAs and circRNAs, the expression profile and functional mechanism of miRNAs are well-characterized in disease resistance in chickens. In fact, differentially expressed miRNAs have a significant effect on oncogenicity (131); the regulation of MAPK, JaK/STAT, and Wnt pathways (132); and suppression of chronic myeloid leukemia caused by avian leukosis virus in chicken (133). In conclusion, non-coding RNAs regulate disease resistance traits, interact with host and pathogen genes, and help to control infectious diseases.

Modern technology and development of disease-resistant chicken

Gene-editing techniques, such as zinc-finger nucleases (ZFNs), transcription activator-like effector nucleases (TALENs), pronuclear injection, sperm-mediated gene transfer, somatic cell nuclear transfer, recombinases, transposons, viral vectors, and CRISPR/Cas9 systems, are novel molecular tools that are efficiently used in mice, cattle, sheep, and goat. For instance, transgenic mice, rabbits, pigs, and sheep were engineered by microinjection of the target DNA into the fertilized embryo (134, 135); lentiviral vectors and embryonic stem cells were used to produce germline transgenic birds (136, 137); and successful knock-out in chickens were achieved by homologous recombination in primordial germ cells (138). In zinc-finger nucleases and transcription activator-like effector nucleases techniques, the proteins bind to the target DNA sequence for modification, whereas the CRISPR requires a guide RNA to recognize the target DNA fragments. Further, the endonuclease enzyme performs a target-specific cut (139). Since the introduction of the CRISPR/Cas9 system in genome editing, substantial progress has been made in the use of the CRISPR/Cas9 technology in chickens. A CRISPR/Cas9-mediated chicken was engineered in 2015 (139) and ovomucoid gene-targeted chickens and knocked-in of human interferon beta into the chicken ovalbumin gene were edited successfully (140, 141). The emerging viral strains of avian leukosis and MDV are highly pathogenic. Further, existing vaccines and antiviral drugs are becoming less effective. Thus, novel antiviral strategies are needed. For instance, through CRISPR/Cas9, the avian leukosis virus subgroup J receptor sodium/hydrogen exchanger type 1 is mutated, which protects the chicken line from avian leukosis virus subgroup J. Subgroup J prototype strain replication is also impaired in mutated birds (142). Resistance was found to develop in chicken cells against avian leukosis virus subgroup J by creating tryptophan mutations at position 38 (143). In another study, genetic resistance to avian leukosis virus subgroups A, C, J was induced by creating frame-shift mutations in *tva* (tumor virus locus A gene), *tvc*, and *tvj* genes (144). Koslová et al. (143) and Hellmich et al. (144) produced ALV-J-resistant chicken lines *via* precise gene editing of chicken sodium/hydrogen exchanger 1. A recent study revealed that transgenic chickens constitutively express Cas9 and guide RNAs specific to the immediate early infected-cell polypeptide-4 (gICP4) of MDV upon challenge with MDV, and exhibit reduced replication compared to wild-type chickens (145). These examples highlight the use of the CRISPR/Cas9 system to edit genes of interest and engineer chicken flocks that

exhibit resistance characteristics to viral infection (146). Lately, CRISPR/Cas9 has been used to develop transgenic animals. Accordingly, transgenic animals are generated *via* the targeted placement of *Streptococcus pyogenes* Cas9 at the ROSA26 locus and endogenous pseudo attP site in pigs and chickens, respectively. Transgenic chickens and pigs constitutively express Cas9. Cas9 was confirmed in pigs and chicken for different target genes in many cell types with the *S. pyogenes* Cas9 platform for *in vitro* and *in vivo* genome editing in livestock species (147). Similarly, different computational and bioinformatics approaches can be used to design synthetic RNA duplexes that would target the mRNA sites of viral, bacterial, and protozoal pathogens. For example, synthetic RNA duplexes that target specific domains of viral genes can inhibit viral replication (148). Techniques, such as RNA interference technology, have strong applications in the development of transgenic poultry that is resistant to microbial infections. RNA interference is the method of choice, where RNA molecules inhibit gene expression by targeting specific mRNA. Similarly, a lentiviral vector containing influenza-specific RNA hairpin rendered the cells refractory to viral infection and inhibited influenza virus replication in mice (149). These results provide evidence and scope for the development of pathogen-resistant poultry flocks *via* the transgenic expression of gene-specific RNA. In an earlier study, a recombinant plasmid with synthetic RNA duplex gene was constructed and transferred into Madin-Darby Canine Kidney cells. The study revealed that the transfected cell lines were resistant to the avian influenza virus (150). This landmark experiment provided the breakthrough for transgenic chicken development and resistance to influenza virus. RNA-Sequencing is another advanced technique that reveals the poultry genome responses to different stresses and diseases. The development of a disease-resistant chick through traditional breeding is a difficult and labor-intensive task, while the use of gene-editing technology and production traits is time-saving and profitable (151). With the development of next-generation sequencing technology, interest in whole-genome sequencing as an alternative to SNP chips for genotyping has increased as it allows the capture of a wide range of variations. For instance, a genome-wide association study and quantitative trait loci mapping identified candidate genes for egg production in ducks (152). These tools would help in the editing of the chicken genome and fulfill the dire need for disease-resistance breeds in poultry.

Applications of chicken-genomics in biomedical research

Chickens are widely used in developmental research owing to their easy rearing, fecundity, growth rates, and genetic variations, thereby advancing the field of biomedical research. The chicken model has been used to evaluate cancer metastasis, test chemotherapy agents, tissue morphogenesis, and angiogenesis, and perform toxicology studies. The egg is an important source of protein and contains phosvitin, which protects against oxidative stress-induced DNA damage in human leukocytes (153), and ovotransferrin, which is used as growth inhibitor for cancer cell lines (154). Avian-derived cell lines are used for viral culture and are helpful in vaccine and recombinant protein production (155). Chicken has also been used as a xenotransplantation model for human stem cells (156), human multiple myeloma xenograft (157), and the production of human antibodies (158). The Omni Chicken by Ligand Pharmaceuticals Inc. is a worldwide unique platform used to produce human monoclonal antibodies from chickens (159). Oishi et al. (141) integrated human interferon beta (hIFN-β) into the chicken ovalbumin locus and produced hIFN-β in egg white. Notably, antibodies produced from humanized chickens and antibodies produced in chicken eggs represent significant industrial applications. Accordingly, chicken is an attractive developmental model for biomedical research.

Conclusion

This review summarized the disease-resistance genes in poultry and provided an outlook of advanced technologies that can be used to engineer disease-resistance characteristics in poultry. The poultry industry is one of the fastest growing sectors of livestock for meat and egg production; however, this industry is threatened by different pathogens, which lead to substantial economic losses. Vaccination, antibiotics, culling, and disease management techniques are frequently employed in flocks to control disease outbreak; however, the success rate is nominal. Genetic resistance is a promising alternative method to augment prophylactic measures. Genetic resistance can be acquired through genetic breeding and genetic modification. Breeding chickens with disease-resistant strains can increase flock resistance; however, the genome modification process can underpin a characteristic of interest and assimilate into offspring to improve immune responses. Currently, genome editing technologies are driving desirable phenotypic traits, as genetic modifications are meeting enhanced production goals in the poultry industry, and engineering elite chicken for breeders. Further studies are required to effectively determine the roles of candidate genes in generating an ideal disease-resistant chicken.

Future prospective

Next-generation sequencing of chicken-genome and pathogens helps in the understanding of host-pathogen interactions, natural variations, and the discovery of new QTLs that may be associated with disease-resistance and susceptibility traits in poultry. The use of lentiviral vectors is very efficient for gene delivery in animals and poultry compared

to homologous recombination of embryonic and somatic cells. Other alternatives for embryonic stem cells include RNAi and ZFNs technologies, which may be used for gene targeting and disruption in animals. The amplified genomic information of poultry and the advent of more sophisticated transgenic tools would result in resistance against pathogens. By investigating the genomics of chickens, new genes with divergent characteristics may lead to enhanced chicken yield. The use of other bird species with similar and unique characteristics will also advance avian research.

Author contributions

HG, IK, and YL contributed to conceptualization. GH contributed to the methodology. IK and SR contributed to software. YL and HG contributed to validation and original draft. NK and SR contributed to investigation. YL contributed to resources and funding acquisition. GH, IK, HW, and NK contributed to the final draft and editing. All authors contributed to the article and approved the submitted version.

Funding

This work was funded by Industry-University-Research Project of Fuyang Normal University (HX2021027000 and HX2022048000).

Conflict of interest

The authors declare that the research was conducted in the absence of any commercial or financial relationships that could be construed as a potential conflict of interest.

Publisher's note

All claims expressed in this article are solely those of the authors and do not necessarily represent those of their affiliated organizations, or those of the publisher, the editors and the reviewers. Any product that may be evaluated in this article, or claim that may be made by its manufacturer, is not guaranteed or endorsed by the publisher.

References

1. Gogoi A, Das B, Chabukdhara P, Phookan A, Phangchopi DJAR. Livestock breeding for disease resistance: a perspective review. *Agric Rev*. (2022) 43:116–21. doi: 10.18805/ag.R-2169

2. Mountford J, Gheyas A, Vervelde L, Smith JJAG. Genetic variation in chicken interferon signalling pathway genes in research lines showing differential viral resistance. *Anim Genet.* (2022) 53:640–56. doi: 10.1111/age.13233

3. Zekarias B, Ter Huurne AA, Landman WJ, Rebel JM, Pol JM, Gruys E. Immunological basis of differences in disease resistance in the chicken. *Vet Res.* (2002) 33:109–25. doi: 10.1051/vetres:2002001

4. Dar MA, Mumtaz PT, Bhat SA, Nabi M, Taban Q, Shah RA, et al. Genetics of disease resistance in chicken. *Appl Genet Genomics Poult Sci.* (2018) 168–74. doi: 10.5772/intechopen.77088

5. Alberts B, Johnson A, Lewis J, Raff M, Roberts K, Walter P. T cells and MHC proteins. In: *Molecular Biology of the Cell*. 4th edition. New York, NY: Garland Science (2002).

6. Kinome M. Metabolism when stimulated early in life with CpG. *Poult Sci.* (2022) 101:101775. doi: 10.1016/j.psj.2022.101775

7. Gul H, Chen X, Geng ZJA. Comparative yolk proteomic analysis of fertilized low and high cholesterol eggs during embryonic development. *Animals*. (2021) 11:744. doi: 10.3390/ani11030744

8. Gul H, Geng Z, Habib G, Hayat A, Rehman MU, Khan IJTAH, et al. Effect of ellagic acid and mesocarp extract of *Punica granatum* on productive and reproductive performances of laying hens. *Trop Anim Health Prod.* (2022) 54:228. doi: 10.1007/s11250-022-03222-7

9. Stear M, Bairden K, Bishop S, Buitkamp J, Duncan J, Gettinby G, et al. The genetic basis of resistance to Ostertagia circumcincta inlambs. *Vet J.* (1997) 154:111–9. doi: 10.1016/S1090-0233(97)80049-4

10. Cole R. Studies on genetic resistance to marek's disease. *Avian Dis.* (1968) 12:9–28. doi: 10.2307/1588081

11. Heringstad B, Klemetsdal G, Ruane JJLPS. Selection for mastitis resistance in dairy cattle: a review with focus on the situation in the Nordic countries. *Livest Prod Sci*. (2000) 64:95–106. doi: 10.1016/S0301-6226(99)00128-1

12. Wilkie B, Mallard BJ. Genetic aspects of health and disease resistance in pigs. In: *Breeding for Disease Resistance in Farm Animals 2.* (2000). p. 379–96.

13. Lyall J, Irvine RM, Sherman A, McKinley TJ, Núñez A, Purdie A, et al. Suppression of avian influenza transmission in genetically modified chickens. *Science.* (2011) 331:223–6. doi: 10.1126/science.1198020

14. Yu M, Muteti C, Ogugo M, Ritchie WA, Raper J, Kemp S. Cloning of the African indigenous cattle breed Kenyan Boran. *Anim Genet*. (2016) 47:510. doi: 10.1111/age.12441

15. Whitworth KM, Rowland RR, Ewen CL, Trible BR, Kerrigan MA, Cino-Ozuna AG, et al. Gene-edited pigs are protected from porcine reproductive and respiratory syndrome virus. *Nat Biotechnol.* (2016) 34:20–2. doi: 10.1038/nbt.3434

16. Kalds P, Zhou S, Cai B, Liu J, Wang Y, Petersen B, et al. Sheep and goat genome engineering: from random transgenesis to the crispr era. *Front Genet.* (2019) 10:750. doi: 10.3389/fgene.2019.00750

17. Golding MC, Long CR, Carmell MA, Hannon GJ, Westhusin M. Suppression of prion protein in livestock by Rna interference. *Proc Natl Acad Sci U S A.* (2006) 103:5285–90. doi: 10.1073/pnas.0600813103

18. Plachy J, Pink JR, Hala K. Biology of the chicken MHC (B complex). *Crit Rev Immunol.* (1992) 12:47–79.

19. Kaufman J, Venugopal K. The importance of MHC for Rous sarcoma virus and marek's disease virus—some payne-ful considerations. *Avian Pathol.* (1998) 27:S82–7. doi: 10.1080/03079459808419297

20. Lopez-Botet M, Llano M, Navarro F, Bellon T. NK cell recognition of non-classical HLA class I molecules. *Semin Immuno*. (2000) 12:109–19. doi: 10.1006/smim.2000.0213

21. Bertzbach LD, Tregaskes CA, Martin RJ, Deumer U-S, Huynh L, Kheimar AM, et al. The diverse major histocompatibility complex haplotypes of a common commercial chicken line and their effect on marek's disease virus pathogenesis and tumorigenesis. *Front Immunol.* (2022) 13:908305. doi: 10.3389/fimmu.2022.908305

22. Boodhoo N, Gurung A, Sharif S, Behboudi S. Marek's disease in chickens: a review with focus on immunology. *Vet Res.* (2016) 47:1–19. doi: 10.1186/s13567-016-0404-3

23. Dong K, Chang S, Xie Q, Black-Pyrkosz A, Zhang H. Comparative transcriptomics of genetically divergent lines of chickens in response to marek's disease virus challenge at cytolytic phase. *PLoS ONE.* (2017) 12:e0178923. doi: 10.1371/journal.pone.0178923

24. Lee HJ, Lee KY, Jung KM, Park KJ, Lee KO, Suh J-Y, et al. Precise gene editing of chicken Na+/H+ exchange type 1 (Chnhe1) confers resistance to avian leukosis virus subgroup J (Alv-J). *Dev Comp Immunol.* (2017) 77:340–9. doi: 10.1016/j.dci.2017.09.006

25. Kolaczkowski B, Thornton J. Performance of maximum parsimony and likelihood phylogenetics when evolution is heterogeneous. *Nature.* (2004) 431:980–4. doi: 10.1038/nature02917

26. Staeheli P, Haller O, Boll W, Lindenmann J, Weissmann CJC. Mx protein: constitutive expression in 3t3 cells transformed with cloned Mx Cdna confers selective resistance to influenza virus. *Cell.* (1986) 44:147–58. doi: 10.1016/0092-8674(86)90493-9

27. Arnheiter H, Skuntz S, Noteborn M, Chang S, Meier EJC. Transgenic mice with intracellular immunity to influenza virus. *Cell.* (1990) 62:51–61. doi: 10.1016/0092-8674(90)90239-B

28. Müller M, Brenig B, Winnacker E-L, Brem GJG. Transgenic pigs carrying Cdna copies encoding the murine Mx1 protein which confers resistance to influenza virus infection. *Gene.* (1992) 121:263–70. doi: 10.1016/0378-1119(92)90130-H

29. Gavora JS. Progress and prospects in resistance to disease. *Proc 6th World Congr Genet Appl Livest Prod, Armidale, NSW*. Ottawa, ON: Centre for Food and Animal Research Agriculture and Agri-Food Canada. (1998).

30. Salter D, Crittenden LJT, Genetics A. Artificial insertion of a dominant gene for resistance to avian leukosis virus into the germ line of the chicken. *Theor Appl Genet.* (1989) 77:457–61. doi: 10.1007/BF00274263

31. Clements J, Wall R, Narayan O, Hauer D, Schoborg R, Sheffer D, et al. Development of transgenic sheep that express the visna virus envelope gene. *Virology.* (1994) 200:370–80. doi: 10.1006/viro.1994.1201

32. Smith J, Lipkin E, Soller M, Fulton JE, Burt DW. Mapping Qtl associated with resistance to avian oncogenic Marek's disease virus (Mdv) reveals major candidate genes and variants. *Genes.* (2020) 11:1019. doi: 10.3390/genes11091019

33. Sironi L, Williams JL, Moreno-Martin AM, Ramelli P, Stella A, Jianlin H, et al. Susceptibility of different chicken lines to H7n1 highly pathogenic avian influenza virus and the role of Mx gene polymorphism coding amino acid position 631. *Virology.* (2008) 380:152–6. doi: 10.1016/j.virol.2008.07.022

34. Ichikawa K, Motoe Y, Ezaki R, Matsuzaki M, Horiuchi H. Knock-in of the duck retinoic acid-inducible gene I (rig-I) into the Mx gene in Df-1 cells enables both stable and immune response-dependent rig-I expression. *Biochem Biophys* Rep. (2021) 27:101084. doi: 10.1016/j.bbrep.2021.101084

35. Ezema WS, Eze DC, Shoyinka SVO, Okoye JOA. Atrophy of the lymphoid organs and suppression of antibody response caused by velogenic newcastle disease virus infection in chickens. *Trop Anim Health Prod.* (2016) 48:1703–9. doi: 10.1007/s11250-016-1147-x

36. Zhang J, Kaiser MG, Deist MS, Gallardo RA, Bunn DA, Kelly TR, et al. Transcriptome analysis in spleen reveals differential regulation of response to newcastle disease virus in two chicken lines. *Sci Rep.* (2018) 8:1–13. doi: 10.1038/s41598-018-19754-8

37. Del Vesco AP, Kaiser MG, Monson MS, Zhou H, Lamont SJ. Genetic responses of inbred chicken lines illustrate importance of EIF2 family and immune-related genes in resistance to newcastle disease virus. *Sci Rep.* (2020) 10:1–9. doi: 10.1038/s41598-020-63074-9

38. Tudeka CK, Aning GK, Naazie A, Botchway PK, Amuzu-Aweh EN, Agbenyegah GK, et al. Response of three local chicken ecotypes of Ghana to lentogenic and velogenic newcastle disease virus challenge. *Trop Anim Health Prod.* (2022) 54:1–12. doi: 10.1007/s11250-022-03124-8

39. Touko H, Keambou T, Han J, Bembide C, Cho C, Skilton RA, et al. The major histocompatibility complex B (MHC-B) and QTL microsatellite alleles of favorable effect on antibody response against the Newcastle disease. *Int J Genet Res.* (2013) 1:1–8.

40. Wang Y, Lupiani B, Reddy S, Lamont S, Zhou H. RNA-Seq analysis revealed novel genes and signaling pathway associated with disease resistance to avian influenza virus infection in chickens. *Poult Sci.* (2014) 93:485–93. doi: 10.3382/ps.2013-03557

41. Lee J, Hong Y, Vu TH, Lee S, Heo J, Truong AD, et al. Influenza a pathway analysis of highly pathogenic avian influenza virus (H5n1) infection in genetically disparate RI chicken lines. *Vet Immunol Immunopathol.* (2022) 246:110404. doi: 10.1016/j.vetimm.2022.110404

42. Adkins HB, Brojatsch, Young JA. Identification and characterization of a shared Tnfr-related receptor for subgroup B, D, and E avian leukosis viruses reveal cysteine residues required specifically for subgroup e viral entry. *J Virol.* (2000) 74:3572–8. doi: 10.1128/JVI.74.8.3572-3578.2000

43. Prikryl D, Plachý J, Kučerová D, Koslová A, Reinišová M, Šenigl F, et al. The novel avian leukosis virus subgroup K shares its cellular receptor with subgroup A. *J Virol.* (2019) 93:e00580–19. doi: 10.1128/JVI.00580-19

44. Schat KA, Skinner MA. Avian immunosuppressive diseases and immune evasion. *Avian Immunology*, 3rd Edition. Boston, MA: Academic Press (2022). p. 387–417. doi: 10.1016/B978-0-12-818708-1.00018-X

45. Xiang S, Huang R, He Q, Xu L, Wang C, Wang Q. Arginine regulates inflammation response-induced by fowl adenovirus serotype 4 Via Jak2/Stat3 pathway. *BMC Vet Res.* (2022) 18:1–10. doi: 10.1186/s12917-022-03282-9

46. Davis MM, Bjorkman PJ. T-Cell antigen receptor genes and T-cell recognition. *Nature.* (1988) 334:395–402. doi: 10.1038/334395a0

47. Lahti J, Chen C, Tjoelker L, Pickel J, Schat K, Calnek B, et al. Two distinct alpha beta T-cell lineages can be distinguished by the differential usage of T-cell receptor V beta gene segments. *Proc Nat Acad Sci.* (1991) 88:10956–60. doi: 10.1073/pnas.88.23.10956

48. Wilson TJ, Van de Water J, Mohr FC, Boyd RL, Ansari A, Wick G, et al. Avian scleroderma: evidence for qualitative and quantitative T cell defects. *J Autoimmun.* (1992) 5:261–76. doi: 10.1016/0896-8411(92)90142-D

49. Cihak J, Hoffmann-Fezer G, Wasl M, Merkle H, Kaspers B, Hála K, et al. Prevention of spontaneous autoimmune thyroiditis in the obese strain (Os) chickens by treatment with a monoclonal anti-Cd4 antibody. *J Vet Med Series A.* (1996) 43:211–6. doi: 10.1111/j.1439-0442.1996.tb00446.x

50. Vermeulen AN. Avian coccidiosis: a disturbed host-parasite relationship to be restored. *Host-Parasite Interact.* (2004) 211–41. doi: 10.4324/9780203487709-10

51. Zekarias B, Landman WJ, Tooten PC, Gruys E. Leukocyte responses in two breeds of layer chicken that differ in susceptibility to induced amyloid arthropathy. *Vet Immunol Immunopathol.* (2000) 77:55–69. doi: 10.1016/S0165-2427(00)00233-6

52. Luhtala M, Tregaskes CA, Young JR, Vainio O. Polymorphism of chicken Cd8-alpha, but not Cd8-beta. *Immunogenetics.* (1997) 46:396–401. doi: 10.1007/s002510050293

53. Davison T. The immunologists' debt to the chicken. *Br Poult Sci.* (2003) 44:6–21. doi: 10.1080/0007166031000085364

54. Wu Z, Ding L, Bao J, Liu Y, Zhang Q, Wang J, et al. Co-infection of mycoplasma gallisepticum and escherichia coli triggers inflammatory injury involving the Il-17 signaling pathway. *Front Microbiol.* (2019) 10:2615. doi: 10.3389/fmicb.2019.02615

55. Gross W, Siegel P, Hall R, Domermuth C, DuBoise R. Production and persistence of antibodies in chickens to sheep erythrocytes: 2. Resistance to Infectious Diseases. *Poult Sci.* (1980) 59:205–10. doi: 10.3382/ps.0590205

56. Parmentier HK, Kreukniet MB, Goeree B, Davison TF, Jeurissen SH, Harmsen EG, et al. Differences in distribution of lymphocyte antigens in chicken lines divergently selected for antibody responses to sheep red blood cells. *Vet Immunol Immunopathol.* (1995) 48:155–68. doi: 10.1016/0165-2427(94)05411-K

57. Parmentier H, Abuzeid SY, Reilingh GDV, Nieuwland M, Graat E. Immune responses and resistance to eimeria acervulina of chickens divergently selected for antibody responses to sheep red blood cells. *Poult Sci.* (2001) 80:894–900. doi: 10.1093/ps/80.7.894

58. Infante-Duarte C, Kamradt T. Th1/Th2 Balance in Infection. *Springer Semin Immunopathol.* (1999) 21:317–38. doi: 10.1007/BF00812260

59. Skånseng B, Kaldhusdal M, Rudi K. Comparison of chicken gut colonisation by the pathogens campylobacter Jejuni and clostridium perfringens by real-time quantitative PCR. *Mol Cell Probes.* (2006) 20:269–79. doi: 10.1016/j.mcp.2006.02.001

60. Saif Y. *Diseases of Poultry.* Ames, IA: John Wiley and Sons (2009).

61. Andino A, Hanning I. Salmonella enterica: survival, colonization, and virulence differences among serovars. *ScientificWorldJournal.* (2015) 2015:520179. doi: 10.1155/2015/520179

62. Calenge F, Kaiser P, Vignal A, Beaumont C. Genetic control of resistance to salmonellosis and to salmonella carrier-state in fowl: a review. *Genet Sel Evol.* (2010) 42:1–11. doi: 10.1186/1297-9686-42-11

63. Tohidi R, Javanmard A, Idris I. Immunogenetics applied to control salmonellosis in chicken: a review. *J Appl Anim Res.* (2018) 46:331–9. doi: 10.1080/09712119.2017.1301256

64. Ferro PJ, Swaggerty CL, Kaiser P, Pevzner IY, Kogut MH. Heterophils isolated from chickens resistant to extra-intestinal salmonella enteritidis infection express higher levels of pro-inflammatory cytokine mRNA following infection than heterophils from susceptible chickens. *Epidemiol Infect.* (2004) 132:1029–37. doi: 10.1017/S0950268804002687

65. Swaggerty CL, Kogut MH, Ferro PJ, Rothwell L, Pevzner IY, Kaiser P. Differential cytokine mRNA expression in heterophils isolated

from salmonella-resistant and-susceptible chickens. *Immunology.* (2004) 113:139–48. doi: 10.1111/j.1365-2567.2004.01939.x

66. Foster N, Tang Y, Berchieri A, Geng S, Jiao X, Barrow P. Revisiting persistent salmonella infection and the carrier state: what do we know? *Pathogens.* (2021) 10:1299. doi: 10.3390/pathogens10101299

67. Redmond SB, Chuammitri P, Andreasen CB, Palić D, Lamont SJ. Genetic control of chicken heterophil function in advanced intercross lines: associations with novel and with known salmonella resistance loci and a likely mechanism for cell death in extracellular trap production. *Immunogenetics.* (2011) 63:449–58. doi: 10.1007/s00251-011-0523-y

68. Fife M, Salmon N, Hocking P, Kaiser P. Fine mapping of the chicken salmonellosis resistance locus (Sal1). *Anim Genet.* (2009) 40:871–7. doi: 10.1111/j.1365-2052.2009.01930.x

69. Elsharkawy MS, Wang H, Ding J, Madkour M, Wang Q, Zhang Q, et al. Transcriptomic analysis of the spleen of different chicken breeds revealed the differential resistance of salmonella typhimurium. *Genes.* (2022) 13:811. doi: 10.3390/genes13050811

70. Sun H, Li N, Tan J, Li H, Zhang J, Qu L, et al. Transcriptional regulation of RIP2 gene by NFIB is associated with cellular immune and inflammatory response to APEC infection. *Int J Mol Sci.* (2022) 23:3814. doi: 10.3390/ijms23073814

71. Wang Y, Wang L, Luo R, Sun Y, Zou M, Wang T, et al. Glycyrrhizic acid against mycoplasma gallisepticum-induced inflammation and apoptosis through suppressing the MAPK pathway in chickens. *J Agric Food Chem.* (2022) 70:1996–2009. doi: 10.1021/acs.jafc.1c07848

72. Connell S, Meade KG, Allan B, Lloyd AT, Kenny E, Cormican P, et al. Avian resistance to campylobacter jejuni colonization is associated with an intestinal immunogene expression signature identified by mRNA sequencing. *PLos ONE.* (2012) 7:e40409. doi: 10.1371/journal.pone.0040409

73. Psifidi A, Fife M, Howell J, Matika O, Van Diemen P, Kuo R, et al. The genomic architecture of resistance to campylobacter jejuni intestinal colonisation in chickens. *BMC Genomics.* (2016) 17:1–18. doi: 10.1186/s12864-016-2612-7

74. McDougald L. Blackhead disease (histomoniasis) in poultry: a critical review. *Avian Dis.* (2005) 49:462–76. doi: 10.1637/7420-081005R.1

75. Adamu M, Boonkaewwan C, Gongruttananun N, Vongpakorn M. Hematological, Biochemical and histopathological changes caused by coccidiosis in chickens. *Agric Nat Resour.* (2013) 47:238–46.

76. Ruhnke I, Andronicos NM, Swick RA, Hine B, Sharma N, Kheravii SK, et al. Immune responses following experimental infection with *Ascaridia galli* and necrotic enteritis in broiler chickens. *Avian Pathol.* (2017) 46:602–9. doi: 10.1080/03079457.2017.1330536

77. Kim E-S, Hong Y, Lillehoj H. Genetic effects analysis of myeloid leukemia factor 2 and T cell receptor-B on resistance to coccidiosis in chickens. *Poult Sci.* (2010) 89:20–7. doi: 10.3382/ps.2009-00351

78. Lühken G, Gauly M, Kaufmann F, Erhardt G. Association study in naturally infected helminth layers shows evidence for influence of interferon-gamma gene variants on *Ascaridia galli* worm burden. *Vet Res.* (2011) 42:1–7. doi: 10.1186/1297-9716-42-84

79. Worley K, Collet J, Spurgin LG, Cornwallis C, Pizzari T, Richardson DSJME, et al. Heterozygosity and survival in red junglefowl. *Mol Ecol.* (2010) 19:3064–75. doi: 10.1111/j.1365-294X.2010.04724.x

80. Norup LR, Dalgaard TS, Pleidrup J, Permin A, Schou TW, Jungersen G, et al. Comparison of parasite-specific immunoglobulin levels in two chicken lines during sustained infection with *Ascaridia galli*. *Vet Parasitol.* (2013) 191:187–90. doi: 10.1016/j.vetpar.2012.07.031

81. Yang Q, Whitmore MA, Robinson K, Lyu W, Zhang G. Butyrate, forskolin, and lactose synergistically enhance disease resistance by inducing the expression of the genes involved in innate host defense and barrier function. *Antibiotics.* (2021) 10:1175. doi: 10.3390/antibiotics10101175

82. Giansanti F, Rossi P, Massucci MT, Botti D, Antonini G, Valenti P, et al. Antiviral activity of ovotransferrin discloses an evolutionary strategy for the defensive activities of lactoferrin. *Biochem Cell Biol.* (2002) 80:125–30. doi: 10.1139/o01-208

83. Chang HM, Ou-Yang RF, Chen YT, Chen CC. Productivity and some properties of immunoglobulin specific against streptococcus mutans serotype c in chicken egg yolk (IgY). *J Agric Food Chem.* (1999) 47:61–6. doi: 10.1021/jf980153u

84. Zhu W, Zhang J, He K, Geng Z, Chen XJPs. Proteomic analysis of fertilized egg yolk proteins during embryonic development. *Poult Sci.* (2020) 99:2775–84. doi: 10.1016/j.psj.2019.12.056

85. Young D, Fan MZ, Mine Y. Egg yolk peptides up-regulate glutathione synthesis and antioxidant enzyme activities in a porcine model of intestinal oxidative stress. *J Agric Food Chem.* (2010) 58:7624–33. doi: 10.1021/jf1011598

86. Lim W, Song G. Differential expression of vitelline membrane outer layer protein 1: hormonal regulation of expression in the oviduct and in ovarian carcinomas from laying hens. *Mol Cell Endocrinol.* (2015) 399:250–8. doi: 10.1016/j.mce.2014.10.015

87. Wicher KB, Fries E. Haptoglobin, a hemoglobin-binding plasma protein, is present in bony fish and mammals but not in frog and chicken. *Proc Nat Acad Sci.* (2006) 103:4168–73. doi: 10.1073/pnas.0508723103

88. Davalos A, Miguel M, Bartolome B, Lopez-Fandino R. Antioxidant activity of peptides derived from egg white proteins by enzymatic hydrolysis. *J Food Prot.* (2004) 67:1939–44. doi: 10.4315/0362-028X-67.9.1939

89. Nakamura S, Kato A. Kobayashi KJJoA, Chemistry F. Enhanced antioxidative effect of ovalbumin due to covalent binding of polysaccharides. *J Agric Food Chem.* (1992) 40:2033–7. doi: 10.1021/jf00023a001

90. Correnti C, Clifton MC, Abergel RJ, Allred B, Hoette TM, Ruiz M, et al. Galline Ex-FABP is an antibacterial siderocalin and a lysophosphatidic acid sensor functioning through dual ligand specificities. *Structure.* (2011) 19:1796–806. doi: 10.1016/j.str.2011.09.019

91. Mahon MG, Lindstedt KA, Hermann M, Nimpf J, Schneider WJ. Multiple involvement of clusterin in chicken ovarian follicle development: binding to two oocyte-specific members of the low density lipoprotein receptor gene family. *J Biol Chem.* (1999) 274:4036–44. doi: 10.1074/jbc.274.7.4036

92. Liu Y, Cheng Y, Shan W, Ma J, Wang H, Sun J, et al. Chicken interferon regulatory factor 1 (IRF1) involved in antiviral innate immunity via regulating IFN-B production. *Dev Comp Immunol.* (2018) 88:77–82. doi: 10.1016/j.dci.2018.07.003

93. Kogut MH, Chiang H-I, Swaggerty CL, Pevzner IY, Zhou HJ. Gene expression analysis of toll-like receptor pathways in heterophils from genetic chicken lines that differ in their susceptibility to salmonella enteritidis. *Front Genet.* (2012) 3:121. doi: 10.3389/fgene.2012.00121

94. Tsuchiya K, Nakajima S, Hosojima S, Thi Nguyen D, Hattori T, Manh Le T, et al. Caspase-1 initiates apoptosis in the absence of gasdermin D. *Nat Commun.* (2019) 10:1–19. doi: 10.1038/s41467-019-09753-2

95. Yu J, Nagasu H, Murakami T, Hoang H, Broderick L, Hoffman HM, et al. Inflammasome activation leads to caspase-1–dependent mitochondrial damage and block of mitophagy. *Proc Nat Acad Sci.* (2014) 111:15514–9. doi: 10.1073/pnas.1414859111

96. Suzuki T, Franchi L, Toma C, Ashida H, Ogawa M, Yoshikawa Y, et al. Differential regulation of caspase-1 activation, pyroptosis, and autophagy via Ipaf and ASC in shigella-infected macrophages. *PLoS Pathog.* (2007) 3:e111. doi: 10.1371/journal.ppat.0030111

97. Hong Y, Kim E-S, Lillehoj H, Lillehoj E, Song K-DJ. Association of resistance to avian coccidiosis with single nucleotide polymorphisms in the zyxin gene. *Poult Sci.* (2009) 88:511–8. doi: 10.3382/ps.2008-00344

98. Krkavcová E, Kreisinger J, Hyánková L, Hyršl P, Javurková V. The hidden function of egg white antimicrobials: egg weight-dependent effects of avidin on avian embryo survival and hatchling phenotype. *Biology Open.* (2018) 7:bio031518. doi: 10.1242/bio.031518

99. Wellman-Labadie O, Picman J, Hincke MJ. Comparative antibacterial activity of avian egg white protein extracts. *Br Poult Sci.* (2008) 49:125–32. doi: 10.1080/00071660801938825

100. Matulova M, Rajova J, Vlasatikova L, Volf J, Stepanova H, Havlickova H, et al. Characterization of chicken spleen transcriptome after infection with *Salmonella enterica.* serovar enteritidis. *PLos ONE.* (2012) 7:e48101. doi: 10.1371/journal.pone.0048101

101. Sedger LM, McDermott M. Tnf and Tnf-receptors: from mediators of cell death and inflammation to therapeutic giants–past, present and future. *Cytokine Growth Factor Rev.* (2014) 25:453–72. doi: 10.1016/j.cytogfr.2014.07.016

102. Falschlehner C, Schaefer U, Walczak HJI. Following trail's path in the immune system. *Immunology.* (2009) 127:145–54. doi: 10.1111/j.1365-2567.2009.03058.x

103. Li M, Lai P, Chou Y, Chi A, Mi Y, Khoo K, et al. Protein tyrosine phosphatase PTPN3 inhibits lung cancer cell proliferation and migration by promoting EGFR endocytic degradation. *Oncogene.* (2015) 34:3791–803. doi: 10.1038/onc.2014.312

104. Liu H-C, Kung H-J, Fulton JE, Morgan RW, Cheng H. Growth hormone interacts with the Marek's disease virus SORF2 protein and is associated with disease resistance in chicken. *Proc Natl Acad Sci U S A.* (2001) 98:9203–8. doi: 10.1073/pnas.161466898

105. Awwad K, Hu J, Shi L, Mangels N, Abdel Malik R, Zippel N, et al. Role of secreted modular calcium-binding protein 1 (SMOC1) in transforming growth factor B signalling and angiogenesis. *Cardiovasc Res.* (2015) 106:284–94. doi: 10.1093/cvr/cvv098

106. Chen S, Wang L, Chen J, Zhang L, Wang S, Goraya MU, et al. Avian interferon-inducible transmembrane protein family effectively restricts avian tembusu virus infection. *Front Microbiol.* (2017) 8:672. doi: 10.3389/fmicb.2017.00672

107. Asiamah CA, Liu Y, Ye R, Pan Y, Lu L-l, Zou K, et al. Polymorphism analysis and expression profile of the estrogen receptor 2 gene in leizhou black duck. *Poult Sci*. (2022) 101:101630. doi: 10.1016/j.psj.2021.101630

108. Bello SF, Adeola AC, Nie QJ. The study of candidate genes in the improvement of egg production in ducks-a review. *Poult Sci.* (2022) 101:101850. doi: 10.1016/j.psj.2022.101850

109. Kang L, Zhang Y, Zhang N, Zang L, Wang M, Cui X, et al. Identification of differentially expressed genes in ovaries of chicken attaining sexual maturity at different ages. *Mol Biol Rep.* (2012) 39:3037–45. doi: 10.1007/s11033-011-1066-x

110. Xu J, Gao X, Li X, Ye Q, Jebessa E, Abdalla BA, et al. Molecular characterization, expression profile of the FSHR gene and its association with egg production traits in muscovy duck. *J Genet.* (2017) 96:341–51. doi: 10.1007/s12041-017-0783-x

111. Ye Q, Xu J, Gao X, Ouyang H, Luo W, Nie QJP. Associations of Igf2 and Drd2 polymorphisms with laying traits in muscovy duck. *PeerJ.* (2017) 5:e4083. doi: 10.7717/peerj.4083

112. Lestari D, Murtini S, Ulupi N, Sumantri C. Polymorphism and association of DMA gene with total IGY concentration and ND antibody titer in Ipb-D2 chicken line. *Trop Anim Sci J.* (2022) 45:1–8. doi: 10.5398/tasj.2022.45.1.1

113. Lee KP, Anthony NB, Orlowski SK, Rhoads DD. SNP-based breeding for broiler resistance to ascites and evaluation of correlated production traits. *Hereditas.* (2022) 159:1–15. doi: 10.1186/s41065-022-00228-x

114. Cubas-Gaona LL, Diaz-Beneitez E, Ciscar M, Rodríguez JF, Rodríguez DJ. Exacerbated apoptosis of cells infected with infectious bursal disease virus upon exposure to interferon alpha. *J Virol.* (2018) 92:e00364–18. doi: 10.1128/JVI.00364-18

115. Xu S, Xue C, Li J, Bi Y, Cao YJ. Marek's disease virus type 1 microRNA miR-M3 suppresses cisplatin-induced apoptosis by targeting Smad2 of the transforming growth factor beta signal pathway. *J Viol.* (2011) 85:276–85. doi: 10.1128/JVI.01392-10

116. Hu J, Bumstead N, Barrow P, Sebastiani G, Olien L, Morgan K, et al. Resistance to salmonellosis in the chicken is linked to NRAMP1 and TNC. *Genome Res.* (1997) 7:693–704. doi: 10.1101/gr.7.7.693

117. Liu W, Kaiser M, Lamont S. Natural resistance-associated macrophage protein 1 gene polymorphisms and response to vaccine against or challenge with *Salmonella enteritidis* in young chicks. *Poult Sci.* (2003) 82:259–66. doi: 10.1093/ps/82.2.259

118. Liu X-Q, Wang F, Jin J, Zhou Y-G, Ran J-S, Feng Z-Q, et al. Myd88 polymorphisms and association with susceptibility to *Salmonella pullorum*. *BioMed Res Int.* (2015) 2015:692973. doi: 10.1155/2015/692973

119. Lee JT. Epigenetic regulation by long noncoding RNAs. *Science.* (2012) 338:1435–9. doi: 10.1126/science.1231776

120. Chen X, Ali Abdalla B, Li Z, Nie QJL. Epigenetic regulation by non-coding RNAs in the avian immune system. *Life.* (2020) 10:148. doi: 10.3390/life10080148

121. Tahira AC, Kubrusly MS, Faria MF, Dazzani B, Fonseca RS, Maracaja-Coutinho V, et al. Long noncoding intronic RNAs are differentially expressed in primary and metastatic pancreatic cancer. *Mol Cancer.* (2011) 10:1–19. doi: 10.1186/1476-4598-10-141

122. Heward JA, Lindsay MAJTii. Long non-coding RNAs in the regulation of the immune response. *Trends Immunol.* (2014) 35:408–19. doi: 10.1016/j.it.2014.07.005

123. Riege K, Hölzer M, Klassert TE, Barth E, Bräuer J, Collatz M, et al. Massive effect on lncrnas in human monocytes during fungal and bacterial infections and in response to vitamins A and D. *Sci Rep.* (2017) 7:1–13. doi: 10.1038/srep 40598

124. Yu H, Mi C, Wang Q, Dai G, Zhang T, Zhang G, et al. Long noncoding RNA profiling reveals that LncRNA BTN3A2 inhibits the host inflammatory response to Eimeria tenella infection in chickens. *Front Immunol.* (2022) 13:891001. doi: 10.3389/fimmu.2022.891001

125. Burnside J, Bernberg E, Anderson A, Lu C, Meyers BC, Green PJ, et al. Marek's disease virus encodes MicroRNAs that map to meq and the latency-associated transcript. *J Virol.* (2006) 80:8778–86. doi: 10.1128/JVI.00831-06

126. Zhao P, Li X-J, Teng M, Dang L, Yu Z-H, Chi J-Q, et al. *In vivo* expression patterns of MicroRNAs of gallid herpesvirus 2 (Gahv-2) during the virus life cycle and development of marek's disease lymphomas. *Virus Genes.* (2015) 50:245–52. doi: 10.1007/s11262-015-1167-z

127. Han B, He Y, Zhang L, Ding Y, Lian L, Zhao C, et al. Long intergenic non-coding RNA GALMD3 in chicken marek's disease. *Sci Rep.* (2017) 7:1–13. doi: 10.1038/s41598-017-10900-2

128. Zhao C, Li X, Han B, Qu L, Liu C, Song J, et al. Gga-miR-130b-3p inhibits MSB1 cell proliferation, migration, invasion, and its downregulation in MD tumor is attributed to hypermethylation. *Oncotarget.* (2018) 9:24187. doi: 10.18632/oncotarget.24679

129. Zhang X, Yan Y, Lei X, Li A, Zhang H, Dai Z, et al. Circular RNA alterations are involved in resistance to avian leukosis virus subgroup-j-induced tumor formation in chickens. *Oncotarget.* (2017) 8:34961. doi: 10.18632/oncotarget.16442

130. Qiu L, Chang G, Bi Y, Liu X. Chen G. Circular RNA and mRNA profiling reveal competing endogenous RNA networks during avian leukosis virus, subgroup J-induced tumorigenesis in chickens. *PLoS ONE.* (2018) 13:e0204931. doi: 10.1371/journal.pone.0204931

131. Li H, Ji J, Xie Q, Shang H, Zhang H, Xin X, et al. Aberrant expression of liver microrna in chickens infected with subgroup J avian leukosis virus. *Virus Res.* (2012) 169:268–71. doi: 10.1016/j.virusres.2012.07.003

132. Wang Q, Gao Y, Ji X, Qi X, Qin L, Gao H, et al. Differential expression of micrornas in avian leukosis virus subgroup J-induced tumors. *Vet Microbiol.* (2013) 162:232–8. doi: 10.1016/j.vetmic.2012.10.023

133. Ji J, Shang H, Zhang H, Li H, Ma J, Bi Y, et al. Temporal changes of MicroRNA Gga-Let-7b and Gga-Let-7i expression in chickens challenged with subgroup J avian leukosis virus. *Vet Res Commun.* (2017) 41:219–26. doi: 10.1007/s11259-017-9681-1

134. Gordon JW, Scangos GA, Plotkin DJ, Barbosa JA, Ruddle FH. Genetic transformation of mouse embryos by microinjection of purified DNA. *Proc Nat Acad Sci.* (1980) 77:7380–4. doi: 10.1073/pnas.77.12.7380

135. Hammer RE, Pursel VG, Rexroad CE, Wall RJ, Bolt DJ, Ebert KM, et al. Production of transgenic rabbits, sheep and pigs by microinjection. *Nature.* (1985) 315:680–3. doi: 10.1038/315680a0

136. McGrew MJ, Sherman A, Ellard FM, Lillico SG, Gilhooley HJ, Kingsman AJ, et al. Efficient production of germline transgenic chickens using lentiviral vectors. *EMBO Rep.* (2004) 5:728–33. doi: 10.1038/sj.embor.7400171

137. Zhu L, Van de Lavoir M-C, Albanese J, Beenhouwer DO, Cardarelli PM, Cuison S, et al. Production of human monoclonal antibody in eggs of chimeric chickens. *Nat Biotechnol.* (2005) 23:1159–69. doi: 10.1038/nbt1132

138. Schusser B, Collarini EJ, Yi H, Izquierdo SM, Fesler J, Pedersen D, et al. Immunoglobulin knockout chickens via efficient homologous recombination in primordial germ cells. *Proc Nat Acad Sci.* (2013) 110:20170–5. doi: 10.1073/pnas.1317106110

139. Véron N, Qu Z, Kipen PA, Hirst CE. Marcelle CJ. CRISPR mediated somatic cell genome engineering in the chicken. *Dev Biol.* (2015) 407:68–74. doi: 10.1016/j.ydbio.2015.08.007

140. Oishi I, Yoshii K, Miyahara D, Kagami H, Tagami TJ. Targeted mutagenesis in chicken using CRISPR/cas9 system. *Sci Rep*. (2016) 6:1–10. doi: 10.1038/srep23980

141. Oishi I, Yoshii K, Miyahara D, Tagami T. Efficient production of human interferon beta in the white of eggs from ovalbumin gene–targeted hens. *Sci Rep.* (2018) 8:1–12. doi: 10.1038/s41598-018-28438-2

142. Kheimar A, Klinger R, Bertzbach LD, Sid H, Yu Y, Conradie AM, et al. A genetically engineered commercial chicken line is resistant to highly pathogenic Avian leukosis virus subgroup. *J Microorganisms.* (2021) 9:1066. doi: 10.3390/microorganisms9051066

143. Koslová A, Trefil P, Mucksová J, Reinišová M, Plachý J, Kalina J, et al. Precise CRISPR/Cas9 editing of the nhe1 gene renders chickens resistant to the J subgroup of avian leukosis virus. *Proc Nat Acad Sci.* (2020) 117:2108–12. doi: 10.1073/pnas.1913827117

144. Hellmich R, Sid H, Lengyel K, Flisikowski K, Schlickenrieder A, Bartsch D, et al. Acquiring resistance against a retroviral infection via CRISPR/Cas9 targeted genome editing in a commercial chicken line. *Front Genome Ed.* (2020) 2:3. doi: 10.3389/fgeed.2020.00003

145. Challagulla A, Jenkins KA, O'Neil TE, Shi S, Morris KR, Wise TG, et al. *In Vivo* inhibition of Marek's disease virus in transgenic chickens expressing Cas9 and Grna against Icp4. *Microorganisms.* (2021) 9:164. doi: 10.3390/microorganisms9010164

146. Koslová A, Kučerová D, Reinišová M, Geryk J, Trefil P, Hejnar J. Genetic resistance to Avian leukosis viruses induced by CRISPR/Cas9 editing of specific receptor genes in chicken cells. *Viruses.* (2018) 10:605. doi: 10.3390/v10110605

147. Rieblinger B, Sid H, Duda D, Bozoglu T, Klinger R, Schlickenrieder A, et al. Cas9-expressing chickens and pigs as resources for genome editing in livestock. *Proc Nat Acad Sci.* (2021) 118:e2022562118. doi: 10.1073/pnas.2022562118

148. Tan FL, Yin JQ. RNAi a new therapeutic strategy against viral infection. *Cell Res.* (2004) 14:460–6. doi: 10.1038/sj.cr.7290248

149. Manjunath N, Wu H, Subramanya S, Shankar P. Lentiviral delivery of short hairpin RNAs. *Adv Drug Deliv Rev.* (2009) 61:732–45. doi: 10.1016/j.addr.2009.03.004

150. Zhang P, Wang J, Wan J, Liu W. Screening efficient Sirnas *in vitro* as the candidate genes for chicken anti-avian influenza virus H5n1 breeding. *Mol Biol.* (2010) 44:37–44. doi: 10.1134/S0026893310010061

151. Wang S, Qu Z, Huang Q, Zhang J, Lin S, Yang Y, et al. Application of gene editing technology in resistance breeding of livestock. *Life.* (2022) 12:1070. doi: 10.3390/life12071070

152. Bello SF, Xu H, Guo L, Li K, Zheng M, Xu Y, et al. Hypothalamic and ovarian transcriptome profiling reveals potential candidate genes in low and high egg production of white muscovy ducks (*Cairina moschata*). *Poult Sci.* (2021) 100:101310. doi: 10.1016/j.psj.2021.101310

153. Moon SH, Lee JH, Lee M, Park E, Ahn DU, Paik HD. Cytotoxic and antigenotoxic activities of phosvitin from egg yolk. *Poult Sci.* (2014) 93:2103–7. doi: 10.3382/ps.2013-03784

154. Moon SH, Lee JH, Lee YJ, Chang KH, Paik JY, Ahn DU, et al. Screening for cytotoxic activity of ovotransferrin and its enzyme hydrolysates. *Poult Sci.* (2013) 92:424–34. doi: 10.3382/ps.2012-02680

155. Nassar FS. Poultry as an experimental animal model in medical research and pharmaceutical industry. *Biomed J Sci Tech Res.* (2018). doi: 10.26717/BJSTR.2018.02.000751

156. Boulland J-L, Halasi G, Kasumacic N, Glover JCJJ. Xenotransplantation of human stem cells into the chicken embryo. *J Vis Exp*. (2010) 11:e2071. doi: 10.3791/2071

157. Martowicz A, Kern J, Gunsilius E, Untergasser GJJ. Establishment of a human multiple myeloma xenograft model in the chicken to study tumor growth, invasion and angiogenesis. *J Vis Exp.* (2015) 99:e52665. doi: 10.3791/52665

158. Ching KH, Collarini EJ, Abdiche YN, Bedinger D, Pedersen D, Izquierdo S, et al. Chickens with humanized immunoglobulin genes generate antibodies with high affinity and broad epitope coverage to conserved targets. *MAbs*. (2018) 10:71–80. doi: 10.1080/19420862.2017.1386825

159. Flemming Alexandra. Human Antibodies from Chicken Eggs. *Nature Reviews Drug Discovery*. (2005) 4:884-5. doi: 10.1038/nrd1883

Frontiers in Veterinary Science

Transforms how we investigate and improve animal health

The third most-cited veterinary science journal, bridging animal and human health with a comparative approach to medical challenges. It explores innovative biotechnology and therapy for improved health outcomes.

Discover the latest Research Topics

See more →

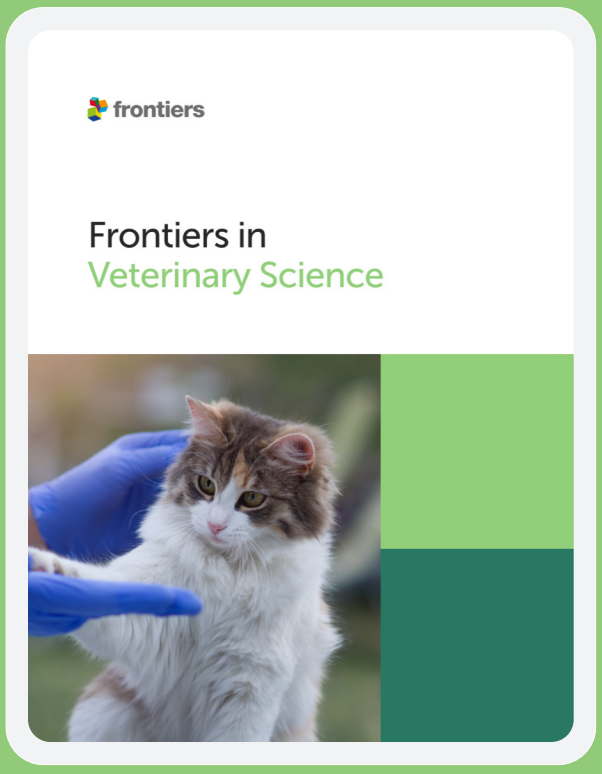

Frontiers

Avenue du Tribunal-Fédéral 34
1005 Lausanne, Switzerland
frontiersin.org

Contact us

+41 (0)21 510 17 00
frontiersin.org/about/contact